Title of the Project: Ganges Aquifer Management in the context of Monsoon Runoff Conservation for Sustainable River Ecosystem Services – A Pilot Study

National Hydrology Project (NHP)
Department of Water Resources, River Development and Ganga Rejuvenation, Ministry of Jal Shakti, New Delhi

National Institute of Hydrology, Roorkee

Study Area: Sot River Catchment

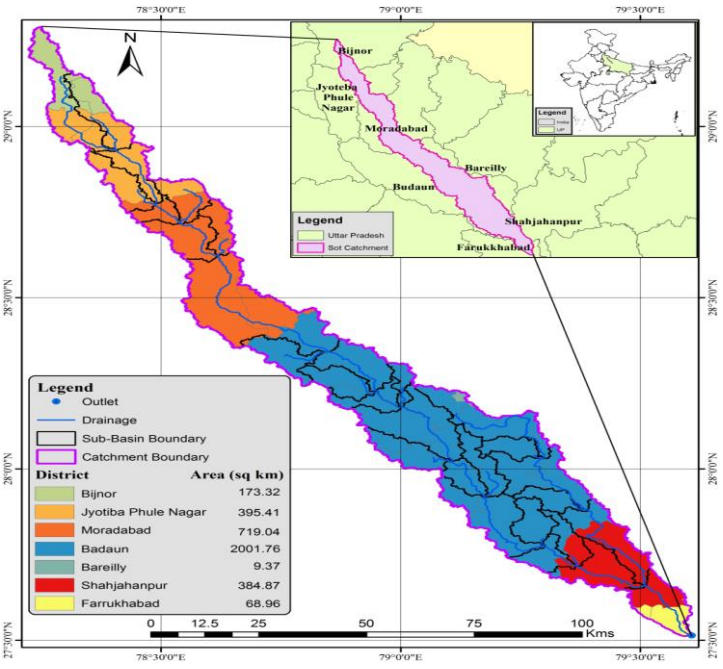

National Institute of Hydrology (NIH)
Roorkee – 247667, Uttarakhand

October 2022

Name: Dr. Surjeet Singh
Designation: Scientist 'F'

National Institute of Hydrology (NIH)
Roorkee – 247667, Uttarakhand

PREFACE

The Ganges is the main river system, in northern India, covering an area of 1.08 million sq.km, which is supported by many perennial tributaries. In various stretches of the Ganga River, contribution of these perennial rivers during lean season cannot be ignored. If these small and medium rivers are endangered, there will be threat in future to the aviral and nirmal dhara of the Ganga River. Groundwater is the main source for sustaining flow in most of the non-glacial perennial rivers during the lean season. Flow in such rivers is highly influenced by the groundwater contribution from the catchment. Both river and groundwater interact in an integral manner. In some reaches, river contributes to the groundwater and in some reaches, groundwater contributes to the river in the form of base flow depending on the hydraulic gradient between these two.

Declining groundwater levels, diminishing river flows, being perennial rivers into ephemeral, and the impact of climate change are posing extreme scarcity of water availability in many tributaries of the Ganga river. Such phenomena are not only affecting the water resources but also the livelihood of farmers and the river ecosystem. The Sot river, earlier used to be perennial, has now become a seasonal river. Under this background, it was felt necessary to investigate the river-aquifer interactions to identify causes of drying of river and suggest rejuvenation measures. It is in that context, groundwater management study of the Sot river catchment with special reference to augmentation of groundwater through monsoon recharge measures is undertaken as a purpose driven study entitled "*Ganges Aquifer Management in the context of Monsoon Runoff Conservation for Sustainable River Ecosystem Services – A Pilot Study*" in collaboration with the Ground Water Department, Lucknow, Govt. of Uttar Pradesh under the National Hydrology Project (NHP) awarded vide letter No. X-63016/1/2017-NHP/7426-7427 dated 04.12.2017 for a period of 4 years duration. The activities to meet the objectives of the project were started from the month of April 2018 by recruitment of project staff, literature survey, field visit of the study area and by organizing three training courses. Support and help provided by Sri Ravikant Singh, Sr. Hydrogeologist and Sh. Anupam Srivastava, Assistant Engineer (Civil), Ground Water Department, Lucknow is highly appreciated. Groundwater level and litho log data provided by GW Department, Lucknow are duly acknowledged. The Technical Report entitled "**Ganges Aquifer Management in the context of Monsoon Runoff Conservation for Sustainable River Ecosystem Services – A Pilot Study**" is prepared based on the work carried out under this PDS by Dr. Surjeet Singh, Scientist 'F' & Principal Investigator of the PDS and his team. The findings of the study would help in solving the problem of declining groundwater levels and reducing base flow to the Sot river in the state of Uttar Pradesh by adopting the suggested measures in the appropriate zones.

Place: Roorkee

Signature

Date: 14.11.2022

(Surjeet Singh)

Project Team	
Lead Organization	Name and Designation (PI)*: Dr. Surjeet Singh, Scientist 'F' Name and Designation (Co-PI)*: Dr. N.C. Ghosh, Scientist 'G' (up to 31.03.2019) Dr. Sudhir Kumar, Scientist 'G' & Director, NIH Sh. C.P. Kumar, Scientist 'G' (up to 30.09.2020) Dr. Gopal Krishan, Scientist 'D' Ms. Suman Gurjar, Scientist 'C' (up to 31.03.2021) Dr. Priyanka Sharma, Research Associate Name and address of lead organization: National Institute of Hydrology, Roorkee – 247667, Uttarakhand Name and address of IA (if different from lead organization): Ground Water Department, Lucknow, Govt. of UP
Partner Organization	Name and Designation (PI)*: Sh. Ravikant Singh, Senior Hydrogeologist Name and Designation (Co-PI)*: Sh. Anupam Srivastava, Assistant Engineer (Civil) Name and address of partner organization: Ground Water Department, Lucknow, Govt. of UP Name and address of IA (if different from partner organization): Same
Consultant/s, if any	Not applicable

*If PI/ Co-PI are changed/ retired, enter those names as follows in above table
Name and designation (PI up to _____)
Name and designation (Co-PI up to _____)

Document Control Sheet

Title	Ganges Aquifer Management in the context of Monsoon Runoff Conservation for Sustainable River Ecosystem Services – A Pilot Study
PDS Number	PDS No.: NIH-7_2016_10
Date of Approval	04 December 2017
Budget in time of original approval (For Partner and for Lead)	Rs. 57,70,674.00 (for Lead – NIH) Nil (for Partner – WRD, Raipur)
Revised Budget (For Partner and for Lead)	Rs. 38,28,174.00 (for Lead – NIH) Nil (for Partner – WRD, Raipur)
Date of commencement	01 April 2018
Date of completion	31 October 2022
Number of page	134
Number of figures and tables	Figure – 73, Table - 17

Abstract

The study area comprises of Sot river catchment. The Sot river is a tributary of the Ganga river. The Sot river flows in between the Ganga and the Ramganga river. Though both these rivers have good water potential, the Sot river is drying-up after the monsoon season in recent years, and its catchment is facing acute water problem and many hydrological problems, including deep groundwater levels, recurrent droughts, soil erosion and desertification in some areas. These factors coupled with the threat of climate change may aggravate crop losses in the area and poor health of river ecosystem. The catchment area falls in districts of JP Nagar, Moradabad, Budaun, Shahjahanpur and Farrukhabad. The Sot river, earlier used to be perennial, has now become a seasonal river.

The geographical area of the Sot river catchment is 3,752.73 sq.km. The elevation of catchment varies from 138 to 245 m above mean sea level. The catchment receives an average annual rainfall of 882 mm, with very hot summer and cold winter. During summers, temperature normally varies from 30 °C to 43 °C and during winters from 5 °C to 25 °C. Average groundwater level varies from 0.90-26.2 mbgl during pre-monsoon and 0.3-25.9 mbgl during post-monsoon. Groundwater levels are shallow in the lower catchment and deep in the middle part of catchment. Groundwater levels are found declining during the period of investigation from 2009 to 2018. Groundwater fluctuation up to 14.85 m is found in the lower part of the catchment. Literature survey was done and various thematic maps, such as catchment boundary, catchment location, DEM, drainage, slope, soil, sub-basin, district/tehsil/road network, grid and land use, were prepared. Daily river flow data was collected and processed to analyse variations along with rainfall. Changes in land use and meteorological variables were also assessed. Infiltration and hydraulic conductivity tests were conducted at 48 locations in the entire catchment. The soil infiltration and conductivity were found to vary from 0.3 to 51.5 cm/hr and 0.05 to 2.3 m/d, respectively. Disturbed and undisturbed soil samples were collected from the same 48 locations of the catchment for the determination of soil properties. Forty-nine litho logs of underground formations were analysed and geological sections and fence diagram were developed to find aquifers geometry which indicate that the alluvial formations are in alternate layers of aquifers and aquitards. ANN model was applied to model the river flow for the period 2009 to 2016.

SWAT model was also setup for extending the river flow records for the historical period 1985 to 2008, as river flow data for this period was not available.

Groundwater modelling was done using the Visual MODFLOW software to model the four-layer groundwater system and assess impacts of groundwater recharge interventions in the catchment. The data for the period from 2009 to 2018 were used. The model was calibrated for the period 2009 to 2014 and validated for the period 2014 to 2018. This calibrated and validated model was then used for assessing the impact of groundwater recharge structures in the catchment.

To implement the groundwater recharge structures in the Sot catchment, potential zones for groundwater recharge were identified. Eleven thematic layers, namely ground elevation, LULC, surface slope, soil, geology, geomorphology, drainage density, recharge, depth to aquifer, depth to groundwater and groundwater fluctuation, were used for identifying these zones. Saaty's Analytic Hierarchy Process (AHP) was used to finalize the consistent weights of various thematic layers. The groundwater potential zones were delineated into six classes viz. unsuitable, very low suitable, low suitable, moderately suitable, suitable and very suitable, using the Prajal tool. The maximum area was found under the moderately suitable condition followed by suitable and very suitable condition. The zones were used to implement the groundwater recharge structures in the catchment.

Finally, few scenarios on groundwater recharge structures are suggested in the Sot catchment for augmentation of groundwater so as to contribute to river in the form of base flow. Three types of recharge structures are suggested depending on the local conditions. These structures include check dams, percolation tanks and recharge shafts. Eight check dams are suggested mainly in the upper part of the catchment. Seven percolation tanks are distributed in the catchment wherever thickness of surface soil is less. Seven recharge shafts are suggested where upper unconfined aquifer is deeper and separated by thick aquitard layer. The impact of these structures is presented with and without these recharge interventions in the form of change in groundwater level profiles. It is seen that the groundwater levels show rise in water table profiles after implementation of the recharge interventions. The water table profiles show rise during the period of recharge and decline during the period of no recharge. It is also observed that in general the water table profiles show rising trend after the recharge interventions. Similar structures can be implemented at other feasible locations (falling under the suitable and moderate suitable zones).

The condition of the Sot river is already very much deteriorated in past few decades and lot of sediment and mud is deposited in the river course. Because of this, capacity of river is reduced a lot. Also due to deposition of mud on the river bed, water exchange capacity between river and groundwater is reduced considerably. Developmental activities and land use changes have also impacted the runoff and groundwater recharge conditions in the river catchment. Considering all these aspects, various measures are suggested for rejuvenation of the Sot river.

Originating unit	National Institute of Hydrology, Roorkee
Key words	Groundwater, River Rejuvenation, Sot, Modelling, Recharge Structures, MODFLOW
Security classification	~~Restricted~~/ Unrestricted
Distribution	~~Restricted~~/ General

CONTENTS

LIST OF FIGURES

LIST OF TABLES

1. INTRODUCTION

Water is regarded as the important natural resource for the well-being of Society and existence of life on the earth. Increasing population and industrialization reduces the water supply for agricultural and domestic purposes. Major reason of reduced water supply is lack of precipitation, which leads to affect the usual social, economic and developmental activities of that region. Anthropogenic disturbances such as river regulation and the clearing of riparian vegetation have contributed to widespread geomorphic adjustment and the degradation of rivers across the globe (Galay, 1983; Nilsson and Berggren, 2000). Declining groundwater levels, diminishing river flows, turning perennial rivers into ephemeral rivers, and impact of climate change are posing extreme scarcity of water availability in many tributaries of the Ganga River. Such phenomena are not only affecting the water resources but also the livelihood of farmers and the river ecosystem. Water resources are inextricably linked with climate. Climate change may also alter the spatial and temporal patterns in rainfall, temperature and evapotranspiration. Based on various projections of future climate change, there will be increased demand of crop water requirements. This may result in huge loss of crops, reduced agricultural production, encroachment of river bed and desertification owing to reduced water resources in the basin. Such phenomena may also contribute to poor water quality problems in the basin.

Groundwater is the main source for sustaining flow in most of the non-glacial perennial rivers during lean season. Flow in rivers is highly influenced by the groundwater in its catchment. Both of these interact in an integral manner. In some reaches, river contributes to the groundwater and conversely in some reaches, groundwater contributes to the river in the form of base flow depending on the hydraulic gradient between these two. These interactions, in future, will also be exacerbated by the climate change which may intensify the dying of many small tributaries of the Ganga River.

The river-aquifer interaction studies are therefore very necessary to understand the processes happening underground for the sustainability of the rivers.

View above in view, the study was proposed with the following objectives:

- Hydro-geological characterization of the area.
- Analysis of meteorological and hydrological variables *vis-a-vis* cessation of river flows during lean season.
- Estimation of surface water and groundwater availability.
- Analysis of stream-aquifer interaction.
- Aquifer management measures for enhancing river flow during lean season.

2. REVIEW OF LITERATURE

An extensive review of the literatures related to the study have been done and presented below:

2.1 River Degradation

The rivers around the globe went through changes due to engineering development, change in land use, construction of flood control, diversion and irrigation structures, and pollution causing from heavy metals. The rivers in different continents are at different stages of adjustment due to increasing industrialization and urbanization, subsequently raises the attention towards then river rehabilitation. Rehabilitation of rivers along with repairing of water quality and ecological losses are the issues of international concern, for the sustainability of ecosystem (Langhans et al., 2013; Pan et al., 2016; Paillex et al., 2017). Anthropogenic activities like regulation of river flow and removal of vegetation from riparian zone are the major factors contributing to geomorphic alteration and river degradation (Galay, 1983; Nilsson and Berggren, 2000). During last three decades, river management becomes a multi-disciplinary initiative to address the diversity of river values and needs of the ecosystem (Piegay et al., 2008; Wohl et al., 2008; Fryirs et al., 2013). It is not only expensive and tough to stop the deterioration in riparian zone once it started, but even mild degradation can cause remarkable damage to freshwater ecosystems (Chessman et al., 2006).

The health of river ecosystem is very important for human being as it provides the vital source of water for humans (Menget al., 2009). Cheng et al. (2018) assess the health of river ecosystem in Haihe River Basin by sampling 148 river sites during pre and post monsoon season. Their study revealed that the change in land use and socio-economic development are major factors responsible for the river deterioration.

The three major factors responsible for river degradation are: (i) Physical disturbance, (ii) Hydrological manipulations, and (iii) Chemical disturbance

2.1.1 Physical disturbance

Physical disturbance of the river is the outcome of anthropogenic activities within the catchment or channel. Channelization and canalization are two common disturbances in channel. Deepening, strengthening, narrowing/widening of channel, erecting embankments comes under the channelization while canalization is the extreme form of channelization which includes lining of channel bed with concrete.

2.1.2 Hydrological manipulations

The interference of humans is gradually increasing across the land-based portion of hydrologic cycle. Construction of dams, inter basin transfer, agriculture, direct abstraction and urbanization are the major human interferences which affects the river ecosystem. These interferences have significantly changed the form of high and low flows and river sediment regimes, which subsequently alters morphology of channel, water quality and biota. Groundwater abstraction is increasing at alarming rate across the globe leading to reduced water table, a subsequent decrease in stream flow, possibly with an intrusion of saline water, and so a decrease in water quality.

2.1.3 Chemical disturbance

Naturally water quality of different rivers varies because of climate and underlying geological formations, and due to seasonal changes in flow and temperature throughout the year, and responding biological activity. Altering drainage pattern to the rivers and chemicals that may be carried by water are the major impacts of humans on water quality. Rivers are also used as wastewater conduit and to feed urban storm-water drains into them. Pollutants impact aquatic ecosystems by reducing abundances and biodiversity, and their general ability to function efficiently.

2.2 River Restoration

Human interventions such as dam construction, channelization and gravel extraction affects the physical and ecological processes in rivers from many years across the world (Gore, 1985; Gregory, 2006). Today in the world of increasing water demand, the restoration of rivers has drawn the attention of researchers around the globe (Bates et al., 2008; Vörösmarty et al., 2010). Meier (1998) defines *river restoration* as, “an attempt to bring the river back to as high a level of ecological integrity as possible, taking into account the prevailing socio-economic, political, and technological constraints. In highly managed rivers, the objective should be to maintain a healthy ecosystem that is able to meet the societal needs in a sustainable manner.” Despite of lot of efforts and funds devoted for the river recovery, the rate of success for river restoration is not up to the mark (Bernhardt et al., 2005; Roni et al., 2008). Planning restoration efforts in a more organized way (Hermoso et al., 2012) may help improving their efficacy, meeting management goals set by global conventions and directives. The number of projects for restoration of river are gradually increasing to stop the losses in freshwater diversity and to enhance the ecological state of rivers

(Bernhardt et al., 2005). Eden et al. (2000) examines the process of river restoration at the river Cole in southern England. The study revealed that the translation perspective is less helpful in evaluating or prescribing restoration as environmental management. Xu et al., (2015) carried out a case study for the restoration of the Jiangshui River in Longkou City, Shandong province considering integrated aspects of flood control, water resources allocation, environmental protection, ecological restoration, and river landscape. Minakshi and Goswami (2009) carried out a study for the restoration of Kolong River in Nagaon, Assam, India using field survey and geo-informatics. The study reveals the fact that a restoration standard is essential for management of the river's health and ecosystem. An outline of the restoration program is discussed.

2.3 River Rejuvenation

Succession and rejuvenation are the two major factors which shapes the landscape unit pattern in natural river systems. Succession is the local transition of a landscape unit to another by changing species composition (Forman and Godron, 1986), while erosion in outer river bends and sedimentation in inner bends rejuvenates the vegetation types to a previous stage. The rejuvenation of river is an effort made in order to restore the poor health of overexploited and polluted rivers. The process of river rejuvenation requires good understanding of the causes for the poor health and the restoration efforts from source to sink (ICFR 2014). The rejuvenation of rivers aimed at building a new sustainable healthy ecosystem which is based on level of river deterioration. This can also be attained by restoring health of the river back to previous state (Shekhar, 2016). The health of the river can be improved by treating the domestic sewage and industrial wastes before disposing into the river. The river flow is the most significant variable of a river system and besides performing various functions; it gives self-cleaning and healing powers to a river (Shekhar, 2016). Thus, the river rejuvenation broadly calls for optimal fresh water flow through the river system during different seasons. The river rejuvenation can be best attained by ensuring minimum amount of flow required in the river for a healthy and sustainable ecosystem. Sinha et. al (2013) gave much emphasis on estimating recovery potential of river and path along with threshold conditions for sustainable management of the river systems in the Ganga River basin. The notion of environmental flow in river management is already being applied in some or other form in 72 countries around the world (IWMI, 2005).

2.4 River-Aquifer Interaction

Groundwater and rivers are conventionally considered as different entities in most of the ecological research. Rivers are characterized by the flow creating turbulent hydraulic forces, variable discharge, small time of retention of the water masses, material transport in one direction, varying chemical conditions and dynamic channel morphology. On the other hand, groundwater ecosystem is relatively more stable, flow is laminar, high residence time, a largely constant sediment structure and permanent darkness (Brunke and Gonser, 1997). Initially, Hynes (1983) was the first to give importance to the hydrological connectivity between rivers and groundwater, by emphasizing the significance of interactions for the water balance and metabolism of streams. Simultaneously, the connections with surface water have become important in groundwater ecological research because upper layers of porous aquifers are biologically most active (Danielopol, 1980, 1989). The exchanges between rivers and groundwater play a crucial role in nearly in all groundwater models. Rivers may get water from aquifers or may lose water to aquifers (Doppler et al., 2007). There are two ways by which aquifers and rivers interact: rivers obtain water by river flow through the riverbed from the aquifer or lose water through the riverbed/bank to the aquifer, which depends on stage of the river and head of the aquifer (McCallum et al., 2012). Engeler et al., (2011) assessed the river aquifer interactions for the area Hardhof situated in Limnat valley in Zurich, Switzerland. The interaction between aquifer and river was modelled by using a leakage concept. The analysis revealed that during flood events the linear leakage concept does not produce the seepage flux in downstream section. In recent decades, a large number of studies have been carried out on river-aquifer interactions (Wroblicky et al. 1998; Hathaway et al. 2002; Storey et al. 2003; Kasahara and Wondzell 2003; Rodgers et al.2004). Frei et al., (2009) studied about the pattern and dynamics of the river-aquifer exchange with variably saturated flow using a coupled model. It is concluded that typical alluvial heterogeneity is an important control of river–aquifer exchange in rivers overlying deep water tables. The Simulated patterns and dynamics are found to be in line with the field observations. McCallum et al., (2012) investigated the aquifer-river interaction in semi-arid environment which is largely affected by groundwater abstraction. The analysis indicated that the groundwater levels have declined (~ 3 m) since the onset of groundwater abstraction. The decline is predominantly due to the abstraction rather than changing climate. Sophocleous et al., (1988) studied the interaction of stream and aquifer along the Arkansas River in Central Kansas. The analysis indicated that the alluvial aquifer has high transmissibility and pumping stress with radius of influence greater than 1.77 km, impacting both the aquifer levels and flow of the stream in the

nearby Arkansas River. Ala Eldin et al., (2000) carried out groundwater modeling to assess the aquifer-river interaction in Ganga-Mahawa sub-basin located in Central Ganga Plain in Moradabad and Budaun districts of Uttar Pradesh, India. The river stage data at Ahar, Naora and Ramghat has been used to provide surface water level and bed elevation in model. The analysis shows an agreement in estimated groundwater balance and that of field observations.

2.5 Aquifer Management

The use of groundwater has been exponentially increased during last 40 years in developed and rapidly growing countries (Bocanegra et al., 2009). The process of abstraction of groundwater has not been monitored, controlled and managed so as to avoid the depletion in quality and level of water. A generalized consequence is deterioration in quality of groundwater, which is mainly due to excessive exploitation, insufficient protection at the land surface and land use change. In literature, remediation and flow exploration aspect of groundwater management problems, both are widely discussed (Gorelick, 1983; Ahlfeld, 1986; Willis and Yeh, 1987; Gorelick *et al*., 1993; Wagner, 1995). Umar et al., (2008) analyzed the water balance components for management of groundwater of Kali-Hindon inter-stream aquifer located in west Uttar Pradesh. The analysis revealed that the groundwater balance is very sensitive to rainfall variability followed by draft through pumping. In northern part depth of the basin water level are shallow while the southern part has deeper water level. It can be concluded that the pumping of groundwater water should be from northern part not from the southern part of the basin, where more abstraction will lead to rapid falling of water level. Ahmad and Umar (2009) modelled the groundwater flow Yamuna–Krishni inter-stream, a part of central Ganga Plain located in Muzaffarnagar district of Uttar Pradesh. The total recharge to the study area is 160.21 million m^3. The groundwater draft through pumping is of the order of 233.56 million m^3, thus leaving a deficit balance of −73.35 million m^3.

Various hydrogeological investigations in Muzaffarnagar are carried out by Central Ground Water Board (CGWB) and Groundwater Department of Uttar Pradesh (U.P.) government. Khan (1992) and Kumar (1994) carried out organized hydrogeological investigations in Muzaffarnagar district and studied the first group of aquifer. They identified a number of blocks that were under and over exploited.

2.6 River Management

The most important natural resource for the well-being of human and the environment on the earth is fresh water (Gleick, 1993). There is increase in water demand globally due to the lack of water supply which is coupled with increasing population and industrialization. This leads to scarcity of fresh water resource on the earth (Wang and Lu, 2009). Water has to be sustained in rivers for conservation of natural ecosystem, and therefore, the minimum amount of water flow required for river's survival. The increase in global water demand made the researcher to think about the assessment of flow requirement for the river management (Stalnaker and Arnette 1976; Jowett 1997; Dunbar et al. 1998; Annear et al. 2002; Linnansaari et al. 2013).

The dynamics of runoff are regulated by different mechanisms, which act on a range of spatial and temporal scale (Sivakumar et al., 2001). The health of river ecosystem can be determined by many factors such as flow, channel structure and riparian zone, quality of water, exploitation level and macrophyte cutting and dredging (Norris and Thomas, 1999). Initially, it was believed that all the problems related to health of the river are associated with low flows and that the river ecosystem will be conserved till a minimum flow is maintained in the river, but as time lapses people become more aware about importance of all the other elements of flow regimes such as floods, medium and low flows (Poff et al., 1997; Hill et al., 1991).The management of river biodiversity and riparian zones sometimes includes direct addition or removal of biota, such as the replenishing of fish populations or the control of alien pest species. More often, however, goals for fluvial biodiversity are pursued indirectly through the manipulation of environmental drivers such as the flow regime (Stanford et al., 1996; Poff et al., 1997; Robinson and Uehlinger, 2003) and physical structure (Frissell et al., 1986; Rhoads et al., 1999). Gupta (2008) studied about the implication of environmental flow (EF) in management of river basin. The approaches for the assessment of environmental flow are evaluated in perspective of flow characteristics of river. The study revealed that EF can be integrated in the mainstream of operation of infrastructure (such as dams and pumps) to modulate the flow of water for the aquatic and other environment in the basins having regulated flows. Vaughan et al., (2009) integrated the ecology and hydro-morphology for river management. The study indicated that the assessment of relations between ecology and physical habitat are serious problem in river research and management.

3. **STUDY AREA**

Sot River is a tributary of the River Ganga. Catchment of the river Sot falls between the Ganga River and the Ramganga River. Drainage area of the catchment is 3,752.73 km^2. The catchment receives average rainfall of 950 mm annually, with very hot summer and cold winter. During summers, temperature usually varies from 30 °C to 43 °C and during winters from 5 °C to 25 °C. The area faces acute water problem and many hydrological problems, including extra-deep groundwater levels, recurrent droughts, soil erosion and desertification in some of the areas. The catchment area falls in the districts of JP Nagar, Moradabad, Budaun, Shahjahanpur and Farrukhabad. The region suffers from extended droughts, depleted water resources, declining groundwater levels, and uncontrolled developmental activities. The location map of the study area is presented in Figure1. In addition to the above, various thematic maps such as catchment boundary, catchment location, DEM, drainage, slope, soil, sub-basin, district/tehsil/road network, grid and land use have been prepared and presented below.

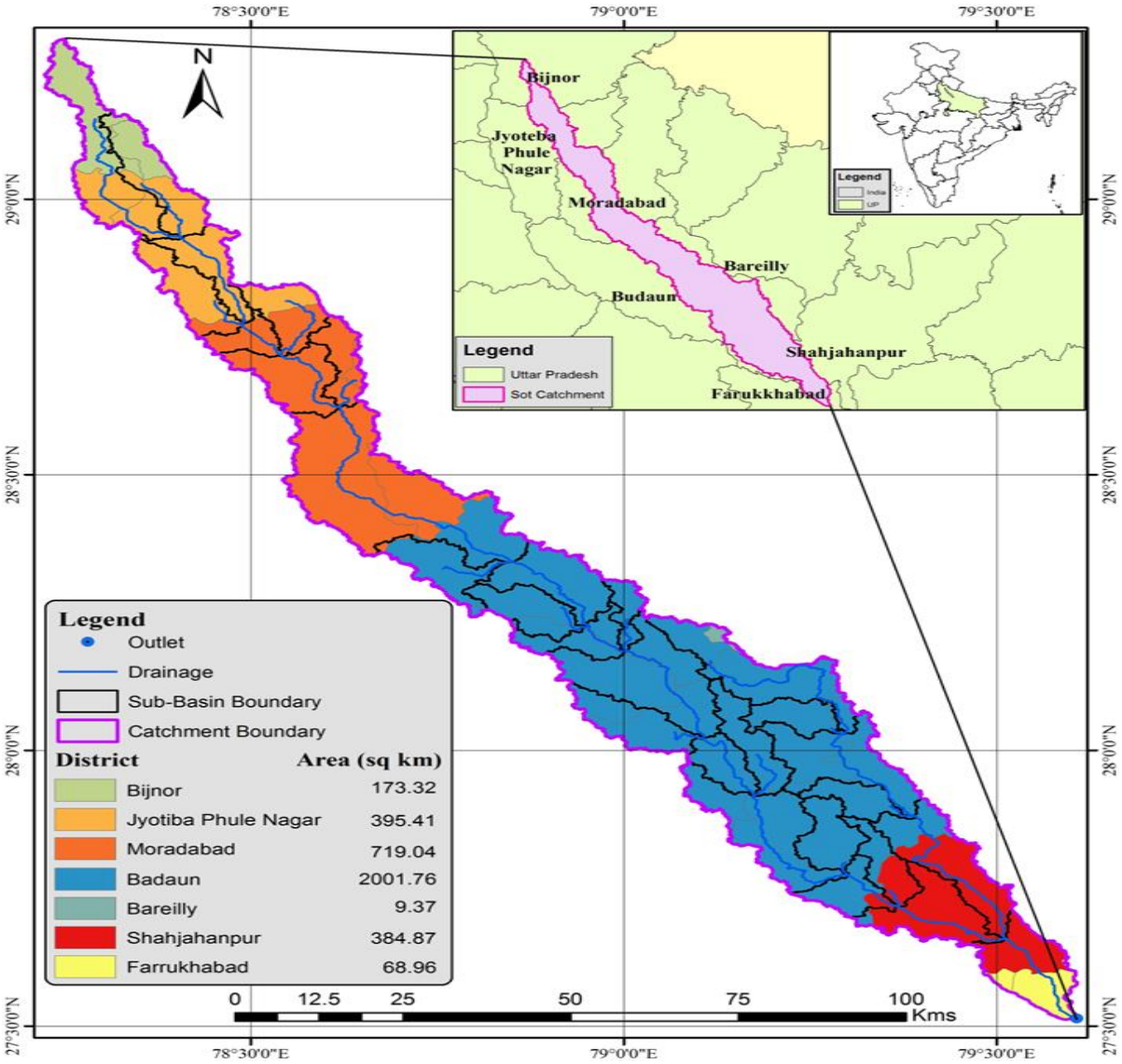

Figure 1. Location map of the Sot catchment

Index map of the Sot catchment is depicted in Figure 2 which shows the area of various tehsils, road network, drainage network and other details falling in the catchment.

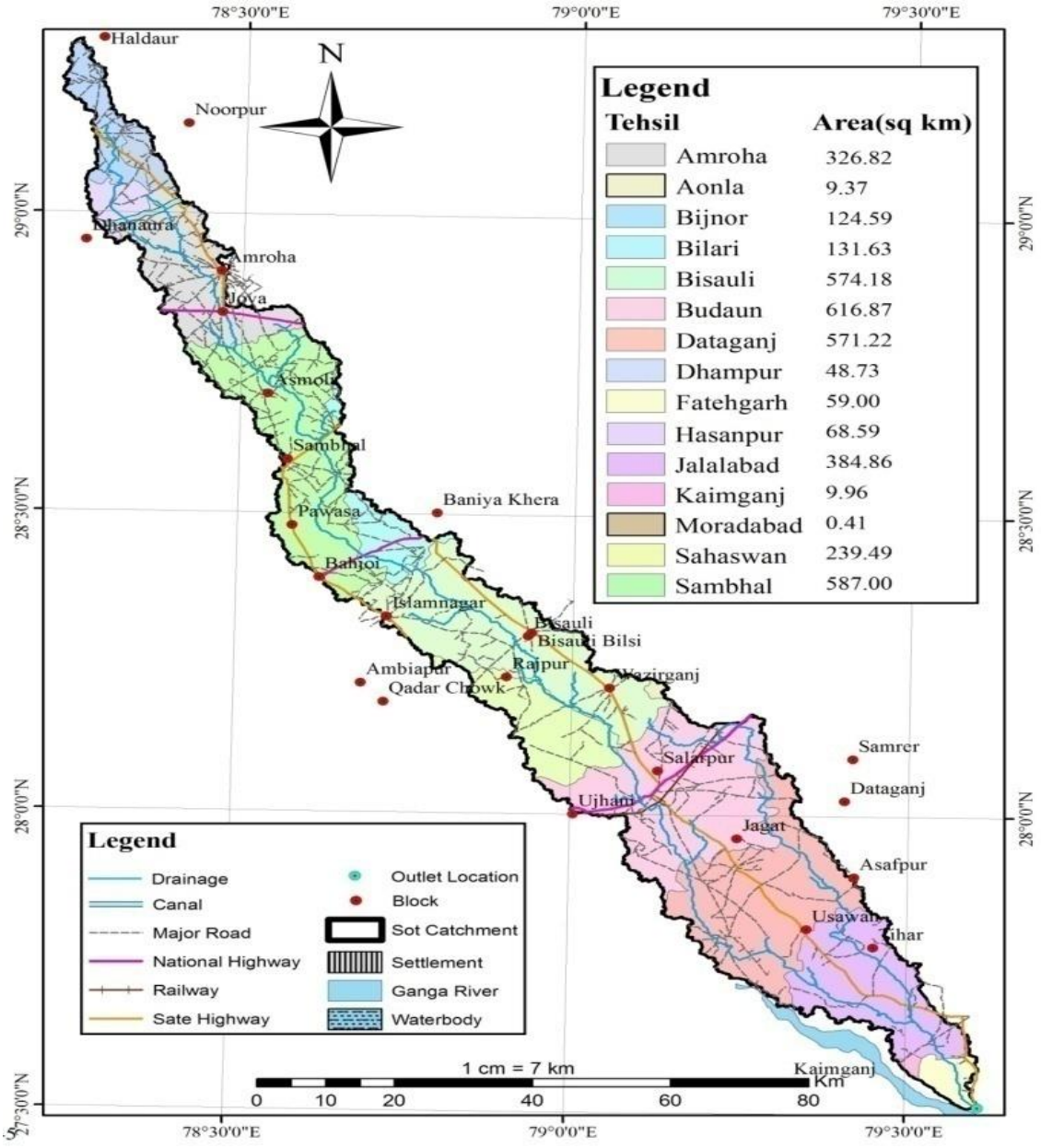

Figure 2. Index map of the Sot catchment

Elevation and drainage network map of the Sot catchment are presented in Figure 3. The elevation of the catchment varies between 138 to 245 m above mean sea level as seen from the Figure 3. Figures 4a and 4b show the 3D map and soil map prepared for the study area. The major soil types in the catchment are silty, clay loam, silt clay and clay.

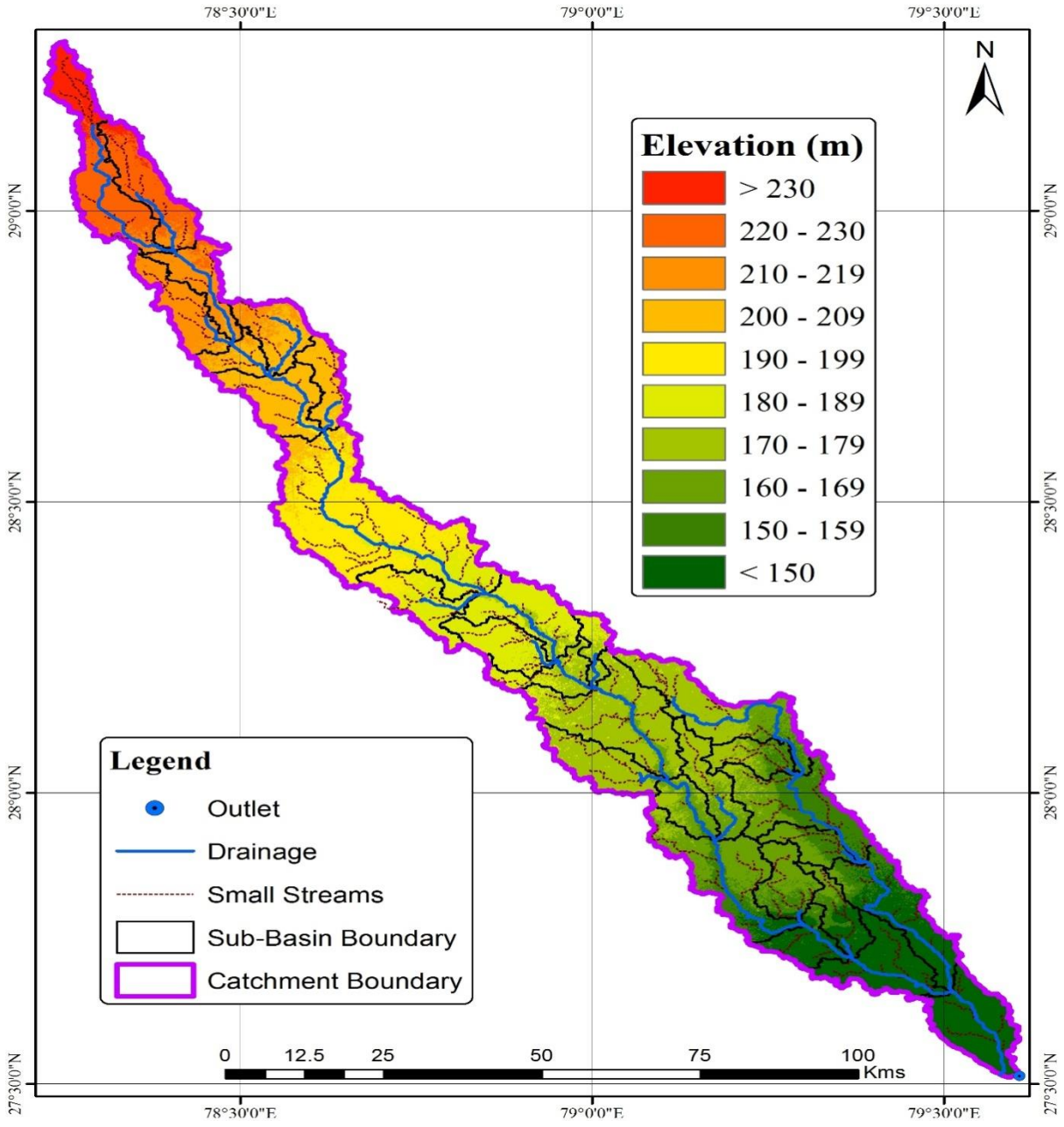

Figure 3. Elevation and drainage network map of the Sot catchment

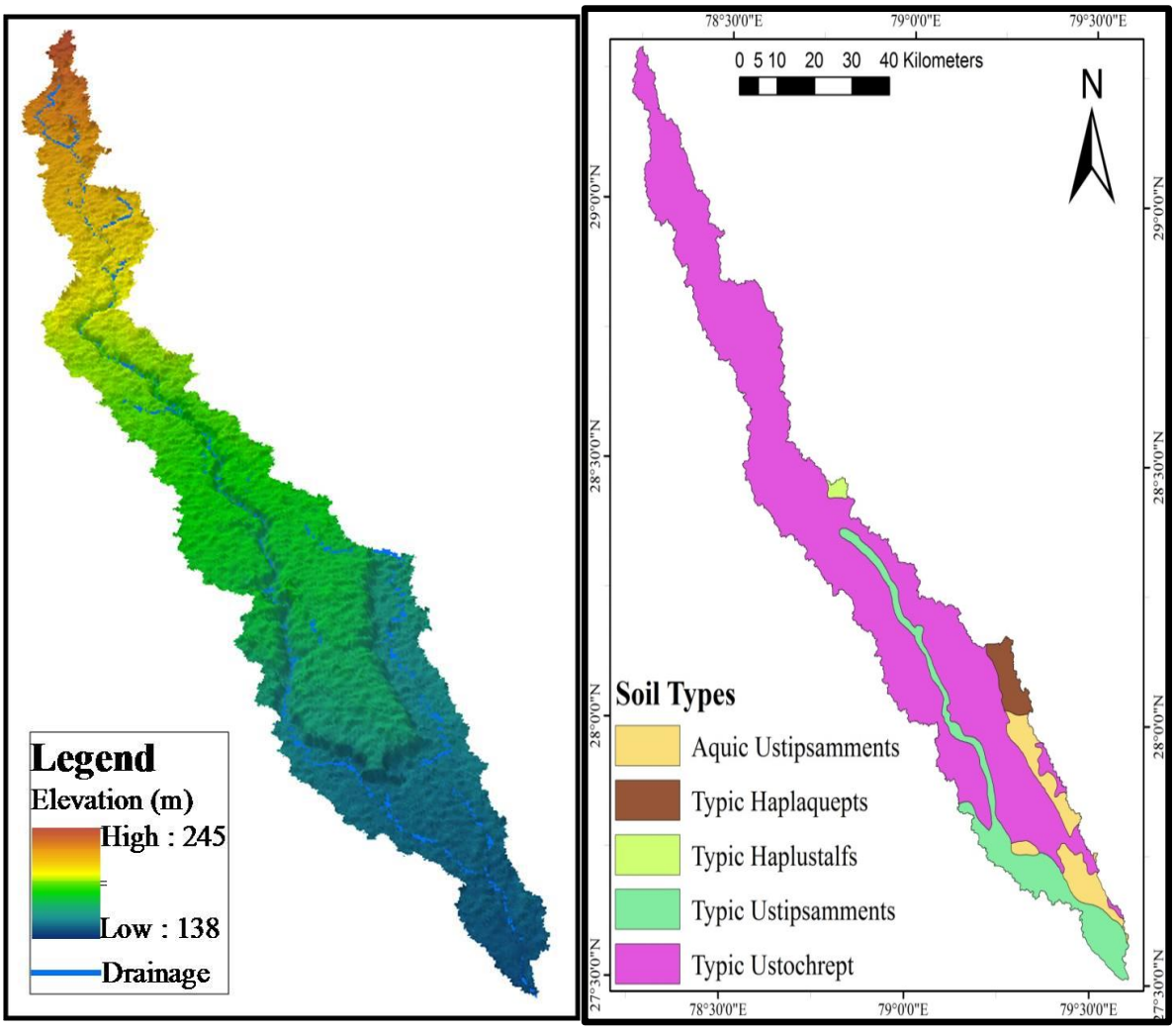

Figure 4(a). 3D map showing the Sot river catchment, and (b) Soil types in the catchment

3.1 Minimum and Maximum Discharge of the Sot River

Variation of minimum and maximum river flow during monsoon and lean season are presented in Figure 5(a) and 5(b), respectively. It is seen from Figure 5(a) and 5(b) that the minimum and maximum river flows during the lean season has drastically reduced after the year 2000. These scenarios shall be studied further along with the variation of precipitation and groundwater withdrawal patterns.

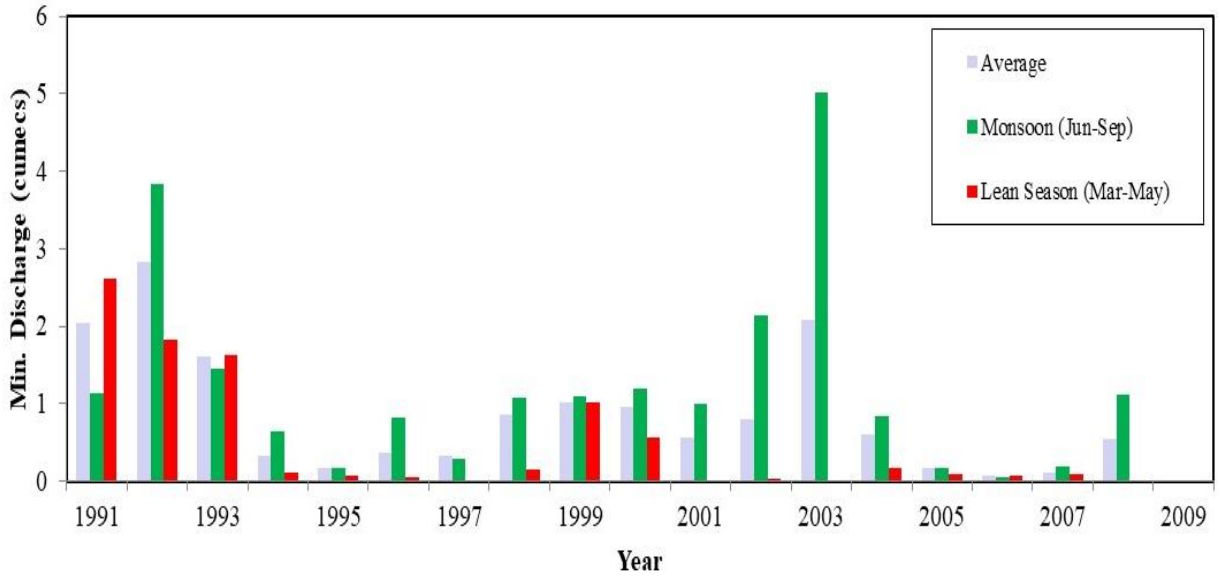

Figure 5a. Variation of minimum river flow during monsoon and lean season

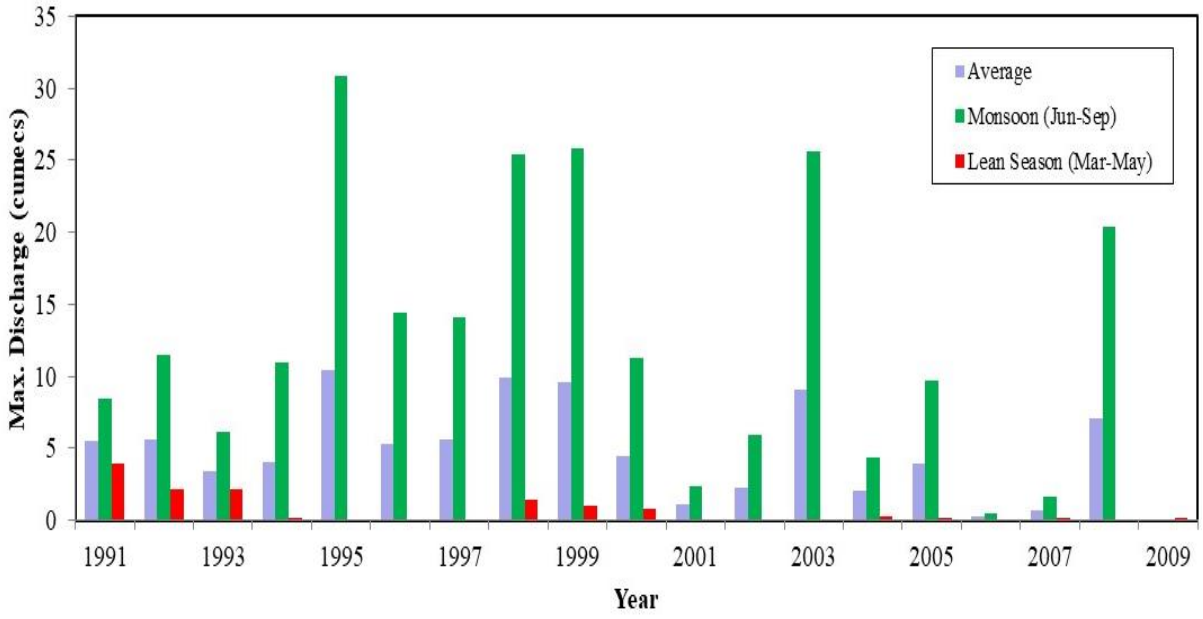

Figure 5b. Variation of maximum river flow during monsoon and lean season

3.2 Rainfall and Temperature Analysis for the Sot River Catchment

Variation of annual, monthly and weekly rainfall is shown in Figures 6 (a, b and c) for the Sot catchment. The annual rainfall varies between 450.50 to 1366.32 mm in the Sot catchment with an average annual rainfall of 881.69 mm, out of which 90% rainfall occurs during the five monsoon months from June to October. Highest amount of rainfall is received in the month of July.

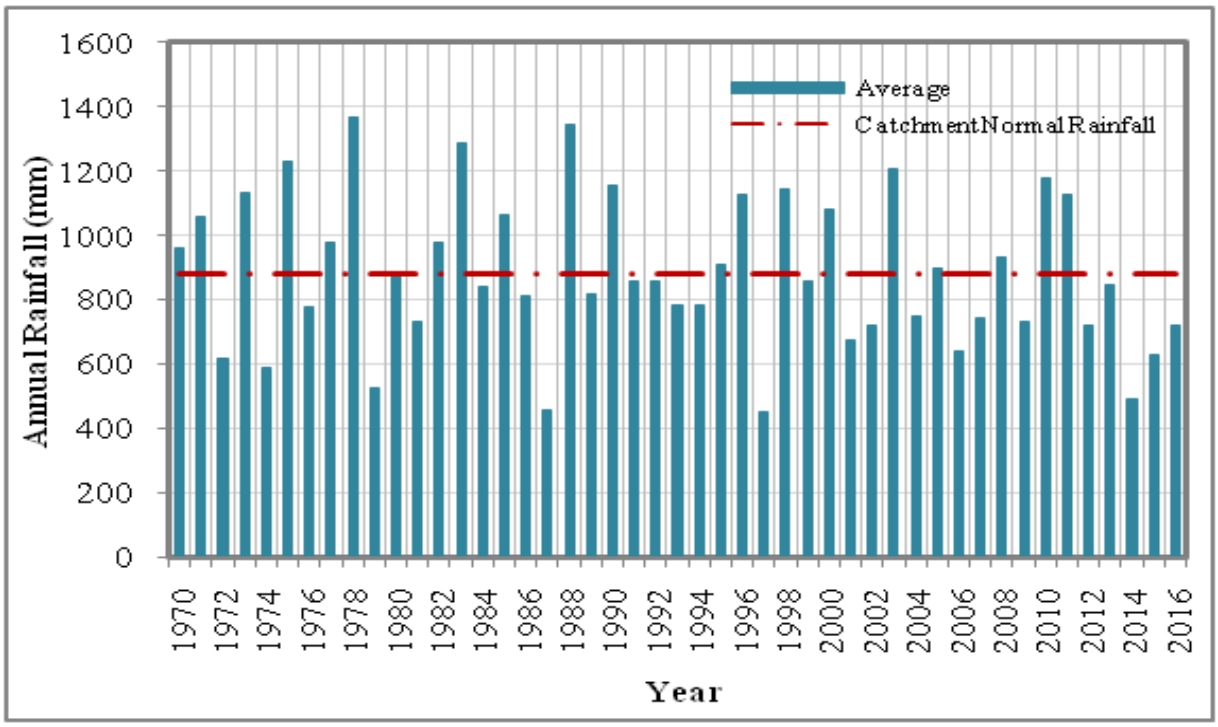

Figure 6a. Annual variation of rainfall

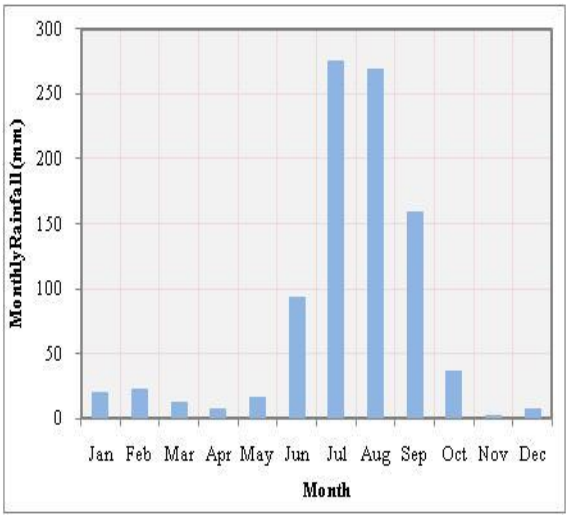

Figure 6b Monthly rainfall variation

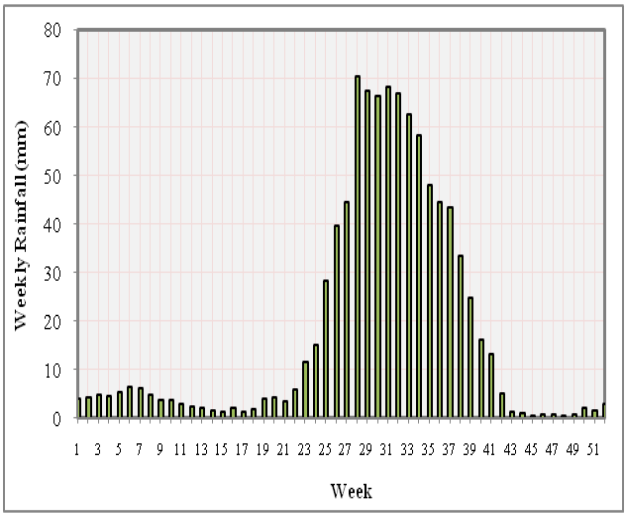

Figure 6c Weekly rainfall variation

Figure 6 Variation of rainfall over the different time periods (annual, monthly and weekly) of the Sot river catchment

Figure 7 shows the spatial variation of the average monthly rainfall in the whole catchment based on the data for the period 1970 to 2016.

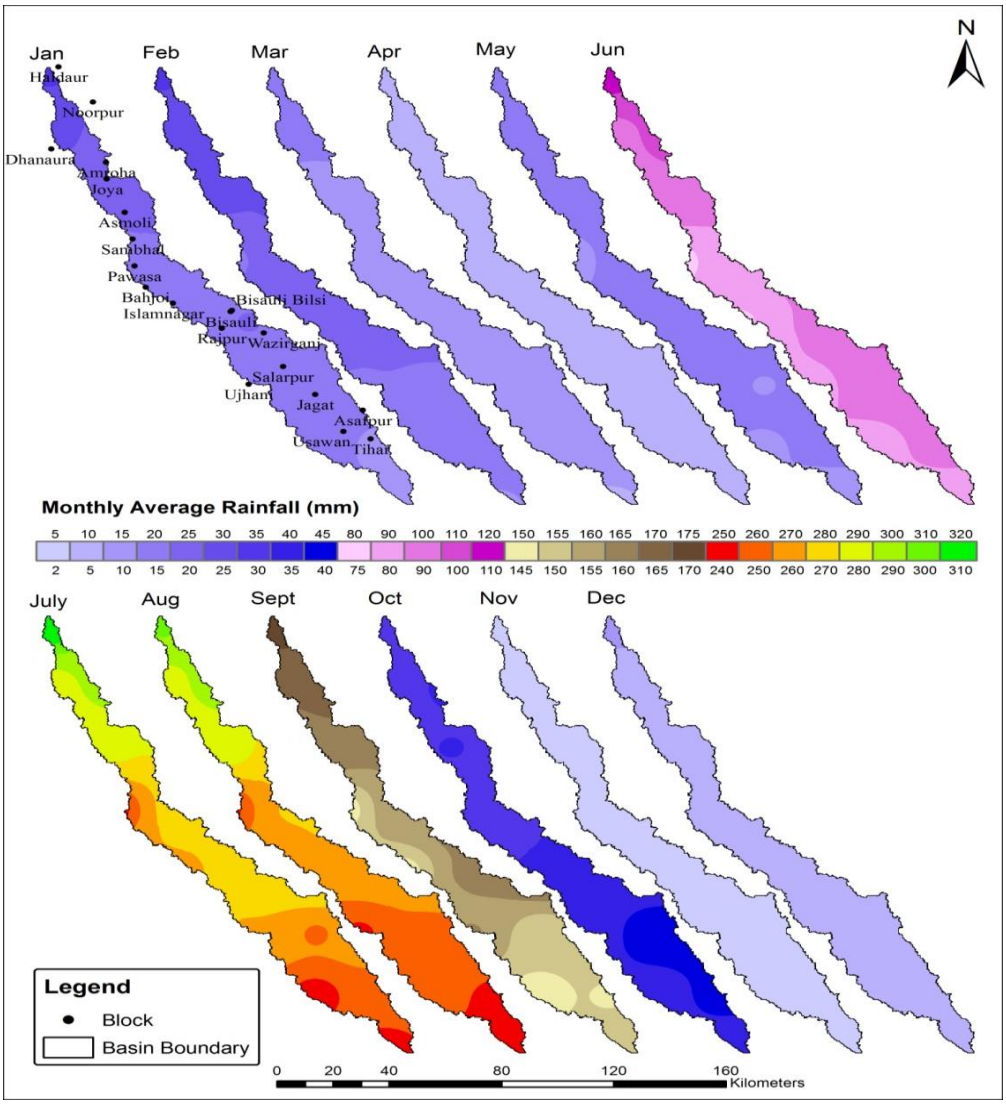

Figure 7. Spatial variation of the average monthly rainfall in the study area

4. DATA COLLECTION AND PROCESSING

The various data collected under the study are given in Table **1**.

Table 1. Data type and period of availability

S. N.	Data	Period
1	Rainfall	1970-2016
2	Temperature (minimum and maximum)	1970-2015
3	River flows	2009-2016
4	Groundwater levels	1998-2017

4.1 Locations of Soil sampling, Infiltration and Conductivity Test Site

A number of field visits were carried-out to monitor the in-situ infiltration rate and hydraulic conductivity of soils in the catchment as well as to collect the soil samples. There are 48 locations where the soils were sampled, and soil infiltration rates and hydraulic conductivity tests were conducted. The locations of these sampling sites are presented in Figure 8.

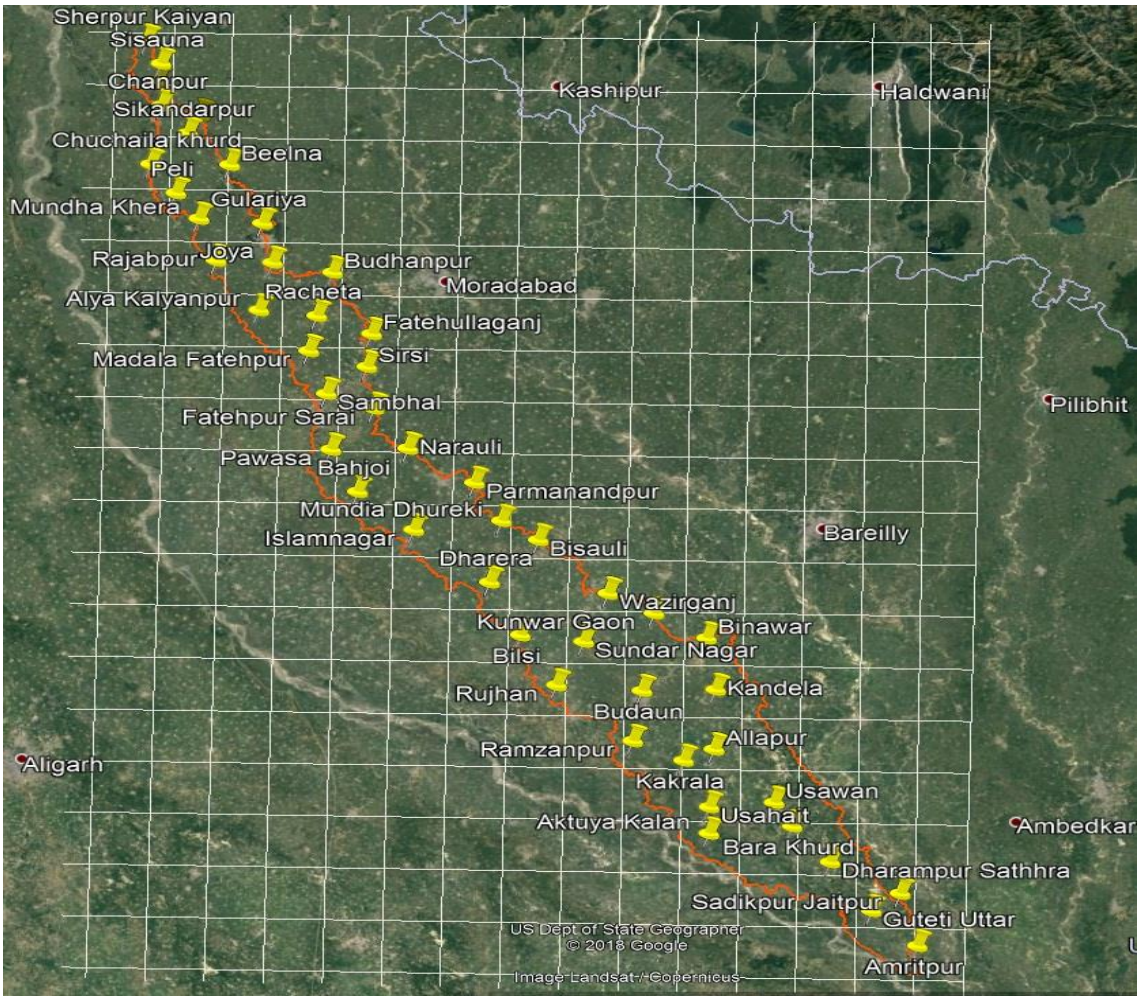

Figure 8. Location of various sampling sites in the Sot catchment

4.2 Infiltration Rates

Infiltration tests were conducted at 48 locations in the entire Sot river catchment using the double ring infiltrometer to estimate the variation in infiltration rate of soil across the catchment. Spatial variation of the infiltration rate in the Sot catchment is presented in Figure 9. It can be seen from the Figure 9 that values of infiltration rate vary between 0.3 to 51.5 cm/hr in the catchment. Major portion of catchment indicates low to moderate infiltration rate.

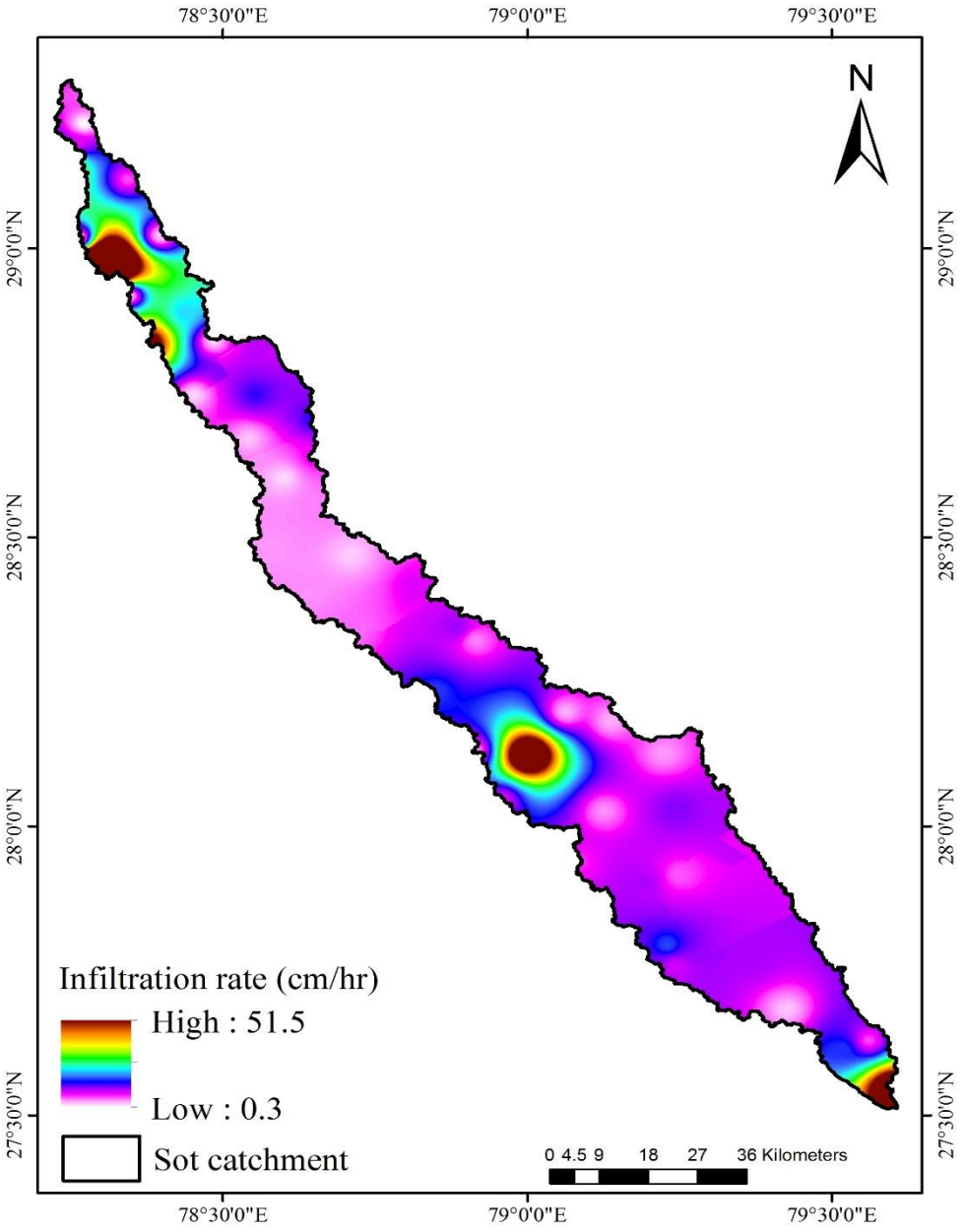

Figure 9. Spatial variation of the infiltration rate in the Sot catchment

4.3 Hydraulic Conductivity

Soil hydraulic conductivity tests were also carried out at 48 locations in the entire catchment using the Guelph permeameter to estimate the variation in soil hydraulic conductivity across the catchment. It is found that the soil hydraulic conductivity in the catchment varies in the range of 5.9×10^{-7} to 2.7×10^{-2} mm/sec (Figure 10). The upper and lower part of the catchment has relatively higher conductivity than the middle part of the catchment.

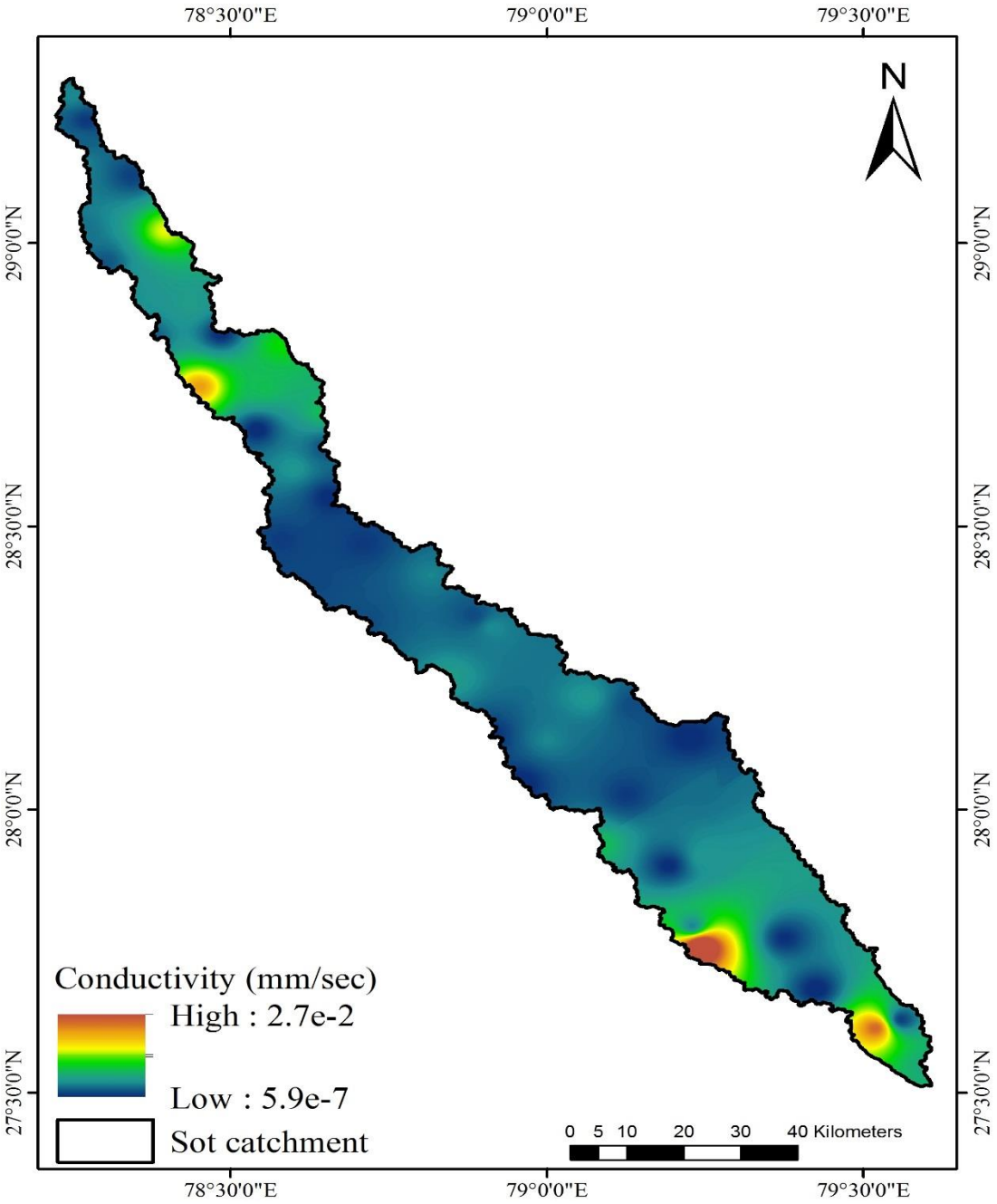

Figure 10. Spatial variation of the hydraulic conductivity in the Sot catchment

4.4 Water Quality sampling and analysis

In order to study the river-aquifer interactions as well as to identify the areas of potential recharge in the Sot catchment, quarterly water sampling is being done at 48 locations. These locations are same as the soil sampling sites as shown in Figure 8. A random distributed sampling method was followed in deciding the location of all these sites. The water sampling shall undergo for both hydro-geochemistry and isotopic analysis of river and groundwater. Few rainwater samples are also being collected. Water sampling was done in the month of March, June, August and September, 2019 at all the 48 locations for water chemistry and isotopic analysis. These samples are under testing in the Water Quality Laboratory, GWQ Lab Annex and Nuclear Hydrology Laboratory of NIH. The water sampling shall be repeated quarterly (pre-monsoon, monsoon, post-monsoon and winter seasons).

4.5 Variation of historical observed rainfall versus river flow data

Variation of historical observed IMD daily rainfall and river flow data for the period of 2009 to 2016 are presented in Figure 11. It is seen from Figure 11 that the rainfall occurs mainly in the monsoon season i.e. (June to October). The daily rainfall varies from 0 to 94.37 mm in the Sot catchment, and the daily river flow data varies from 0 to 12.63 cumecs, respectively. Thus, the river is a monsoonal river having more than 90 per cent rainfall and river flow in monsoon season. The average annual daily rainfall, that occurs during dry season, is 10 mm and at the same time the river flow in the dry season is near to zero or negligible. It may be possible due to high soil infiltration, evaporation or negligible base flow contribution to the Sot river. Figure 11 clearly shows that the river flow data is very complex and non-linear mainly due to the high variation in rainfall data during the dry season to wet season.

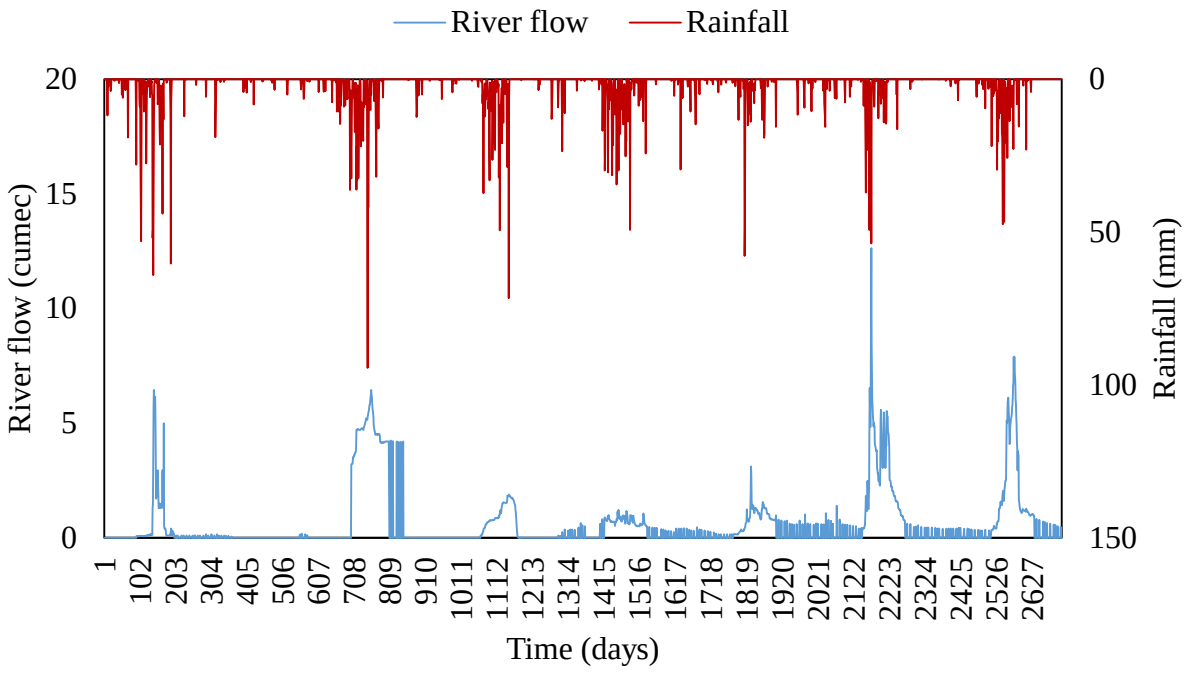

Figure: 11 Variation of daily rainfall and river flow in the Sot river catchment

5. METHODOLOGY

This section presents various methodologies that will be used to accomplish the objectives of the study.

5.1 Checking the presence of trends

In the present study, parametric and non-parametric trend analyses of hydro-meteorological variables are used to find the declining trends in river flows vis-à-vis groundwater levels particularly during the non-monsoon season using Mann-Kendall and Sen-Slope Estimator.

5.1.1 Modified Mann-Kendall (MMK) Test

The Mann-Kendall (MK) test is a rank based non-parametric test for assessing the significance of a trend and has been widely used for trend detection studies. It is based on the test statistic S as defined below:

$$S = \sum_{i=1}^{n-1} \sum_{j=i+1}^{n} \operatorname{sgn}(x_j - x_i) \quad \ldots \quad (1)$$

where, x_1, x_2, … x_n represent n data points, where x_j represents the data point at time j and sign represents the signum function, which returns -1, 0 or 1 depending on whether the difference (x_j-x_i) is negative, zero or positive respectively.

It has been documented that when n ≥10, the statistic S is approximately normally distributed with the mean E (S) = 0 and variance, given by:

$$\mathrm{VAR}(S) = \frac{n(n-1)(2n+5) - \sum_{i=1}^{m} t_i(t_i-1)(2t_i+5)}{18} \quad \ldots \quad (2)$$

where, n is the number of data points, m is the number of tied groups, and t_i is the number of data points in the i^{th} group.

The standardized test statistic Z is computed as follows:

$$Z = \begin{cases} \frac{S-1}{\sqrt{\mathrm{VAR}(S)}} \text{ if } S > 0 \\ 0 \text{ if } S = 0 \\ \frac{S+1}{\sqrt{\mathrm{VAR}\,(S)}} \text{ if } S < 0 \end{cases} \quad \ldots \quad (3)$$

It is well known that the original Mann–Kendall test does not consider the autocorrelation factor that may be present in the time series. The presence of an autocorrelation in a dataset may lead to

inaccurate interpretations of the MK test (Hamed and Rao, 1998; Ehsanzadeh et al., 2011). Hamed and Rao (1998) proposed a Modified Mann Kendall (MMK) test in order to deal with the issue of autocorrelation structures for all lags in a dataset, because autocorrelations may still exist past the first lag. The method proposed by Hamed and Rao (1998) modifies the calculation for the variance of the MK test when the data are serially correlated by using an empirical formula. Thus, MMK test was found to be practically as powerful when applied to auto-correlated data with a large sample size, as the MK test applied to an independent data (Hamed and Rao, 1998).

The calculation of the variance of the test statistics S is altered and given by an empirical formula (equation 4) (Hamed and Rao, 1998):

$$V^*(S) = VAR(S) \cdot \frac{n}{n_s^*} = \frac{n\,(n-1)(2n+5) - \sum_{i=1}^{m} t_i(t_i-1)(2t_i+5)}{18} \cdot \frac{n}{n_s^*} \quad \dots \quad (4)$$

where, n/n_s^*represents a correction due to the autocorrelation in the data. The best approximation to the theoretical values was obtained by using n/n_s^*given by the empirical expression:

$$\frac{n}{n_s^*} = 1 + \frac{2}{n\,(n-1)(n-2)} \times \sum_{i=1}^{n-1}(n-i)(n-i-1)(n-i-2)\rho_s\,(i) \quad \dots \quad (5)$$

where, ρ_s is the serial autocorrelation in the series which is as given by:

$$\rho_s(i) = \frac{\frac{1}{n-i}\sum_{t=i+1}^{n}(x_t - \bar{x})(x_{t-i} - \bar{x})}{\sqrt{\frac{1}{n}\sum_{t=1}^{n}(x_t - \bar{x})}\sqrt{\frac{1}{n}\sum_{t=i+1}^{n}(x_{t-i} - \bar{x})}} \quad \dots \quad (6)$$

Autocorrelation, significant in the time series at the 95% confidence level, was used for evaluating the modified variance of S using equations (4) and (5).

5.1.2 Sen's slope estimator

The slope of the data set can be estimated using the Sen's slope estimator. This equation is used instead of a linear regression because it has limited influence of the outliers on the slope (Hirsch et al. 1982).

$$\beta = Median\left[\frac{X_j - X_i}{j-i}\right] \quad For\ all\ i < j \quad \dots \quad (7)$$

where, X_j and X_i are data values at times j and i (i > j), respectively.

$$Intercept = Median\,[X(i) - \beta \times i] \quad For\ \ i = 1\ to\ n \quad \dots \quad (8)$$

To compute the relative change of different climatic parameters, the following equation was used (Some'e et al. 2012):

$$RC = \frac{n*\beta}{|x|} * 100 \quad \ldots \quad (9)$$

where, n is the length of trend period (years), β is the magnitude of the trend slope of the time series which is determined by Sen's median estimator, and |x| is the absolute average value of the time series.

Further, in the study aquifers will be delineated. Making use of bore logs and geological cross-sections, fence diagrams and a 3D model will be developed in the Rockworks Software.

Soil Water Assessment Tool (SWAT) will be used for hydrological modeling.

5.2 Data Limitation and Estimation of Historical River Flow

The daily river flow data for the Sot river catchment was available from 2009 to 2016 for the GD site at Budaun. Therefore, the river flow needs to be estimated for the historical period for the period 1980 to 2008. In order to model the river flow, ANN, SWAT and NAM models are being used. ANN model has been calibrated and validated for the period 2009 to 2014 and 2015 to 2016, respectively by using MATLAB (R2013a) with compatible nntool. SWAT model is also being setup to model the river flow in various reaches of the catchment. NAM model is being used to extend the river flow series for the historical period.

5.2.1 Artificial Neural Network model for river flow prediction

ANNs are mathematical models with a highly interconnected structure inspired by the structure of the human brain and nervous systems. ANN processes operate in parallel, which differentiates them from conventional computational methods. An ANN consists of a number of neurons that are arranged in an input layer, an output layer, and one or more hidden layers. The input neurons receive and process the input signals and send the output to other neurons in the network where this process is continued. These processes are carried out in a forward manner hence the term multi-layer feed-forward model is used. In a feed-forward network, the weighted connections feed activations only in the forward direction from an input layer to output layer. Training of a neural network to perform particular function is done by adjusting the values of connections (weights) between elements. It is well known that the relationship of rainfall and river flow is known to be highly non-linear and complex. Therefore, it is extremely necessary to evaluate the performance

of ANN model for modeling river flow by utilizing different input parameters such as daily rainfall, lag one or two daily rainfall, and lag one daily river flow.

5.2.2 Data Used for ANN modeling

For this study, continuous river flow time series were available from the period 2009 to 2016, which was collected from the Water Resources Department, Bareilly, UP. Further, rainfall data for the same period (2009 to 2016) were obtained from Indian Meteorological Department, Pune, India. First six years (2009 to 2014) of the obtained records of the daily river flow data was used to calibrate the ANN model while the remaining two years (2015-2016) of the observed river flow records were used for verification of the ANN models.

5.2.3 ANN Architecture

In this study, multilayer feed forward neural network was used in combination with back-propagation training algorithm, namely, the BP neural network. The idea of the back propagation algorithm was to reduce this error, until the ANN learns the training data. The training begins with random weights, and the goal was to adjust them so that, the error was minimum. A schematic representation of artificial neuron and multilayer feed forward model is depicted in Figure 12(a) and 12(b).

The architecture of neural network consists of one to four input parameters such as rainfall (P_t), lag 1 rainfall (P_{t-1}), lag 2 rainfall (P_{t-2}), and lag 1 river flow (Q_{t-1}), one hidden layer and one output parameter (Q_t). In order to optimize the best ANN architecture, trial and error procedure was adopted with different architectural configurations. In the trial and error procedure, the number of hidden neurons was varied from 1 to 10. The combinations of input parameters are presented in Table 2 for river modeling of Sot river. The numbers of models developed for river flow prediction for Sot river were four on the basis of different combination of input parameters.

(a) Architecture of an artificial neuron

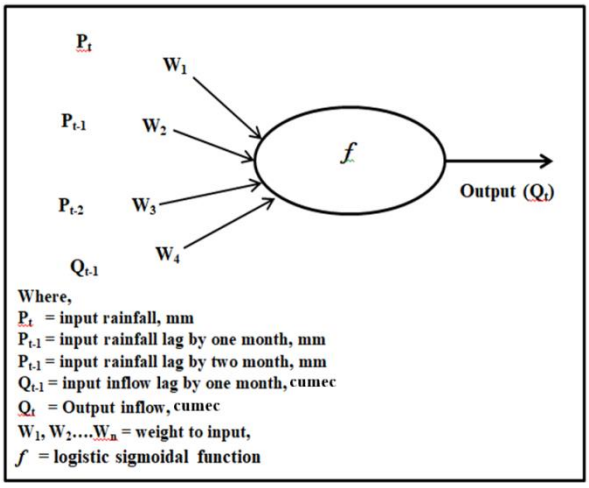

(b) Architecture of multilayer feed forward neural network

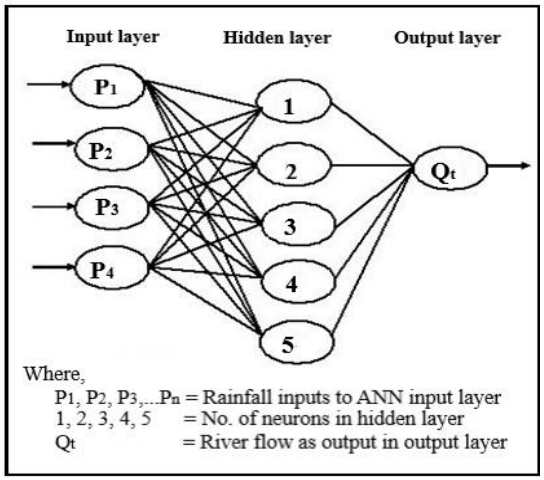

Figure: 12 Architecture of artificial neuron and multilayer feed forward neural network

Table: 2 ANN structure of different model of Sot river

Model No.	Model Descriptions	No. of input parameters	No of Hidden layers	Output layer
1.	$Q_t = P_t$	1	1	1
2.	$Q_t = P_t, P_{t-1}$	2	1	1
3.	$Q_t = P_t, P_{t-1}, P_{t-2}$	3	1	1
4.	$Q_t = P_t, P_{t-1}, P_{t-2}, Q_{t-1}$	4	1	1

P_t – rainfall, mm, P_{t-1} – lag one rainfall, mm, P_{t-2} – lag two rainfall, mm, Q_t – River flow, cumec, Q_{t-1} – lag one River flow, cumec.

5.2.4 Activation function

The transfer function of a neuron in a neural network is only processing function. It is utilized for the limiting the amplitude of the output of a neuron. This transfer function is commonly used in the hidden layers of multilayer, ANN networks, as given in Figure 13 and it is represented by Eq. 10. The symbol in the square to the right of each transfer function graph shown above represents the associated transfer function. These icons replace the general f in the network diagram blocks to show the particular transfer function being used. The mathematical expression of the logistic sigmoid function is given by Eq. (10).

$$f(\alpha) = \frac{1}{1 + e^{-\alpha}} \qquad \ldots(10)$$

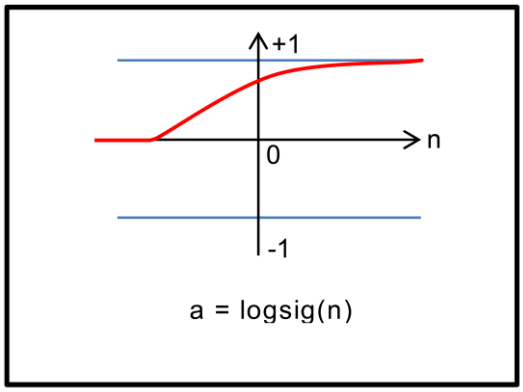

Fig. 13 Log sigmoid transfer function

5.2.4 Procedure for ANN Model Operation

The procedure was adopted to run the ANN in Matlab (R2014) software as depicted in flowchart (Figure 14). The program was written to modify the existing nntool model, to make it compatible as per requirement. The input and target files were prepared in Met text file format. The different inputs were selected to execute the program for training data (75 per cent), validation (25 per cent) data set, by selecting the training algorithm trainlm (feed foreword Back-propagation algorithm) and sigmoid function was used to operate the model. In the ANN model epochs were set up to 1000 iterations. Model training was carried out by using Levenberge Marquadt algorithm and performance was checked by using R and mean square error (MSE). The data was divided on random basis while add an input and output in neural network toolbox in Matlab (R2014) for training of the network to automatically stops whenever recommended output reached with least errors. After the training of ANN, it gives output in the form of performance plot, training state plot, fit plot and regression plot. These plots were used for finding best ANN architecture for the estimation of river flow. The model tries by changing number of neuron in hidden layers and changing the hidden layer and neurons simultaneously. This procedure was repeated until the expected results not achieved in terms of R and MSE. The model with R approaching to 1 and MSE approached to 0 indicating the performance of the model as best. And on these criteria models were selected for validation of models. The model with different inputs and best value of R and MSE was selected for statistical performance check and to adopt the model for output estimation, as to be observed as best model.

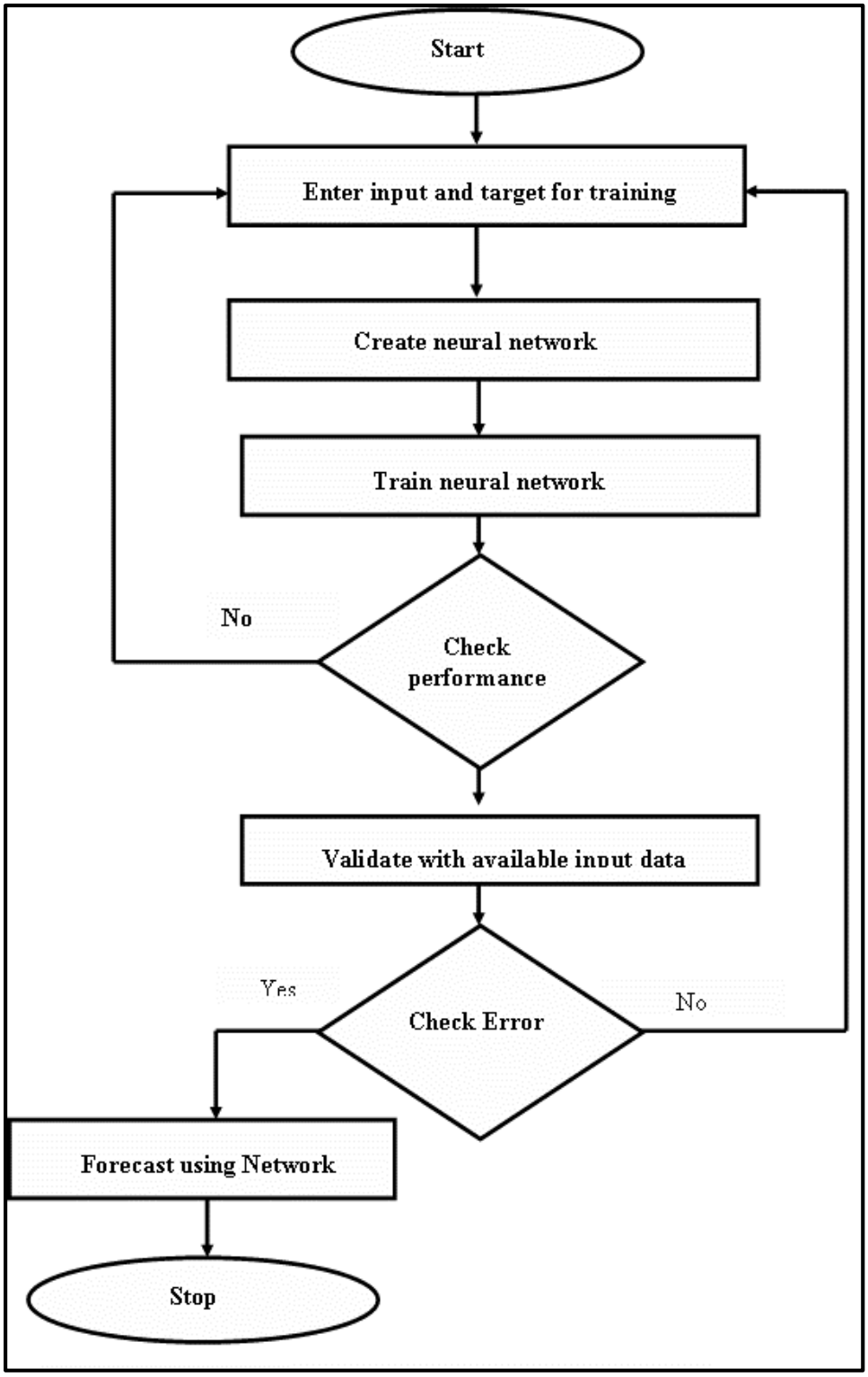

Figure 14 Flowchart illustrating step-by-step procedure of ANN modeling

5.2.5 Statistical Performance Evaluation Indices of ANN Model

The statistical performance indices of different ANN model were evaluated and compared with the observed monthly river flow during the calibration and validation period. These statistical goodness-of-fit measures include correlation coefficient (R) (Butts et al., 2004), root mean square error (RMSE) (Wang et al., 2009), modified Nash-Sutcliffe efficiency (MNSE) (Legates and McCabe, 1999) and Modified Index of Agreement (MIA) (Willmott et al., 1985). These performance evaluation indices are described below

5.3 Stream flow Simulation Using Soil and Water Assessment Tool (SWAT) Model

5.3.1 ArcSWAT model

In this study, the ArcGIS 10.4 interface of SWAT (version 2012) was utilized for hydrological modeling, which is popularly known as ArcSWAT. Soil water assessment tool (SWAT) is a physically based, spatially distributed and continuous-time-step hydrologic model used to simulate the impacts of different land use and land management practices and climate change on hydrology and water quality of a watershed. It is free software and was developed at the USDA-ARS during the early1970's. The hydrological component simulated by ArcSWAT is generally based on the principle of water balance equation, which is mathematically expressed as follows:

$$SW_{t_i} = SW_o + \sum_{i=1}^{t}(R_{day_i} - Q_{surf_i} - E_{a_i} - W_{seep_i} - Q_{gw_i}) \quad \ldots(11)$$

where SW_{t_i} is the soil water content (mm) at time t, SW_o the initial soil water content (mm), t the simulation period (days), R_{day_i} the amount of precipitation on the i^{th} day (mm), Q_{surf_i} the amount of surface river flow on the i^{th} day (mm), E_{a_i} the amount of evapotranspiration on the i^{th} day (mm), W_{seep_i} the amount of water entering the vadose zone from the soil profile on the i^{th} day (mm) and Q_{gw_i} the amount of base flow on the i^{th} day (mm)**.**

5.3.2 Data Preparation and Pre-processing

The input data required for SWAT modeling are Digital Elevation Model (DEM), soil type, land use/land cover (LULC) map and meteorological data. The input forcing data required for SWAT modelling can be broadly classified into two categories: 1) spatial data, and 2) temporal data. The details of spatial and temporal data, procured from different organizations, are given in Table 3.

This data was pre-processed for preparing the input data, which was further used for ArcSWAT model building.

Table 3. Details of input data used for the SWAT model and their sources

Sr. No.	Data Type	Information	Scale/Time Period	Source
A.	**Spatial Data**			
1	Digital elevation model	Raster, 90 m-resolution	-	SRTM DEM, USGS
2	Landsat 8 satellite images used to create LULC Map	Raster, 30 m-resolution	2015	USGS Earth explorer
3	Soil Map	-	1 : 500 000	HWSD, FAO, United Nations
B.	**Temporal data**			
4	Rainfall	Daily	2006-2018	IMD, New Delhi
5	Temperature	Daily	2006-2018	IMD, New Delhi
6	River flow	Daily	2009-2018	Irrigation Department, Bareilly District, UP

5.3.2.1 Digital Elevation Model

DEM file, downloaded from SRTM (Shuttle Radar Topography Mission) at 90 m × 90 m resolution is projected to coordinated system (WGS 1984 UTM Zone 43 N). The DEM is used to define the topography of study area that describes the elevation of any point in a catchment at a specific spatial resolution. It is also used to delineate the network of river streams, sub-basins, and parameters like slopes for HRUs. DEM map of Sot catchment is presented in Fig. 15.

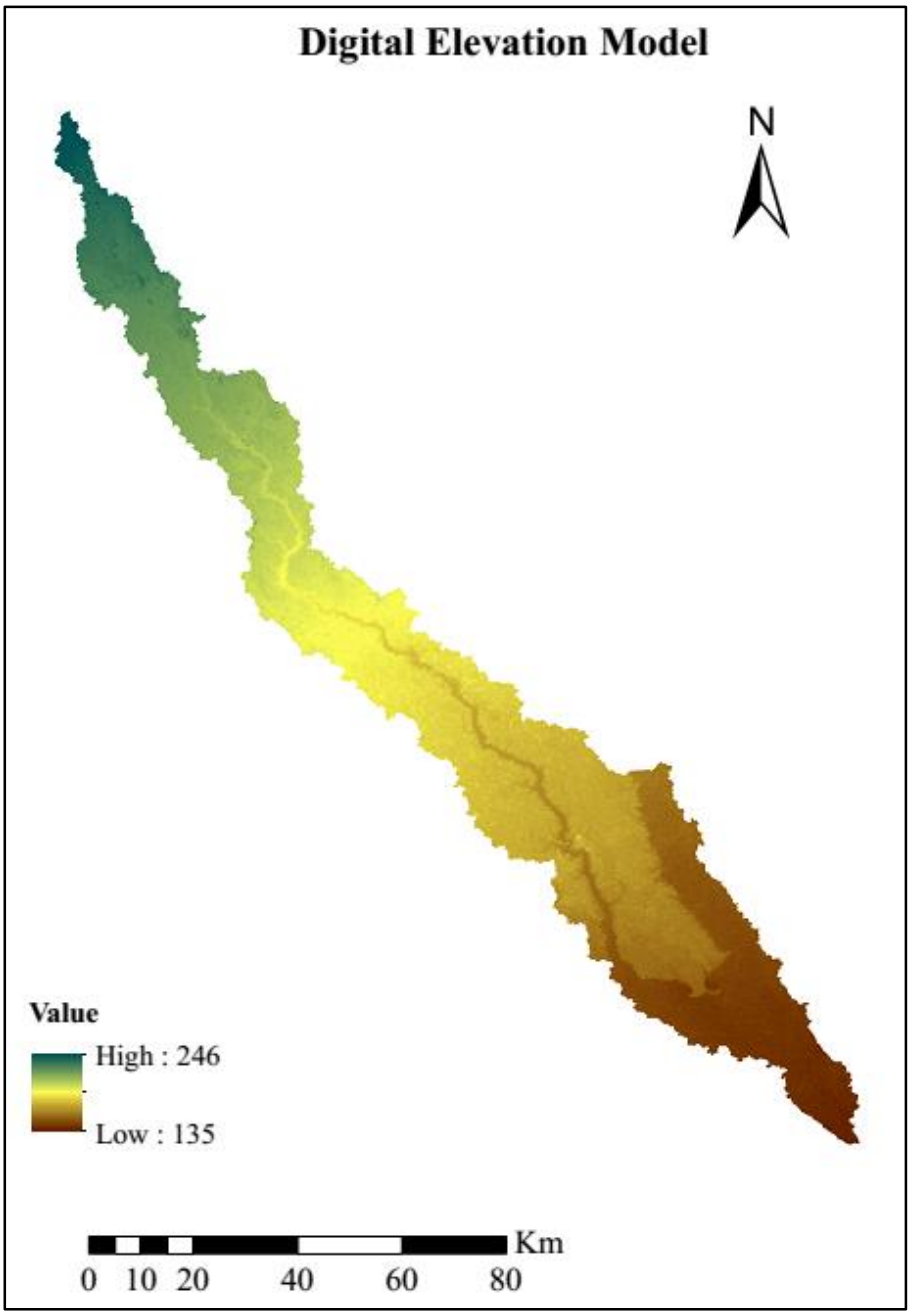

Fig. 15 Digital elevation model of Sot catchment

5.3.2.2 Land Use/Land Cover

For preparing LULC, three satellite imageries were downloaded from the USGS Earth Explorer at 30 m resolution. These images were processed and image classification was performed by using ENVI tool. These satellite images comprised of multiple bands which together form an image. There are mainly two types of image classification techniques: supervised and unsupervised. In this study, supervised classification was used. In this technique, the software is guided by the

researcher in specifying the land cover classes of interest as a signature dataset, which is then automatically used by the software to create the spectral classes. LULC is mainly used to define the factors that affect runoff, evapotranspiration and surface erosion in a watershed. The LULC map of the Sot catchment, for the year 2015, is shown in Fig. 16.

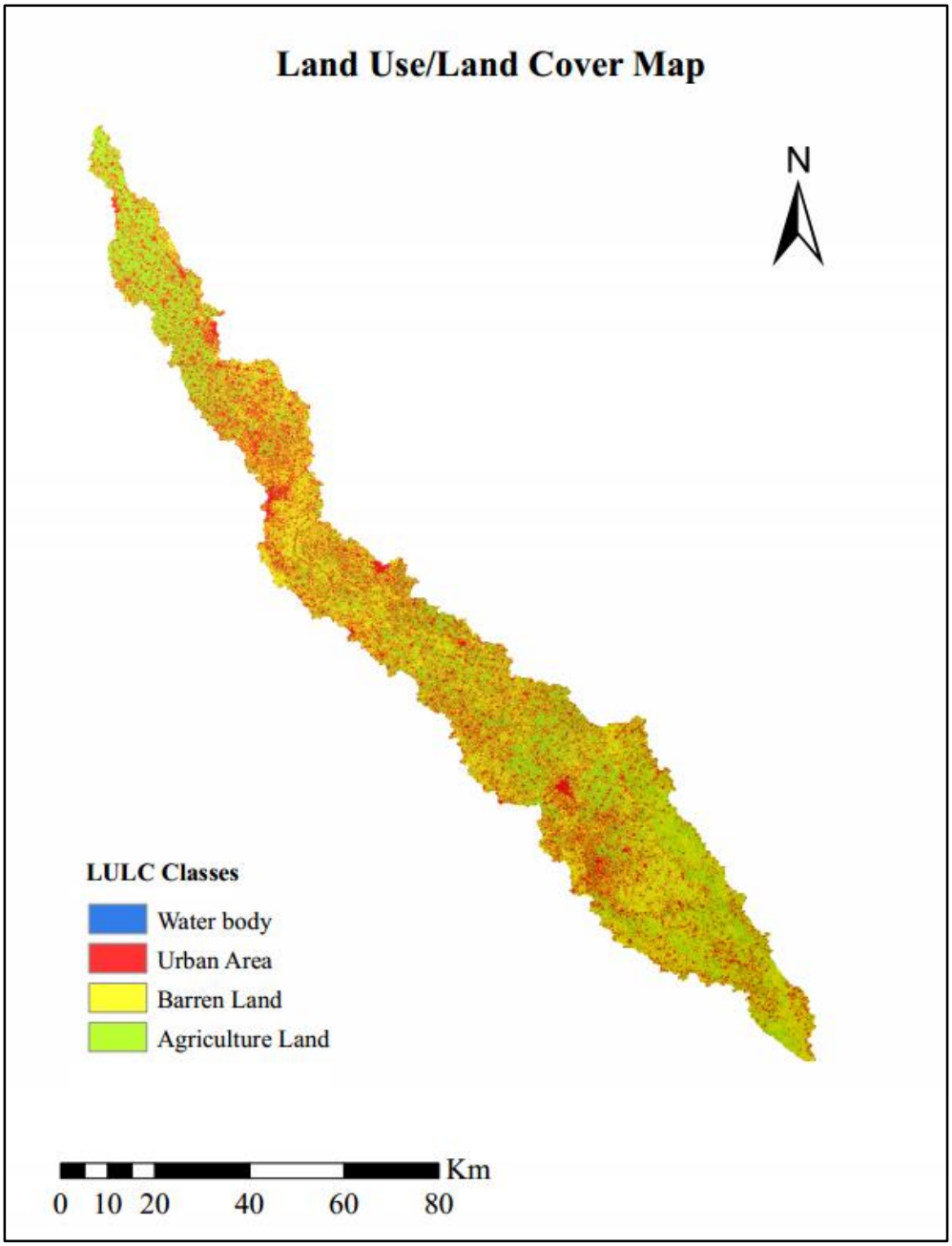

Fig. 16 Land use land cover map of Sot catchment

5.3.2.3 Soil Map

The soil map with spatial resolution of 1:500 000 was obtained from the Food and Agricultural Organization (FAO), United Nations. Soil data of Sot catchment is mainly divided into two different soil groups. It was observed that clay soil is covering more than 90 % area of Sot catchment. The soil map of the Sot catchment is presented in Fig. 17.

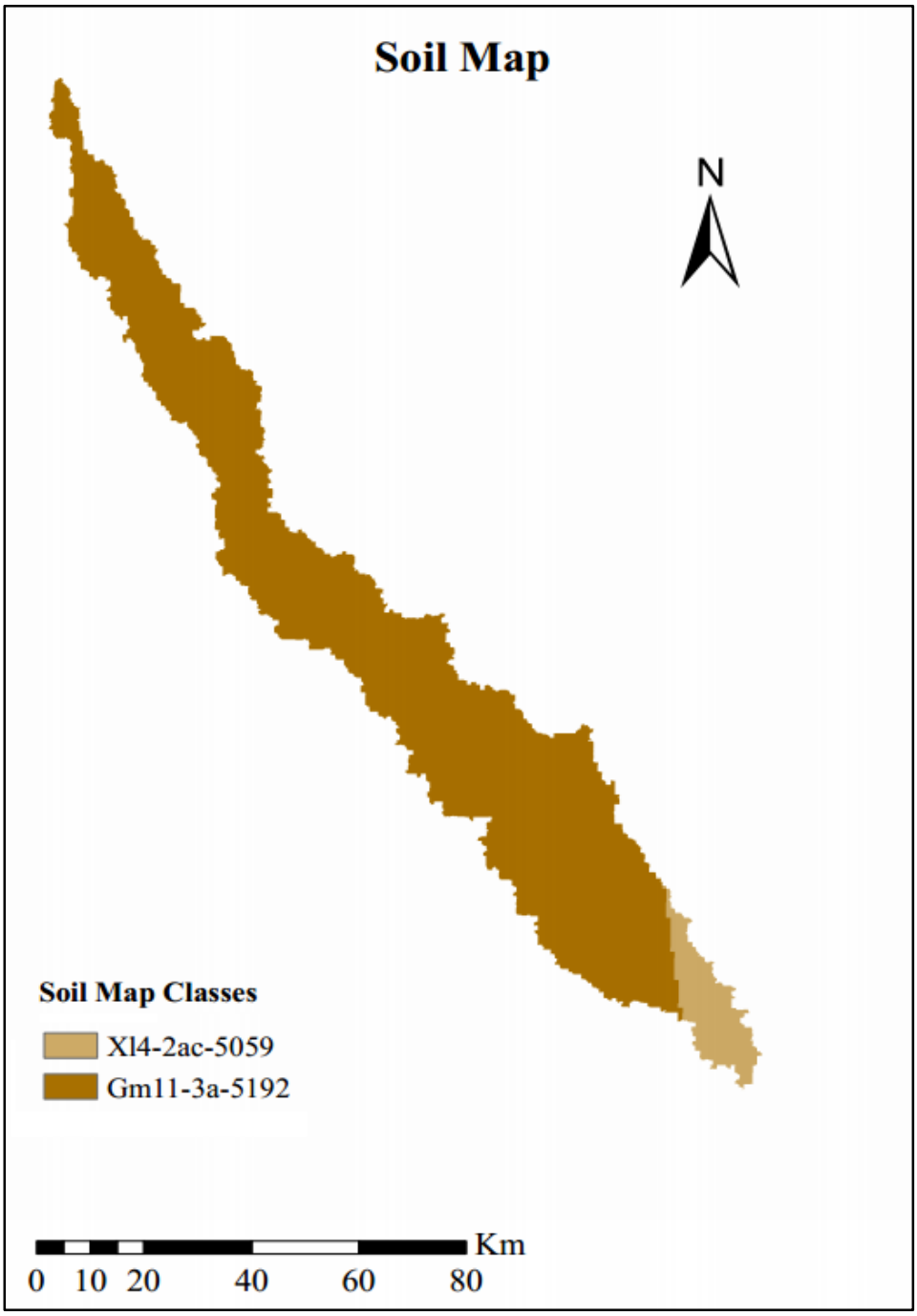

Fig. 17. Soil map of Sot catchment

5.3.3 Model Setup

Watershed delineation is the first step of model setup. DEM data was used as an input to delineate the watershed in several hydrologically connected sub-watersheds. The next step in model setup is the Hydrological Response Units (HRU) analysis. HRUs are the unique combination of land cover, soil type and topographic slope which represent the characteristics of the sub-basins. The SWAT divided the watershed into 29 sub-watersheds and 90 HRUs. Fig. 18 shows the delineated watershed, sub-basins, reach and main outlet of the Sot catchment. After delineating the watershed and defining the HRUs, the surface runoff was calculated using the curve number method.

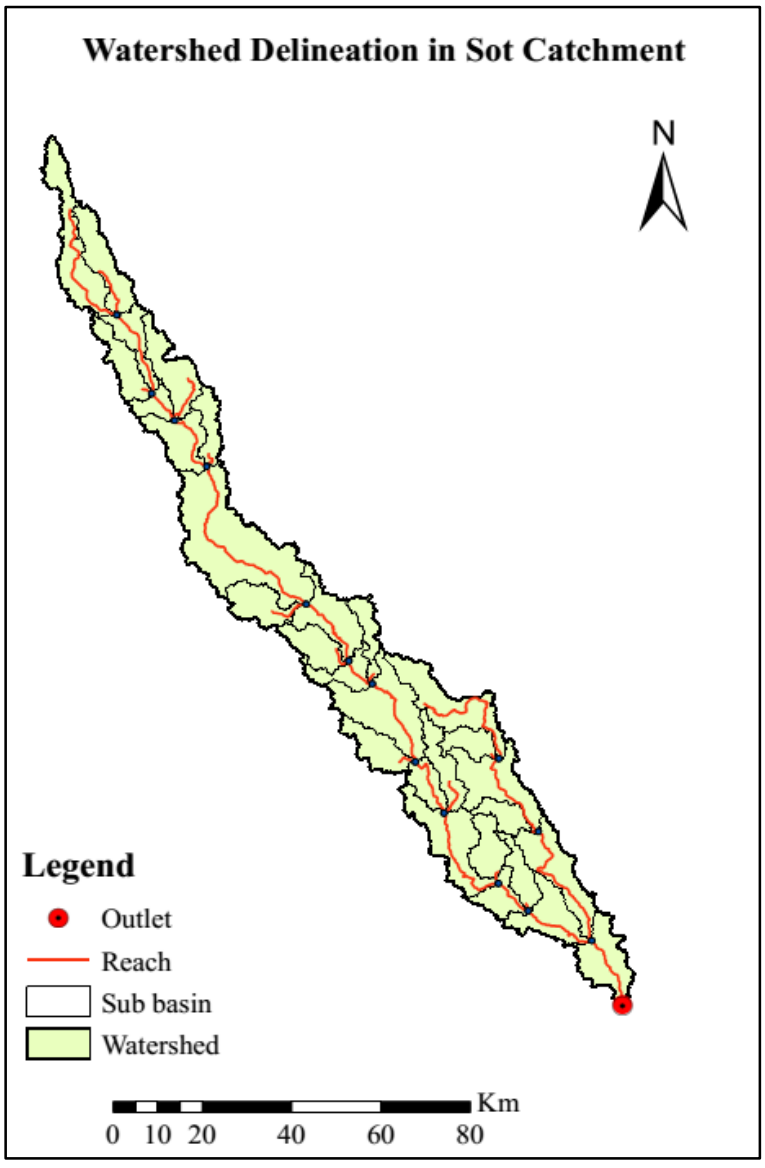

Fig. 18 Watershed Delineation of Sot Catchment

5.3.4 Sensitivity analysis

Sensitivity analysis is conducted to identify the parameters that are important for accurate results. It facilitates understanding the behaviors of the system being modeled, as well as evaluating the applicability of the model. SWAT-CUP, an automatic calibration tool, used the multiple regression analysis equation to find out the most sensitive parameters. Afterwards, the Student's t-distribution test was applied to get the statistic value (p-value) of each parameter. The smaller the p-value i.e. <0.05, the more sensitive and significant the parameter is.

5.3.5 SWAT Calibration and Validation

The calibration of SWAT model can be performed by using two techniques: conventional trial-and-error method and auto-calibration technique. SWAT-CUP (SWAT Calibration and Uncertainty Procedures), a computer programme was used for sensitivity analysis, calibration, validation and uncertainty analysis of SWAT models. The program is linked with many algorithms such as SUFI-2 (sequential uncertainty fitting algorithm), PSO (Particle Swarm Optimization), MCMC (Markov Chain Monte Carlo), GLUE (Generalized Likelihood Uncertainty Estimation), and Parasol (Parameter Solution) procedures to SWAT. The SUFI-2 algorithm was employed to perform calibration and validation of river flow data set. Calibration is the modification of parameters influencing the SWAT yields, which is very essential for the proper hydrological modeling. Validation of the SWAT model compares the results obtained from SWAT without modifying the values of the parameters. After completing the initial building of SWAT model and uploading the rainfall and temperature data, the next step is the calibration and validation of model. In this study, first six years (2009 to 2014) of the monthly river flow data was used to calibrate the SWAT model while the remaining four years (2015-2018) of the observed river flow data was used for validation. Monthly variation in river flow data for the period of Jan, 2009 to Dec, 2018 is presented in Fig 19. There are many parameters which can be used for the calibration purpose.

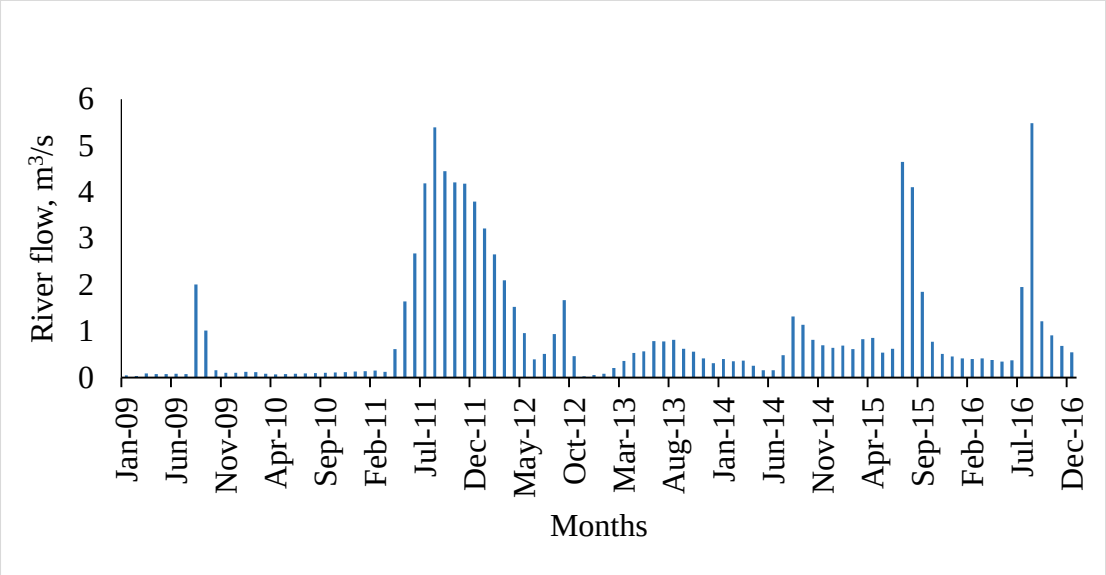

Fig. 19 Monthly variation of river flow data (2009-2016)

Table 4 Parameters used for calibration with their minimum and maximum values

Sr. No.	Parameter name	Description	Minimum	Maximum
1	CN2	SCS runoff curve number	-0.2	0.2
2	GW_DELAY	Groundwater delay (d)	0	500
3	GWQMN	Threshold depth of water in the shallow aquifer required for return flow to occur (mm)	0	2
4	ALPHA_BF	Base flow alpha factor	0	1
5	SOL_AWC	Available water capacity of the soil layer	-0.2	0.2
6	SOL_K	Saturated hydraulic Conductivity	-0.2	0.2
7	CH_N2	Manning's n value for the main channel	-0.01	0.3
8	CH_K2	Effective hydraulic conductivity in main channel alluvium	-0.01	500

5.3.6 Statistical Performance Evaluation Indices of SWAT Model

The statistical performance indices of different ANN model were evaluated and compared with the observed monthly river flow during the calibration and validation period. These statistical goodness-of-fit measures include correlation coefficient (R) (Butts et al., 2004), root mean square error (RMSE) (Wang et al., 2009), modified Nash-Sutcliffe efficiency (MNSE) (Legates and McCabe, 1999) and Modified Index of Agreement (MIA) (Willmott et al., 1985). These performance evaluation indices are described below.

5.4 Groundwater Modelling using MODFLOW

5.4.1 General

The MODFLOW - a three-dimensional finite-difference flow model developed by USGS (Harbaugh, and McDonald, 1996; Harbaugh, 2005) - has a modular structure that allows to simulate steady and non-steady flow in an irregularly shaped flow system in which aquifer layers can be confined, unconfined, or a combination of confined and unconfined. Flow from external stresses, such as flow to wells, areal recharge, evapotranspiration, flow to drains, and flow through river beds, can be simulated. The governing partial differential equation for a confined aquifer used in the MODFLOW is as follows:

$$\frac{\partial}{\partial x}\left[K_{xx}\frac{\partial h}{\partial x}\right]+\frac{\partial}{\partial y}\left[K_{yy}\frac{\partial h}{\partial y}\right]+\frac{\partial}{\partial z}\left[K_{zz}\frac{\partial h}{\partial z}\right]+W=S_S\frac{\partial h}{\partial t} \quad \ldots \quad (12)$$

Where, K_{xx}, K_{yy} and K_{zz} are the values of hydraulic conductivities along the *x*, *y*, and *z* coordinate axes (L/T); *h* is the potentiometric head, (L); *W* is a volumetric flux per unit volume representing sources and/or sinks of water, where *negative* values are extractions and *positive* values are injections, (T^{-1}); S_s is the specific storage of the porous material (L^{-1}); and *t* is time (T).

Groundwater modelling using the MODFLOW is to develop a predictive model using the recharge to study the responses of the groundwater system and to determine responses of the aquifers for various management strategies.

In mathematical terms, the algebraic equation on discrete finite difference form in terms of potential head of water as solved by the MODFLOW (Harbaugh, and McDonald, 1996) is given by:

$$KZ_{i,j,k-\frac{1}{2}}\,h^m_{i,j,k-1}\,KX_{i-\frac{1}{2},j,k}h^m_{i-1,j,k}+KY_{i,j-\frac{1}{2},k}h^m_{i,j-1,k}$$
$$+\left(-KZ_{i,j,k-\frac{1}{2}}-KX_{i-\frac{1}{2},j,k}-KY_{i,j-\frac{1}{2},k}-KY_{i,j+\frac{1}{2},k}-KX_{i+\frac{1}{2},j,k}-KZ_{i,j,k+\frac{1}{2}}+\right.$$
$$\left.HCOF_{i,j,k}\right)h^m_{i,j,k}+KY_{i,j+\frac{1}{2},k}h^m_{i,j+1,k}+KX_{i+\frac{1}{2},j,k}\,h^m_{i+1,j,k}+KZ_{i,j,k+\frac{1}{2}}\,h^m_{i,j,k+1}=RHS_{i,j,k} \quad \ldots(13)$$

in which, $HCOF_{i,j,k}=P_{i,j,k}-\frac{SS_{i,j,k}\,\Delta X_i\,\Delta Y_j\,\Delta Z_k}{t^m-t^{m-1}}$

and, $RHS_{i,j,k}=-Q_{i,j,k}-SS_{i,j,k}\,\Delta X_i\,\Delta Y_j\,\Delta Z_k\,\frac{h^{m-1}_{i,j,k}}{t^m-t^{m-1}}$

Where,

- $h^m_{i,j,k}$ is the hydraulic head at cell (*i*,*j*,*k*) at time step *m*, which is to be calculated;

- *KX, KY* and *KZ* are the hydraulic conductance between node (*i,j,k)* and a neighbouring node;
- $P_{i,j,k}$ is the sum of coefficients of head from source and sink terms, such as aquifer recharge, $W_{rech.sh}$ in the present case;
- $Q_{i,j,k}$ is the sum of constants from source and sink terms, where $Q_{i,j,k} < 0$ is flow out of the groundwater system (such as pumping), and $Q_{i,j,k} > 0$ is flow in (such as injection);
- $SS_{i,j,k}$ is the specific storage;
- $\Delta X_i\ \Delta Y_j\ \Delta Z_k$ are the dimensions of cell (*i,j,k*) which, when multiplied, represent the volume of the cell; and
- t^m is the time at time step *m.*

In matrix form, eq. (1) can be represented as:

$$[A]\,[h] = [C] \qquad \ldots (14)$$

where [A] is a matrix of the coefficients of head for all active nodes in the grid; [h] is a vector of heads at the end of time step m for all nodes in the grid; and [C] is a vector of the constant terms in *RHS of eq. (6)* for all nodes in the grid.

In eq. (3), which represents eq. (1) in matrix form, the elements of the matrices, [A] and [C] are known, the unknowns are the elements of matrix [h].

5.4.2 Modelling Area

The modelling area covers the Sot river catchment. The study area lies in the part of Uttar Pradesh state comprising of districts of JP Nagar, Moradabad, Budaun, Shahjahanpur and Farrukhabad including 3-km buffer on every side of the catchment to take care of any nearby boundary. **Figure 20** shows the modelling area in grey colour (active cells) and bluish colour (inactive cells).

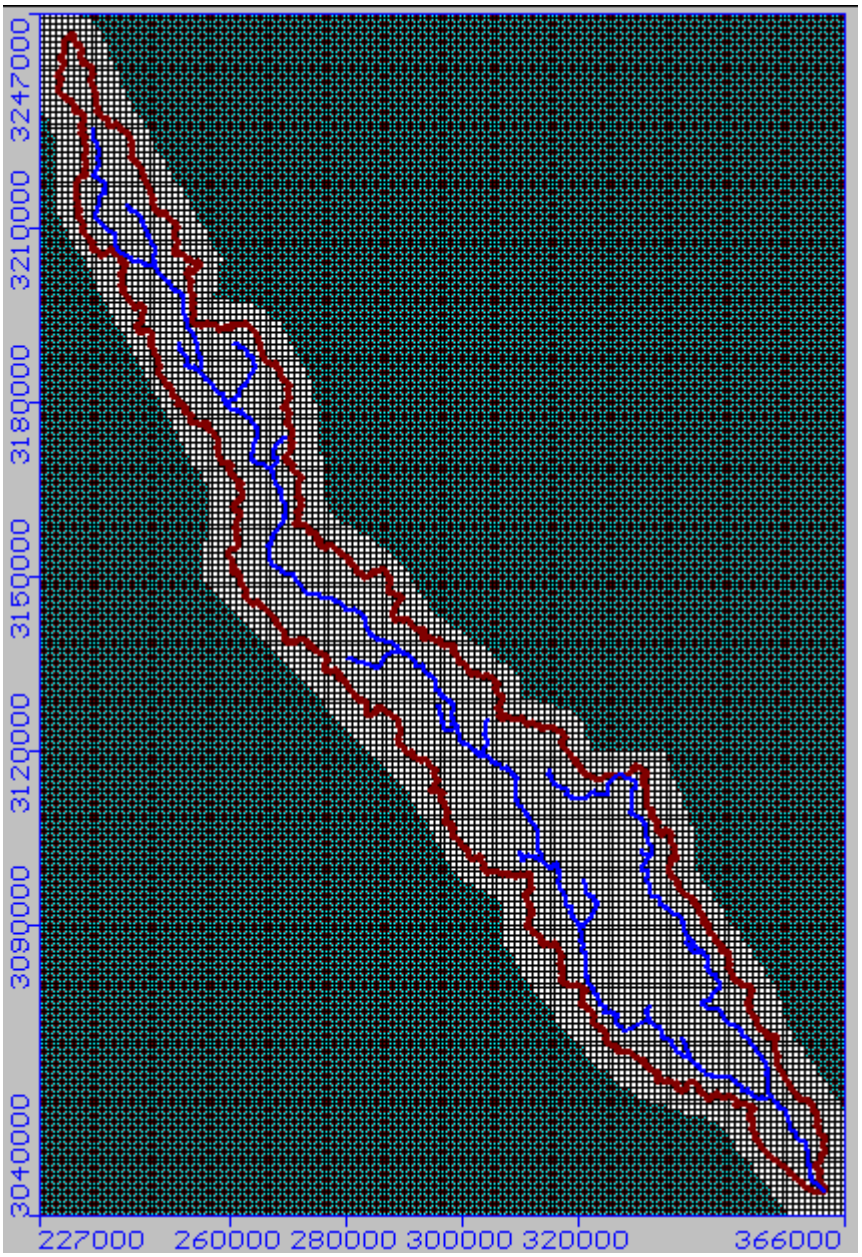

Figure 20. Model domain showing inactive (blue colour cells) and active cells (grey colour cells).

5.4.3 Data Collection and Analysis

Modelling of groundwater needs a lot of data for each and every grid being the MODFLOW, a distributed model. For this purpose, most of the data support was provided by the Ground Water Department, Government of Uttar Pradesh. The groundwater levels and bore log data for the study area were collected from the GW Department, Uttar Pradesh. Digital Elevation Model (DEM) for the modelling area was taken from 90 m SRTM. Groundwater recharge and draft was collected

from CWGB reports. The aquifer properties were taken from the literature, which were finally calibrated during the modelling process. Stages of river flow for the Sot river passing through the modelling area were collected from the Water Resources Department, UP.

5.4.4 Hydro-geology of the Area

The modelling area comprises parts of five districts Uttar Pradesh. These districts include JP Nagar, Moradabad, Budaun, Shahjahanpur and Farrukhabad. The district-wise hydrogeology of the area is described below:

Jyotiba Phuley Nagar: Jyotiba Phuley Nagar is underlain by unconsolidated sediments of quaternary age comprising sand, silt, clay along with occasional kankar. The groundwater occurs in the granular sediments within the zone of saturation under water table conditions in the shallow aquifer and in deeper aquifer below 150 m depth, occurs under semi-confined to confined conditions. On regional scale a single aquifer group extends down to 180 mbgl. The exploratory drilling done by CGWB in the district and adjacent district (Moradabad) down to a depth of 450 mbgl indicate that the first aquifer group may extend down to 215 mbgl below which a 215 m thick clay bed is existing. The change in the sediment facies occur in depth range of 388-400 mbgl and sediments may belong to one system. The sediments below 400 m may belong to different depositional environment. The aquifer system behaves as unconfined to semi confined depending upon the presence of clay beds. The aquifer materials are fine to medium grained and get coarser with depth. Also gravel is encountered at a few places. The presence of clay beds of variable thickness is dominantly confined to areas close to major drainage system namely Ganga. A single aquifer system has been deciphered in the district down to 180.00m. The system at places is separated or divided into a number of aquifers by the intercalation clays. The system behaves as an unconfined to confined depending upon the disposition of clays. The water table of the state tube wells varies from 5 to 12mbgl. General depth of tube wells ranges from 50 to 110 mbgl. The cumulative screened length varies from 20 to 30 m down to the depth of tube well. The average yield varies from 1445 to 3000 lpm for drawdown ranging from 1.85 to 8.70 m. The specific capacity of the tube well varies from 183 to 1129 lit/min/m (CGWB, 2013).

Moradabad: The district is underlain by alluvial sediments having thickness of around 1000 m comprising clay, silt and various grades of sand. Limited drilling carried out for groundwater

exploration down to a depth of 450 mbgl reveals the presence of potential aquifers with a marked change in sedimentation below 390 mbgl. The sediments down to 390 m can be broadly divided into two aquifer groups. The upper aquifer group down to 180 m being exploited extensively by state and private tube wells. The second potential aquifer group present below 180 m depth, still remains to be fully harnessed for optimum utilization. Depth to water level in the area during pre-monsoon period varies from 2.57 to 14.54 mbgl and in post-monsoon period varies from 1.70 to 13.69 mbgl (CGWB, 2009).

Budaun: Geologically, the area is underlain by Quaternary alluvial sediments of Central Ganga Plains. These deposits are fluvial in nature and have been deposited by the drainage system of the Ganga river and its tributaries. General stratigraphic sequence of the formation in the area shows Newer Alluvium of Recent Age comprised of sand, slit and clays. Older Alluvium of Holocene Age having sand, gravel, clay and kankar type of sediment. Upper Siwaliks formation of Pleistocene to Pliocene Age composed of sandstone, shale and limestone. Ground water occurs in the pore spaces of the unconsolidated alluvial sediments in the zone of saturation. The near surface sediments are dominantly sandy clays and clays which grade into sediments having varied proportions of sand and clays. These sediments occur as inter layered sequence and pockets. These mixed sediments occur down to 20 m and support large number of dug wells. The depth of dug wells ranges between 6 to 20 m. Below the top 4 to 10 m silty clays and clays, there occurs sand formations which form a part of aquifer system. This aquifer is largely unconfined to semi-confined and supports a large number of cavity/shallow tube wells. The water level during May, 2012 varies from 3.38 mbgl as seen at Dhanari in Gunnaur Block to 13.50 mbgl at Budaun in Jagat block. In whole of Rajpura, Gunnaur and most parts of Junawai block water level generally ranges between 3 to 5 mbgl. In most parts of Islamnagar, Dahgawan, Sahaswan, Asafpur, Quadar Chowk, Jagat, Ujhani, Samrer, Dataganj blocks water level generally ranges between 5 to 10 mbgl. The water level between 10 to 13.5 mbgl is generally observed in Bisauli, Ambiapur and Wazirganj blocks and in parts of Salarpur, Ujhani, Usawan and Miaon blocks. The water level during November, 2012 varies from 2.5 mbgl as seen at Kachla in Ujhani Block to 14.10 mbgl at Budaun in Jagat block. In the western part of the district covering Rajpura and most parts of Gunnaur and Junawai blocks water level generally ranges between 2 to 5 mbgl. In Samrer, Dataganj, Jagat blocks covering eastern part and parts of Quadar Chowk, Dahgawan blocks water level ranges

between 5 and 10 mbgl. The water level between 10 to 14.10 mbgl is generally observed in Bisauli, Ambiapur and Wazirganj blocks and in parts of Salarpur, Ujhani, Asafpur, Islamnagar, Usawan and Miaon blocks (CGWB, 2013).

Shahjahanpur: The district is underlain by thick pile of Quaternary alluvium deposited over Siwalik Supergroup, which in turn overlies Vindhyan Supergroup unconformably. The Newer Alluvium occurs along the courses of major streams forming wedge shaped cover. The formation consists of fine to medium sand, silt with thin clay lenses. Terrace Alluvium of different rivers exhibits different characteristics. Central Ground Water Board has carried out exploratory drilling in the district up to the maximum depth of 456 m, i.e. mainly within older alluvium. A total of 10 exploratory wells and 1 slim hole have been drilled in the district. Lithological units are composed mainly of fine to medium and coarse sand, gravel, clay and kankar, with sand being the dominant component. Kankar is generally associated with clay capping (3-5 m or more in thickness) existing all over the area. Clay generally occurs in lenticular form in the upper parts and attains regional character at deeper levels. Perusal of electrical logs of the wells apparently suggests that 4 aquifer groups exist at individual sites, with top and bottom of individual aquifer group varying widely (CGWB, 2012). However, on the basis of fence diagram constructed with the help of litho logs of different wells, exhibiting disposition of different aquifers, three aquifer groups, separated by fairly thick clay beds, can be identified in the district down to the maximum explored depth. A conspicuous surface silty clay capping having 3-5m thickness or more also exists almost over entire district. Decreasing resistivity values may point to decreasing granularity with depth. Groundwater in shallow aquifer occurs under unconfined condition and is tapped by dug wells and shallow bore wells. Tube wells drilled by State Government generally tap 30-40 m thickness in this aquifer in the depth range of 70-130 m, with discharge of 2,400 to 3,600 lpm (CGWB, 2006). In deeper aquifers, groundwater occurs under semi-confined to confined conditions. Exploratory wells drilled by CGWB tapping shallow or collectively shallow and deep aquifers have yields ranging from 1,483-2,074 lpm, whereas the well tapping only second aquifer has yielded 904 lpm (CGWB, 2013).

Farrukhabad: The Farrukhabad district occupies a small part of Indo-Gangetic alluvial plains in Ganga-Yamuna Doab. The area is underlain by quaternary sediments comprising mainly a

sequence of clay, silty clay, fine to coarse sand occasionally mixed with kankars and gravels in varying proportions and grades. The Central Ground Water Board, under its exploratory drilling programme, has drilled 5 numbers of boreholes in the district at Khalwara, Sahsapur, Aseh (Nagla Talpur), Rasoolpur and Tahpur. The perusal of sub-surface lithological logs, it reveals that four distinct groups of granular zones occur down to the depth of 450 mbgl separated by poorly permeable / impermeable horizons. Each group of granular zone represent a separate sedimentological environment or cycle. Based on borehole data, four types of aquifer systems exist in Farrukhabad district. The upper unconfined aquifer occurs in the range of 27 to 100 mbgl having fine to medium sand, kankar and occasional presence of coarse sand and gravel; 2^{nd} aquifer exists between 140 to 200 mbgl composed of fine to medium sand; 3^{rd} aquifer between 240 to 310 mbgl comprising of fine grained sand and clay; and the 4^{th} aquifer in between 405 to 440 mbgl composed of fine grained sand (CGWB, 2013).

To delineate the aquifer geometry and lithological stratigraphy, bore log data of 49 locations obtained from Ground Water Deptt., UP, which are scattered in the study area as well as nearby area (**Figure 21**). These bore logs were analyzed and processed to finalize the geometry of underground formations. The depth of those bore logs varied from 89.0 to 150.9 m-amsl.

Bore log data **(Figure 21)** was analysed and discretised into alternate layers of aquifers and aquitards. The bore log data indicates that thickness of the top most layer varies from few centimetres to about 7.4 m. It is characterized by top soil, a mixture of sand silt and clay in varying proportions. These top layer formations are underlain by highly porous and permeable formations of average thickness 22.0 m, comprised of coarse sand and sand mixed with gravels and boulders and sand mixed with kankar in alluvial areas. A clay sequence in patches as well as continuous thick clay comprised of clay mixed with sand, gravel and boulders are available as the next underground formation layer of average thickness 6.75 m. Below this layer, a second aquifer of varying thickness is present of porous and permeable formation similar to the upper aquifer formation of average thickness of 17.70 m. These four layers are considered for the groundwater modelling and are presented in the subsequent sections.

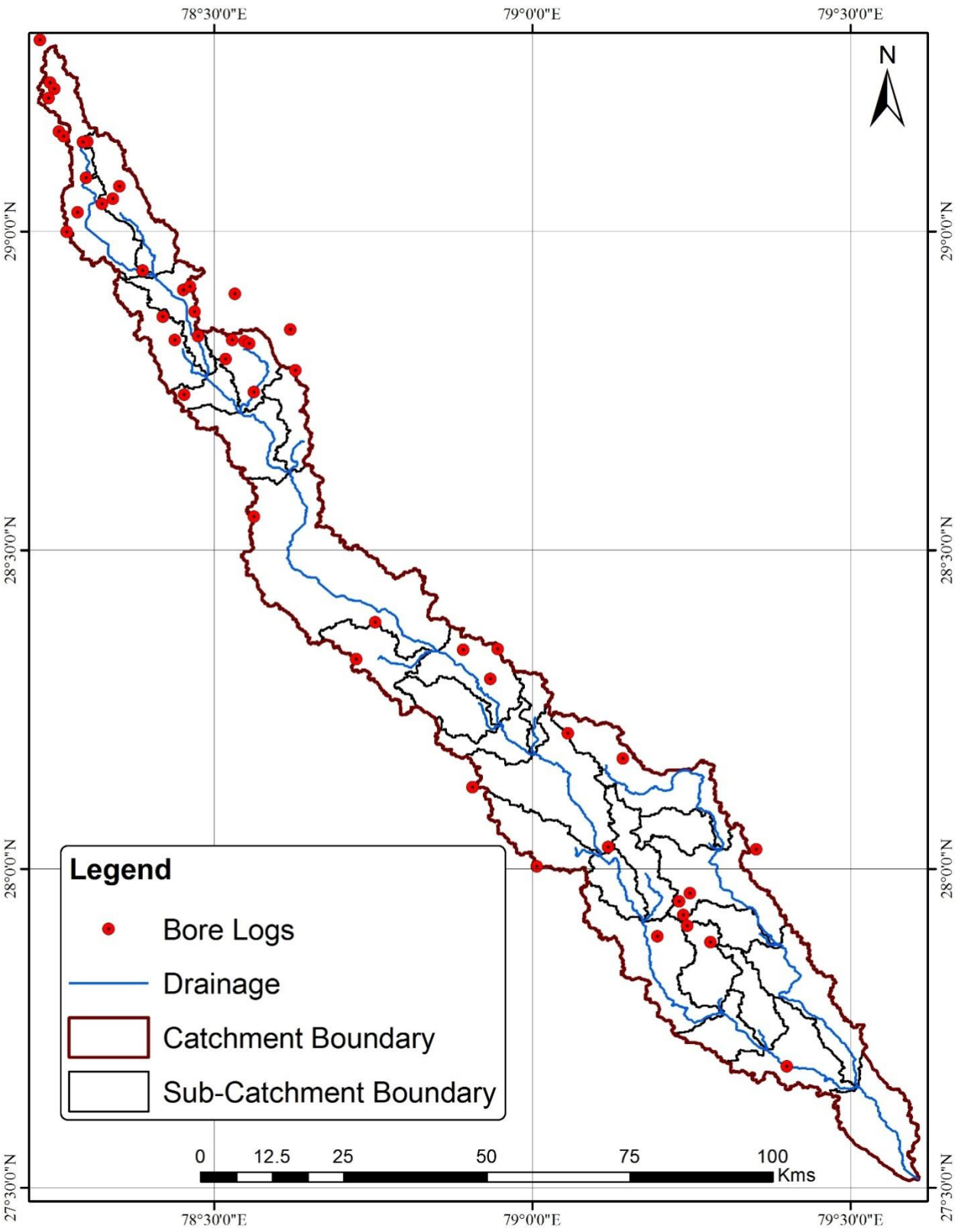

Figure 21. Distribution of bore logs in the study area.

5.4.5 Model Setup and Model Domain

Figure 22 depicts the groundwater model domain map showing various districts of falling fully or partly in the modelling area. Similarly, **Figure 23** presents various administrative blocks falling in the modelling area. The Sot river flows from the north-western side of the area towards the south-eastern side, where it joins the Ganga river (**Figure 24**). All these details have been included in the study area and accordingly the model domain has been finalized.

The easting and northing distances of the model domain vary from 3040000 to 227000 and 3247000 to 336000 m, respectively. To accommodate these distances, the study area was discretized into 2,07,000 m (X- (W-E) direction) and 1,39,000 m (Y- (N-S) direction) gridded network comprising of 28,773 cells per layer with size of each cell of 1000 m x 1000 m. The model domain consists of 207 rows and 139 columns with an area of 28,773 sq.km. The surface flow direction in the study area is largely towards south-east direction. All the cells inside the modelling area are considered active and outside cells were considered inactive. The inactive cells are ignored by the model during model run and no computations are made in these cells.

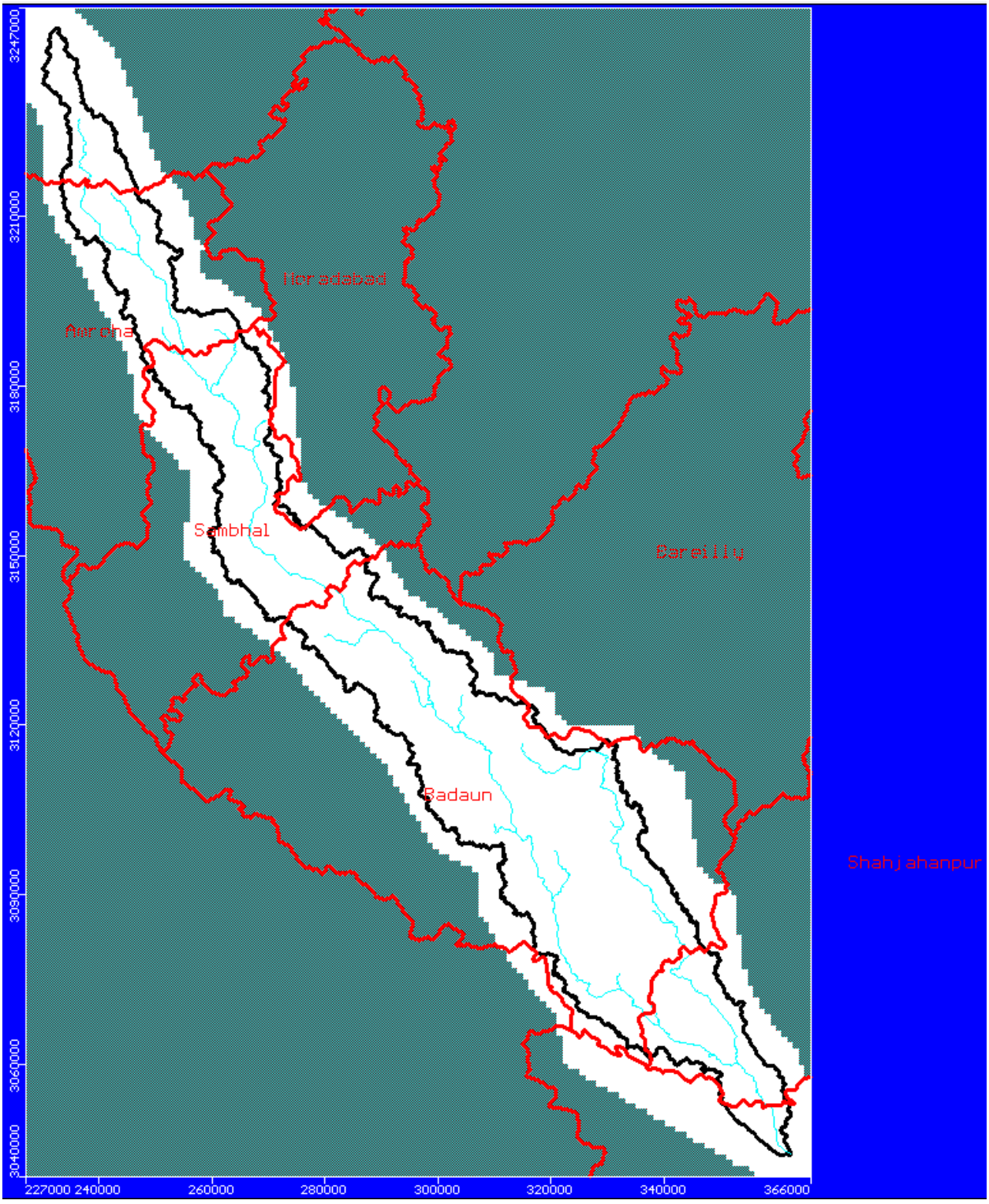

Figure 22. Model domain showing various districts falling in the modelling area (cell size: 1000 m x 1000 m)

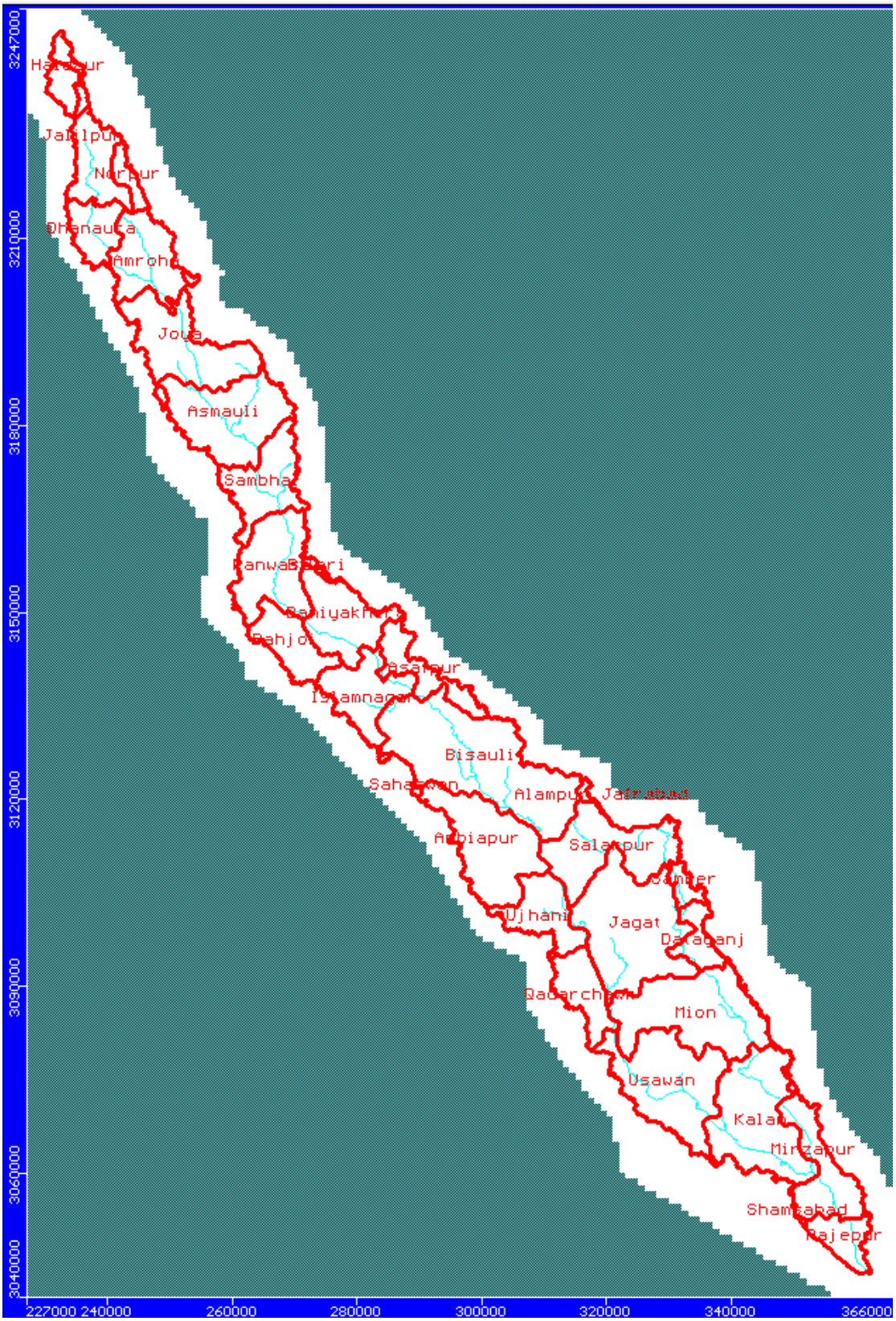

Figure 23. Map showing administrative blocks in the modelling area.

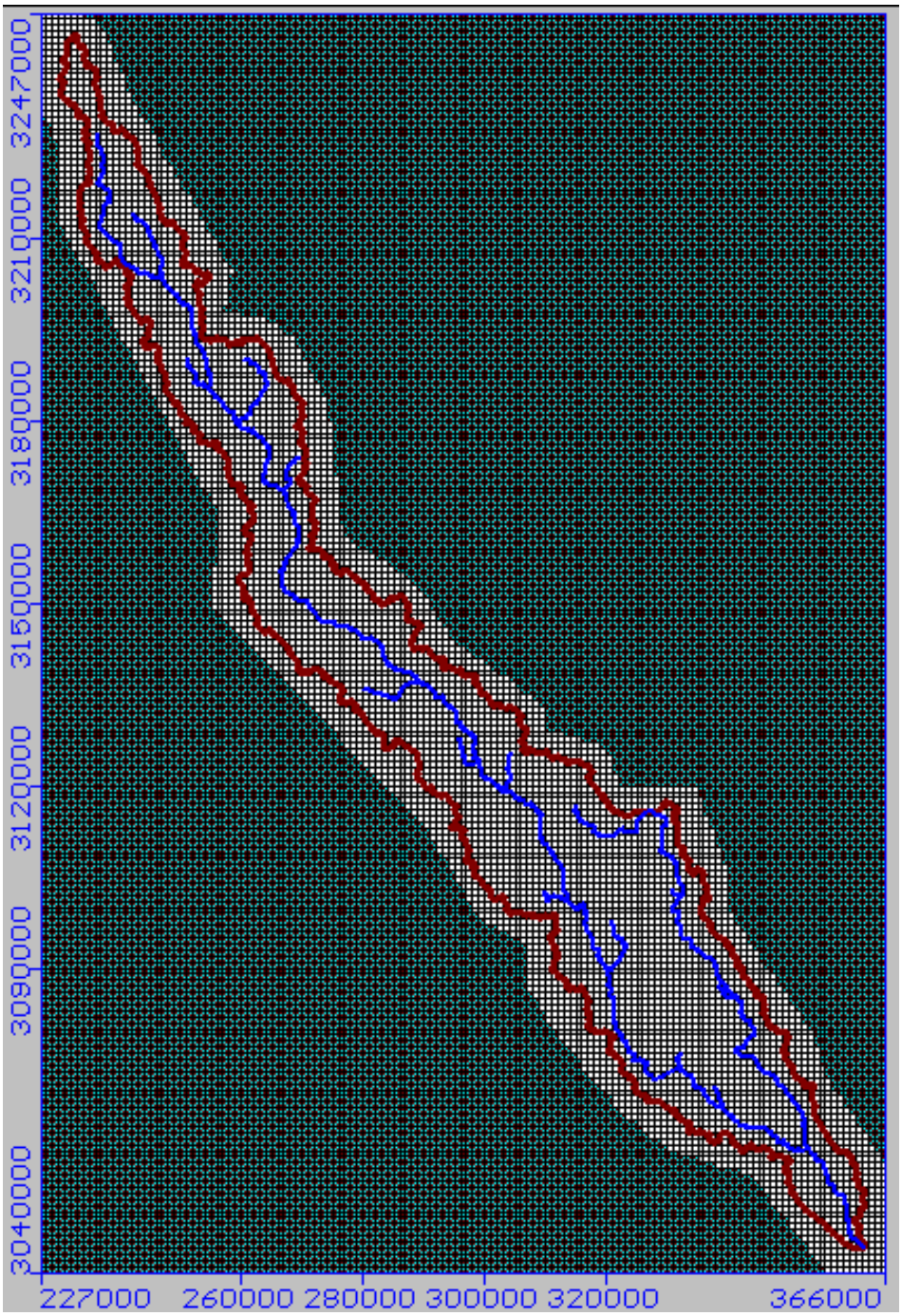

Figure 24. Main river network falling in the model area.

The underground formations comprise of several alternate layers of aquifers and aquitards. Therefore, it was planned to consider a 4-layer groundwater flow model. The vertical cells below the active zone were considered active and inactive below the inactive zone. The vertical discretization of four layers represents the formations as top layer of variable thickness represent top soil having characteristics of aquitard, followed by an unconfined aquifer of varying thicknesses, then an aquitard of varying thicknesses, and then confined aquifer of variable thickness. **Figure 25a** and **25b** show the cross-sectional views of four layers of underground

formation at the middle of the model domain, i.e. at 103rd row and 70th column. Coloured cells are active cells and greyish colour cells are inactive cells.

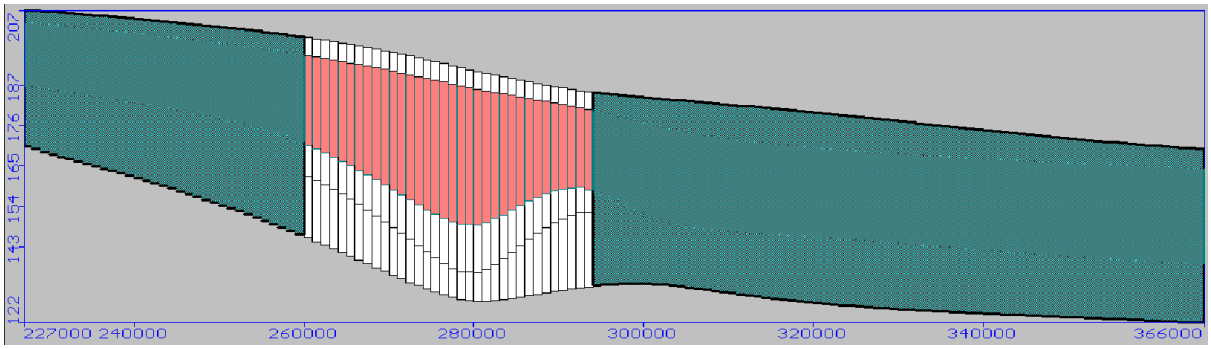

Figure 25a. Sectional view of vertical discretization of model domain showing four layers of underground formations along middle of W-E direction (103rd row).

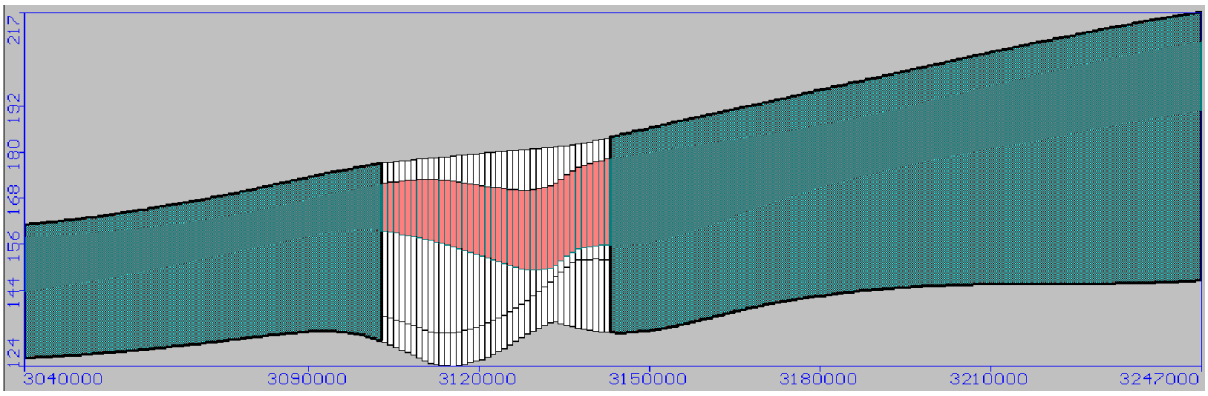

Figure 25b. Sectional view of vertical discretization of model domain showing four layers of underground formations along middle of N-S direction (70th column).

5.4.6 Initial and Boundary conditions

Initial condition

The initial condition is required for the transient simulation run as the initial position of the groundwater table. The pre-monsoon season water level data of June, 2009 was taken as the initial condition for calibration of the groundwater flow model and June, 2014 for the validation of model. The rasterized map from point data of initial water level was then used as initial condition for all the active grid cells. **Figure 26** shows the initial heads considered in the study area along with contours.

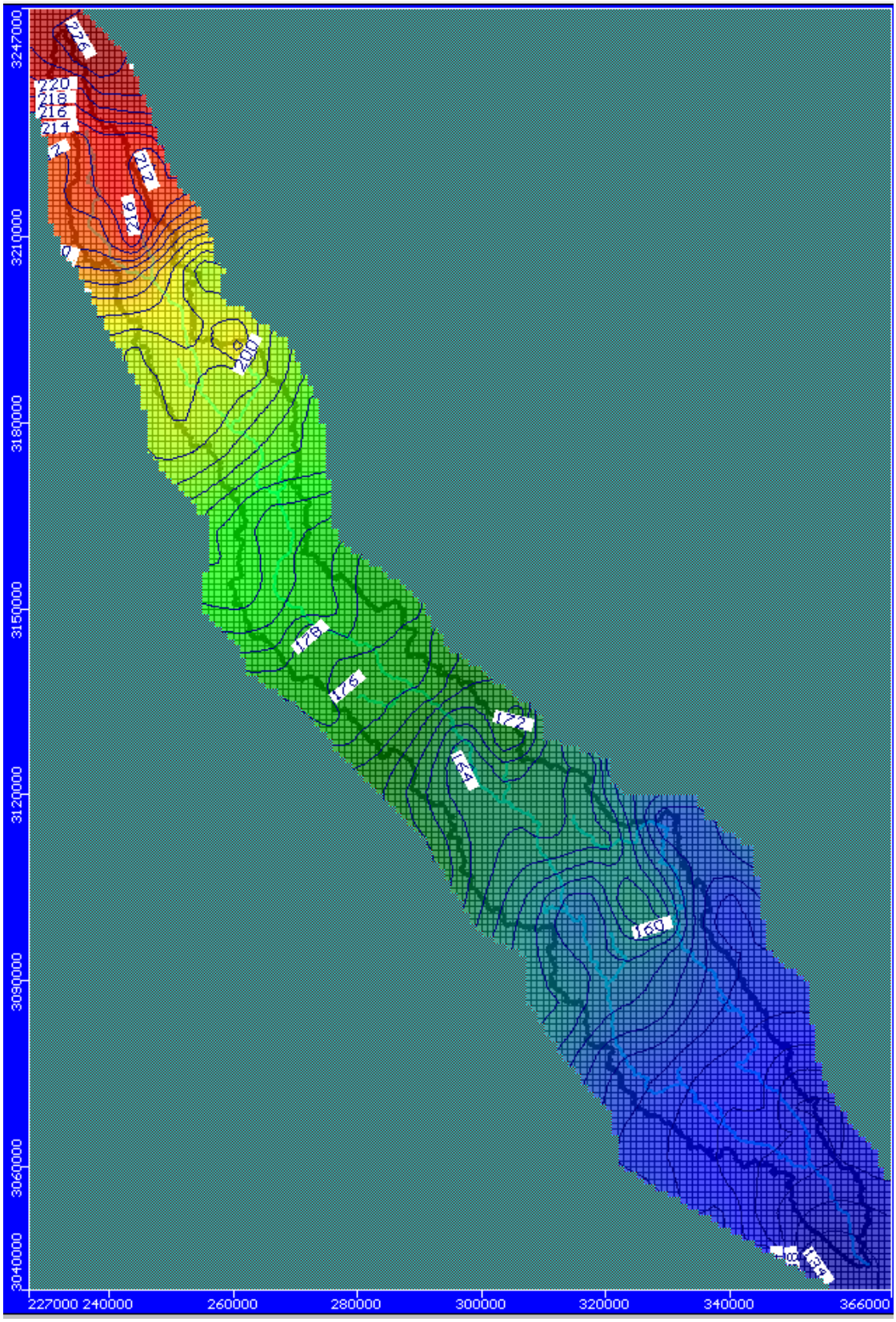

Figure 26. Distribution of initial heads in the modelling area.

Boundary conditions

Ideally - a groundwater basin boundary should form the boundary condition. Since the modelling area fall in the alluvium area, underground aquifer boundaries are not fixed like in the hard rock areas. Therefore, specified head boundaries are assigned all along the modelling boundary. These boundaries are shown in **Figure 27**.

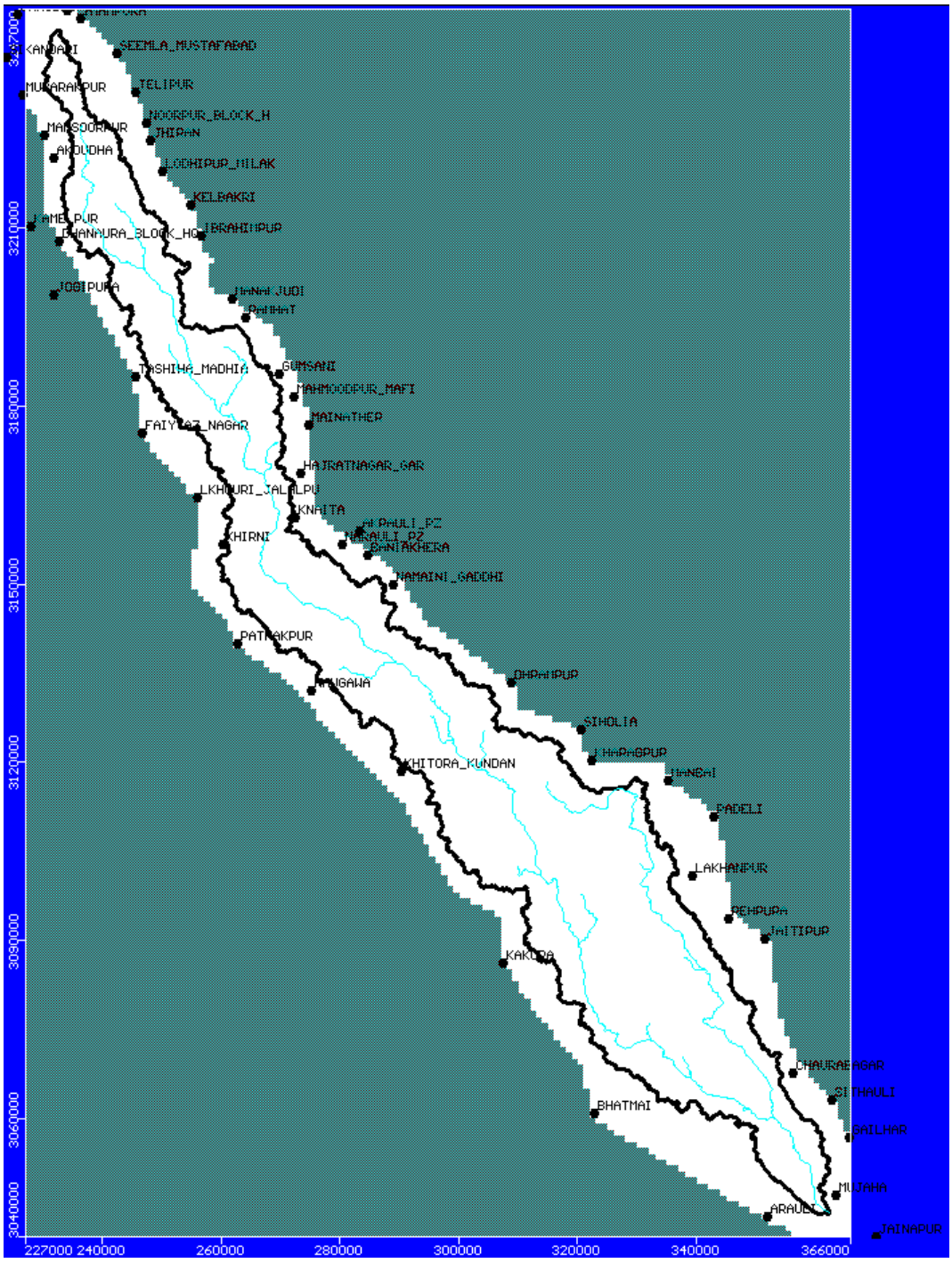

Figure 27. Boundary conditions in the modelling area.

Ideally the groundwater recharge varies point to point and cell-be-cell and accordingly it must be assigned to the model. In the present case, block-wise groundwater recharge and withdrawals are assigned for the whole modelling area. The block-wise monthly values of groundwater recharge were estimated for the Central Ground Water Board (CGWB) reports. The block-wise groundwater draft was also taken from the district brochures report of CGWB of various years and used in the modelling. The map showing block-wise zones of groundwater recharge and draft are shown in **Figure 28**.

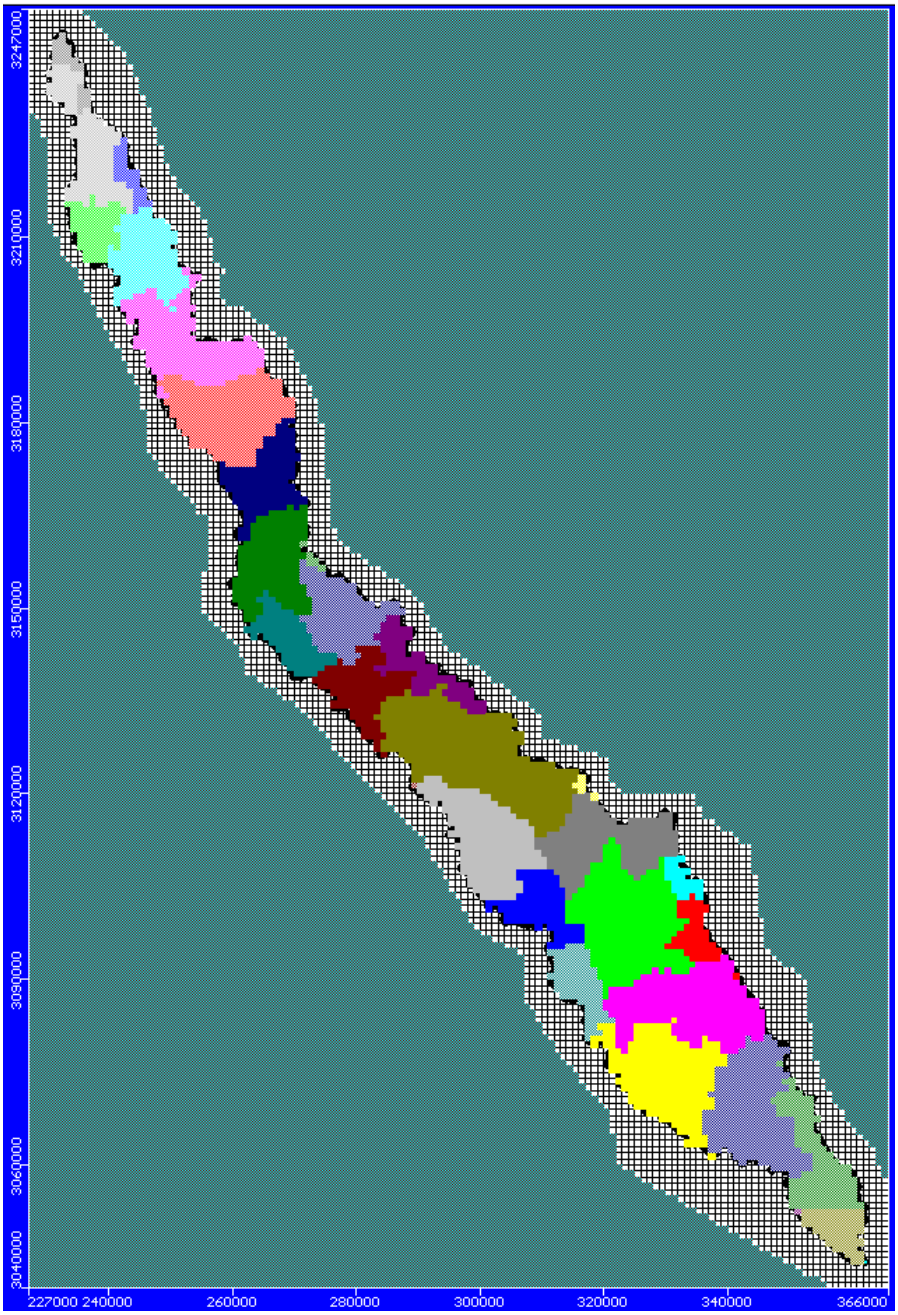

Figure 28. Map showing various recharge zones for assigning recharge and draft.

The groundwater model uses observed groundwater levels for calibration and validation simulation runs. For this purpose, the observed groundwater level data of 212 nos. observation wells was available from Groundwater Department, U.P. for the period 2009 to 2018. Five years' groundwater level data (2009-2014) was used for calibrating the flow model and four years' data (2014-2018) was used for validating the model. The location of various observation wells, falling in the modelling area, is shown in **Figure 29**. Except some patches, the wells are almost well distributed in the whole study area.

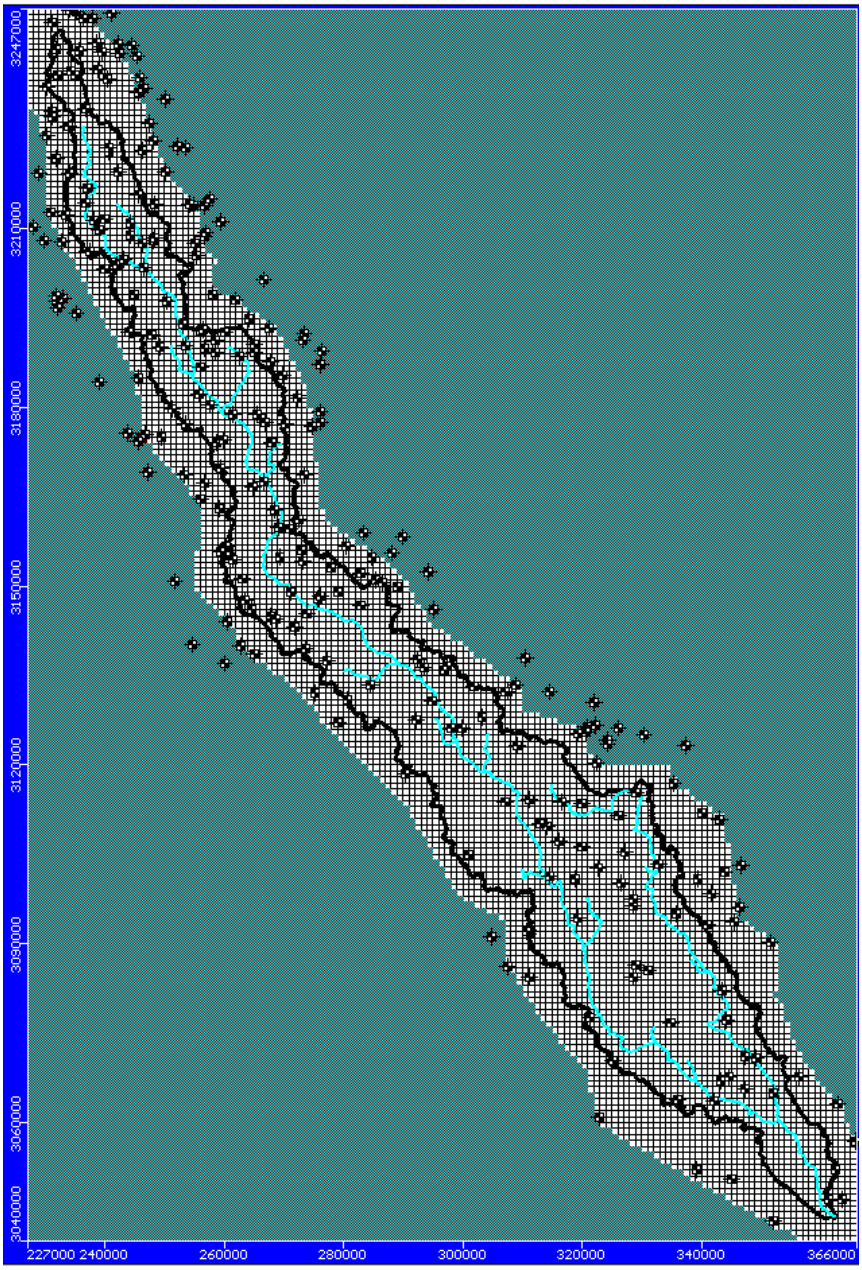

Figure 29. Distributed locations of groundwater level observation points in the modelling area.

5.5 Assessment of Groundwater Potential Zones

5.5.1 Generation of Thematic Maps

To prepare the groundwater potential zone mapping of the Sot catchment, various thematic maps including geology, geomorphology, DEM, soil, slope, LULC, drainage, recharge, groundwater fluctuation, depth to aquifer, and depth to groundwater level for pre-monsoon period are prepared using the remote sensing and GIS applications.

5.5.2 Assignment of Weights Using AHP Method

The most common approach to assigning weight to each parameter is to analyse the inter-relationship between the layers and one layer's effect on another. The more the effect, the higher the weight will be. AHP method is a very helpful method for multi-parameter assessment. In this method, the relative significance of each parameter is resolved with Saaty's 1-9 scale, in which a score of 1 represents equal importance between two parameters and a score of 9 represents extreme significance between two parameters (Saaty, 1980). In the present study, the assignment of weight to the individual thematic layer is done on the basis of previous studies and field observations as recommended by Saaty. The weights thus assigned to different thematic maps and their individual features were normalized by the eigenvector technique and Saaty's analytic hierarchy process (AHP). The AHP picks up the likelihood of uncertainty in assessments through the principal eigenvalue and the index of consistency (Saaty, 2008). The Consistency index (CI), as a measure of consistency, is derived from the following equation.

$$CI = \frac{\lambda_{max} - 1}{n - 1} \quad \ldots(21)$$

where λ_{max} is the significant eigenvalue of the pair-wise comparison matrix, and n is the number of classes. To regulate the assessment of consistency analysis and scale, Consistency ratio (CR) defined as the measure of consistency between pair-wise comparison matrix (Saaty, 1980) is calculated.

$$CR = \frac{CI}{RI} \quad \ldots(22)$$

Where RI is the Ratio Index. The value of CI should always be less than 0.1, so that there should be no revaluation and recalculation of the assigned weights to the individual layers.

After assigning the weights of each thematic layer and its sub parameters, the groundwater potential zones were demonstrated by using the weighted overlay analysis technique. For this the groundwater potential index (GWPI) is computed by the weighted linear combination method. The mathematical expression of GWPI is given below:

$$GWPI = \sum_{w=1}^{m} \sum_{i=1}^{n} (w_j \times x_i) \quad \ldots(23)$$

Where x_i = normalized weight of the i^{th} class of the parameter and w_i = normalized weight of the j^{th} theme, m = total number of parameter and n = total number of classes in a theme.

6 RESULTS AND DISCUSSION

6.1 Analysis of variability in rainfall, temperature and groundwater level of Sot river catchment

The long-term trends of annual and seasonal rainfall have been investigated. It is clear from Figure 30 that the annual and monsoon rainfall show decreasing trend in lower part of the catchment during monsoon season. However, during summer and winter season, rainfall doesn't show any trend.

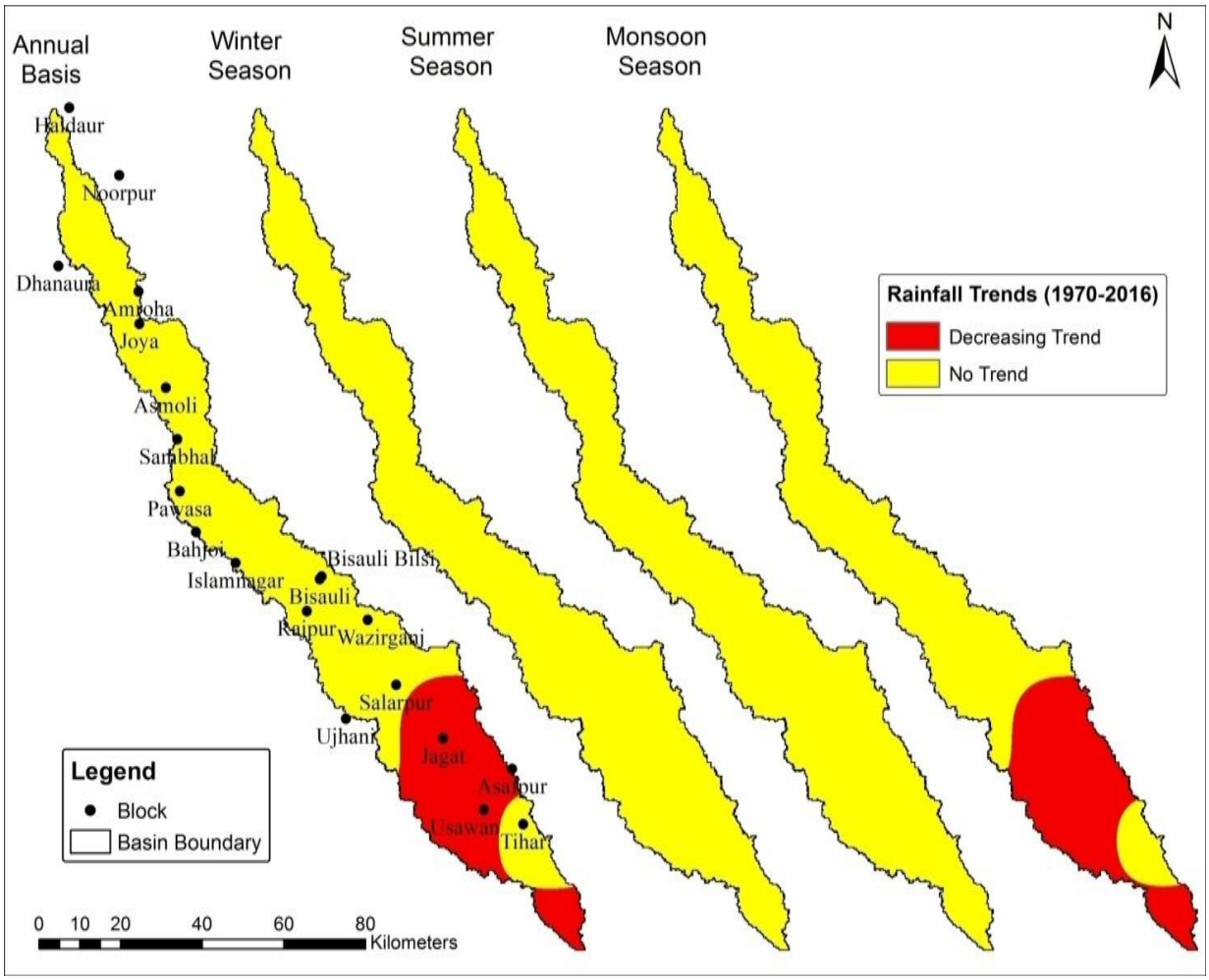

Figure: 30 Annual and seasonal rainfall trend

Figure 31 shows the spatial variation of monthly minimum and maximum temperature in the whole catchment.

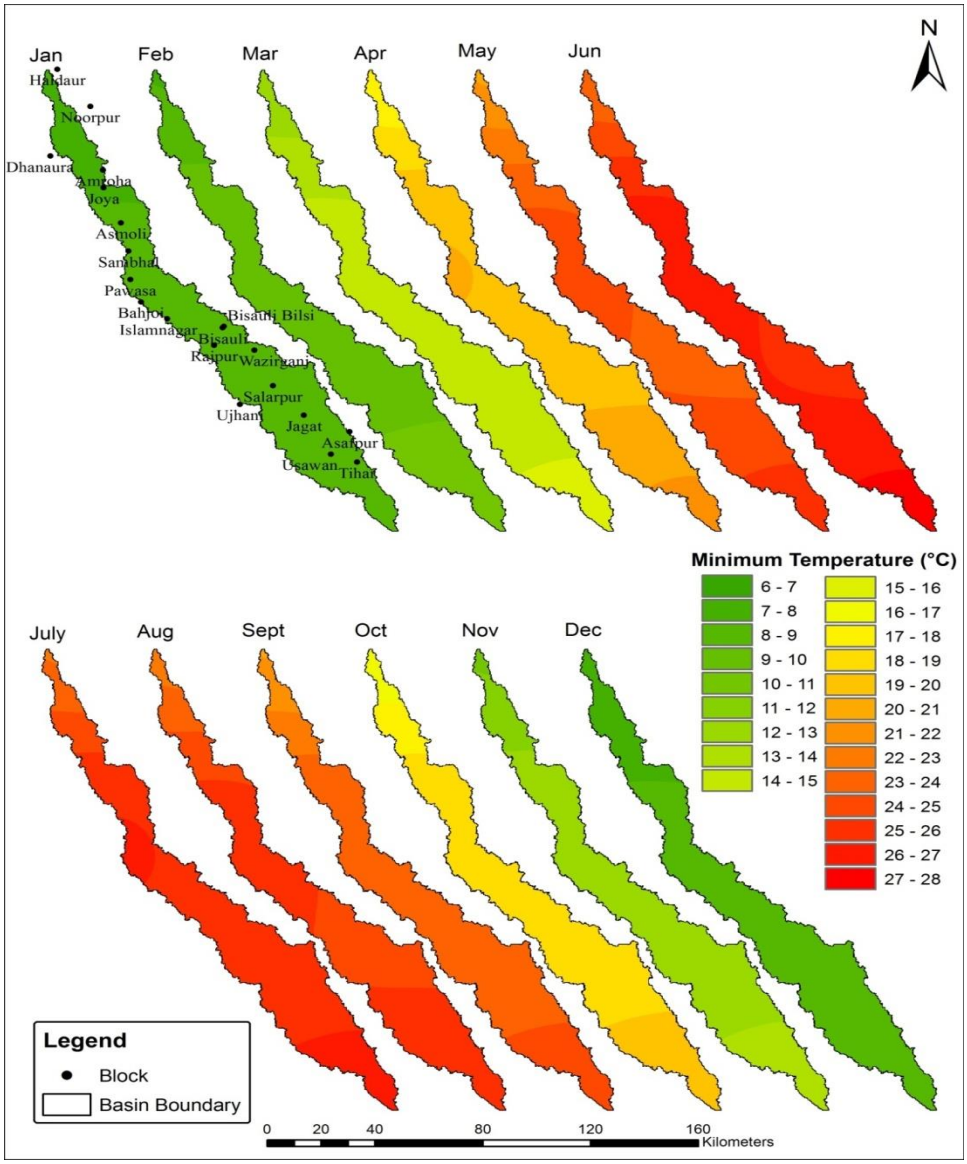

Figure 31a. Monthly variation of minimum temperature in the study area

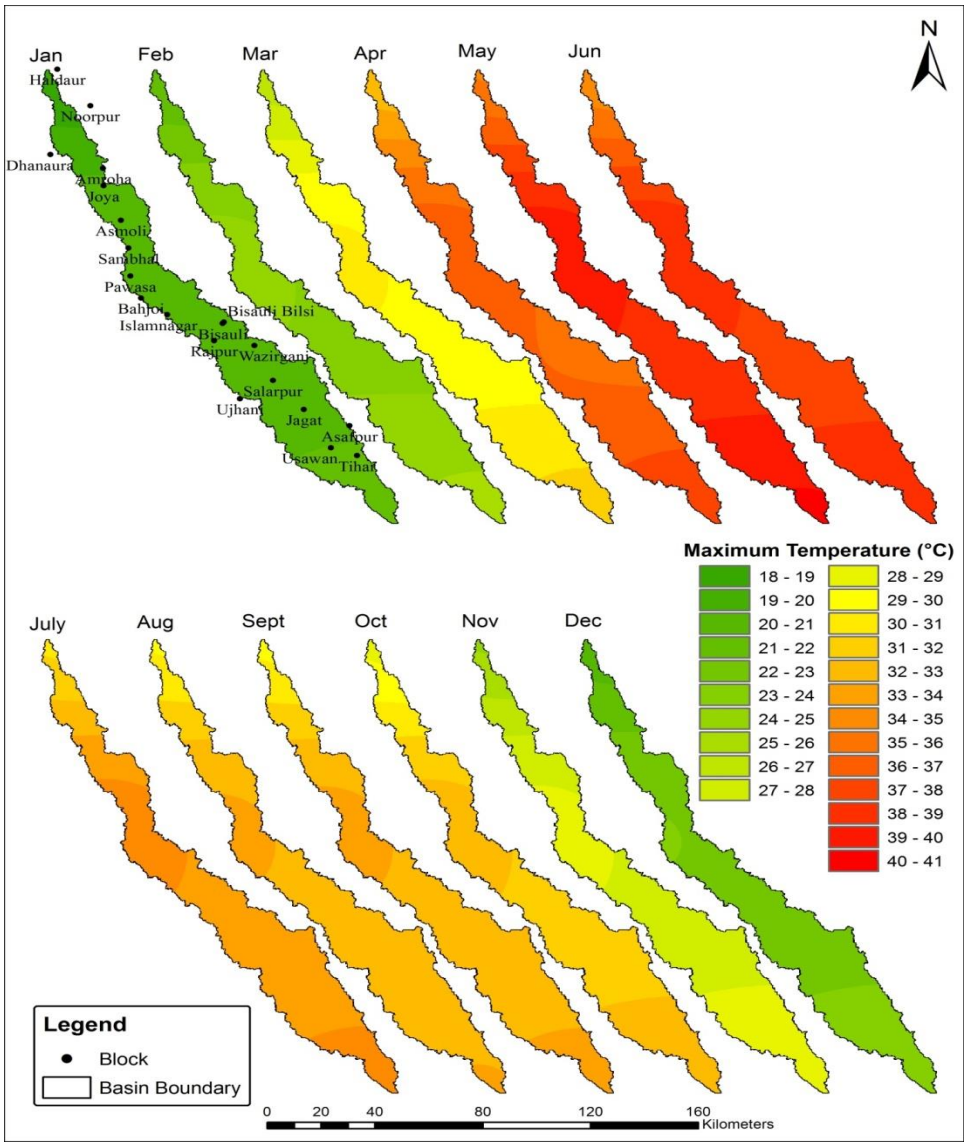

Figure 31b. Monthly variation of maximum temperature in the study area

Figure 32 shows the spatial variation trends of monthly mean temperature in the catchment during the period 1970 to 2015, which indicates increasing temperature trend in the month of August. However, January and February months show decreasing trend in temperature.

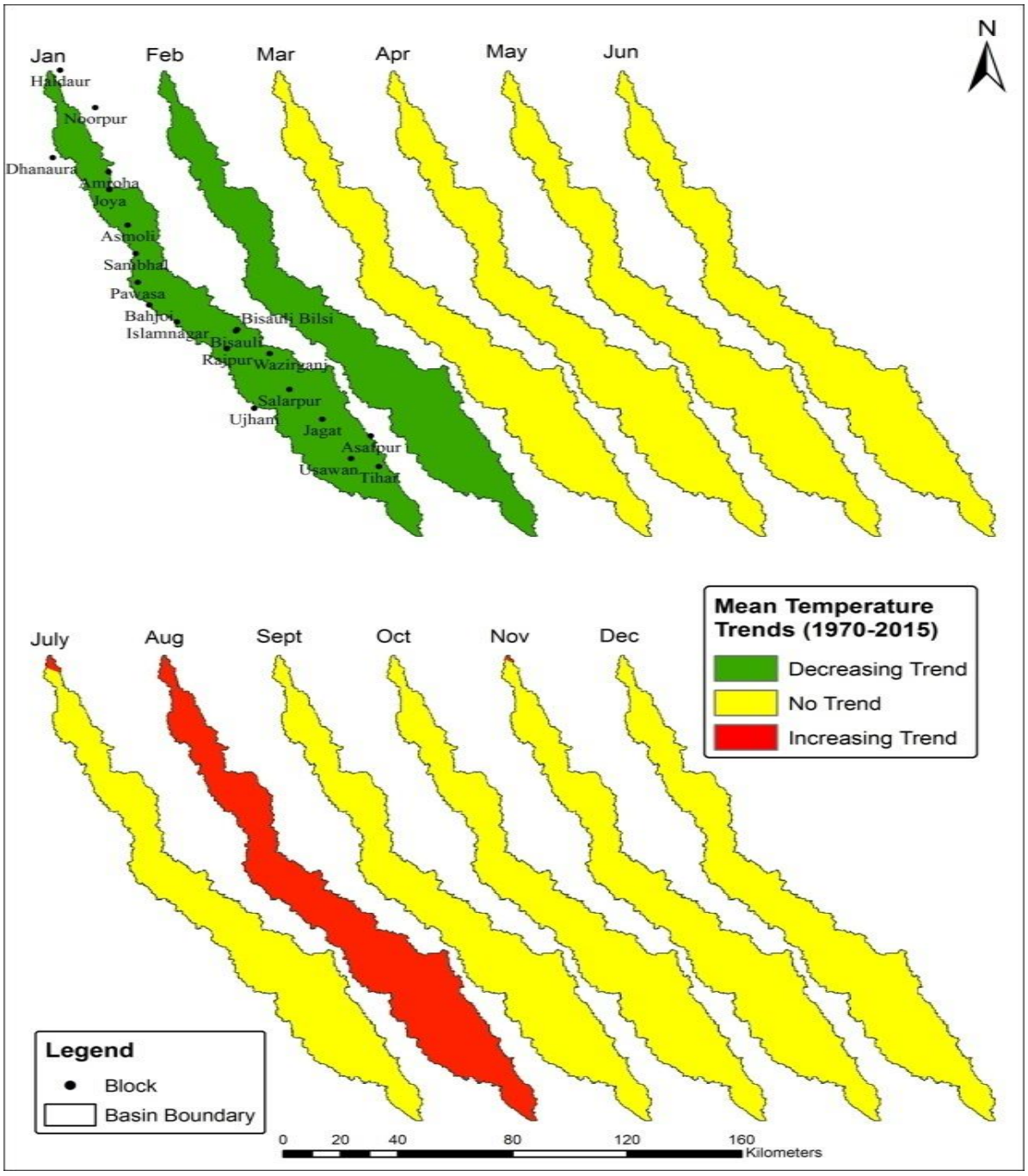

Figure 32. Monthly variation of mean temperature in the study area

The variation of groundwater levels, investigated during pre- and post-monsoon season of 2017 in the catchment, is shown in Figure 33(a) and 33(b). It is seen that the groundwater levels vary from 5 to more than 13 m-bgl in the whole catchment.

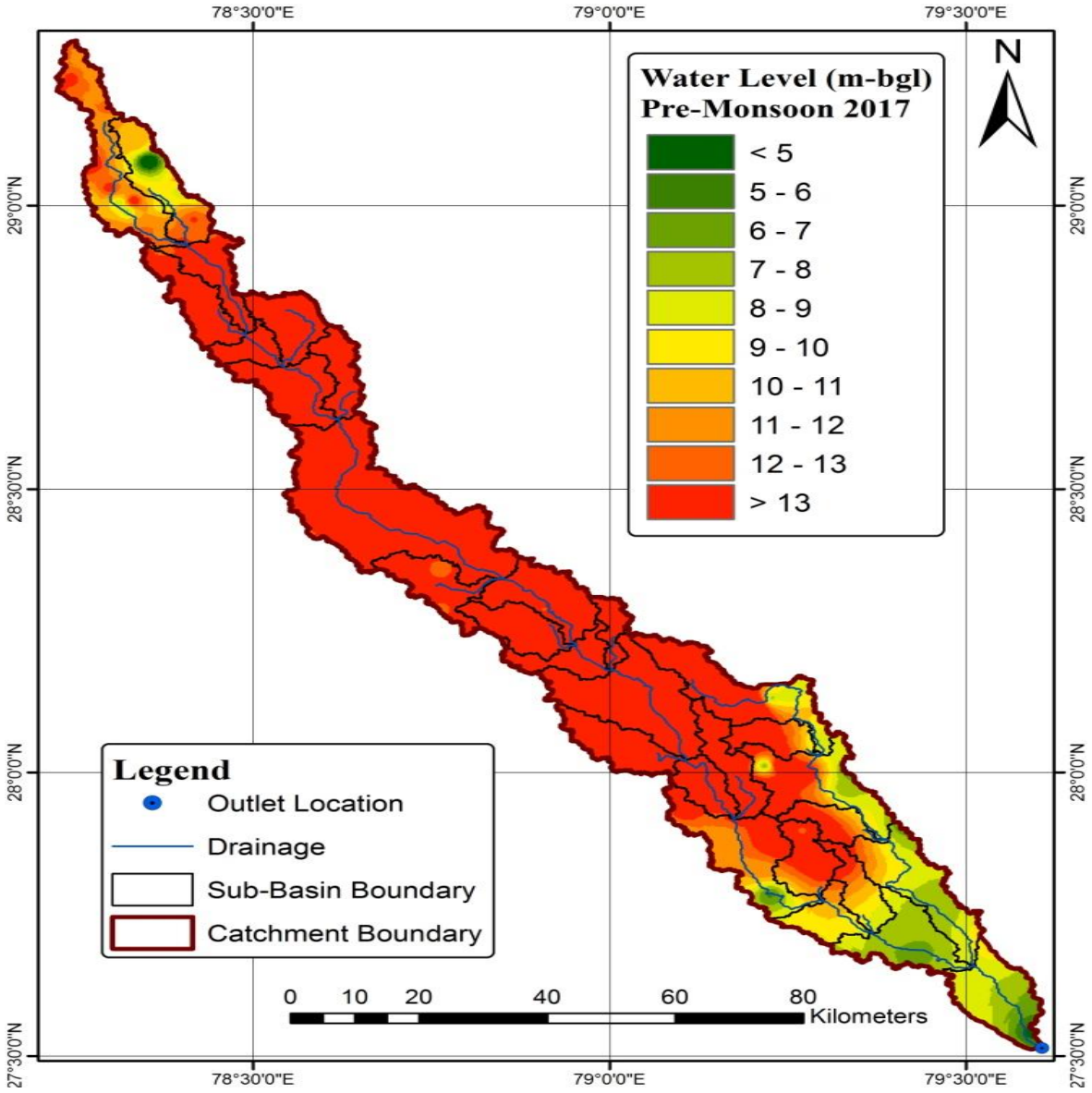

Figure 33a. Variation of groundwater levels during the pre-monsoon season of 2017

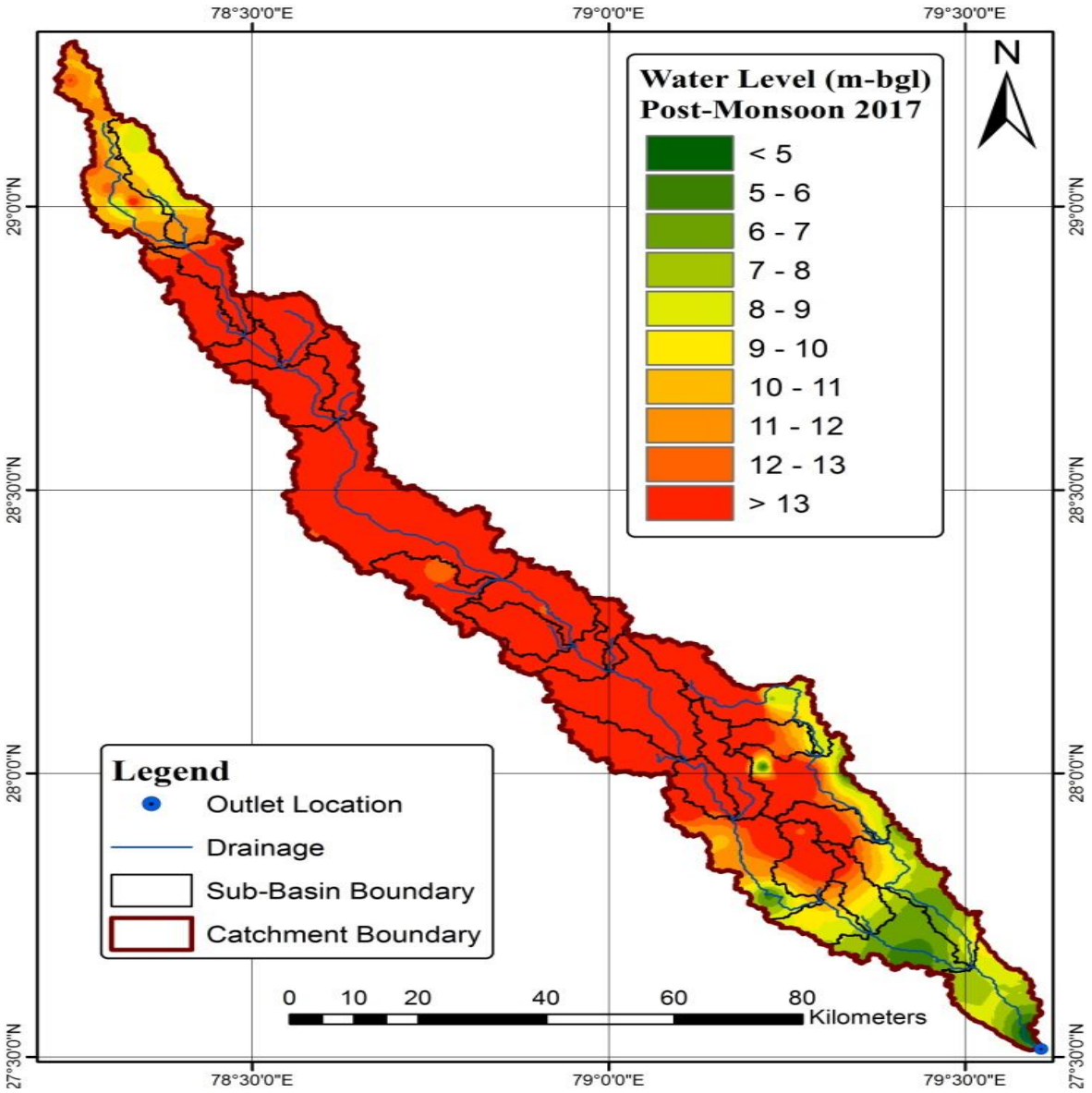

Figure 33b. Variation of groundwater levels during the post-monsoon season of 2017

Figure 34 shows the spatial trend in groundwater levels in the catchment area during the pre-monsoon season based on the data for the period from 2008 to 2017. It is seen that the middle portion of the catchment shows significant declining groundwater level trend. However, the upper and lower catchment portion does not show any trend in the groundwater levels.

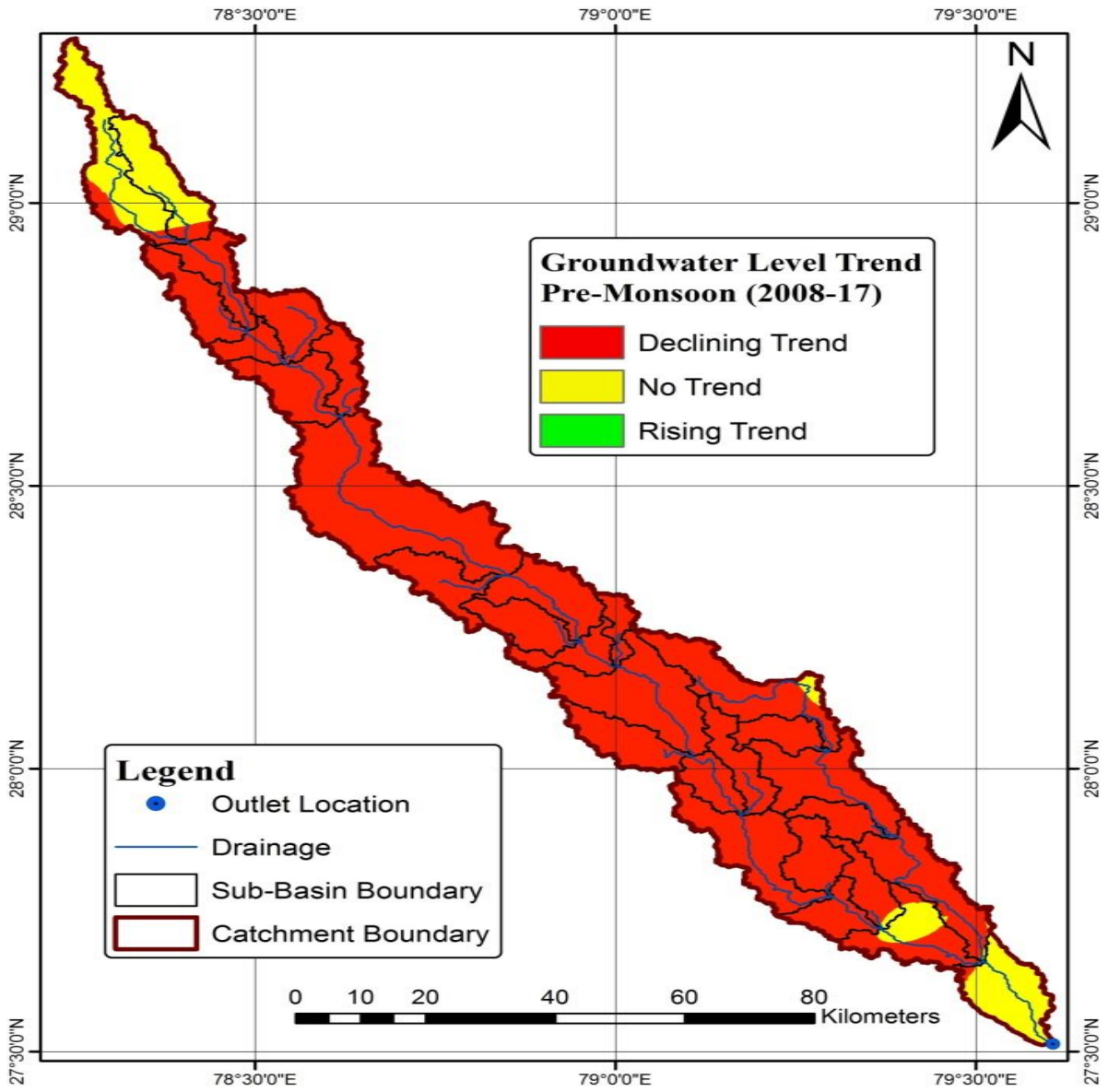

Figure 34. Pre-monsoon groundwater level trend during 2008-2017 in the study area

Figure 35 shows groundwater level fluctuation during 2017 in the catchment. It is obvious from the figure that the fluctuation is more in the upper and lower part of the catchment as compared to the middle part.

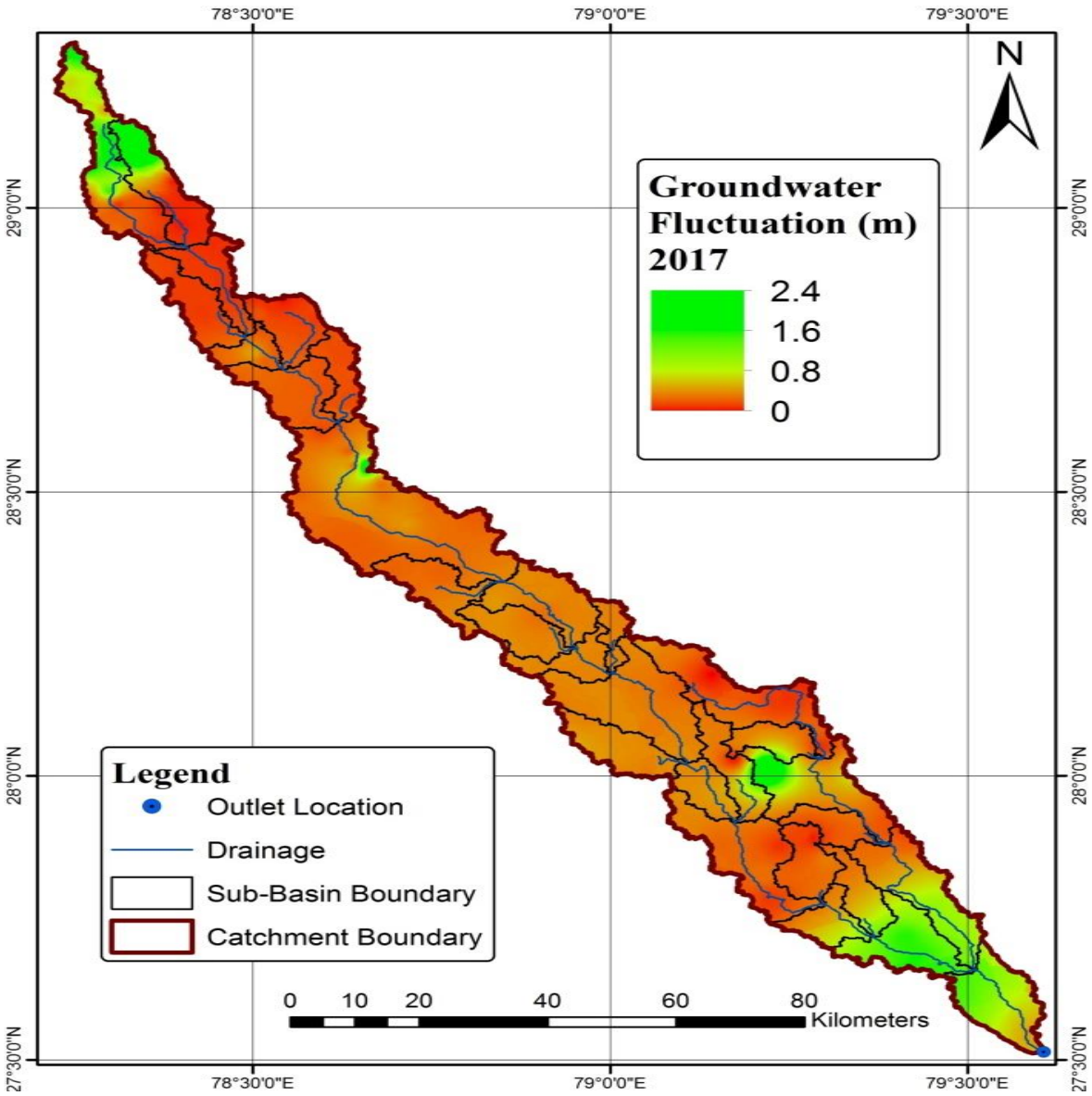

Figure 35. Variation of groundwater fluctuation during 2017 in the study area

6.2 Land Use Changes

Three LANDSAT-8 satellite images of 30 m resolution were retrieved from the USGS Earth Explorer Website to prepare the LULC map for the year 1998, 2008 and 2018. Using ERDAS Imagine 2014, supervised classification of the pre-processed images was carried-out after merging them. The land use type of the study area was divided in five different classes namely agriculture, barren land, orchards, settlements and water bodies. The percentage change obtained in the land use during the period of 1998, 2008 and 2018 is presented in Table 5. The land use maps for the year 1998, 2008 and 2018 are presented in Figures 36 (a, b and c), respectively. It is clear from Figure 37 that the catchment is agriculturally dominant.

Table 5 Percentage of various land use classes in the catchment

Sr. No.	Land Use Class	1998	2008	2018
1	Agricultural Land	87.46	87.82	87.52
2	Barren Land	5.18	3.57	0.32
3	Orchards	5.54	5.07	5.32
4	Settlements	1.77	2.07	6.37
5	Water Bodies	0.06	1.47	0.48

6.3 Drought Analysis for the Sot River Catchment

Droughts, which are regional climatic phenomenon occurring due to less than average rainfall over a given period of time at a given place, lead to short term water deficit and economic loss in the catchment. A season/year is said to be drought season/year if it receives rainfall less than 75% of corresponding long-term average. In the present study, various drought characteristics (i.e. frequency, severity and persistence) have been analyzed for the districts of Bijnor, Moradabad, Budaun and Shahjahanpur located in the western part of Uttar Pradesh. These districts have semi-arid climate with average annual rainfall in the range of 824 - 1042 mm. Based on the analysis of 113 years (1901-2013) data; it has been observed that these districts have experienced frequent droughts once in 5 years. The severity (i.e. magnitude of deficit) of a drought event generally described in terms of rainfall departure from the corresponding long-term mean. The maximum rainfall deficiency of 60.4%, 56.4%, 59.6% and 50.8% has been observed in the districts of Bijnor, Budaun, Moradabad and Shahjahanpur respectively, over the period of 113 years. In addition to the above these districts faced severe rainfall deficiency in years 1907, 1918, 1938, 1972, 1987, 2001 and 2002. Sometimes a drought event may continue for more than one year. The tendency of drought events for more than one successive year is termed as drought persistence. The persistent drought events of 2-, 3- and 4- consecutive years have been identified. The analysis revealed that the maximum drought persistency of 2- and 3- consecutive years are common in this region. This information will be useful in managing the water resources and reduction in crop losses in the catchment and in suggesting artificial recharge measures.

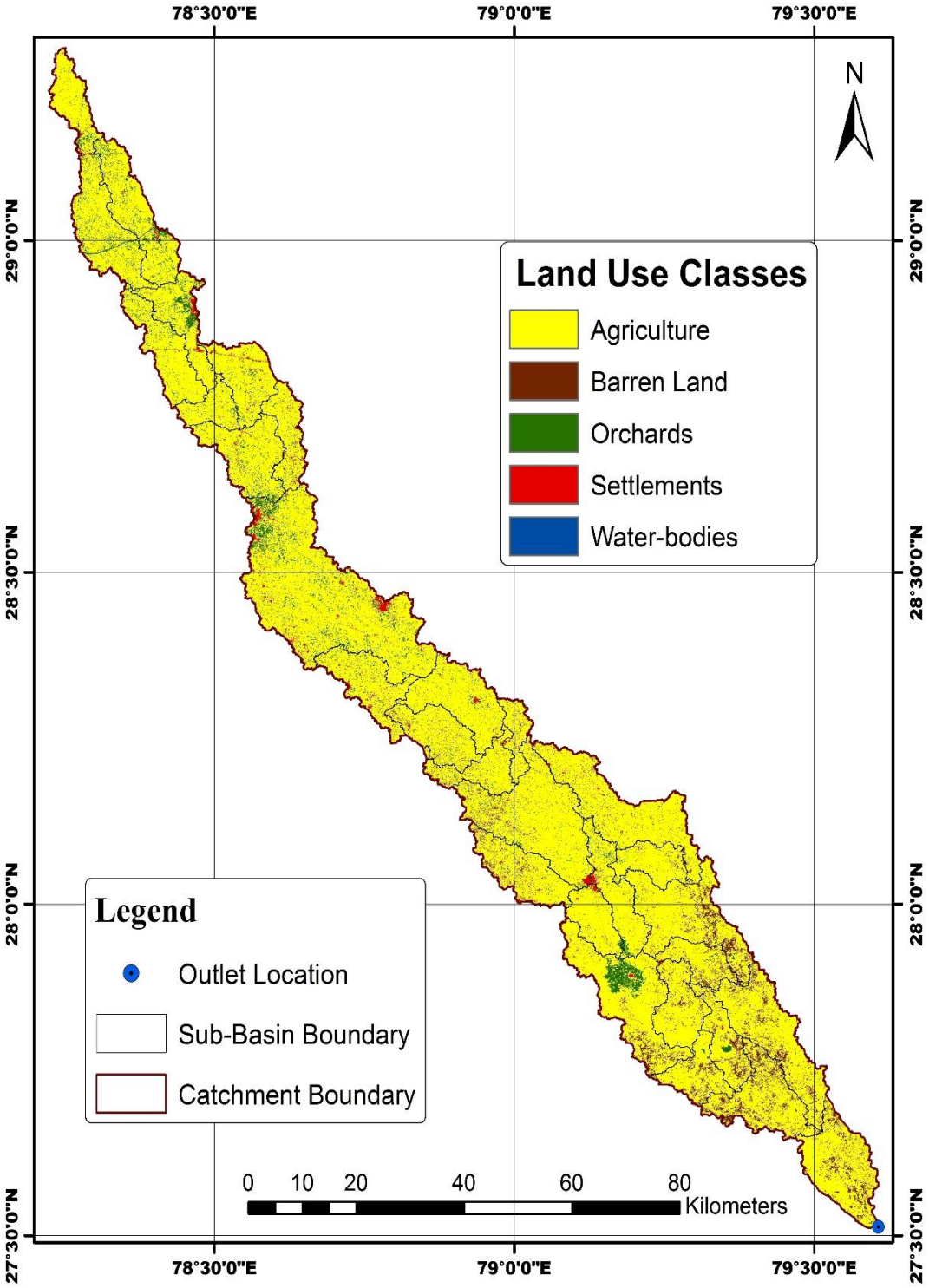

Figure 36a. LULC map of the Sot catchment for the year 1998

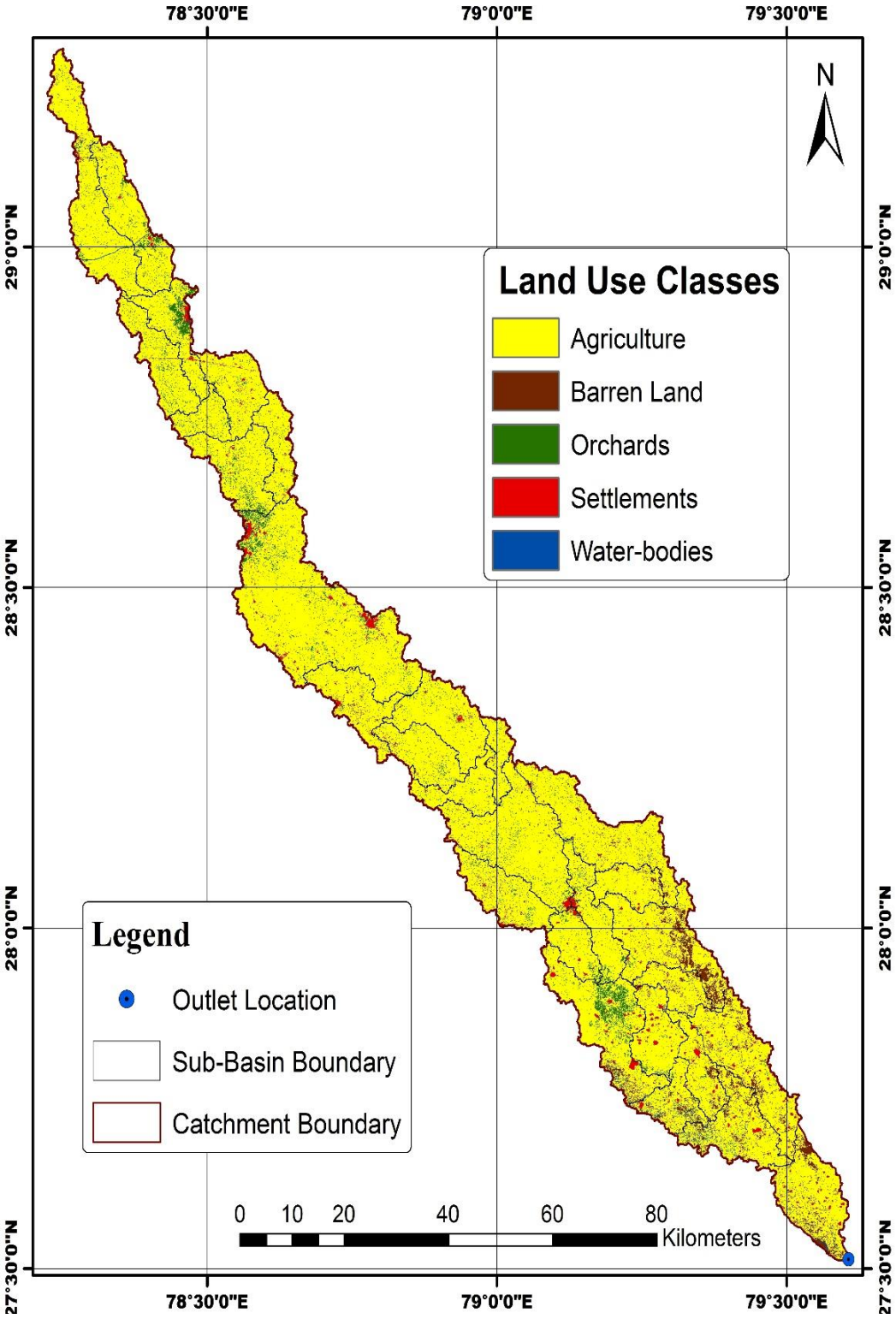

Figure 36b. LULC map of the Sot catchment for the year 2008

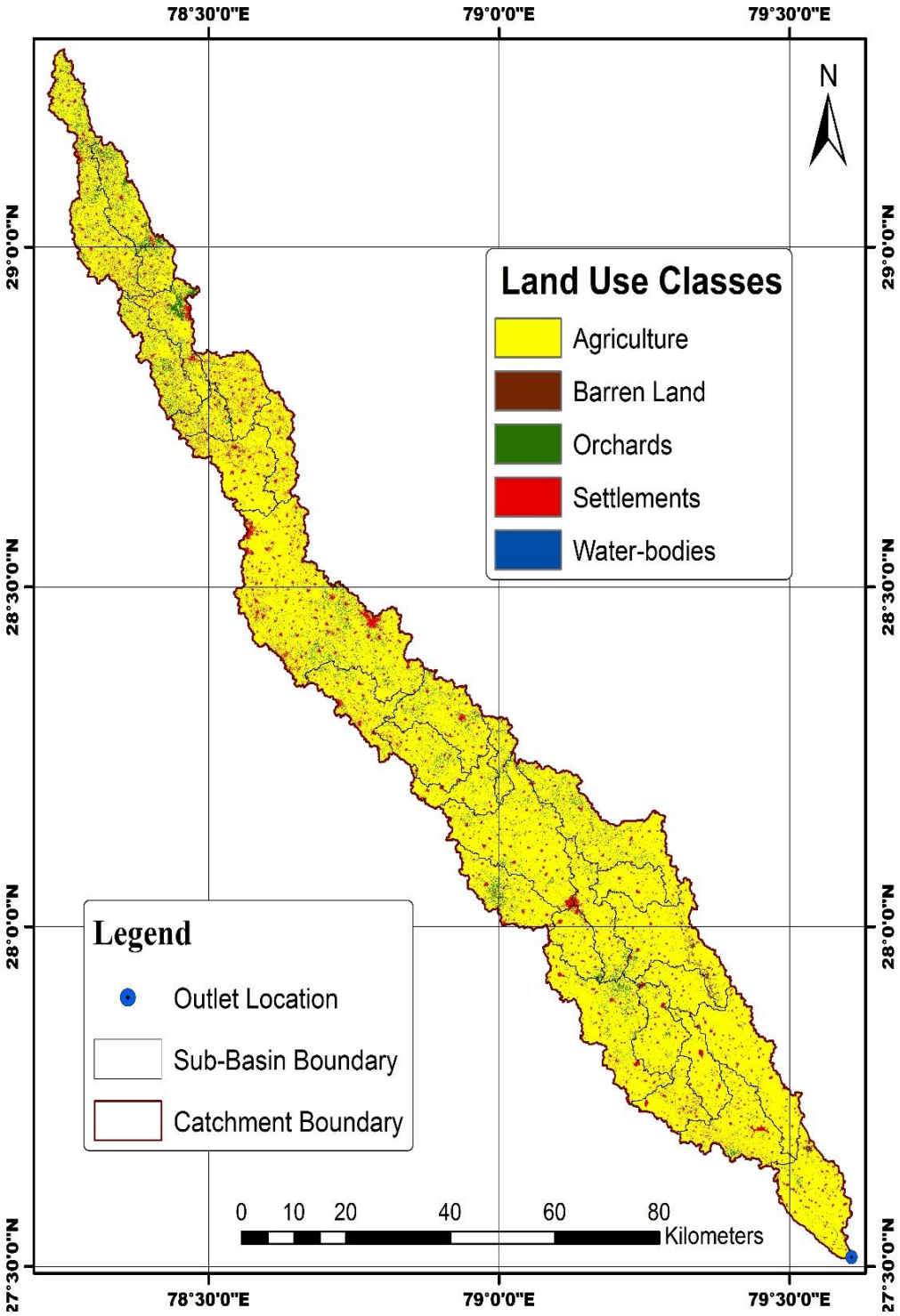

Figure 36c. LULC map of the Sot catchment for the year 2018

6.4 Results of modeling and prediction of river flows using ANN models

6.4.1 Identification of appropriate ANN Architecture

In modeling non-linear hydrological process, identification of appropriate architecture of ANN models is extremely important to get the accurate predicted values of river flow. In this research, the number of neurons in the hidden layer varied between 1 and 10 and models were trained based on the trial and error procedure. In general, networks with less number of hidden neurons are preferred, because they have better generalization capability and less over fitting problems. Input parameters and adopted ANN structure of different models is given in Table 6.

Table 6 Input parameters and adopted ANN structure of different model for Sot river

Model No.	Model Descriptions	No. of input parameters	No of Hidden layers	No of neurons in the hidden layer	Output layer	Model structure
1.	$Q_t = P_t$	1	1	8	1	1 1 8 1
2.	$Q_t = P_t, P_{t-1}$	2	1	5	1	2 1 5 1
3.	$Q_t = P_t, P_{t-1}, P_{t-2}$	3	1	7	1	3 1 7 1
4.	$Q_t = P_t, P_{t-1}, P_{t-2}, Q_{t-1}$	4	1	10	1	4 1 10 1

6.4.2 Predicting daily river flow using ANN models

The selected ANN models i.e. M1, M2, M3 and M4 models were calibrated (April, 2009 to December, 2014) and validated (Jan, 2015 to December, 2016) to predict daily river flow at Sot Basin. These models were calibrated and validated by utilizing different number of input parameters. The performance of the ANN model starts improving when the input vector includes the previous one day or lag 1 of river flow data. The performance of ANN models was assessed using correlation coefficient (R), root mean square error (RMSE), modified index of agreement (MIA) and modified Nash–Sutcliffe efficiency (MNSE) indicators, and through visual inspection by line and scatter diagrams. The value of R, RMSE, MIA and MNSE during calibration and validation periods for model 3 and 4 are summarized in Table 7. It is observed from the performance evaluation indices that ANN model 4 i.e., M4 with maximum R values (0.94 and 0.97), MNSE values (0.77 and 0.78), MIA values (0.88 and 0.89), and minimum RMSE values (0.39 and 0.45) during the calibration and validation period can be best suited for predicting river

flow of Sot river basin. Hence, it can be concluded the ANN model has the ability to solve highly complex non-linear river flow data prediction problems which can be further used for the generation of synthetic river flow data.

Figure 37 and 38 depicts the visual comparison of observed and model-predicted monthly river flow values for calibration and validation period by using line and scatter plot. It can be seen from Figure 37 that ANN model 3 (M3) over-predicted the daily river flow at low peaks and under-predicted at high peaks especially during validation period. A 1:1-line plot between the observed and predicted monthly river flow was drawn for the calibration and validation period, and R^2-value of the fitted linear trend was found to be 0.19 and 0.24 (See Figure 38). It was seen that the monthly river flow could not be adequately fitted by the developed ANN model, when the river flow values are not included as an input. In hydrological modeling, poor-fitting due to peaks and/or extremes are very common mainly due to high variation in rainfall as this may generate natural fluctuations over the physical scale, and natural variabilities associated with the river flow system (e.g., chaotic disturbances, random and non-stationary, complex and non-linear behaviors)

On the other hand, Figure 39 and 40 illustrates the visual comparison of observed and model-predicted monthly river flow values of ANN model 4 (M4) i.e. after including lag-1 river flow data for calibration and validation period by using line and scatter plot. It can be clearly observed from Figure 39 that ANN model 4 over-predicted the daily river flow at low peaks and under-predicted at high peaks especially during validation period. A 1:1-line plot between the observed and predicted monthly river flow was drawn for the calibration and validation period, and R^2-value of the fitted linear trend was found to be 0.89 and 0.93 (See Figure 40). It was observed that R^2-values drastically improved from model 3 (0.19 to 0.24) to model 4 (0.89 and 0.93) on inclusion of lag-1 river flow data during calibration and validation period, respectively. This illustrates satisfactory performance of the developed ANN model 4 in modeling river flow, except at very high peaks.

Table 7 Performance evaluation indices of Sot river flow data during calibration and validation period

	ANN model M3	**ANN model M4**

Performance evaluation indices	(without including river flow data as an input)		(with lag-1 river flow data as an input)	
	Calibration period	Validation Period	Calibration period	Validation Period
Correlation coefficient (R)	0.43	0.49	0.94	0.97
Modified Index of Agreement (MIA)	0.44	0.50	0.88	0.89
Root Mean Square Error (RMSE)	--0.02	0.06	0.39	0.45
Modified Nash-Sutcliffe Efficiency (MNSE)	0.20	0.26	0.77	0.78

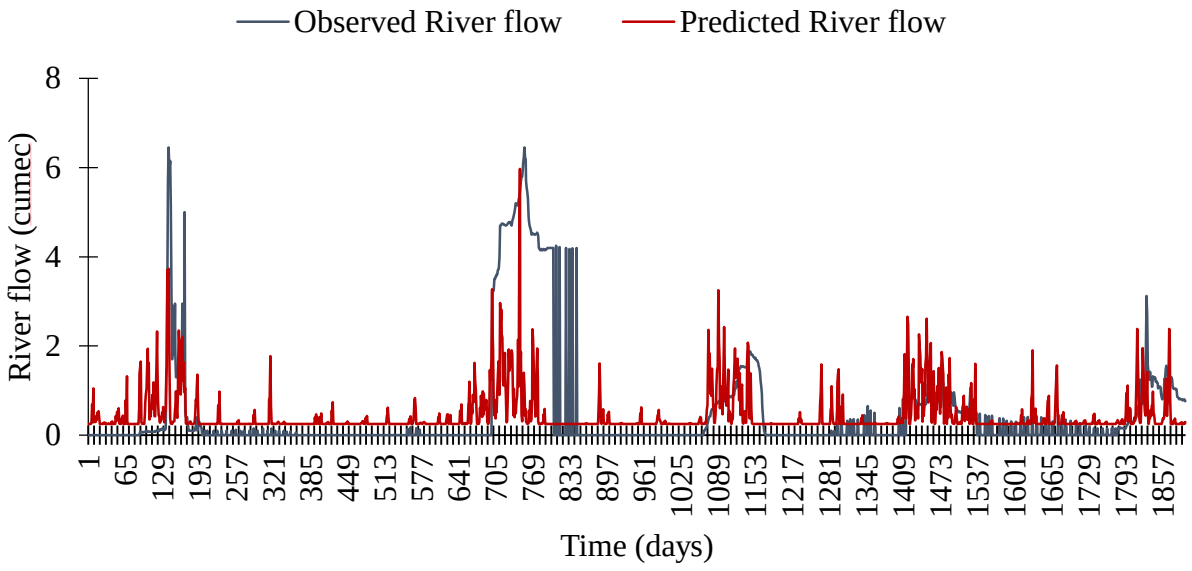

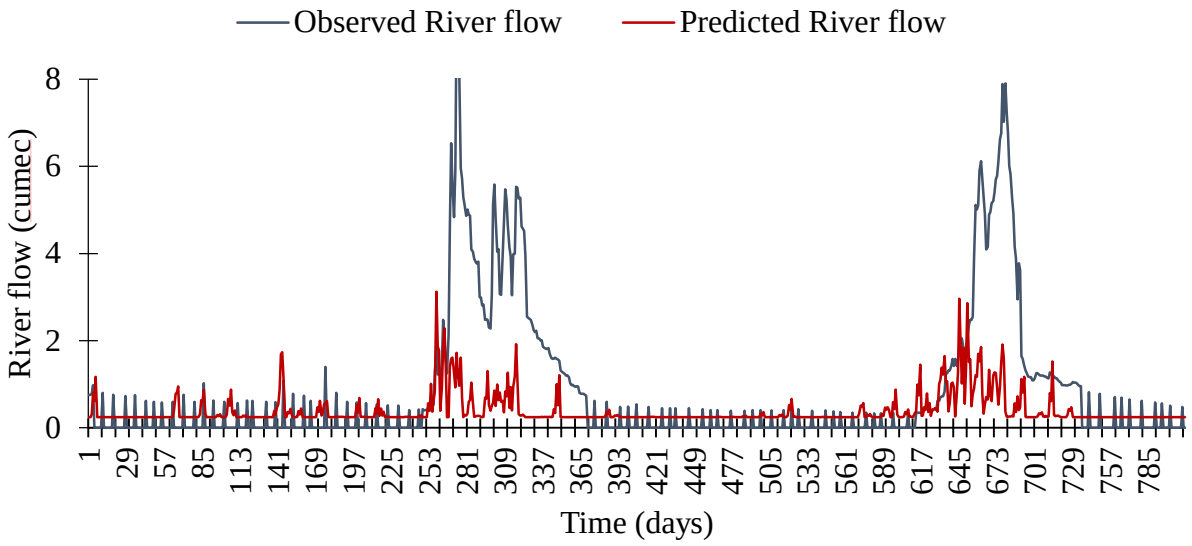

Figure 37. Line diagram of ANN model 3 (M3) between observed and predicted river flow (without including river flow)

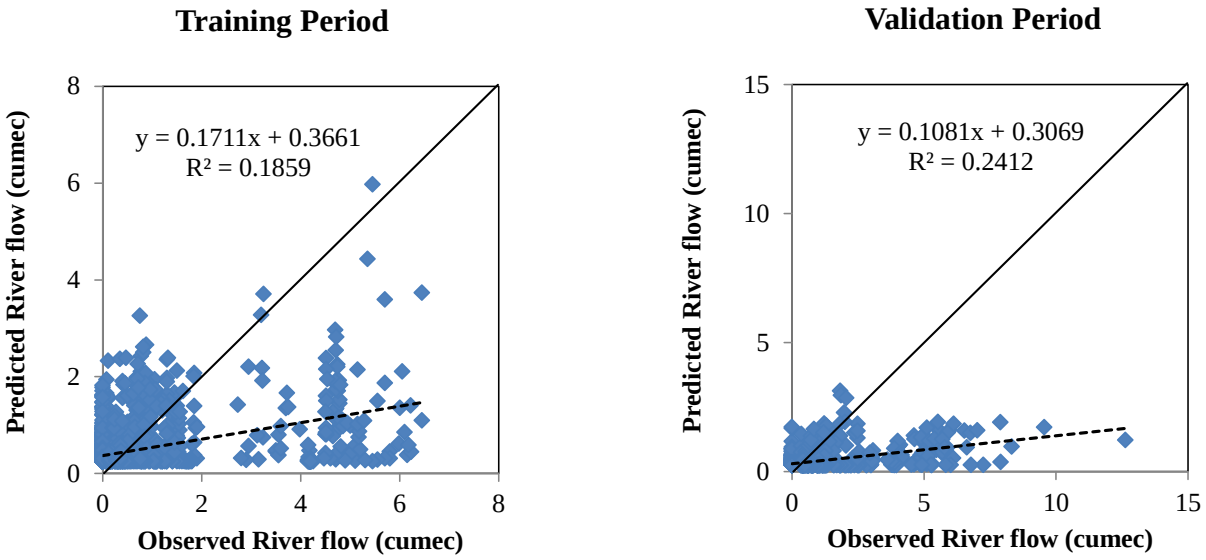

Figure 38. Scatter plot of model 3 (M3) between observed and predicted river flow data (without including river flow)

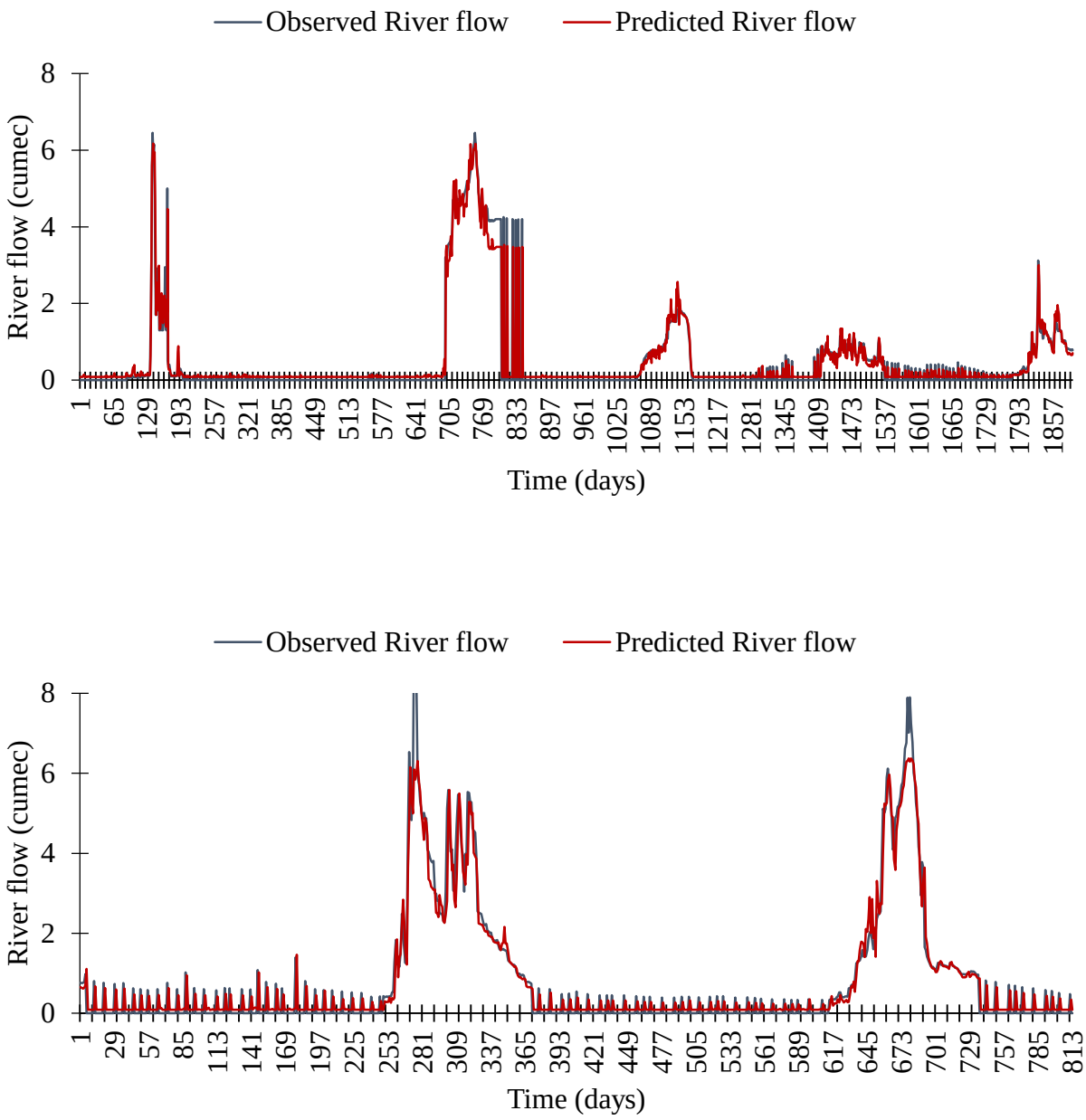

Figure 39. Line diagram of best fit model 4 between observed and predicted river flow data (with lag-1 river flow data as an input)

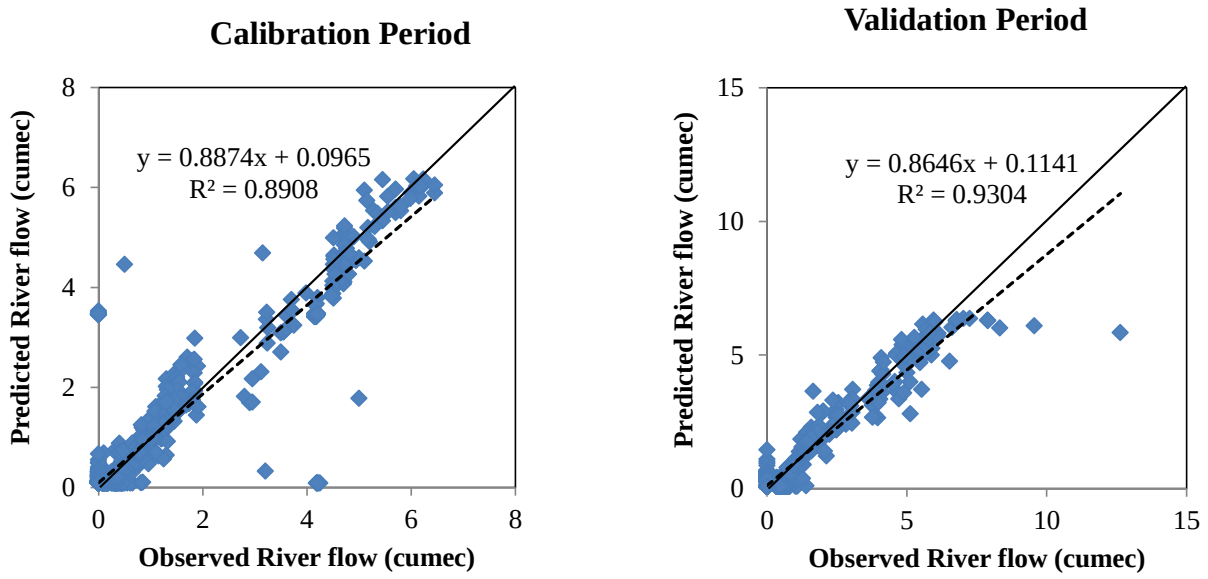

Figure 40. Scatter plot of best-fit model 4 between observed and predicted river flow data during calibration and validation period (with lag-1 river flow data as an input)

6.5 Results of river flow time series using SWAT model

6.5.1 SWAT model output

In this study, the SWAT model was run for the Sot catchment falling in the state of Uttar Pradesh. It was estimated that the average annual rainfall of the catchment is 867.10 mm, snowfall is 0 mm, surface runoff is 145.88 mm, lateral discharge is 0.54 mm, and groundwater discharge from shallow aquifers is 279.99 mm. The average value of total aquifer recharge is 294.04 mm. The evapotranspiration is 426.40 mm. A pictorial representation of the SWAT output with water balance components is shown in Fig. 41. From the Fig. 41, it is clearly observed that, on an average, more than 45 % of the total rainfall water is lost in surface runoff and evapotranspiration.

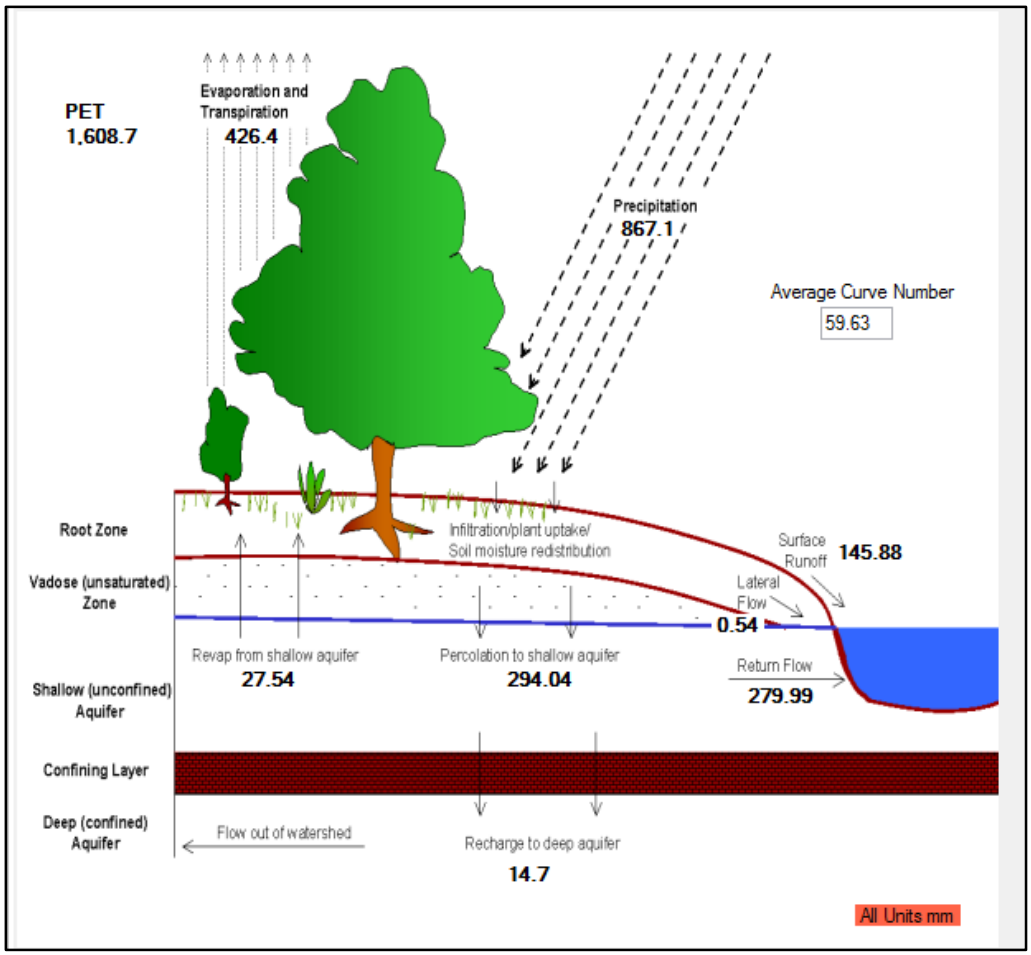

Figure 41 Pictorial representation of SWAT output

6.5.2 Calibration and Validation results for the SWAT model

In this study, first six years (2009 to 2014) of the monthly river flow data was used to calibrate the SWAT model with a 2-year warm-up period from 2009 and 2010 by using SWAT-CUP's SUFI-2 algorithm. Initially, a total of eight parameters such as initial runoff curve number to moisture condition II (CN2), base flow alpha factor (ALPHA_BF), groundwater delay time (GW_DELAY), threshold depth of water in the shallow aquifer for return flow to occur (GWQMN), Manning's "n" value for the main channel (CH_N2), effective hydraulic conductivity in the main channel alluvium (CH_K2), available water capacity of the soil layer (SOL_AWC), saturated hydraulic conductivity (SOL_K) were selected with their minimum and maximum values and updated in the *par.info file*. The results of the parameter sensitivity analysis are identified and presented in Table 8 which shows that the 6 most sensitive parameters related to river flow simulation at outlet of the Sot River catchment among the 8 input parameters. The most sensitive parameters are shown from

the least to the most sensitive, based on their p-values. Table 9 represents the minimum and maximum values of the parameters considered for model calibration in the present study. The calibration process was initiated for 2000 simulations by giving the two years of warm up period for getting the better results.

Table 8 Most sensitive parameters for river flow simulation in the Sot river catchment.

S. No.	Parameter name	Description	Rank	p-value
1	GW_DELAY	Groundwater delay (d)	6	1.23E-06
2	SOL_AWC	Available water capacity of the soil layer	5	1.30E-09
3	CH_K2	Effective hydraulic conductivity in main channel alluvium	4	5.21E-21
4	CN2	SCS runoff curve number	3	1.04E-91
5	ALPHA_BF	Base flow alpha factor	2	9.62E-155
6	CH_N2	Manning's n value for the main channel	1	1.55E-269

The calibration of model is the adjustment of the selected model parameters on the basis of characteristics of watershed or river basin, within the recommended ranges. The calibration is used for the optimization of the model output so the simulated values, obtained from calibration matches with the observed datasets. Calibration provides fitted values of initially selected parameters. Table 9 represents the results of final auto-calibrated values of fitted sensitive parameters. All these parameters can be adjusted manually or automatically until the simulated values best matches with the observed datasets.

The comparison between the observed and simulated river flows was carried out using both graphical approach and quantitative statistics. Table 10 provides a statistical summary of the relationship between observed and simulated river flows over the calibration and validation period based on the performance measurement indices. These performance indices gave satisfactory results between the observed and simulated river flows with statistical values of R (0.73 and 0.84) and NSE (0.49 and 0.63) during the calibration and validation period. The SUFI-2 results indicated that the p-factor for the calibration period was 0.47, while it was 0.80 for the validation period. This means that 47 and 80 % of the data measured during calibration and validation period respectively captured or considered for the correct simulated river flow by the model while the

remaining occur due to errors in input data such as rainfall, temperature, etc. The r-factor that measures the quality of the calibration and the thickness of the 95 ppu is 10.59 for calibration and 5.83 for validation period respectively indicating the performance of the model as average. The hydrograph of the daily observed and simulated river flow with their rainfall values during calibration and validation period are shown in Fig. 42. Scatter plot between daily observed and simulated river flow for the calibration and validation period of the Sot river catchment is shown in Fig. 43.

Table 9 Results of final auto-calibration values of fitted sensitive parameters.

Sr. No.	Parameter name	Description	Minimum	Maximum	Fitted value
1	CN2	SCS runoff curve number	-0.2	0.2	-0.086
2	GW_DELAY	Groundwater delay (d)	0	500	0.062
3	GWQMN	Threshold depth of water in the shallow aquifer required for return flow to occur (mm)	0	2	306.425
4	ALPHA_BF	Base flow alpha factor	0	1	0.657
5	SOL_AWC	Available water capacity of the soil layer	-0.2	0.2	-0.167
6	SOL_K	Saturated hydraulic Conductivity	-0.2	0.2	-0.154
7	CH_N2	Manning's n value for the main channel	-0.01	0.3	0.005
8	CH_K2	Effective hydraulic conductivity in main channel alluvium	-0.01	500	193.869

Table 10 Statistical summary of the relationship between observed and simulated river flows during the calibration and validation period

Period	Performance evaluation indices				
	p-factor	r-factor	R^2	NSE	MSE
Calibration	0.47	10.59	0.73	0.49	1
Validation	0.8	5.83	0.84	0.63	0.91

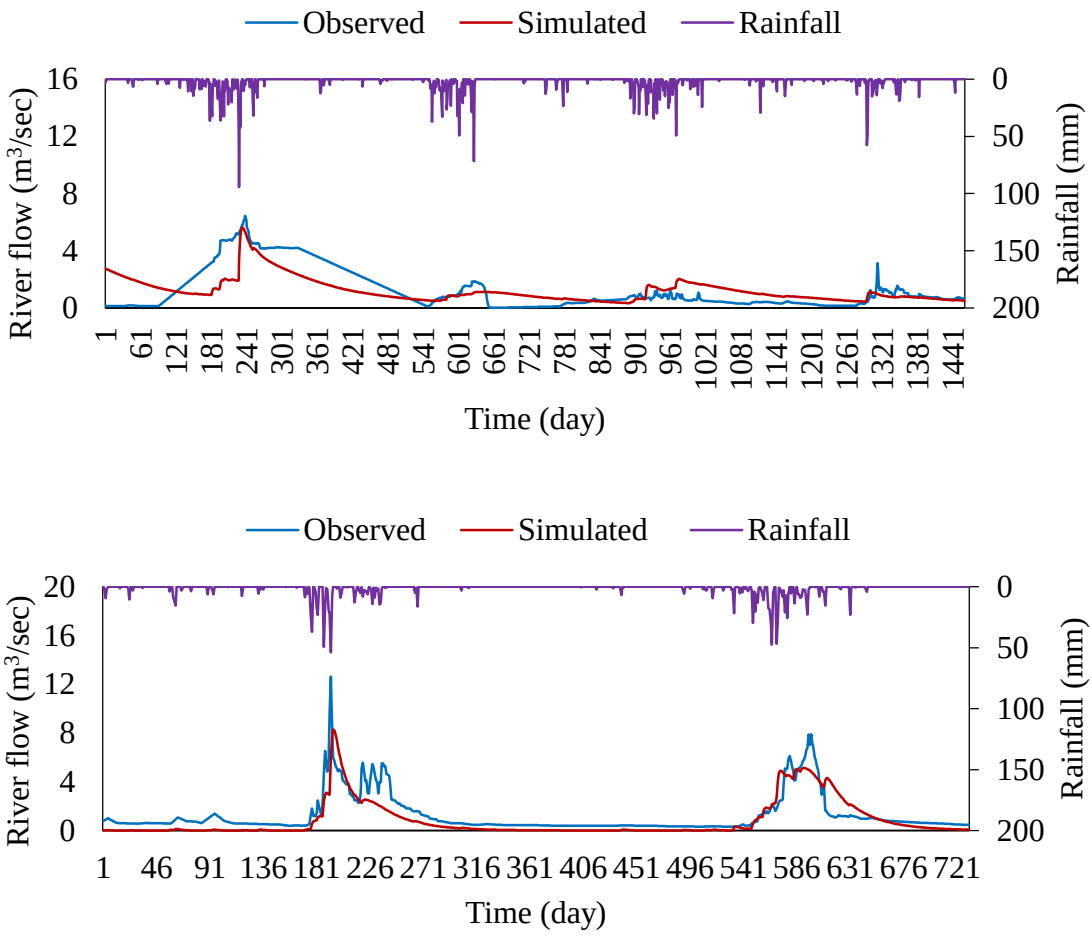

Fig. 42 Hydrographs of the daily observed and simulated river flow during the calibration and validation period

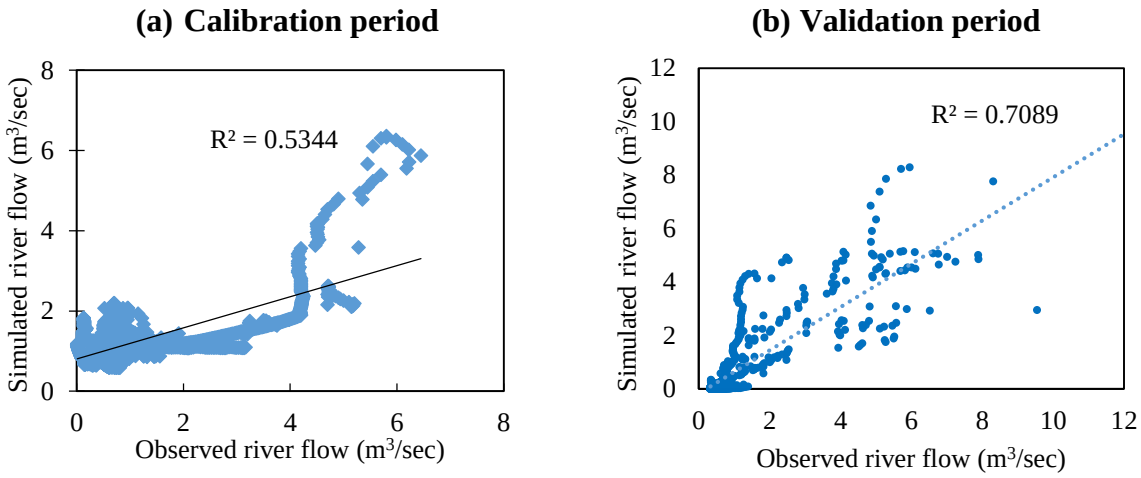

Fig. 43 Scatter plot between daily observed and simulated river flow during the calibration and validation period

6.6 Results of groundwater modeling using MODFLOW

6.6.1 Model Calibration

The MODFLOW model parameters were calibrated in the following ways:

a) First hand calibration of the initial guess values of parameters are considered with initial groundwater levels with no external stresses on the modelling domain, and allowing model to run for a long duration till it reaches to steady state condition;

b) Refinement of the first hand calibrated values of the parameters considering transient state of the domain with a particular set of observed data and by considering all input stresses acting on the domain;

c) Validation of the model's responses comparing with another set of observed data considering refined calibrated values of the parameters.

To develop the MODFLOW simulation model, the parameters were calibrated for the transient state condition by comparing the computed heads with the observed heads. The calibrated parameters were thereafter validated with another set of computed and observed heads. The acceptability of a model's parameters calibration is usually a subjective measure, and must be calibrated to different conditions. However, there are some generally accepted methods of evaluating and interpreting the model calibration using both qualitative and quantitative measures viz. residual mean (RM), absolute residual mean (ARM), standard error of the estimate (SE), root

mean squared error (RMSE), normalized root mean squared error (NRMSE), correlation coefficient (CC), etc. If the responses of the model corresponding to the parameters assumed for calibration were found acceptable with these criteria, then the model's parameters and the setting of the model were said to be calibrated. The calibration of the model was thus a trial and error approach.

The data period length of nine years' period (2009-2018) was used for model simulation. Of which, the period from June, 2009 to May, 2014 was used for calibration and the period from June, 2014 to October, 2018 was used for validating the flow model. For calibration of the model parameters, i.e., hydraulic conductivities, $K_{xx,}$ K_{yy}, and K_{zz} and storage coefficients, $S_{xx,}$ S_{yy}, and S_{zz}; input stresses namely, rainfall recharge, flows through boundaries, and groundwater withdrawals were used for the period from June, 2009 to October, 2018.

For comparison of the simulated model's responses (in terms of heads) with the observed ones, data of 212 observation wells distributed within the study area were used. Making use of the inputs stresses, boundary conditions and initial heads as explained above, the model parameters were calibrated for the period 2009 to 2014. The time length of each stress period was considered 30 days, which indicates that all input and output stresses are uniform within each month, and the simulation was carried out by setting a transient-state condition. Depending upon the data, there were total 71 stress periods. In each stress period, there were 10 time-steps with multiplier of 1.0. The simulation was carried out by setting a transient-state flow model.

After a large number of model runs by changing and optimizing the system parameter values, a quite improved 1:1 plot of calculated heads versus observed heads of various wells was obtained. The 1:1 plots of the calculated heads versus observed heads for the calibration period of the 1^{st}, 913^{rd} and 1827^{th} day are shown in **Figures 44(a) to (c),** respectively. The statistical values of these plots during the calibration period namely, RM (residual mean) ranges between -0.367 and 0.476 m, ARM (absolute residual mean) ranges between 1.658 and 1.988 m, SE (std. error of the estimate) ranges between 0.164 and 0.199 m, RMSE ranges between 2.398 and 2.89 m, NRMSE ranges between 2.516 and 2.983 % and the correlation coefficient that ranges between 0.994 and 0.996 were also indicated in these figures. The histogram **[Figures 45 (a) to (c)]** of residuals between the observed and computed heads for the calibration period showed almost normal distribution, which implied a close agreement of error distribution.

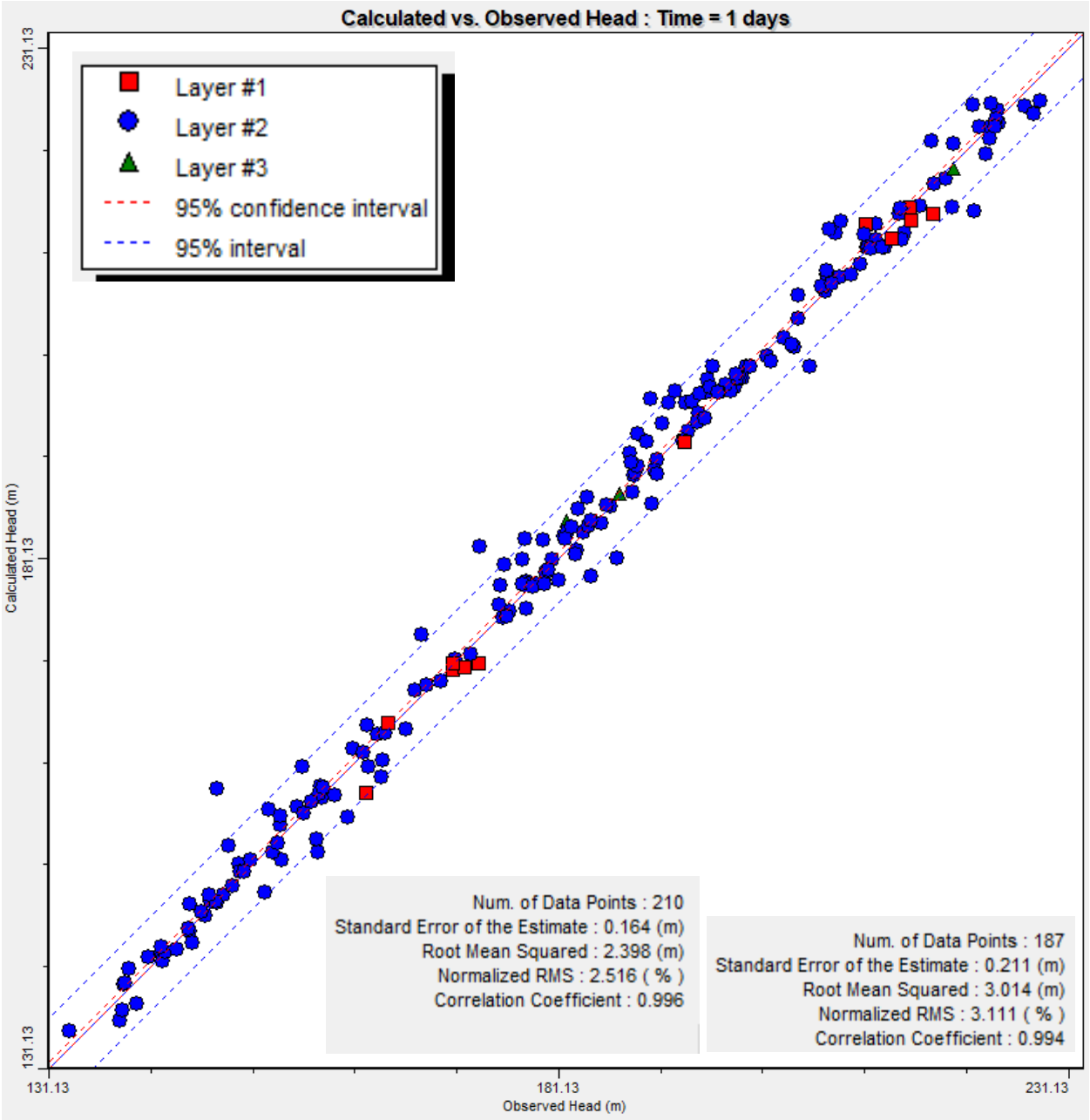
Calculated vs. Observed Head : Time = 1 days
Layer #1
Layer #2
Layer #3
95% confidence interval
95% interval
Num. of Data Points : 210
Standard Error of the Estimate : 0.164 (m)
Root Mean Squared : 2.398 (m)
Normalized RMS : 2.516 (%)
Correlation Coefficient : 0.996
Num. of Data Points : 187
Standard Error of the Estimate : 0.211 (m)
Root Mean Squared : 3.014 (m)
Normalized RMS : 3.111 (%)
Correlation Coefficient : 0.994
Calculated Head (m)
231.13
181.13
131.13
131.13
181.13
231.13
Observed Head (m)

(a)

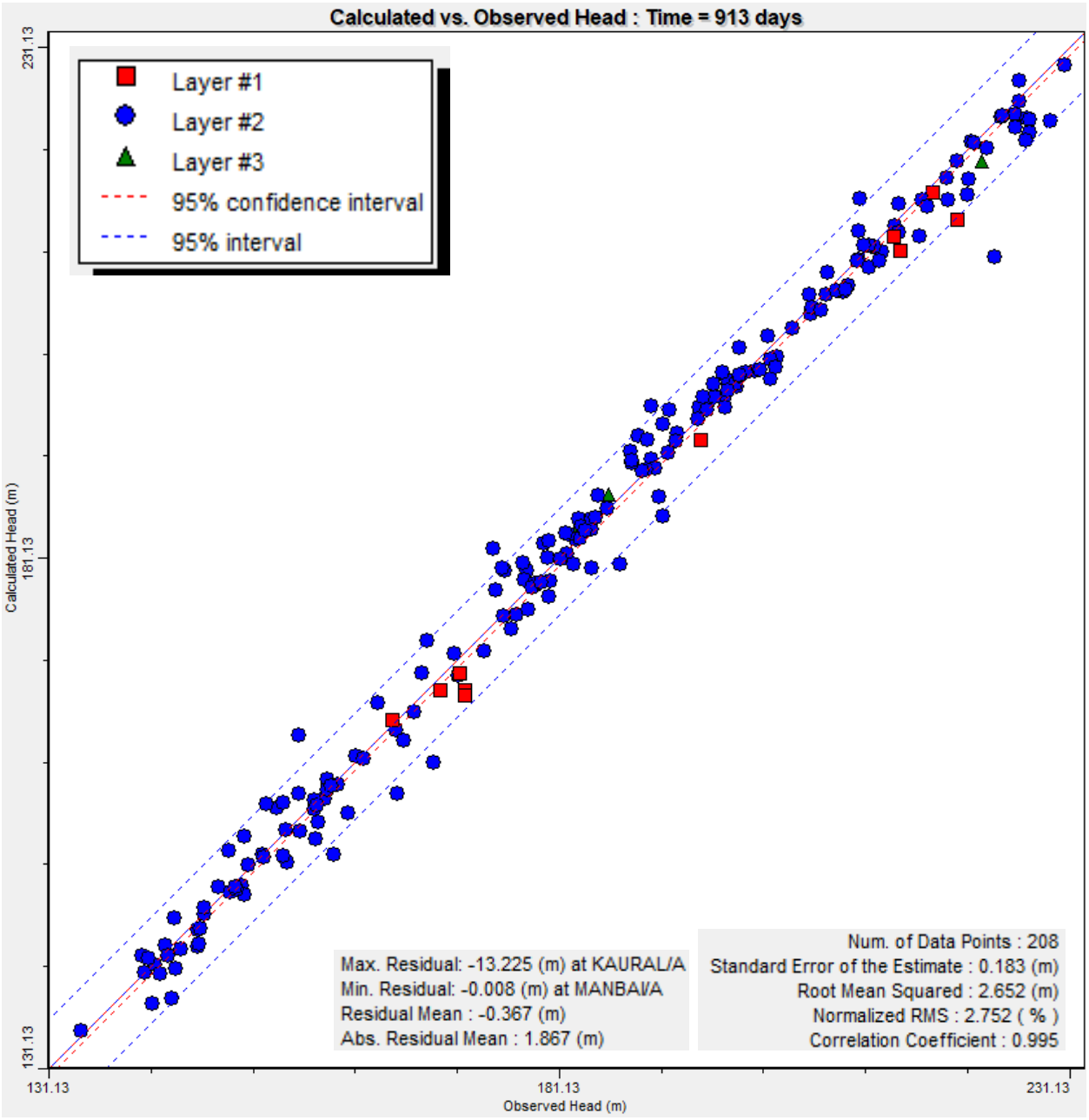
Calculated vs. Observed Head : Time = 913 days
Layer #1
Layer #2
Layer #3
95% confidence interval
95% interval
Max. Residual: -13.225 (m) at KAURAL/A
Min. Residual: -0.008 (m) at MANBAI/A
Residual Mean : -0.367 (m)
Abs. Residual Mean : 1.867 (m)
Num. of Data Points : 208
Standard Error of the Estimate : 0.183 (m)
Root Mean Squared : 2.652 (m)
Normalized RMS : 2.752 (%)
Correlation Coefficient : 0.995
Calculated Head (m)
231.13
181.13
131.13
131.13
181.13
231.13
Observed Head (m)

(b)

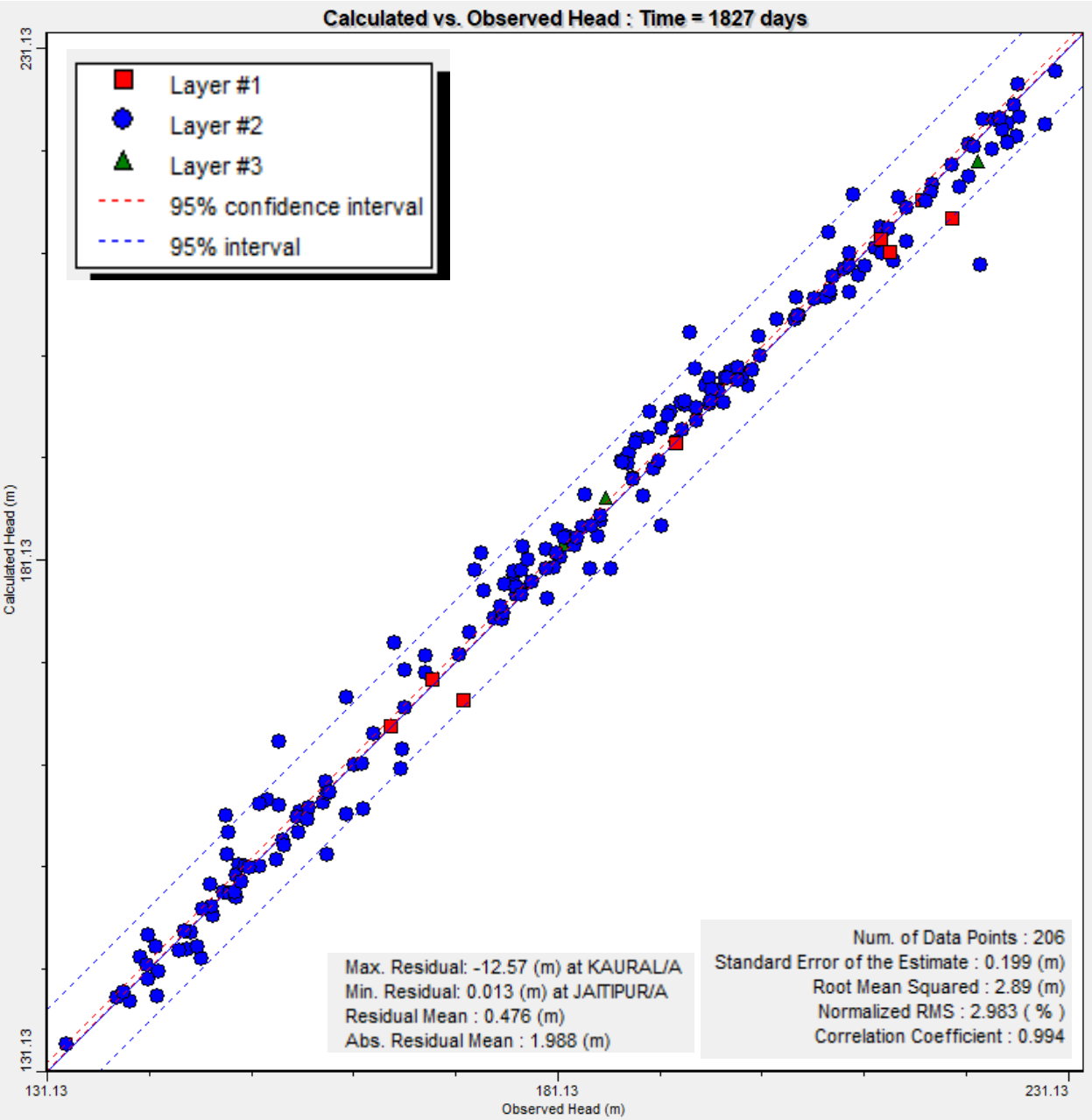

(c)

Figure 44. 1:1 plot of computed and observed heads during the calibration period for the (a) 1st day, (b) 913th day, and (c) 1827th day of simulation.

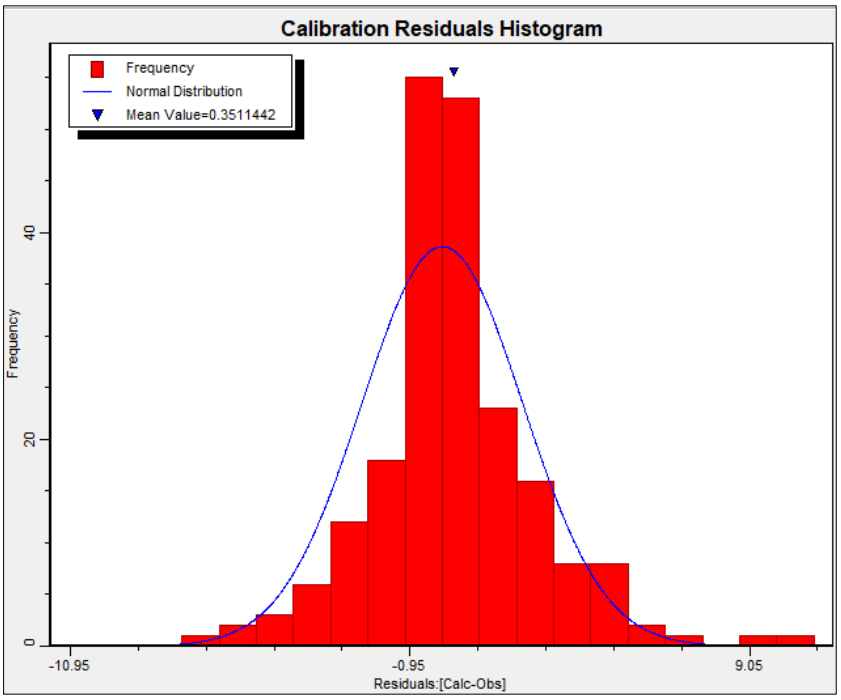
Calibration Residuals Histogram
Frequency
Normal Distribution
Mean Value=0.3511442
Frequency
0
20
40
-10.95
-0.95
9.05
Residuals:[Calc-Obs]

(a)

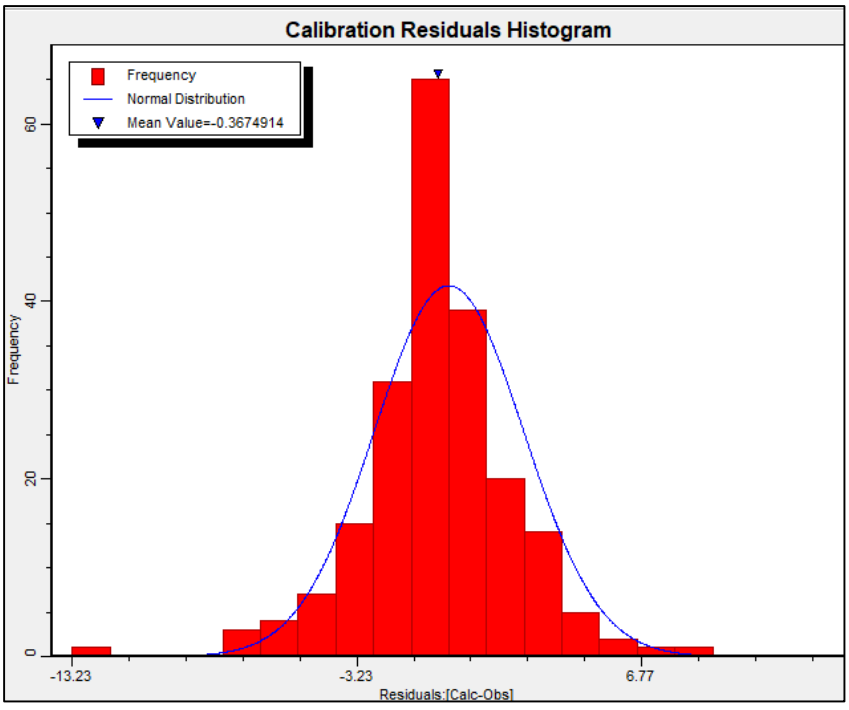
Calibration Residuals Histogram
Frequency
Normal Distribution
Mean Value=-0.3674914
Frequency
0
20
40
60
-13.23
-3.23
6.77
Residuals:[Calc-Obs]

(b)

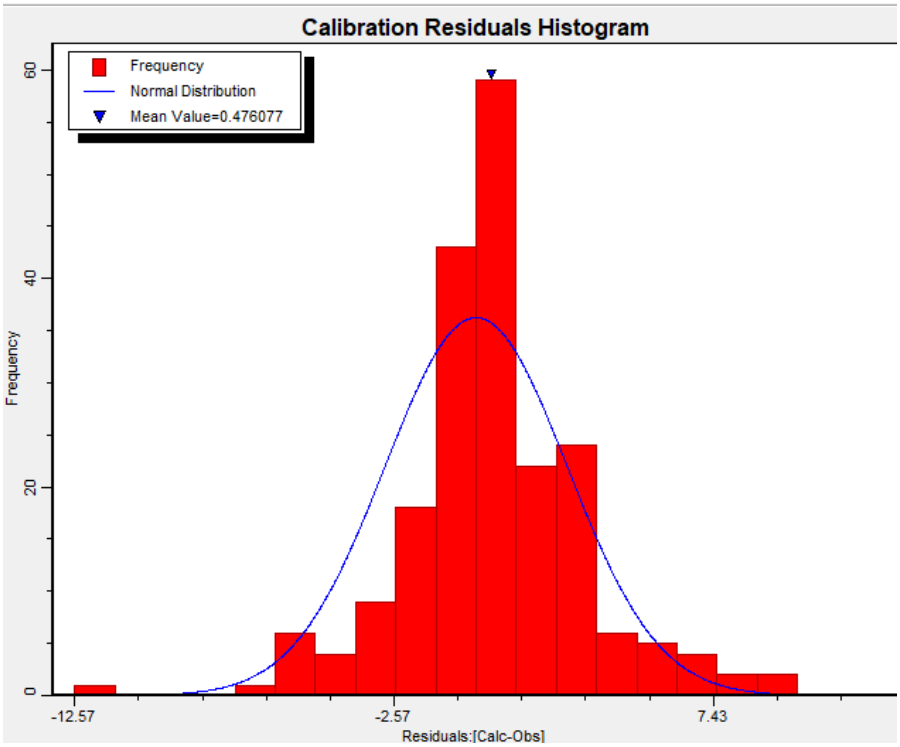

(c)

Figure 45. Histogram of residuals during the calibration period (a) 1st day, (b) 913rd day, and (c) 1827th day of simulation.

The temporal variation of calculated and observed heads of groundwater levels for few locations corresponding to the calibrated parameters was shown in **Figure 46. Figure 46** indicates that the observed and the computed groundwater table profiles are matching reasonably well. The hydraulic properties namely: hydraulic conductivity, specific yield and specific storage corresponding to these scenarios are taken as the calibrated parameters of the aquifer. The calibrated parameters are presented in **Table 11** and **Table 12.**

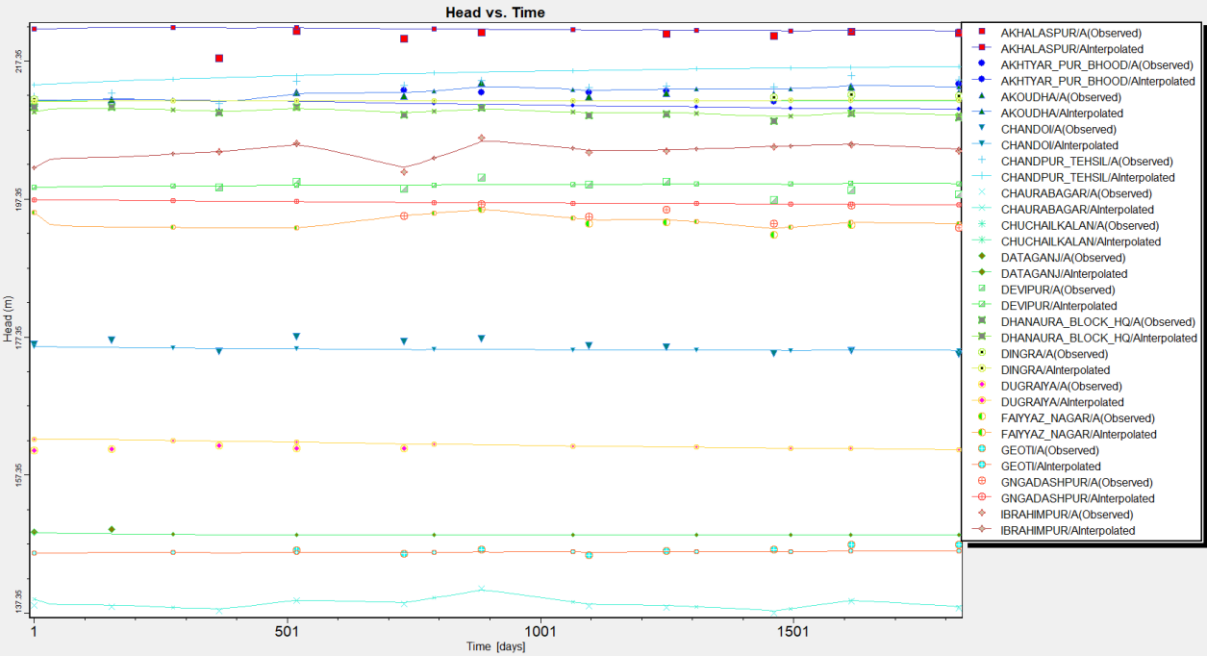

Figure 46. Comparison of temporal variation of computed and observed heads of groundwater table of various wells during the calibration period.

The temporal variation of calculated and observed heads of groundwater levels for few individual groundwater observation wells corresponding to the calibrated parameters is shown in **Figure 47(a) to 47(d).**

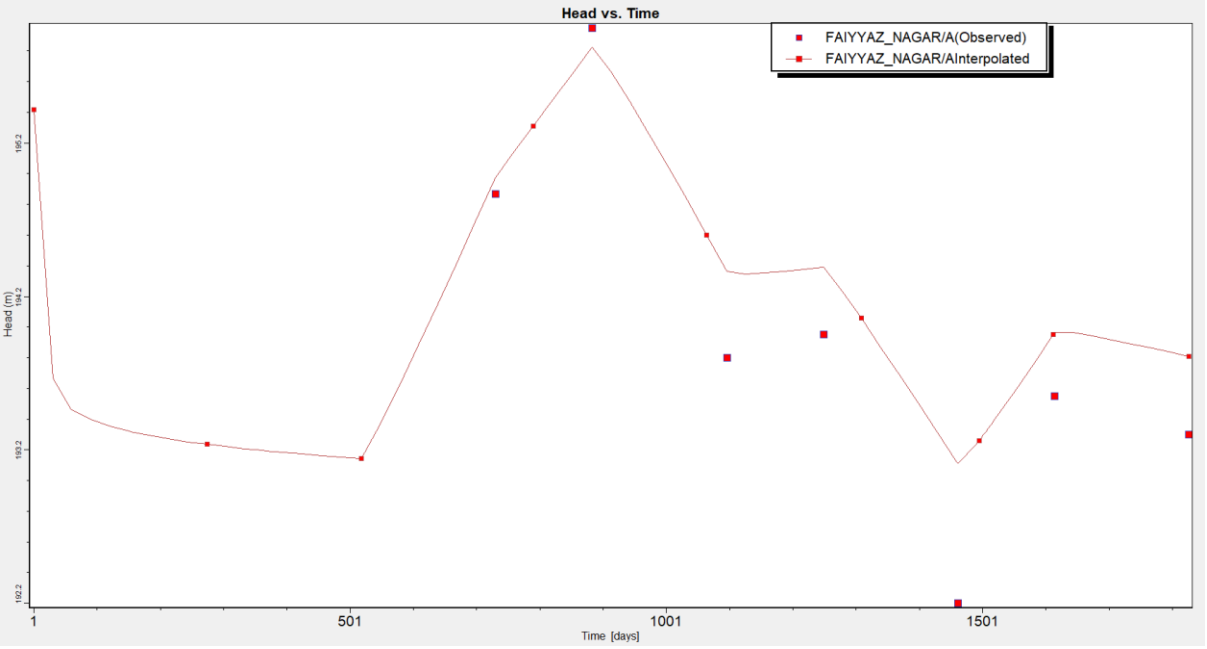

Figure 47(a). Variation of groundwater table for the observation well located at Faiyyaz Nagar.

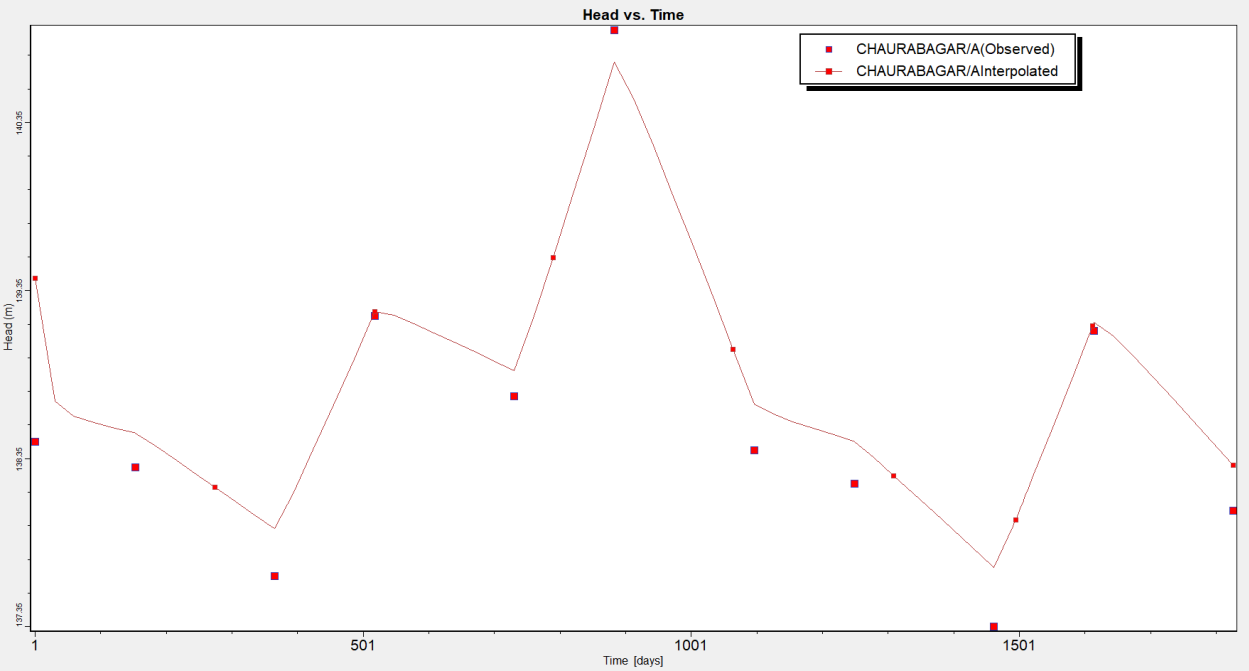

Figure 47(b). Variation of groundwater table for the observation well located at Chaurabagar.

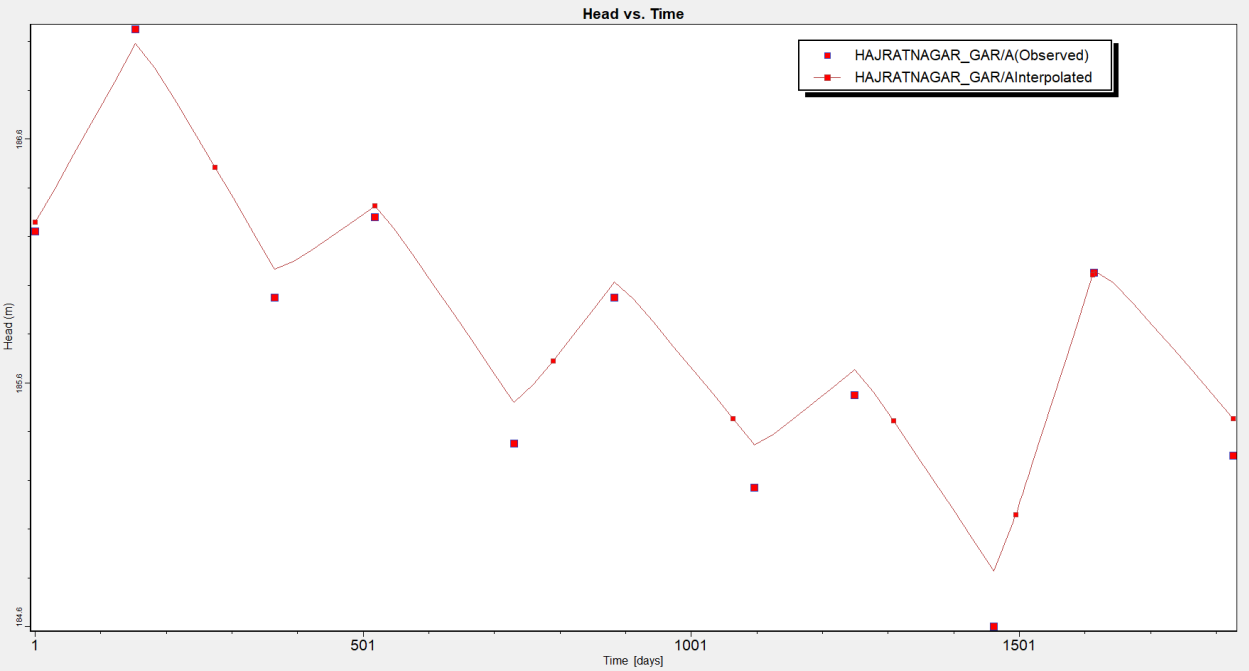

Figure 47(c). Variation of groundwater table for the observation well located at Hajratnagar.

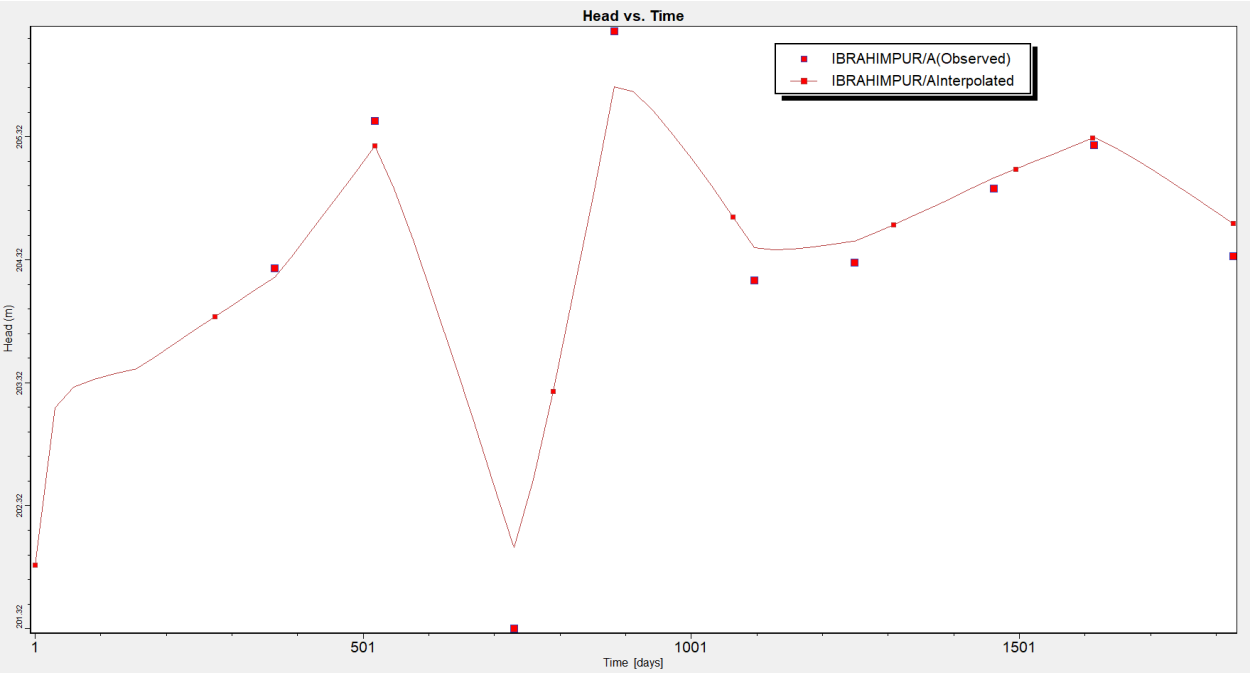

Figure 47(d). Variation of groundwater table for the observation well located at Ibrahimpur.

The spatial groundwater level variation in the modelling area corresponding to t=1827 days is presented in **Figure 48**. The groundwater flow direction map is presented in **Figure 49**. It is seen from **Figure 48** that, in general, groundwater levels are higher in the north-west part of the study area. In south-east part of the area, groundwater levels are shallow. On moving from north-west to south-east, groundwater levels decrease. It is also seen from **Figure 49** that the broadly the groundwater flow direction is towards the south-eastern side.

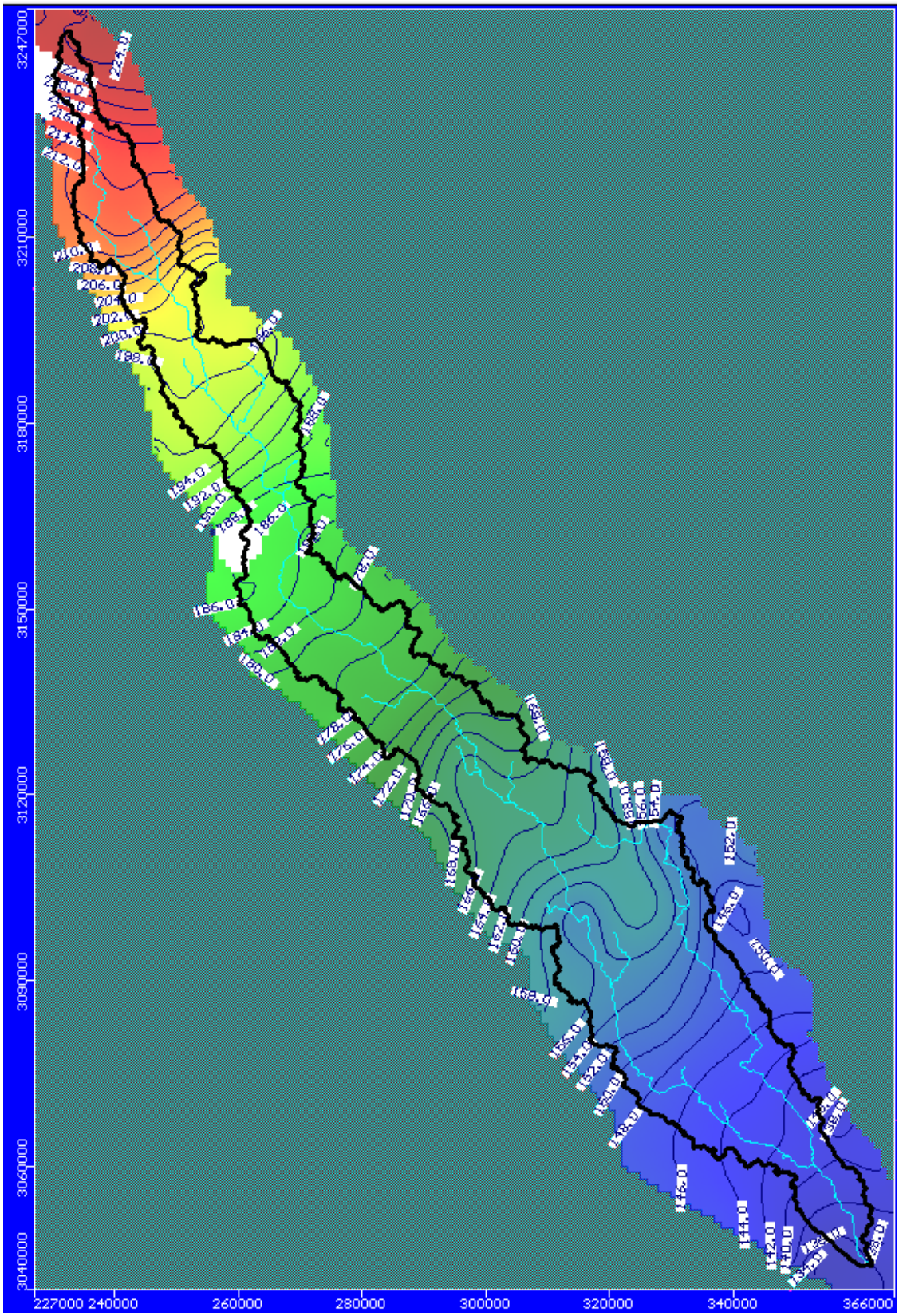

Figure 48. Spatial variation of groundwater heads in the modelling area.

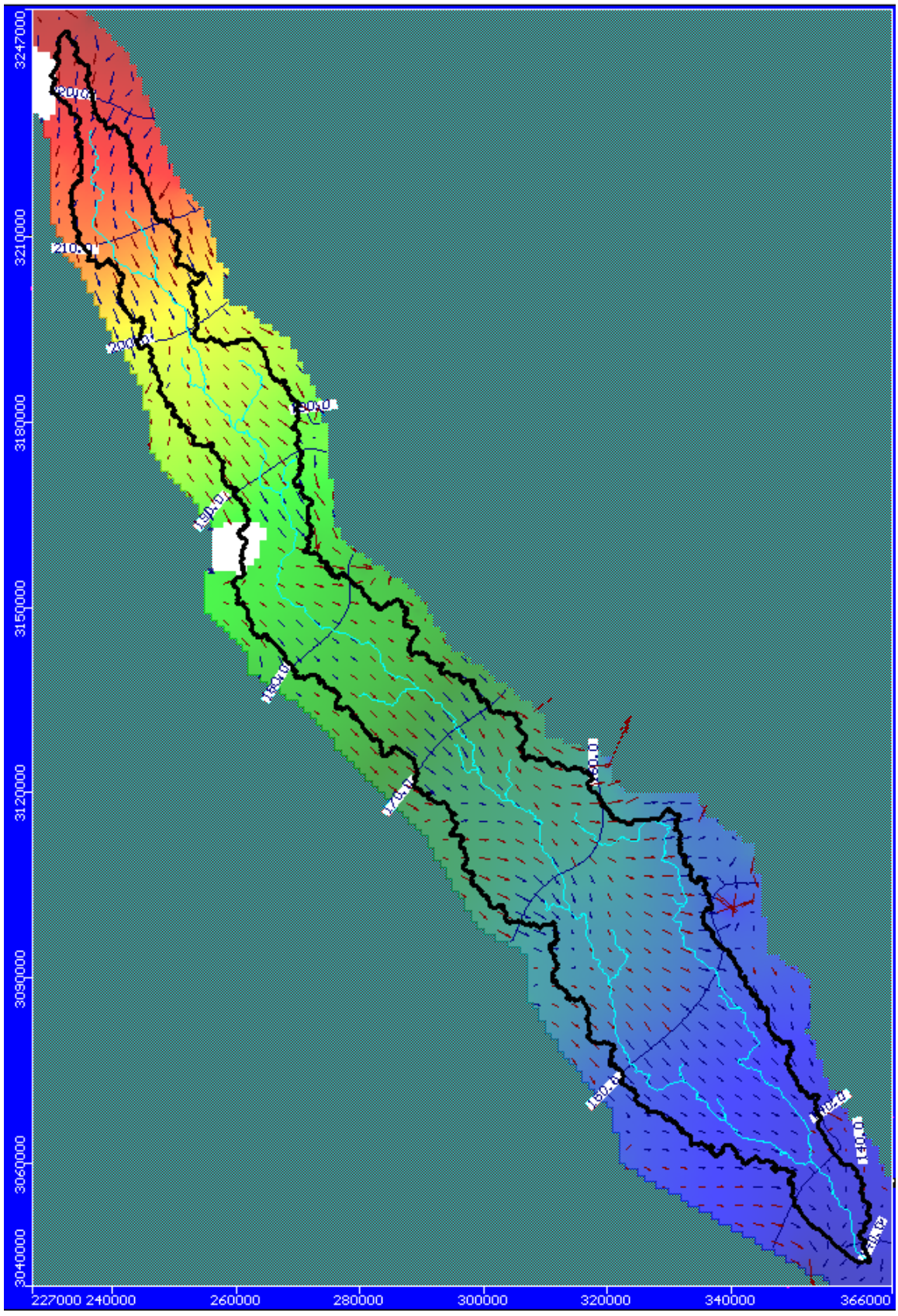

Figure 49. Velocity vectors showing groundwater flow direction in the modelling area.

The spatial variation of groundwater table elevation in the study area is presented in **Figure 50**. The water table elevation varies from 136 to about 224 m above mean sea level. In general, the water table elevation in north-western side is higher and reduces towards south-eastern side.

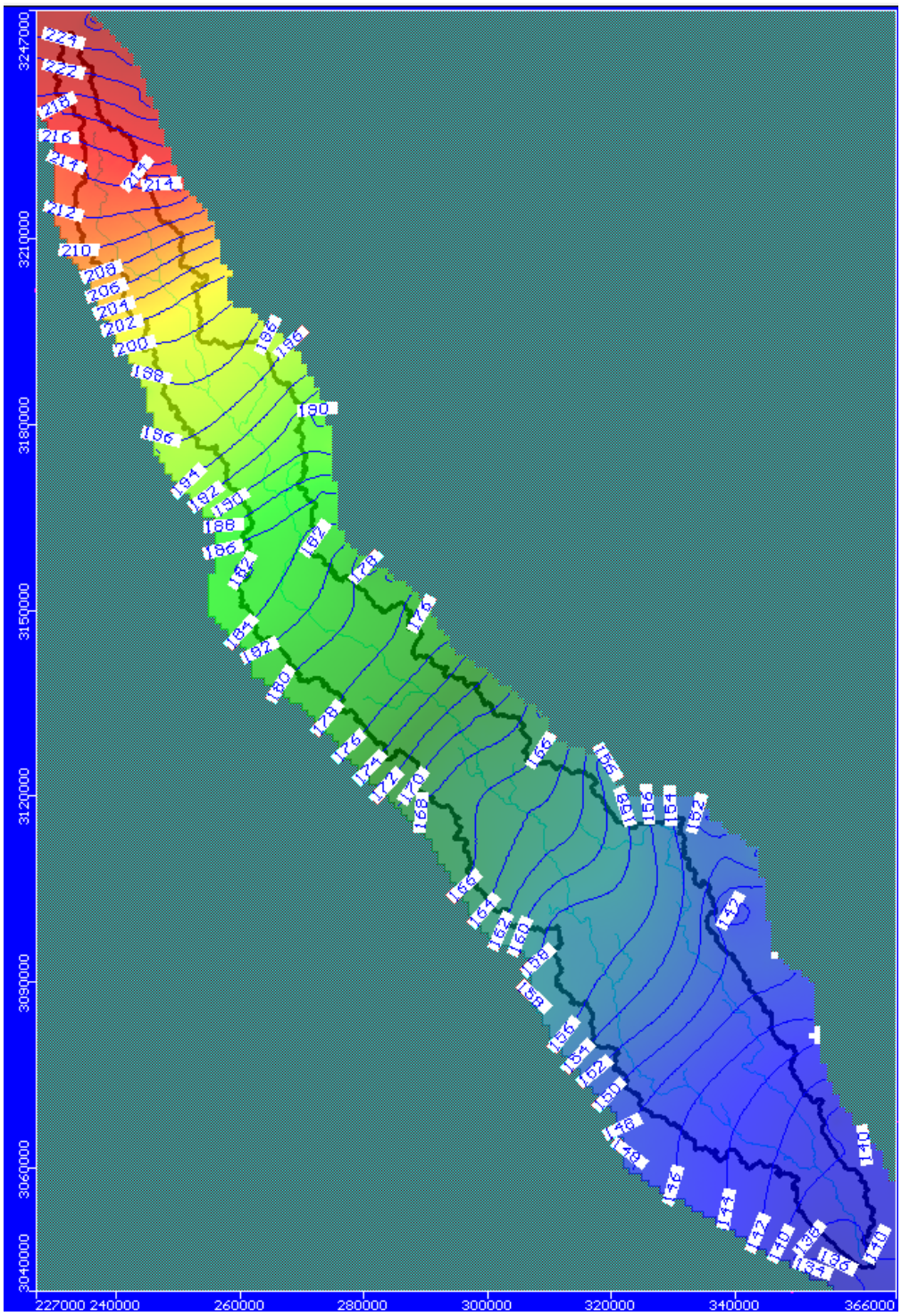

Figure 50. Spatial variation of water table elevation in the modelling area.

Figures 44 to 47 demonstrate that the observed and the computed groundwater table profiles matched satisfactorily, which establishes the calibration of the developed model reasonably well. The hydraulic properties namely: hydraulic conductivity, specific yield and specific storage corresponding to these calibrated results, which were optimized after a number of trial runs and finally obtained as the calibrated parameters of the aquifer are given in **Table 11** and **12**. This calibrated model can now be used for validation purpose.

Table 11. Calibrated conductivity values for different model layers

Layer	Type of layer	Horizontal hydraulic conductivity $K_{xx} = K_{yy}$ (m/day)	Vertical hydraulic conductivity, K_{zz} (m/day)
1	Top Soil	6.64	0.664
2	Unconfined Aquifer	83.0	8.30
3	Aquitard	4.70	0.47
4	Confined Aquifer	52.0	5.20

Table 12. Calibrated storage parameters for different model layers

Model Layer	Specific Storage (1/m)	Specific Yield (dimensionless)
Layer-1	-	0.12
Layer-2	0.0001	0.23
Layer-3	1E-6	-
Layer-4	0.0001	-

6.6.2 Model Validation

The above-mentioned calibrated groundwater flow model was validated for the period 2009-2018. For the validation purposes, all the stresses and boundary conditions for the period from June, 2014 to October, 2018 were considered. The time length of each stress period was considered 30 days, which indicates that all input and output stresses are uniform within each month, and the simulation was carried out by setting a transient-state condition. Depending upon the data, there were total 99 stress periods. In each stress period, there were 10 time-steps with multiplier of 1.0. The simulation was carried out by setting a transient-state flow model. The same calibrated hydraulic conductivity values, specific yield and specific storage, as used in the calibration process, was used for validating the model. **Figures 51 and 52** show the 1:1 plots of the computed

heads versus observed heads of various observation wells during the validation period for the 1st, 822nd and 1615th day, respectively. The statistical values of these plots namely, RM (residual mean) ranges between 0.885 and 2.262 m, ARM (absolute residual mean) ranges between 2.354 and 3.211 m, SE (std. error of the estimate) ranges between 0.211 and 0.302 m, RMSE ranges between 3.104 and 4.65 m, NRMSE ranges between 3.111 and 4.631 % and the correlation coefficient that ranges between 0.988 and 0.994 were also indicated in these figures. These statistical criteria values as well as the histogram **(Figure 52)** of residuals near normal distribution between the observed and computed heads implied a close agreement of error distribution for the validation period.

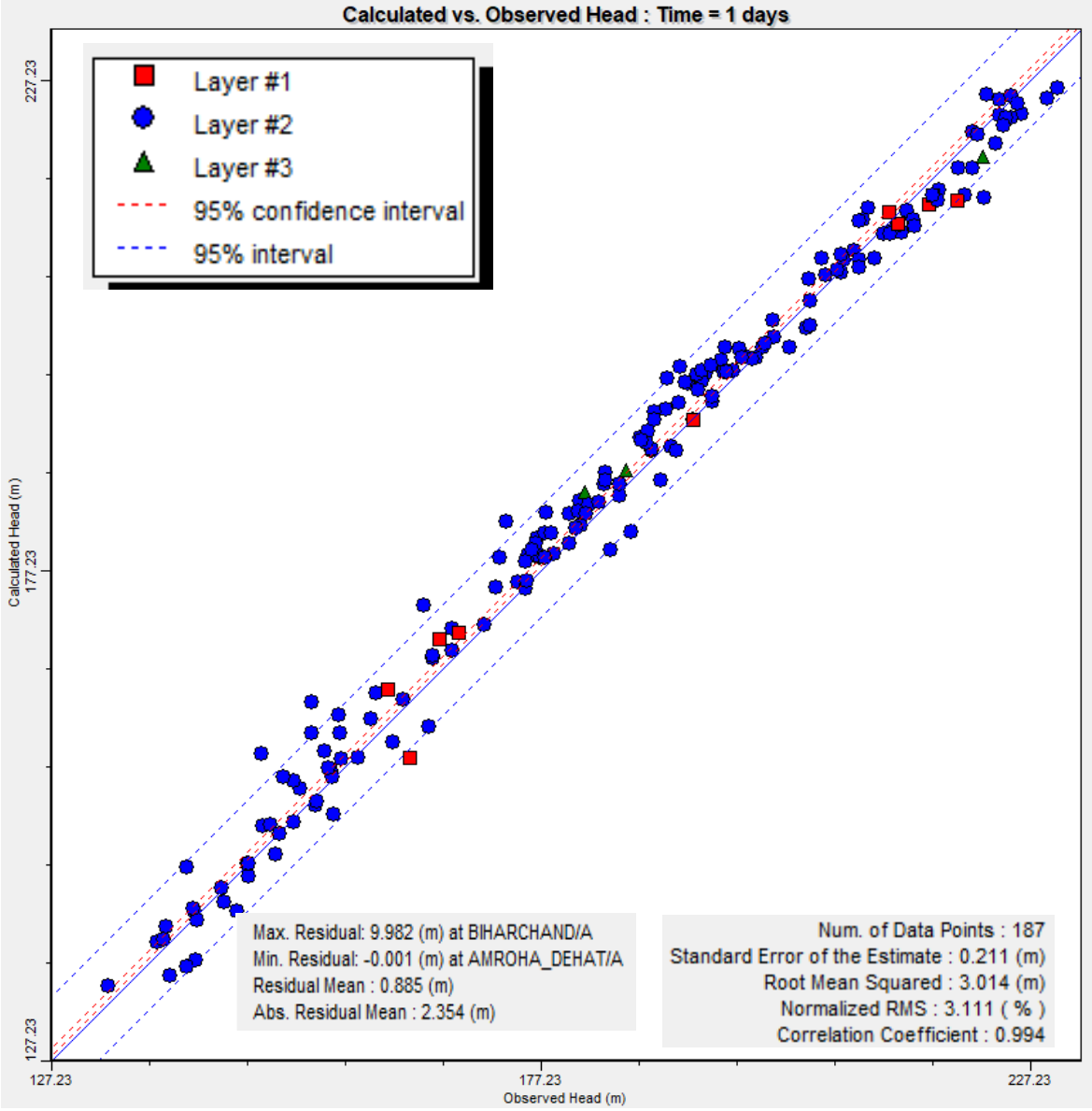

(a)

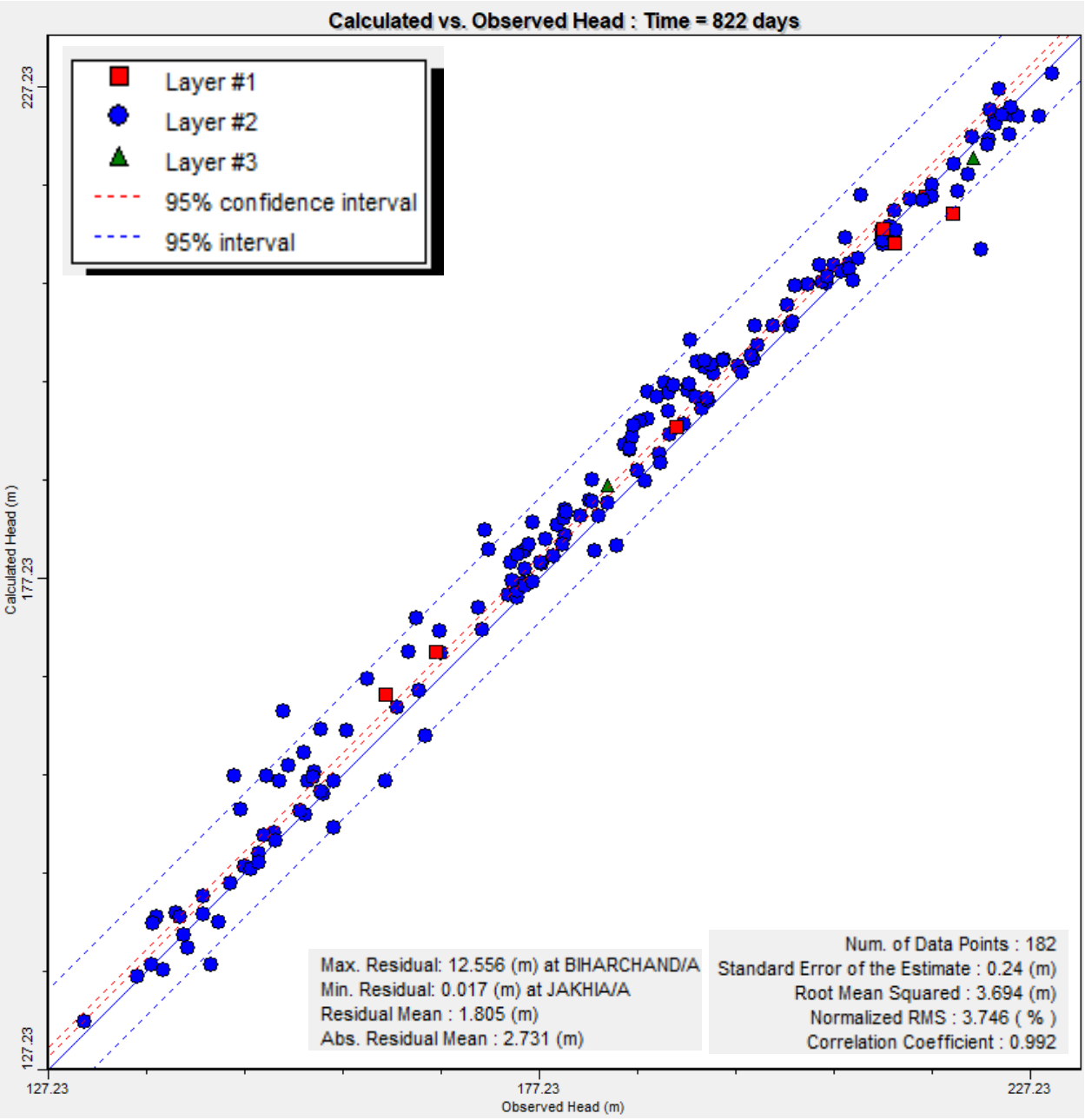
Calculated vs. Observed Head : Time = 822 days
Layer #1
Layer #2
Layer #3
95% confidence interval
95% interval
Max. Residual: 12.556 (m) at BIHARCHAND/A
Min. Residual: 0.017 (m) at JAKHIA/A
Residual Mean : 1.805 (m)
Abs. Residual Mean : 2.731 (m)
Num. of Data Points : 182
Standard Error of the Estimate : 0.24 (m)
Root Mean Squared : 3.694 (m)
Normalized RMS : 3.746 (%)
Correlation Coefficient : 0.992
Calculated Head (m)
227.23
177.23
127.23
127.23
177.23
227.23
Observed Head (m)

(b)

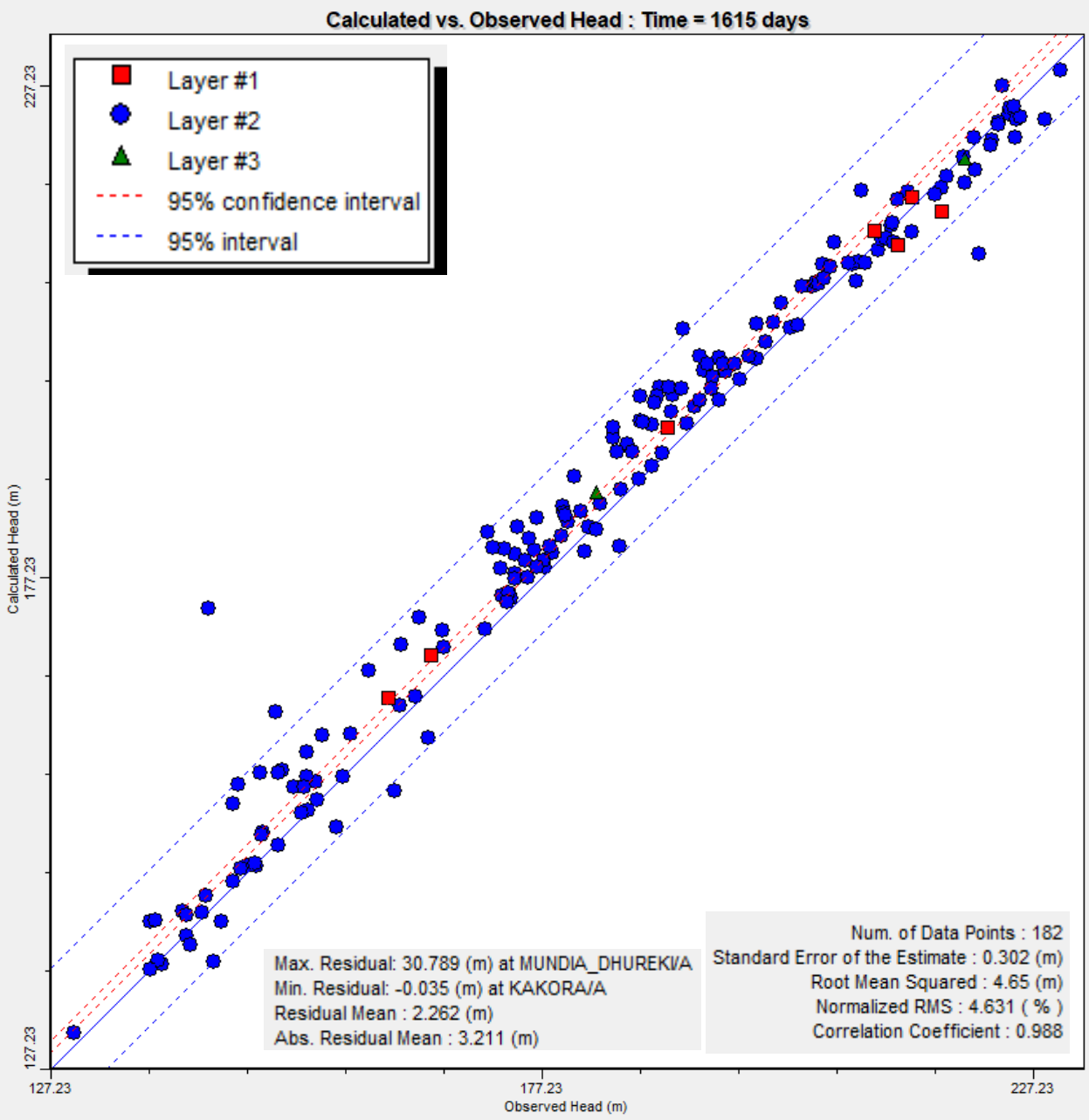

(c)

Figure 51. 1:1 plot of computed and observed heads for during the validation period for the (a) 1st day, (b) 822nd day, and (c) 1615th day of simulation.

.

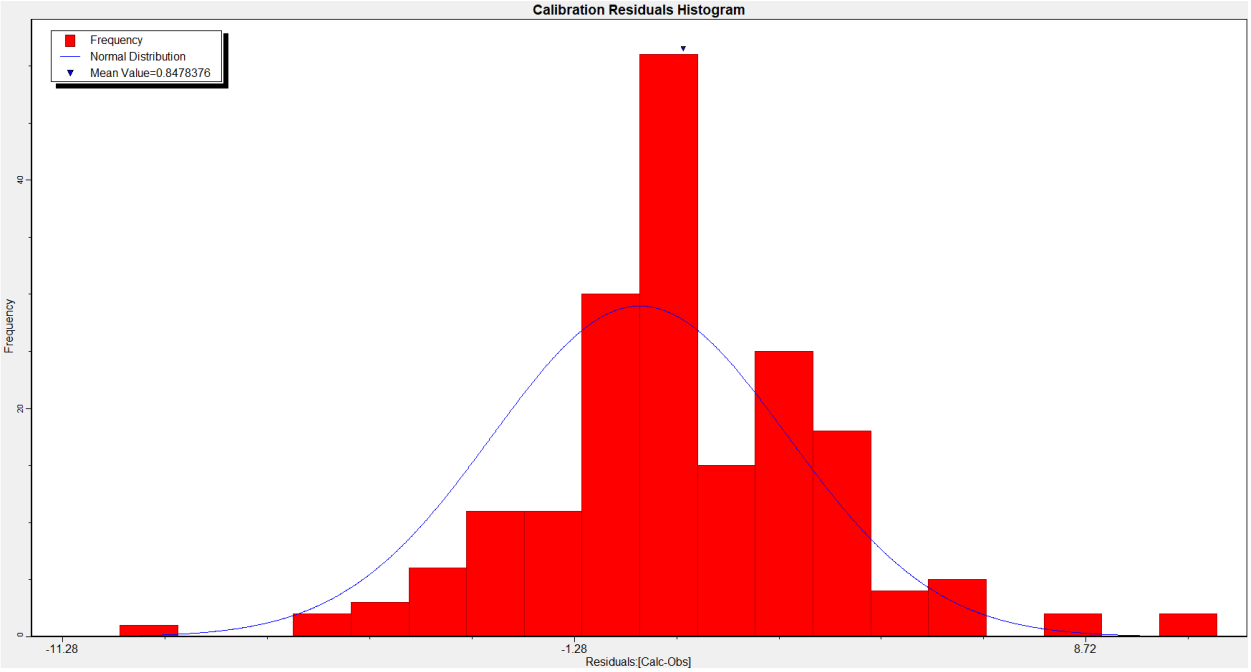
Calibration Residuals Histogram
Frequency
Normal Distribution
Mean Value=0.8478376
Frequency
0
20
40
-11.28
-1.28
8.72
Residuals:[Calc-Obs]

(a)

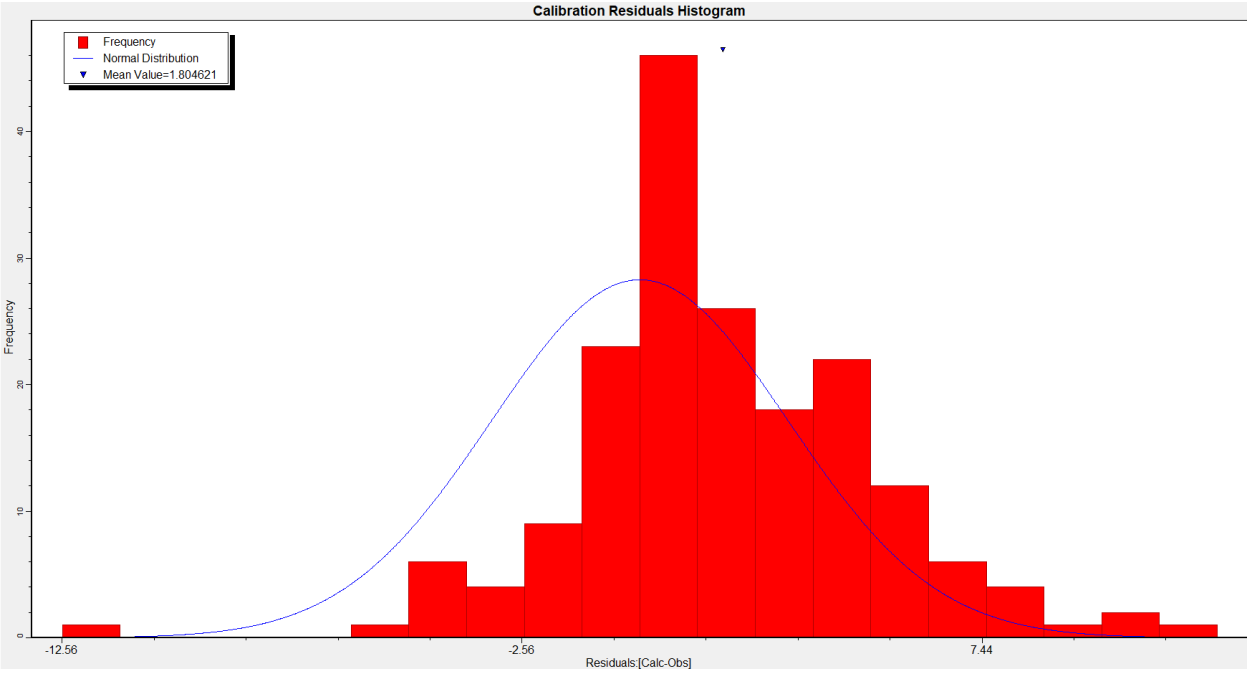
Calibration Residuals Histogram
Frequency
Normal Distribution
Mean Value=1.804621
Frequency
0
10
20
30
40
-12.56
-2.56
7.44
Residuals:[Calc-Obs]

(b)

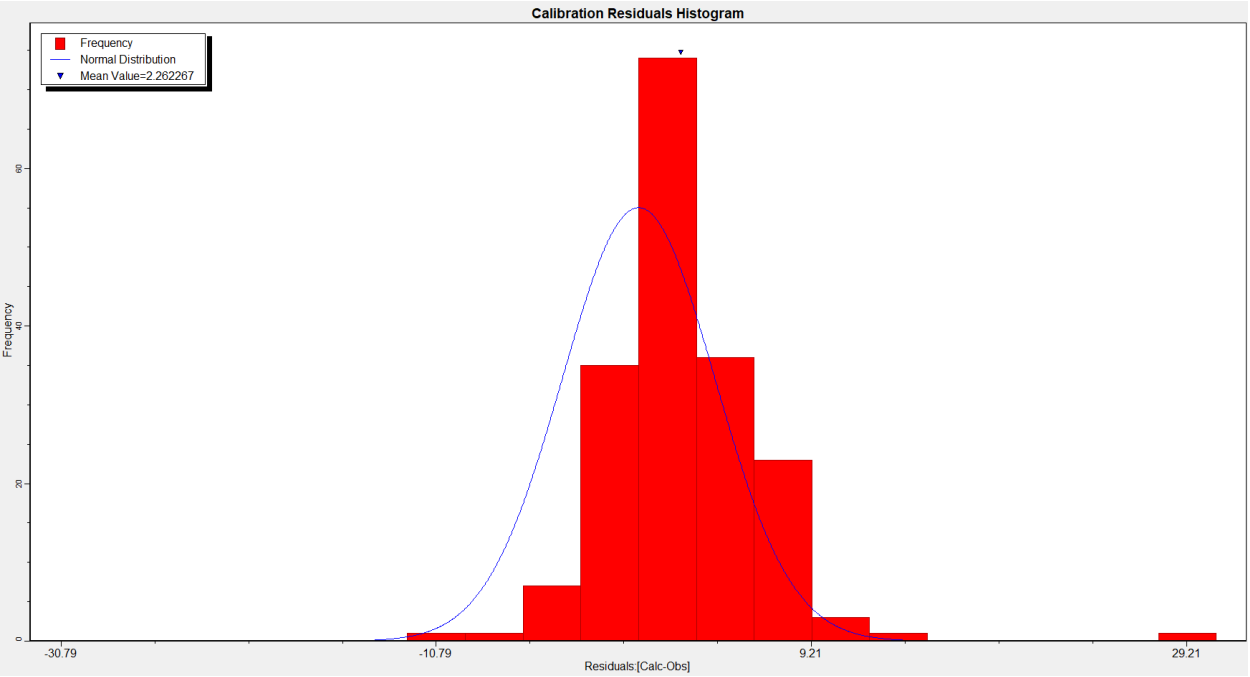

(c)

Figure 52. Histogram of residuals for the (a) 1st day, (b) 822nd day, and (c) 1615th day of simulation during the validation period.

The temporal variation of calculated and observed heads of groundwater levels for few locations corresponding to the calibrated parameters was shown in **Figure 53**.

Figure 53 indicates that the observed and the computed groundwater table profiles are matching reasonably well. The hydraulic properties namely: hydraulic conductivity, specific yield and specific storage corresponding to these scenarios can thus be considered as the validated parameters of the aquifer.

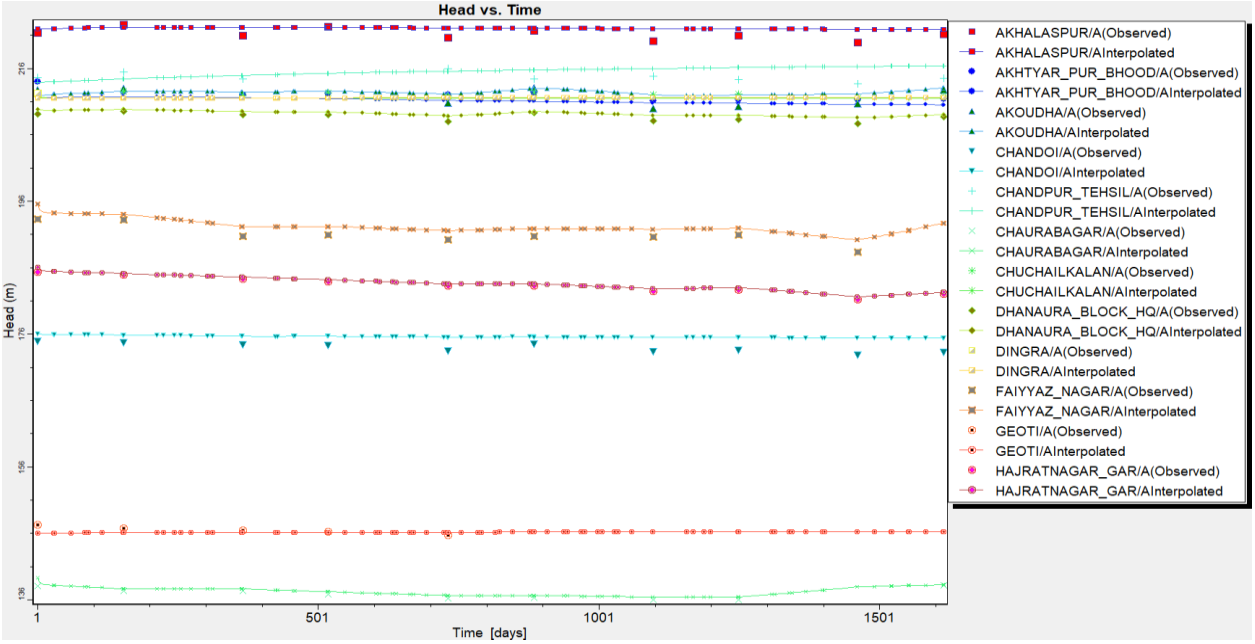

Figure 53. Comparison of temporal variation of computed and observed groundwater heads of few wells for the validation period.

The temporal variation of calculated and observed heads of groundwater levels for few individual groundwater observation wells corresponding to the calibrated parameters is shown in **Figure 54(a) to (d).**

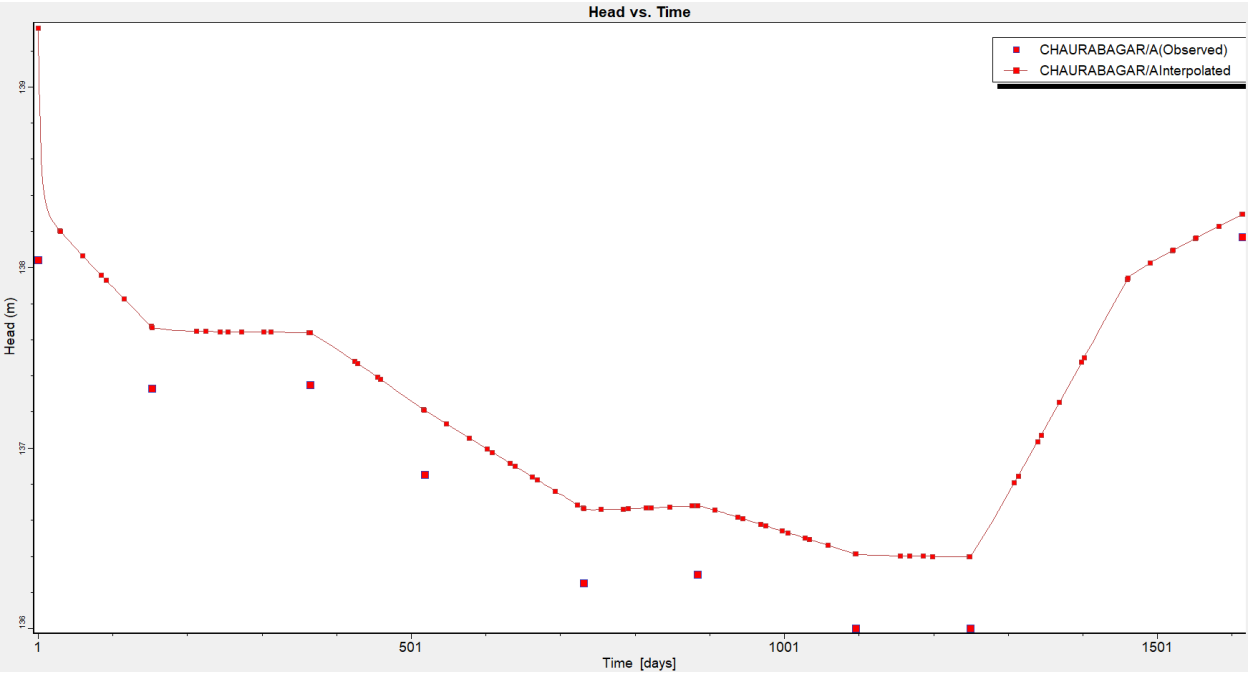

Figure 54(a). Variation of groundwater table for the observation well located at Chaurabagar.

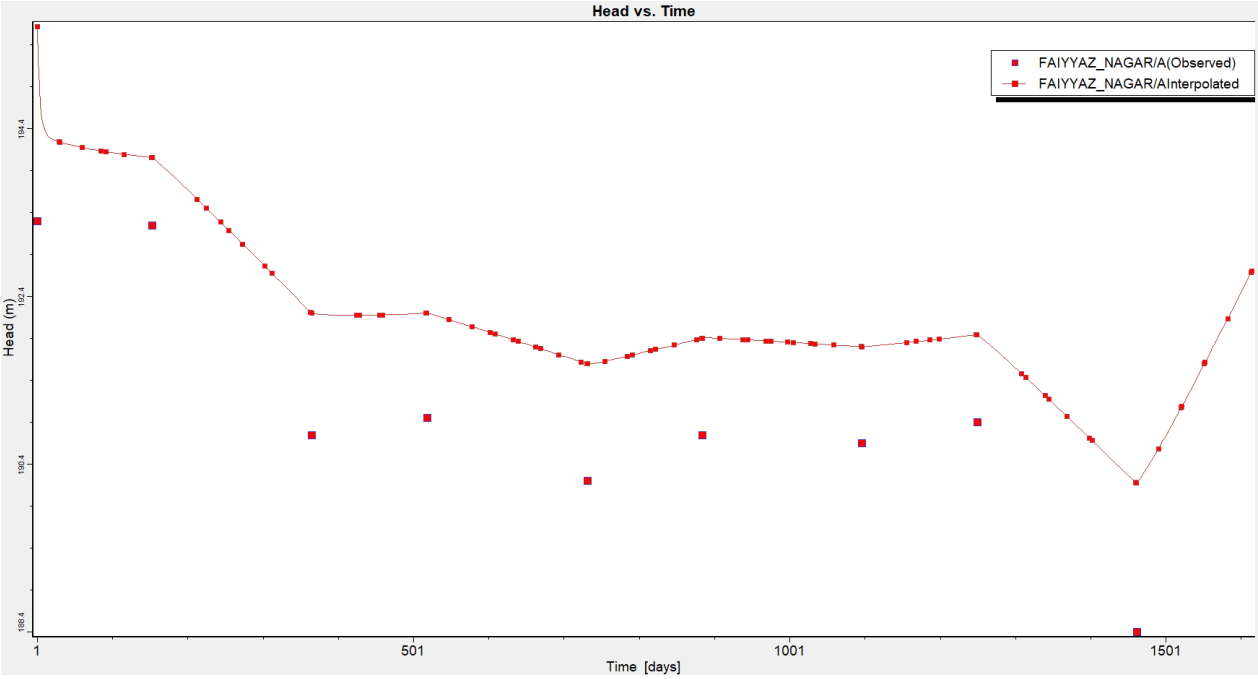

Figure 54(b). Variation of groundwater table for the piezometer well located at Faiyyaz Nagar.

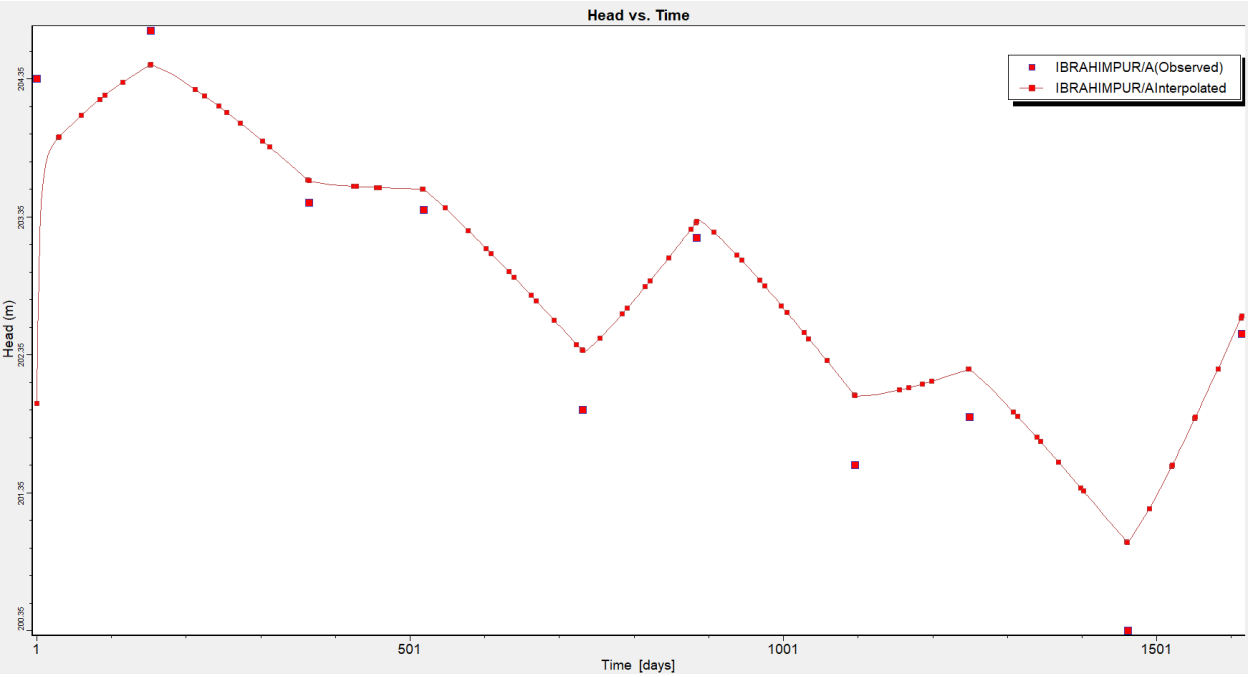

Figure 54(c). Variation of groundwater table for the observation well located at Ibrahimpur.

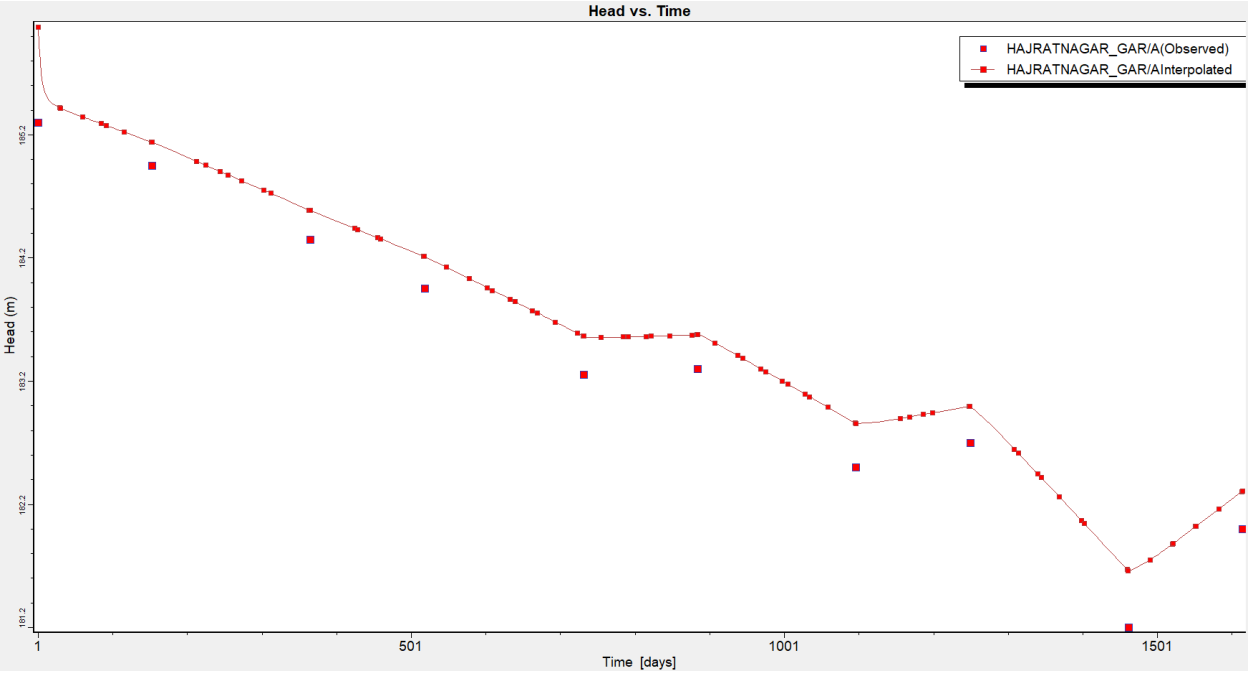

Figure 54(d). Variation of groundwater table for the observation well located at Hajratnagar.

Figures 51 to 54 demonstrates that the observed and the computed groundwater table profiles matched reasonably well, which establishes the validity of the developed model. The validated MODFLOW model can be used as a prediction model for scenario analysis of the modelling area. The spatial groundwater level variation in the modelling area corresponding to t=1615th day is presented in **Figure 55**. The groundwater flow direction map is presented in **Figure 56**. During the validation period, similar kind of variation of groundwater levels is found as during the calibration period.

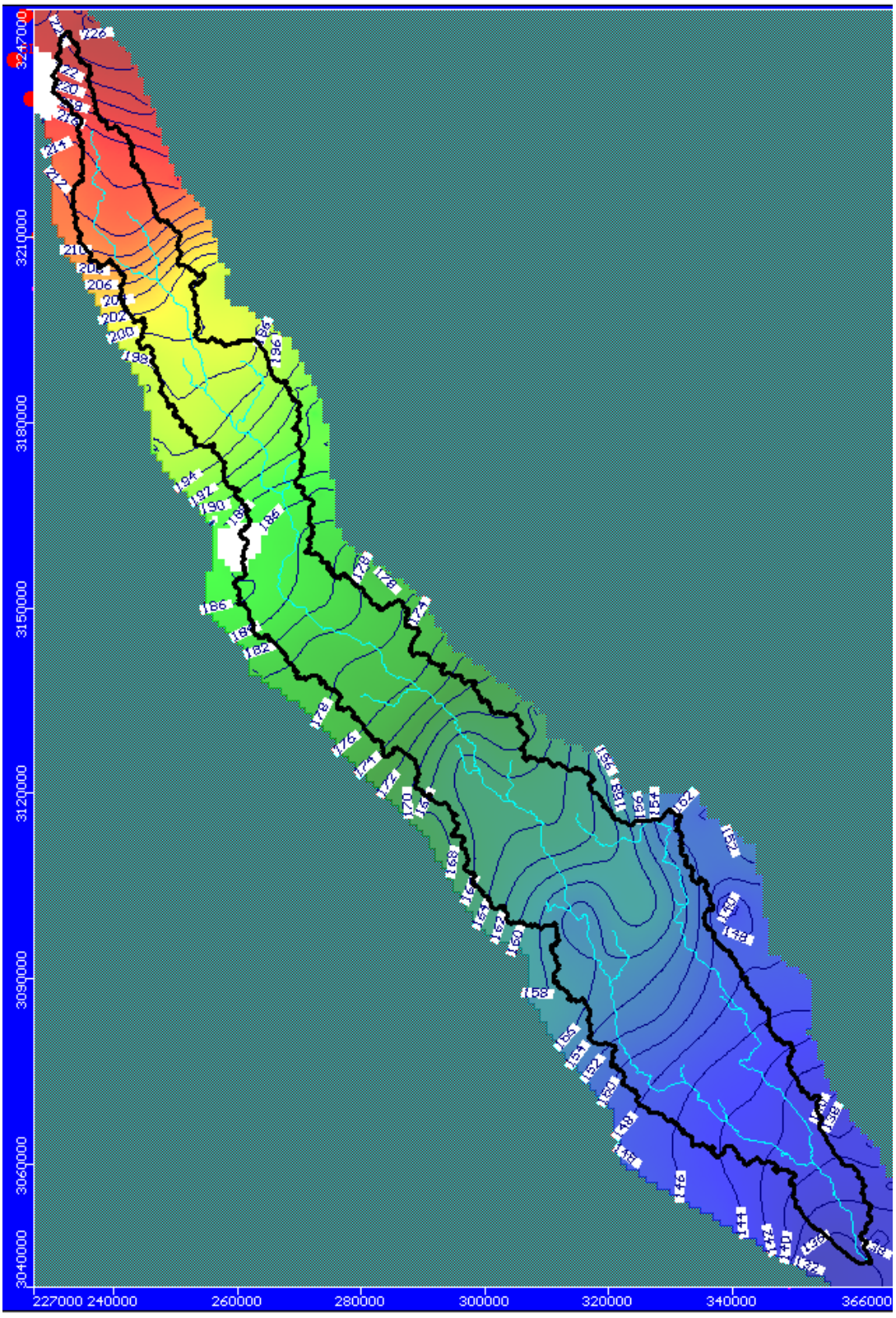

Figure 55. Spatial groundwater head variation in the study area.

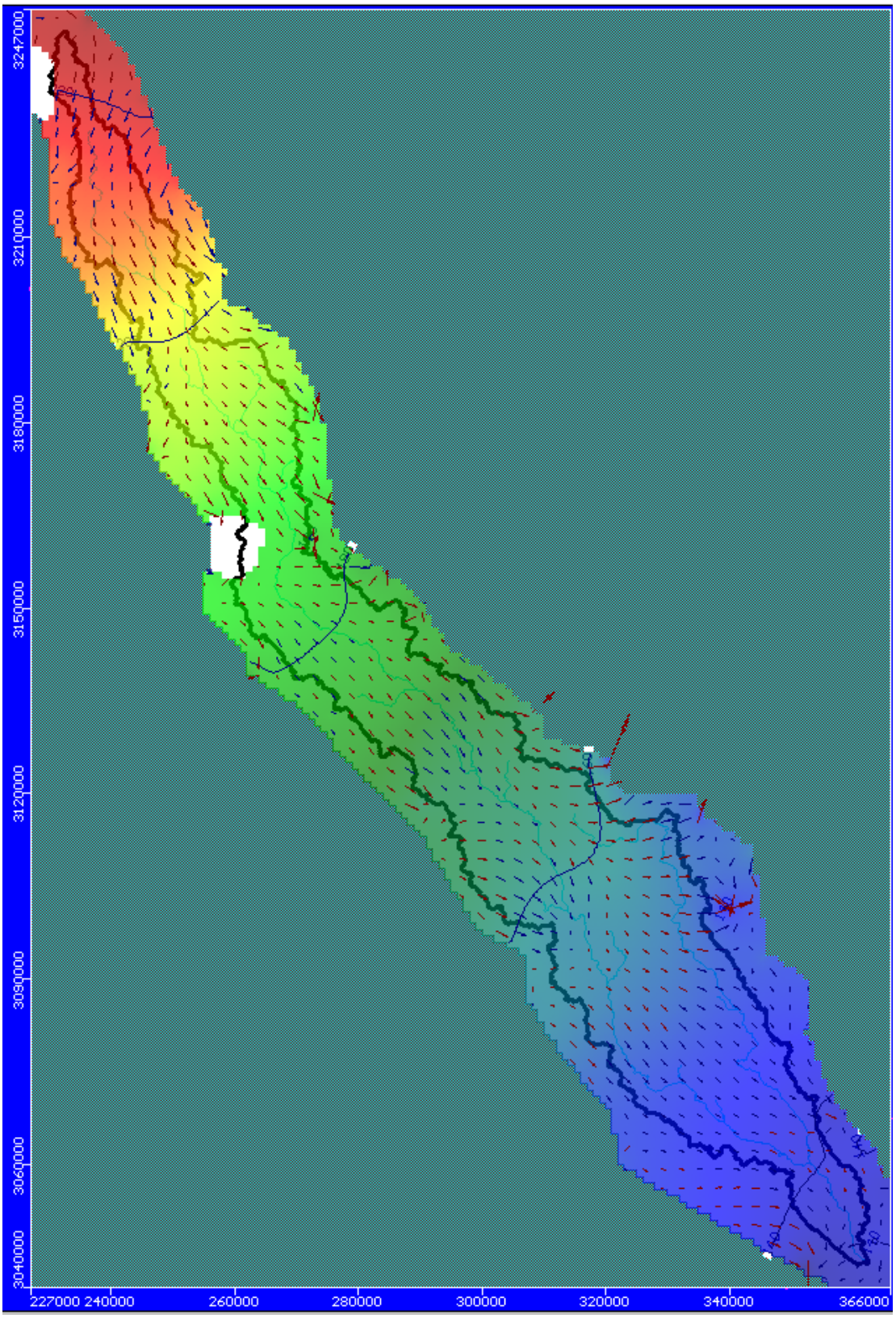

Figure 56. Velocity vectors showing groundwater flow direction in the study area.

The spatial variation of groundwater table in the study area is presented in **Figure 57**. The water table elevation varies from 134 to about 226 m above mean sea level. In general, the water table elevation in north-western side is higher and reduces towards south-eastern side. The direction of groundwater flow is also towards the south-eastern side (**Figure 56**).

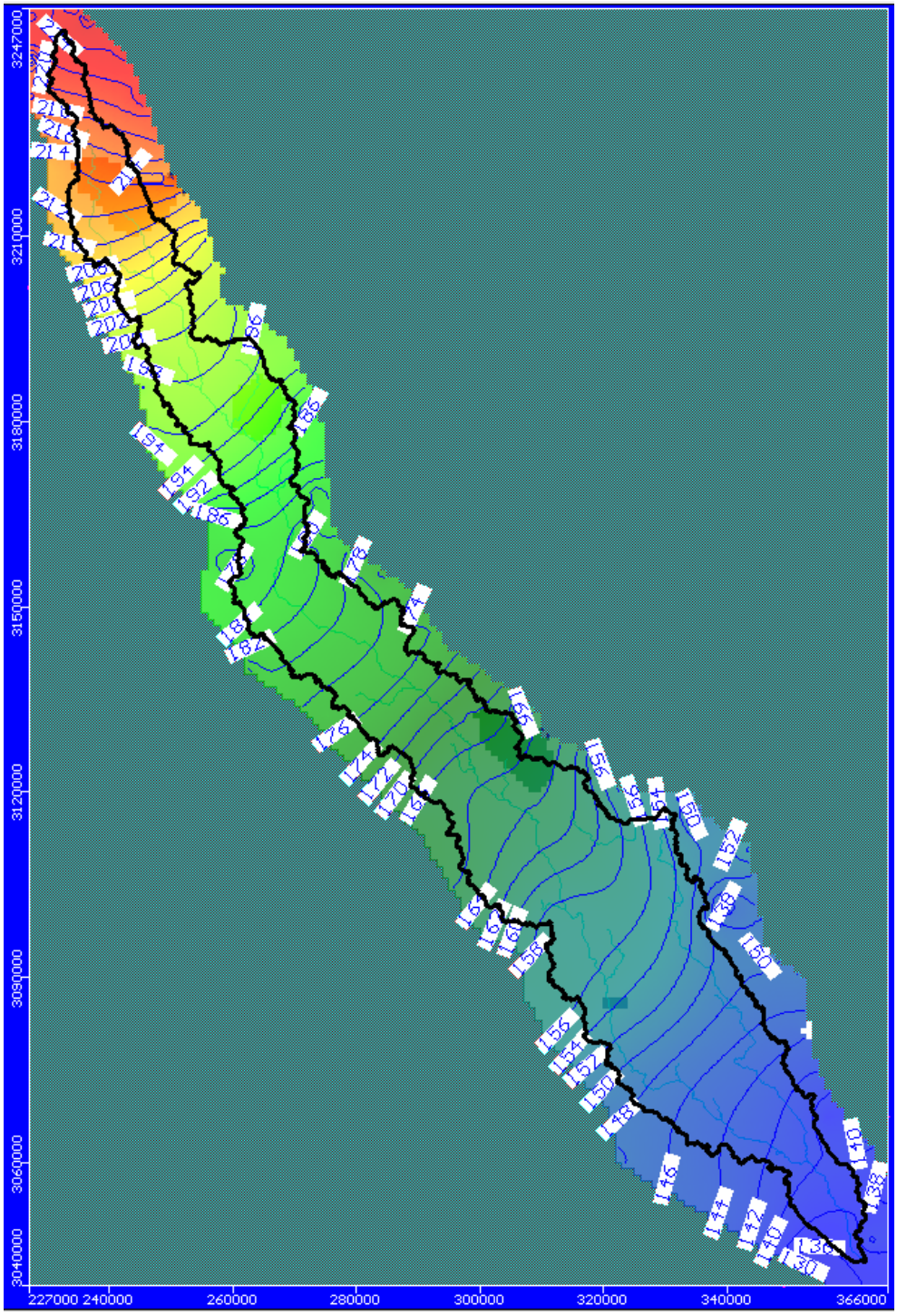

Figure 57. Spatial variation of water table elevation in the modelling area.

6.7 Results of groundwater potential zone mappings

6.7.1 Thematic Layers of the Study Area

Eleven thematic layers have been used for the potential zone mapping. These layers include geology, geomorphology, DEM, soil, slope, LULC, drainage, recharge, groundwater fluctuation, depth to aquifer, and depth to groundwater level for pre-monsoon period. The detailed information and data interrelated to different thematic layers used to prepare the groundwater potential zone maps are briefly described below:

Elevation

The elevation is an important topographic factor to investigate groundwater potential because it is considered as a surface indicator. The altitude of the study area was generated from 90 m STRM DEM and reclassified into five classes viz., 135–160, 160–185, 185–200, 200–225, 225–250 m (Figure 58). Variation of altitude can alter climate conditions, which causes variation in rainfall, soil condition, vegetation, land uses, and vegetation type.

Land Use Land Cover

Land use land cover plays a significant role in finding out the groundwater potential zones. In this study, LULC map was prepared using Sentinel-2 satellite imagery (spatial resolution 10 meter). The LULC was categorized into seven classes, namely, agriculture, urban, water body, Indian grass, pasture, barren, and forest. The majority of the study area is covered with agriculture (86.74%), urban (9.19%), Indian grass (2.09 %), forest (1.89 %), water body (0.08 %), barren land (0.04 %), and pasture (0.006 %). It is clearly shown in Figure 59 that the Sot catchment is dominated by agriculture which has high infiltration but at the same time, the water demand is also high. Compared to urban areas, forest areas will have high levels of infiltration and low levels of runoff. Conversely, urban areas will experience a decrease in infiltration and a higher demand for water. Each sub-class in the LULC class is assigned with different weights on the basis of AHP approach.

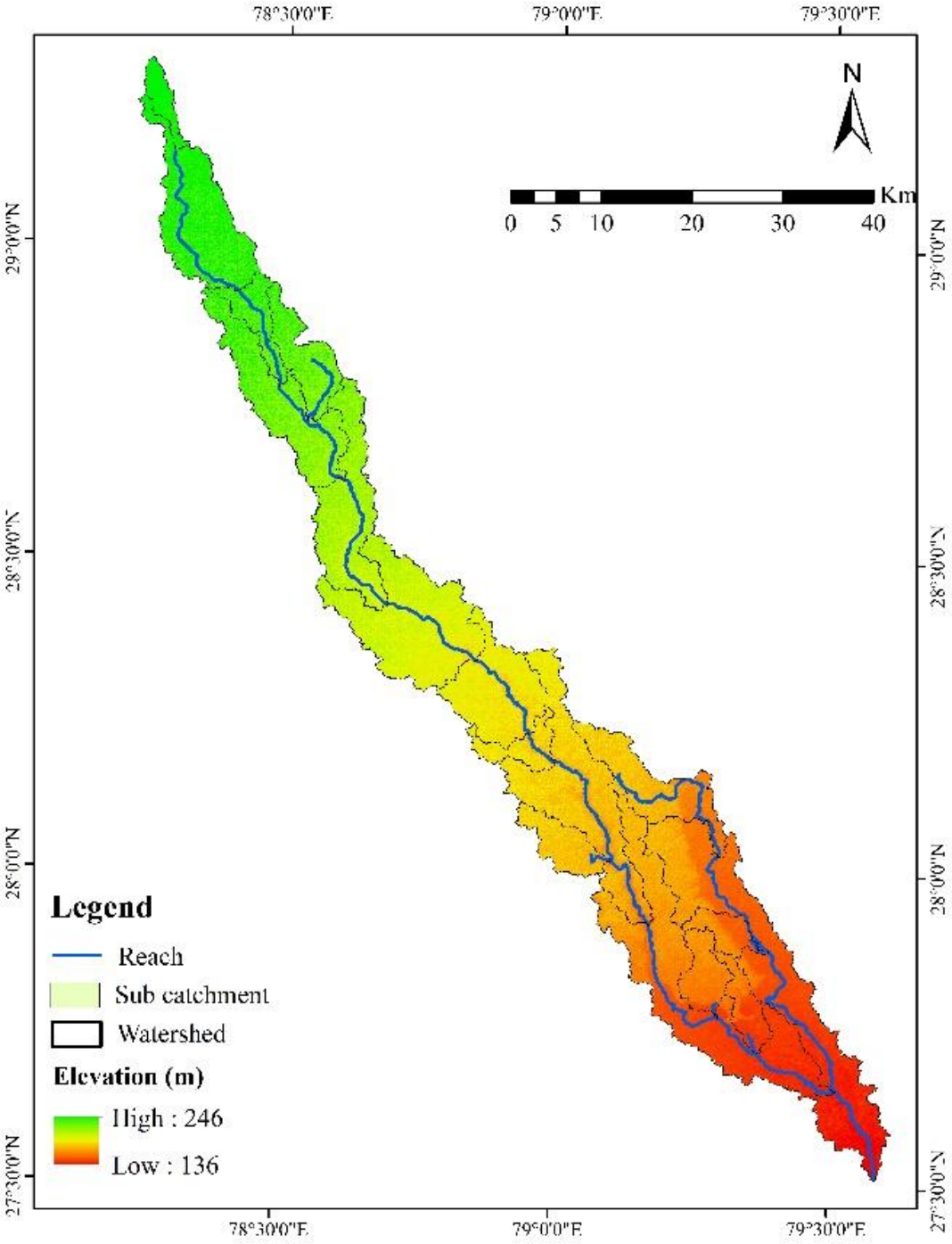

Figure 58. Elevation map of Sot river catchment

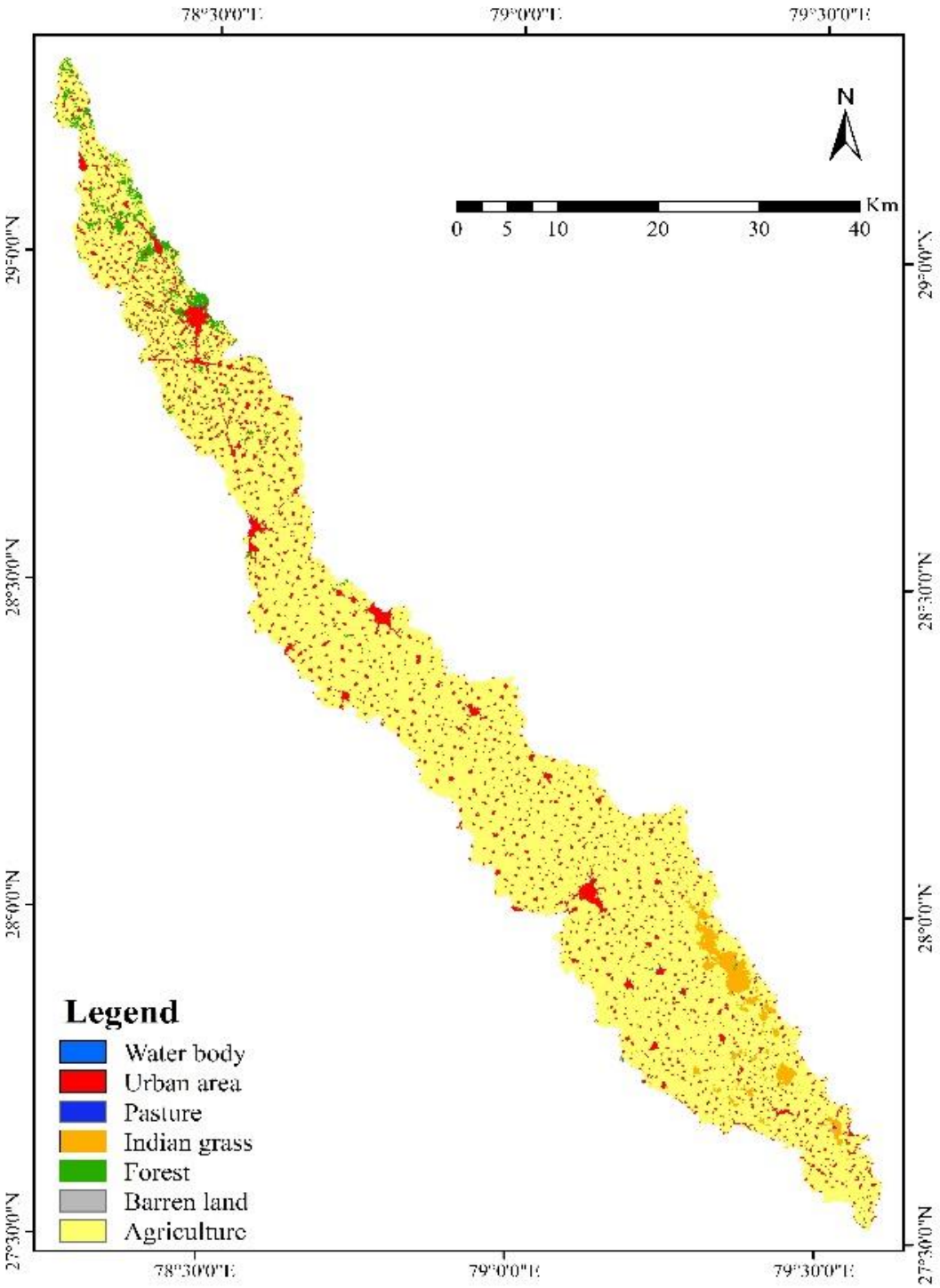

Figure 59. Land use land cover map of Sot river catchment

Slope

The slope is one of the most important criteria for estimating the groundwater potential since it determines how much surface water penetrates. Slope angle indicates flat and steep terrain, respectively, based on its lower and higher values. Slope map of the study area was derived from SRTM-DEM (90 m x 90 m resolution) using the ArcGIS 10.4 tool. It can be seen in Figure 60 that a higher percentage of the study area falls into the moderate and minor slope (0-4) categories.

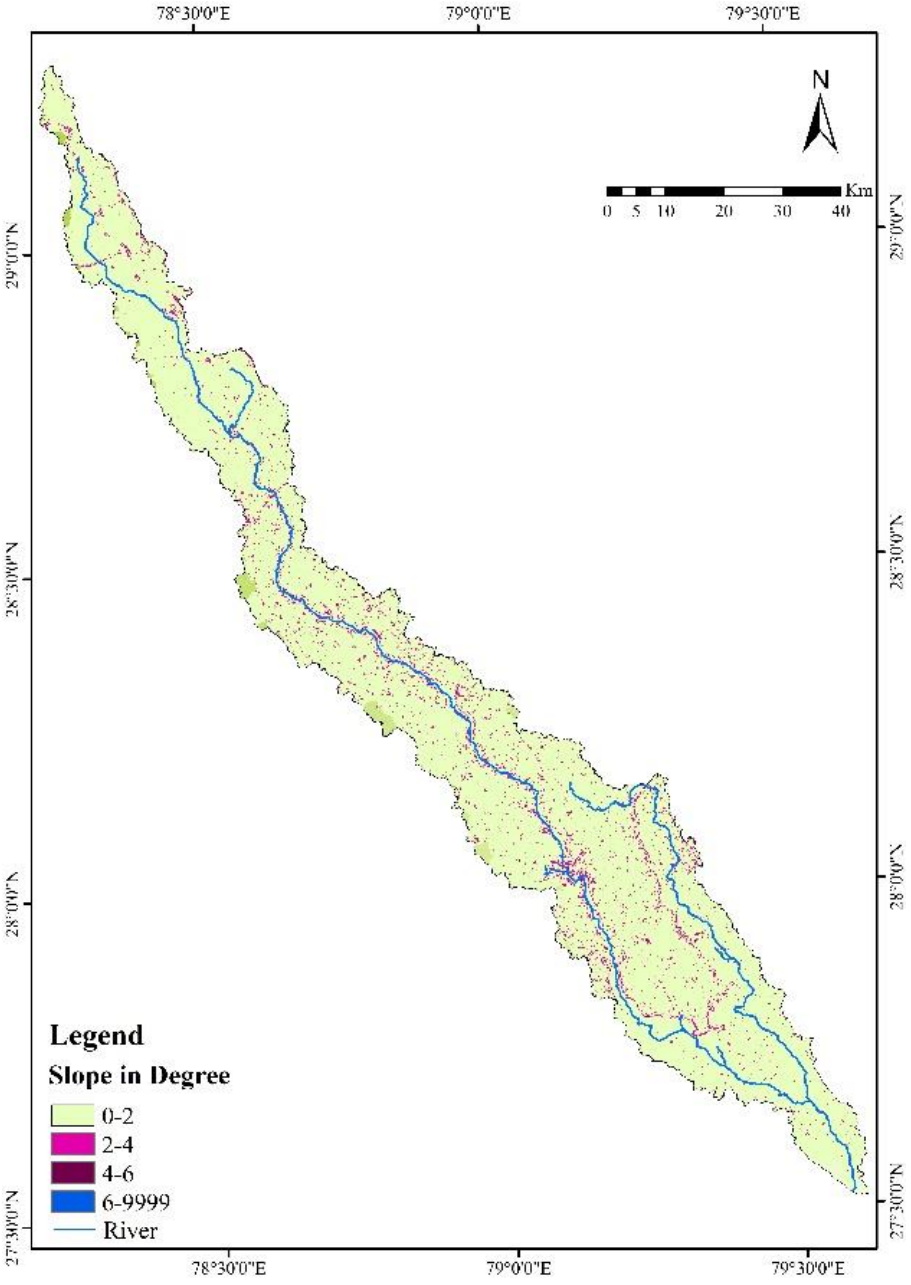

Figure 60. Slope map of Sot river catchment

Soil map

The soil information is taken from the National Bureau of Soil Survey and Land Use Planning with a scale of 1: 50000. The study area covers with different types of soils including typic ustochrept covers 79.47 % of the area, typic ustipsamments cover 11.66 %, aquic ustipsamments covers 5.97 % of the area, typic haplaquepts covers 2.44 % of the area, and typic haplustalfs covers 0.47 % of the area. The different types of soil in Sot river catchment are shown in Figure 61.

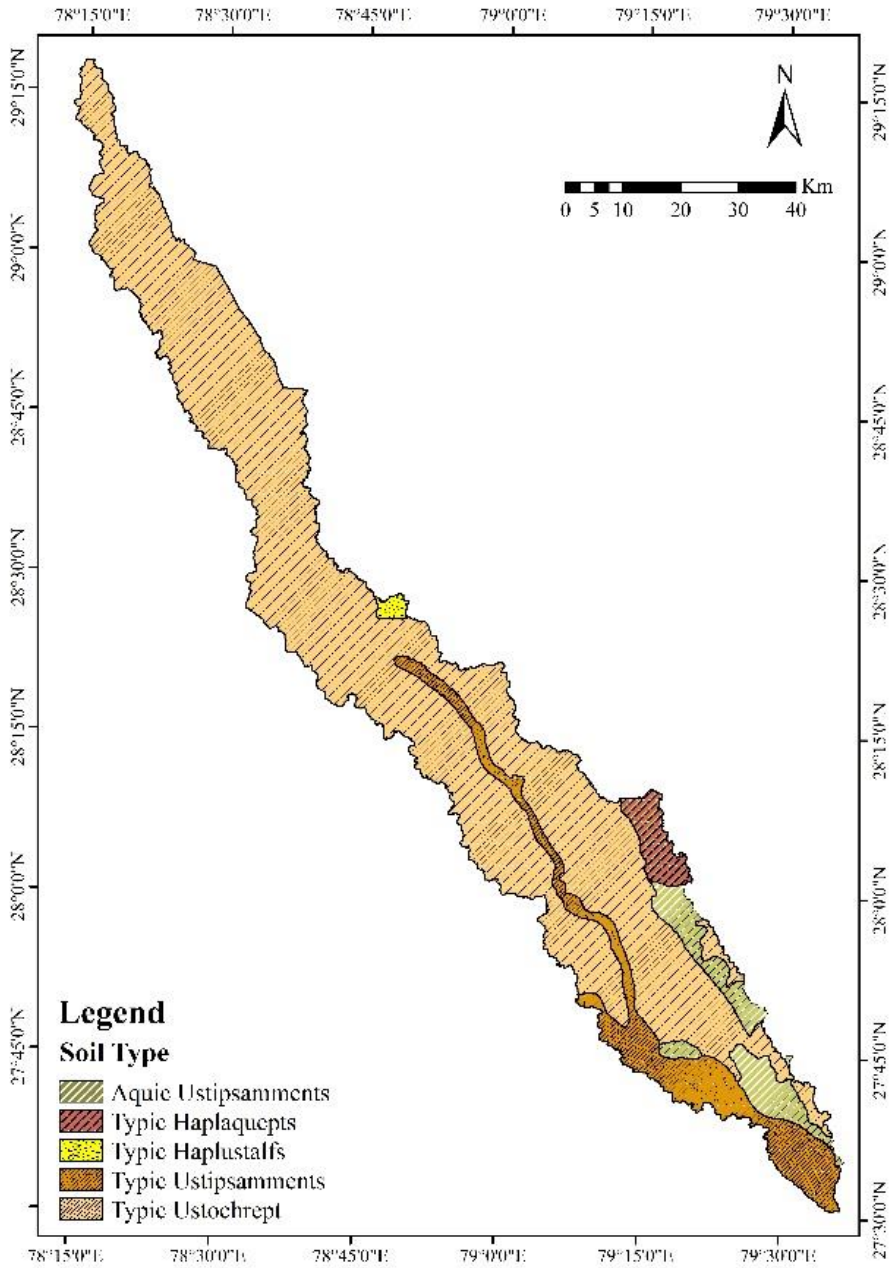

Figure 61. Soil map of Sot river catchment

Geology

The geological map and information are taken from the Geological Survey of India with a scale of 1: 50000. The geological or lithological features of the study area are shown in Figure 62. The study area consists of three different types of lithological features viz., grey micaceous sand, silt and clay, oxidized silt-clay with kankar and micaceous sand, silt clay, sand with gravel and pebbles, and grey sand, silt and clay.

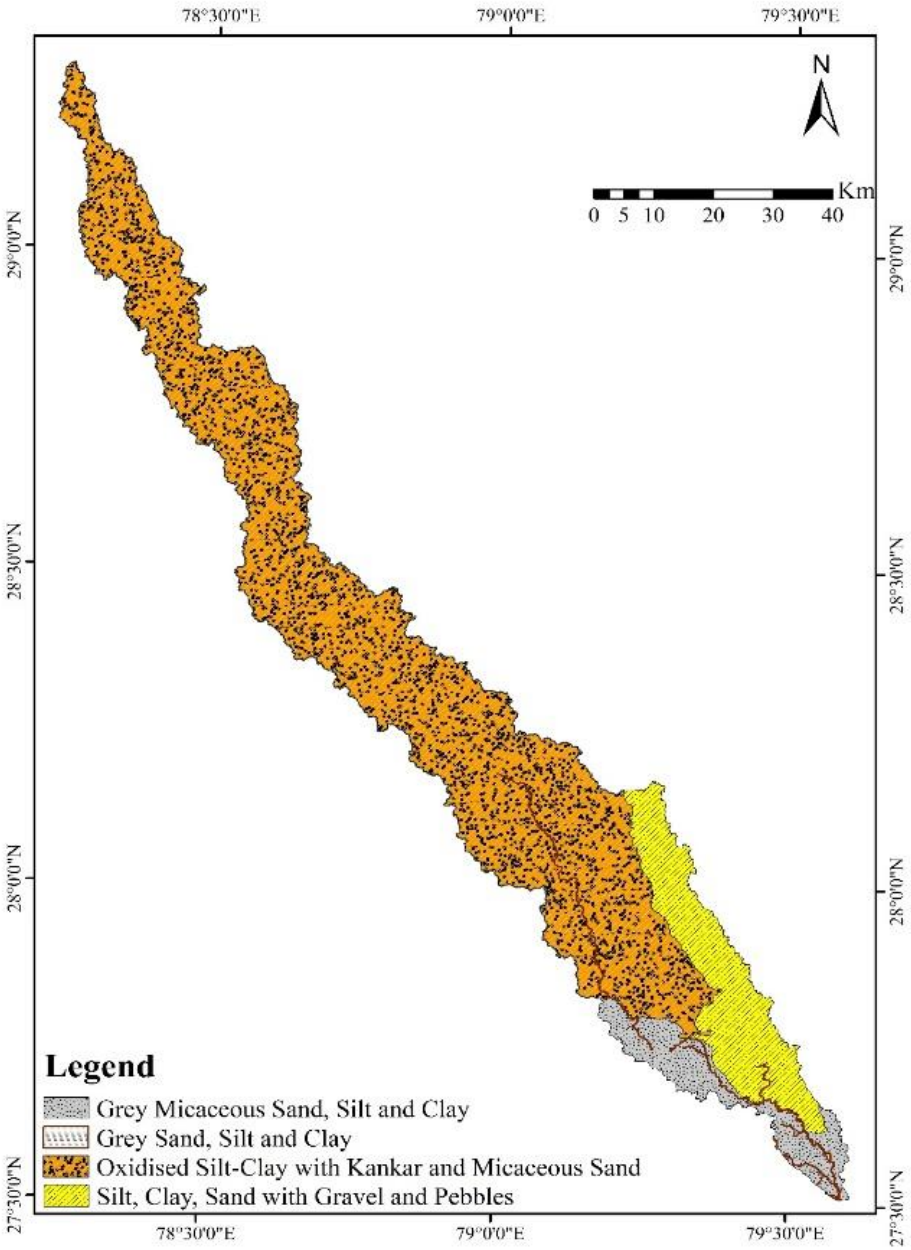

Figure 62. Geological map of Sot river catchment

Geomorphology

Geomorphology of an area is an important factor used for assessing the groundwater potential and prospect because it controls the subsurface movement of groundwater. The geomorphological information is taken from the Geological Survey of India. In the study area, geomorphology was divided into active flood plain, older flood plain, older alluvial plain, oxbow lake and ponds to calculate the potential groundwater zone. The geomorphologic features of the Sot catchment are shown in Figure 63.

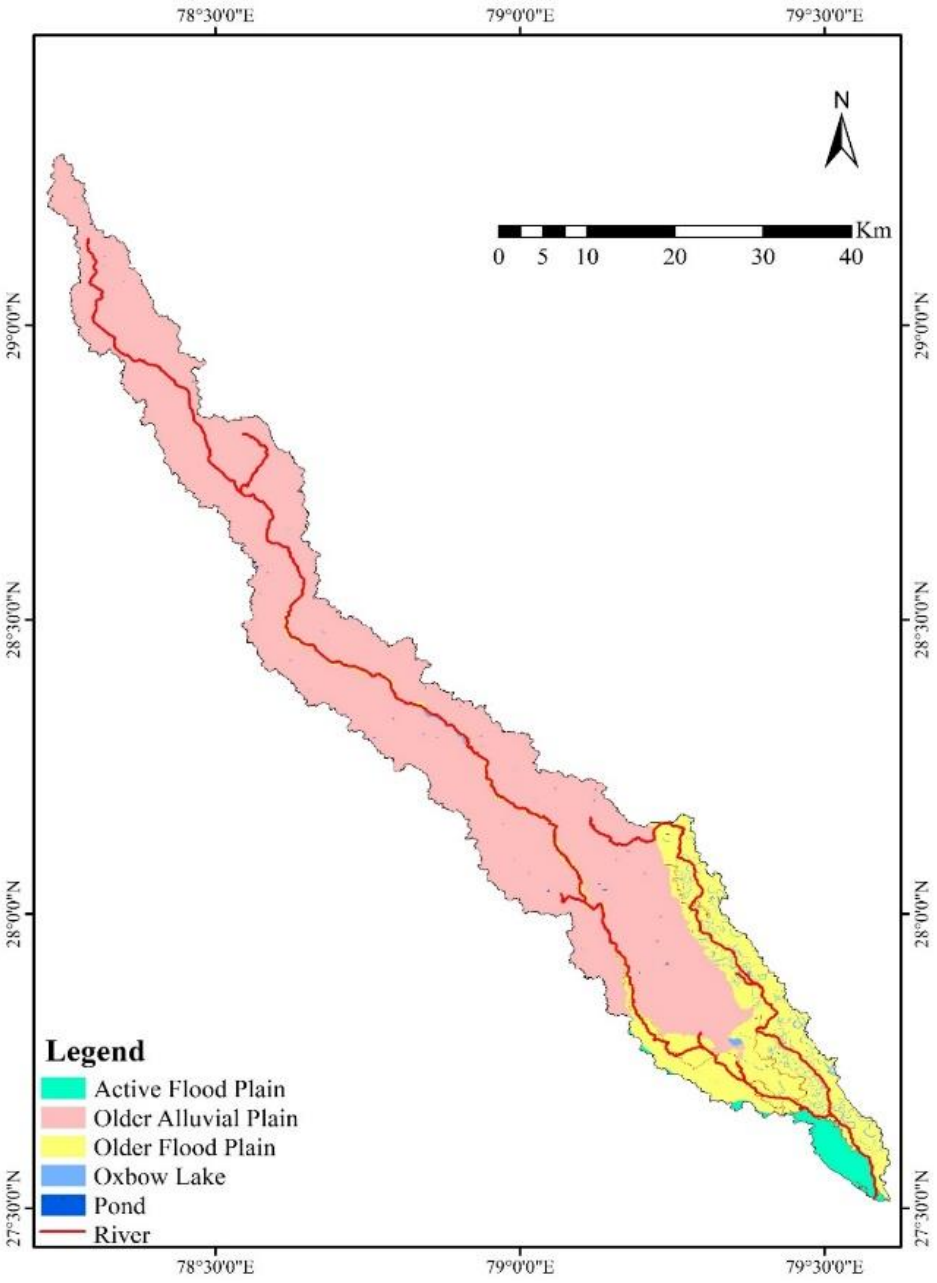

Figure 63. Geomorphology map of Sot river catchment

Drainage density

The drainage density (km/km^2) expresses the closeness of spacing of stream channels, thus providing a quantitative measurement of the average length of stream channels of the whole basin. The drainage density has an inverse relation with the permeability of aquifers and plays a vital role in the runoff distribution and level of infiltration. The drainage density of Sot catchment was prepared from the digital elevation model (90 m x 90 m resolution) in ArcGIS 10.4.1 platform. The study area is divided into five different categories on the basis of their drainage density values (See Figure 64).

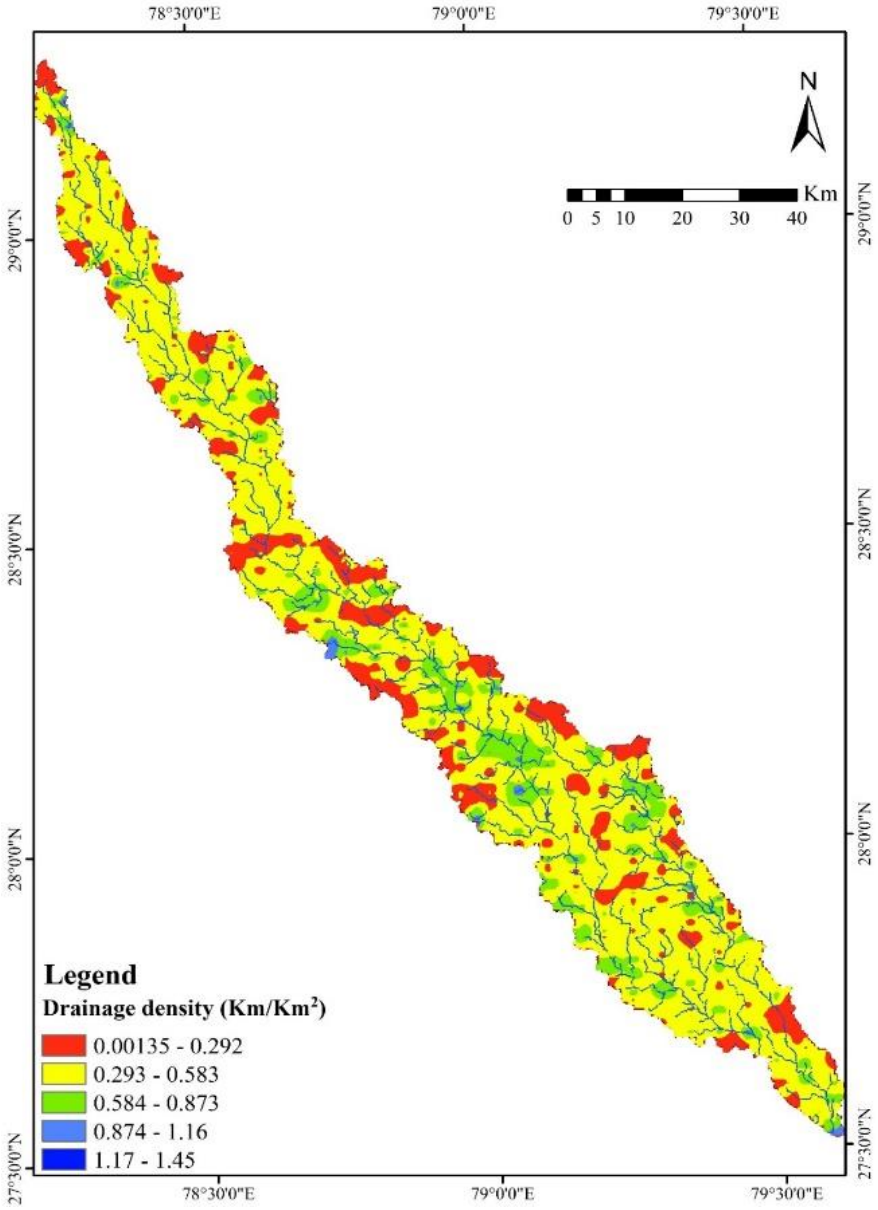

Figure 64. Drainage density map of Sot river catchment

Recharge map

When investigating a groundwater potential zone, the recharge map plays a crucial role, since the higher the recharge, the higher the groundwater potential. The block-wise average recharge is presented in Figure 65. The average recharge for Sot catchment varied from 190 to 315 mm. The values of recharge were further classified into five classes to assign the appropriate weights. The same is shown in Table 14.

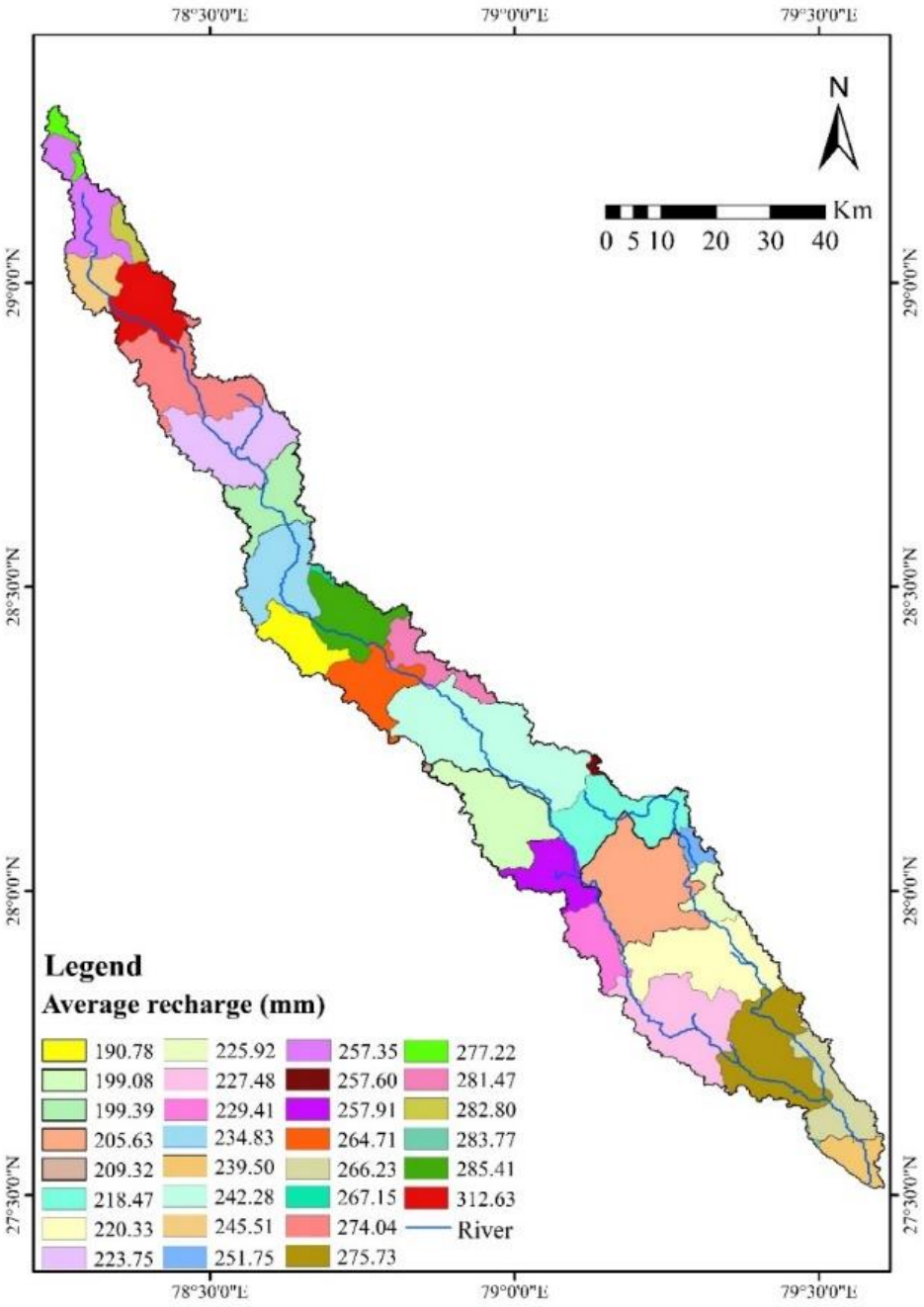

Figure 65. Recharge map of Sot river catchment

Aquifer map

Groundwater potential in alluvial areas is greatly impacted by the depth of aquifers, which are mainly sedimentary formations that store groundwater. The aquifer map is depicted in Figure 66 and the depth of upper unconfined aquifer layer varied up to 10 mm.

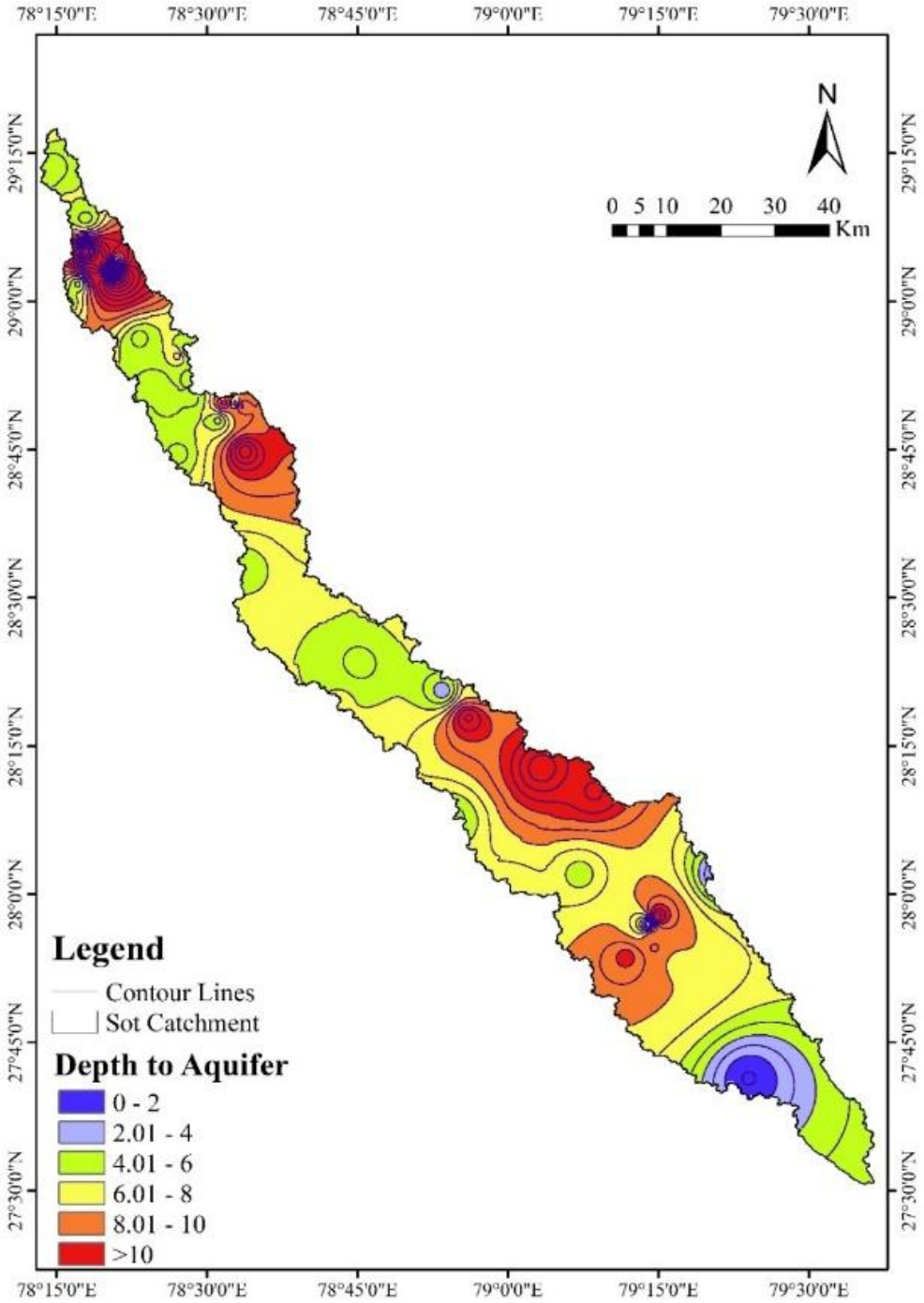

Figure 66. Depth to aquifer map of Sot river catchment

Groundwater fluctuation map

Groundwater fluctuation map shows the variation in groundwater in the different seasons which is determined by the difference of pre and post-monsoon groundwater level data. The groundwater fluctuation map is prepared from the groundwater level data collected from the Ground Water Deptt., Uttar Pradesh. The magnitude of groundwater fluctuation varied up to 3.5 mm (See Figure 67).

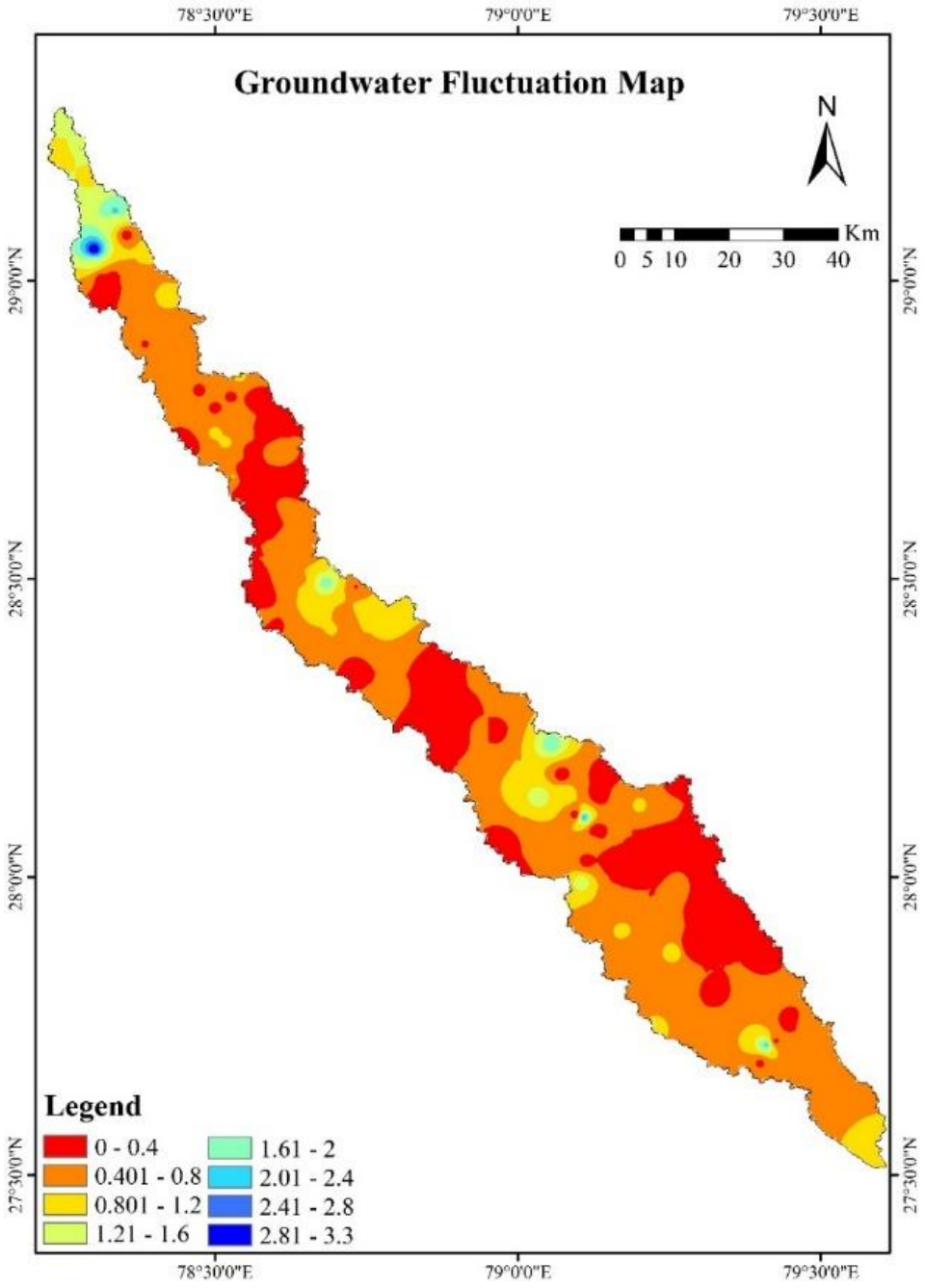

Figure 67. Groundwater fluctuation map of Sot river catchment

Depth to water level map

Depth to groundwater level map was prepared from the groundwater level data and well inventory for the pre-monsoon period. This map indicates the water level below the ground surface at different depths in the Sot catchment. Depth of water level for the Sot catchment is found to vary between 2 to 20 m-bgl (See Figure 68).

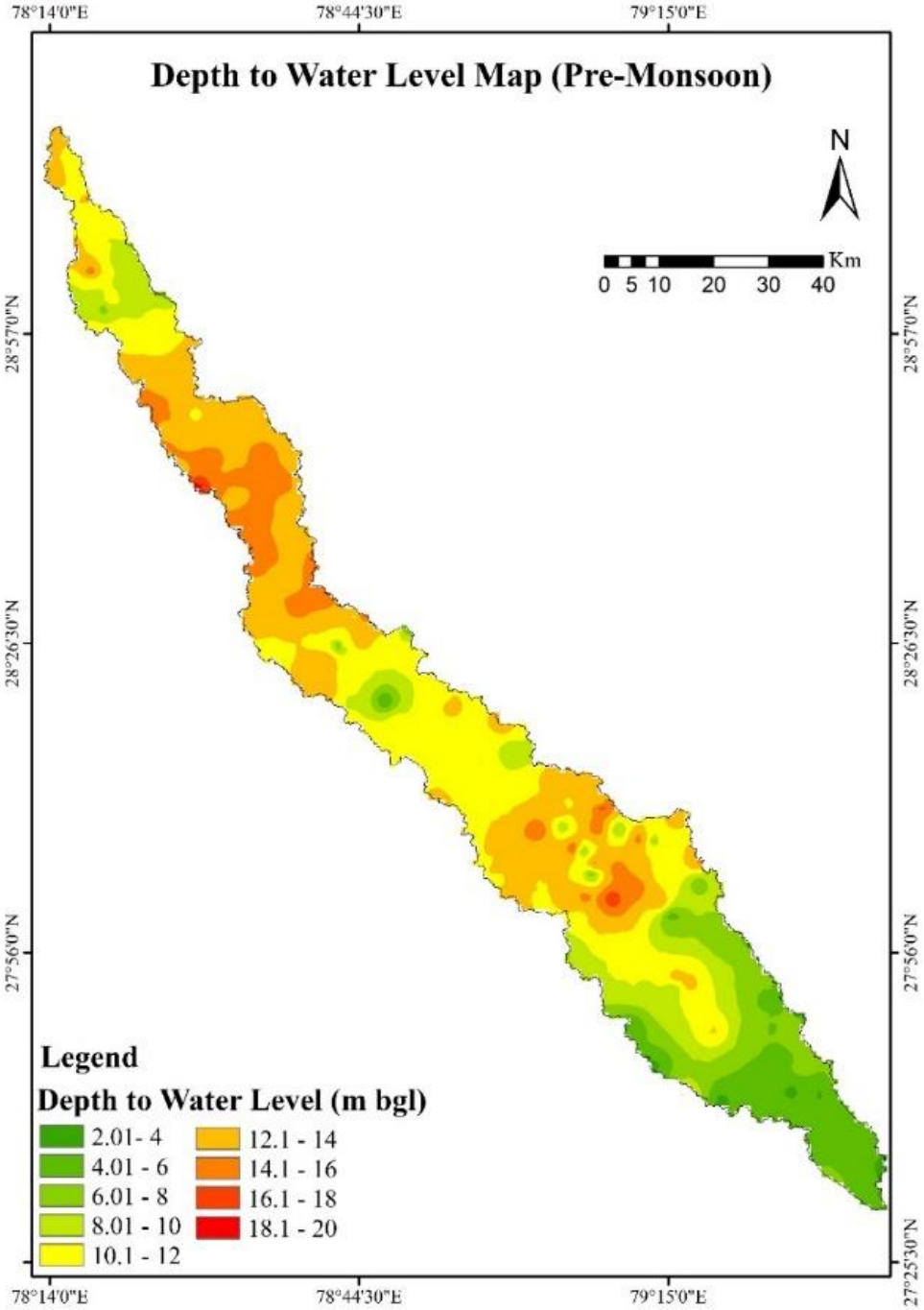

Figure 68. Depth to water level map of Sot river catchment

6.7.2 Generation of weights for groundwater prospecting parameters

After preparing all the eleven thematic layers for the Sot river catchment, weights were generated using the AHP technique. According to Saaty, initially the AHP was used for solving a complex problem by splitting it into different categories and integrating each subsection to find out the big picture that has to be solved. The detailed description of steps involved in the derivation of weights of major thematic layers and their subclasses are available in literature (Saaty 2004; Jhariya et al. 2016; Murmu et al. 2019). The weight of each thematic layer and sub-parameter are given in Table 13 and 14.

Table 13 Weight of various parameters

Map Parameter	Parameter Weight
Geomorphology	10.39
Lithology	12.99
Depth to Aquifer	11.69
Soil Type	9.09
Recharge	9.74
Slope	7.79
Elevation Zones	7.40
Depth to GWL Pre-Monsoon	8.83
GWL Fluctuation	6.49
Land Use and Land Cover	8.44
Drainage Density	7.14

Table 14 Weight of various sub-parameters of each thematic layer

Parameter	Sub-Parameter	Groundwater Prospects	Sub-Parameter Weight
Geomorphology	Active Flood Plain	Excellent	10
	Older Alluvial Plain	Very good	8
	Older Flood Plain	Good	8
	Oxbow Lake	Moderate	4
	Pond	Moderate	4
	River	Excellent	10
Geology	Grey Micaceous Sand, Silt and Clay	Good	6
	Grey Sand, Silt and Clay	Very Good	8
	Oxidised Silt Clay with Kankar and Micaceous Sand	Good	6
	Silt, Clay, Sand with Gravel and Pebbles	Excellent	10

Depth to Aquifer (m-bgl)	≤ 02	Excellent	10
	02 to 04	Very good	8
	04 to 06	Good	6
	06 to 08	Moderate	4
	08 to 10	Poor	3
	> 10	Very Poor	1
Soil map	Aquic Ustipsamments (Sand & Loamy Sand)	Very Good	8
	Typic Haplaquepts (Silty Clay Loam, Silt Clay & Clay)	Very Poor	1
	Typic Haplustalfs (Sandy Clay Loam)	Moderate	4
	Typic Ustipsamments (Silt Loam & Loam)	Poor	3
	Typic Ustochrept (Sandy Clay Loam)	Moderate	4
Recharge (mm)	≤ 50	Very Poor	1
	50 - 100	Poor	3
	100 - 150	Moderate	4
	150 - 200	Good	6
	200 - 250	Very Good	8
	> 250	Excellent	10
Slope (%)	≤ 4	Excellent	10
	4 - 10	Very Good	8
	10 - 20	Good	6
	20 - 50	Moderate	4
	50 - 100	Poor	3
	> 100	Very Poor	1
Elevation Zones (m)	≤ -4	Excellent	10
	-4 to -2	Very good	8
	-2 to 0	Good	6
	0 to 2	Moderate	4
	2 to 4	Poor	3
	> 4	Very Poor	1
Depth to GWL Pre-Monsoon (mbgl)	≤ 2	Very Poor	1
	2 - 4	Poor	3
	4 - 6	Moderate	4
	6 - 8	Good	6
	8 - 10	Very Good	8
	> 10	Excellent	10
GWL Fluctuation (m)	≤ 1	Very Poor	1
	1 - 2	Poor	3
	2 - 4	Moderate	4
	4 - 6	Good	6
	6 - 8	Very Good	8
	> 8	Excellent	10

Land Use and Land Cover	Urban Area	Very Poor	1
	Pasture	Good	6
	Grassland	Excellent	10
	Forest	Excellent	10
	Barren Land	Moderate	4
	Agriculture	Very Good	8
	Water Body	Good	6
Drainage Density (km/km^2)	≤ 0.5	Excellent	10
	0.5 - 1.0	Very good	8
	1.0 - 1.5	Good	6
	1.5 - 2.0	Moderate	4
	2.0 - 2.5	Poor	3
	> 2.5	Very Poor	1

6.7.3 Calculation of groundwater potential zone maps

After assigning the weights of each thematic layer and its sub-parameters, these layers were overlaid to find out the groundwater potential zones using the Prajal tool (http://prajal.org/). During the weighted overlay process, the ranks were given for each individual parameter of each thematic layer according to the influence of the different parameters. For Sot river catchment, the groundwater potential zones were delineated into six classes which include unsuitable, very low suitable, low suitable, moderately suitable, suitable and very suitable on the basis of report titled "T05. GIS multi-criteria decision analysis" given by INOWAS- Free web-based groundwater modeling platform (See Figure 69). It is observed from Figure 69, that the maximum area comes under the moderately suitable category followed by the suitable and very suitable category. As a result of this study, it is found that the groundwater condition of any area is greatly influenced by the LULC and geology. Based on the result of the study, this can be concluded that concerned decision makers can formulate an efficient groundwater utilization plan for the study area.

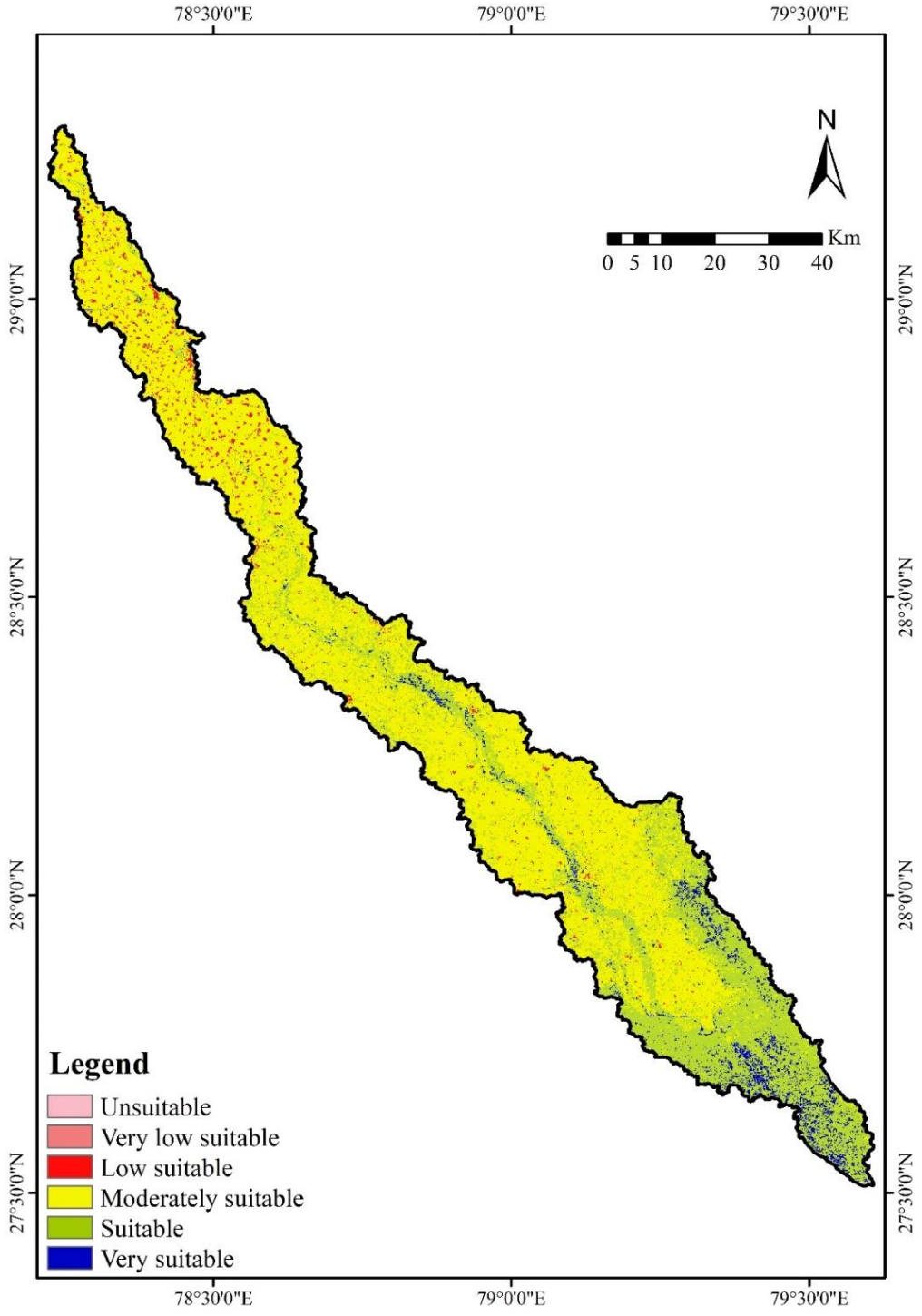

\

Figure 69: Groundwater potential zones in the Sot river catchment

6.8 Surface Water Conservation Measures including Artificial Groundwater Recharge

Sot river catchment, experience acute water shortage and many hydrological problems, including extra-deep groundwater levels, recurrent droughts, soil erosion and desertification in some of the areas due to population growth and economic development activities. Despite the fact, there could be other reasons of river drying up including extreme weather events such as high temperature, heavy rainfall for small duration etc. The Sot river catchment is threatened by multiple factors, such as climate crises, indiscriminate building construction, and other local factors. In the face of rapid drying of the Sot river, the local people are turning to groundwater to meet their demands for drinking and irrigation purposes. This has led to a substantial depletion of groundwater. As per the report published by the Composite Water Management Index, released by the NITI Aayog in June 2018, stated that 600 million people in India are facing high to extreme water stress. Throughout the whole process such as river drying up and declining groundwater levels in semi-arid areas of Uttar Pradesh, the interaction between surface and ground water resources always exists and exert great impact on quantities of surface water and groundwater. Therefore, the interaction between surface and ground water resources should be expressed precisely and in detail. In this study, we propose site-specific water conservation structures in the area that will increase groundwater recharge potential. Surface water conservation measures were selected following the thematic layers including geology, geomorphology, DEM, soil, slope, LULC, drainage, recharge, groundwater fluctuation, depth to aquifer, and depth to groundwater level for pre-monsoon period. Also, groundwater potential zones were delineated into six classes including unsuitable, very low suitable, low suitable, moderately suitable, suitable and very suitable by using eleven thematic layers. Therefore, to find out the suitable surface water conservation measures with artificial groundwater recharge structures, this study integrates the geology, geomorphology, soil, and slope of the area to overcome this problem.

Over the last decades, researchers have proposed many surface water conservation measures which help in regulating the surface runoff. These measures are classified into three categories, 1) engineering 2) vegetation, and 3) agricultural measures. Furthermore, agricultural water-saving potential mainly consist of water savings generated by techniques, engineering project and water-saving management (planting structure adjustment, water resource rational allocation, optimal irrigation schedule and water right policy). Surface water conservation is critical as it impacts the livelihood of the people and agricultural productivity. In order to meet the area's water needs, some

small dams (artificial water ponds) have been constructed. However, due to inadequate site evaluation techniques, many of these water facilities failed to meet the requirements. Due to high evaporation rates, a large quantity of directly stored water dries out before the next rainy season. Therefore, it is important to select suitable site Variation of daily rainfall and river flow data are presented in Figure 11. It can be seen from the Figure 11 that the daily rainfall varies from 0 to 94.37 mm in the Sot catchment, and the daily river flow data varies from 0 to 12.63 cumecs, respectively. Thus, the river is a monsoonal river having more than 90 per cent rainfall and river flow in monsoon season. The catchment area of Sot river is defined by a gentle to moderate slope (1– 4 %) which is one of the principal elements governing water infiltration into the aquifer. Besides this, runoff also is directly controlled by the slope and it is possible to construct a water retention structure on this slope. The study area consists of three different types of lithological features viz., grey micaceous sand, silt and clay; oxidized silt-clay with kankar and micaceous sand; silt clay, sand with gravel and pebbles; and grey sand, silt and clay. In the study area, geomorphology was divided into active flood plain, older flood plain, older alluvial plain, oxbow lake and ponds. On the basis of geological formation, the lithological feature including grey sand, silt and clay, and grey micaceous sand, silt and clay are suitable sites for artificial recharge as the in these sites the permeability is high. In this area rainwater harvesting can be done through percolation tanks, open wells or bore wells as this area will allow retention of substantial volume of water. Artificial recharge techniques enhance the sustainable yield in area and utilize the rainfall runoff which otherwise goes to sewer or storm water drains. Moreover, it restores supplies from aquifers depleted due to excessive groundwater usage and also enriches the groundwater reservoir. Percolation tanks are the most prevalent structures in India to recharge the groundwater reservoir in alluvial soil. One of the advantages to construct percolation tanks in this area is a cultivable land and also has a sufficient number of wells. It is also advisable to construct recharge pit of 1 to 2 m wide with 2 to 3 m deep for shallow aquifer. Rain water harvesting can be done by storage of rain water on surface for future use and recharging groundwater. In other lithological feature where the layer consists of oxidized silt-clay with kankar and micaceous sand, and silt clay, sand with gravel and pebbles is the suitable site for the rainwater harvesting. This area falls in low slope category, and has low permeability and this combination is very suitable for check dams. In this area the infiltration rate is lower than that of the other soil group. Therefore, the site is suitable for constructing check dams and farm ponds as these structures serve the dual purpose of facilitating recharge to ground water as well as for direct use of water. It is an important point to note that a

check dam must be constructed across a water course, and the locations have to be decided considering this factor.

6.9 Groundwater Recharge Structures

In the present study, few scenarios on groundwater recharge structures are suggested in the Sot catchment. Three types of recharge structures are suggested depending on the local conditions, i.e. surface slope, soil types, subsurface strata, etc. These structures include check dams, percolation tanks and recharge shafts. Check dams are suggested mainly in the upper part of the catchment. Percolation tanks are distributed in the catchment wherever thickness of surface soil is less. Recharge shafts are suggested where upper unconfined aquifer is deeper and separated by thick aquitard layer. Some tentative locations of these structures are given in Figure 70. Similar structures can be implemented at other feasible locations (falling under the suitable and moderate suitable zones).

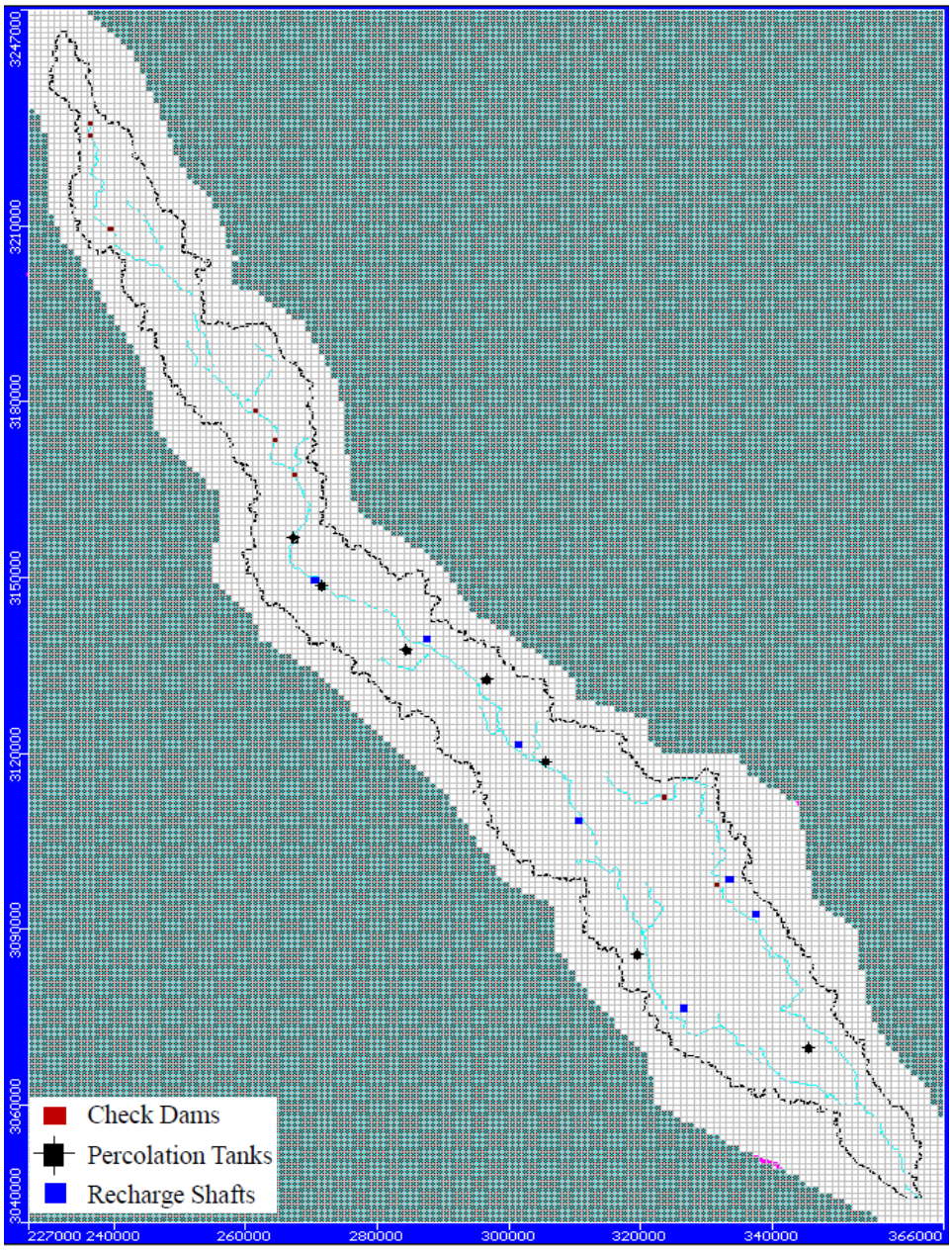

Figure 70. Tentative locations of suggested recharge structures in the catchment.

6.9.1 Impact Assessment of few Recharge Structures on the Groundwater Table

The catchment receives an average annual rainfall of 881.69 mm which indicates that the surface runoff potential is sufficient for groundwater recharge. The proposed sites are tentative, however, pin pointed sites have to be finalized after assessing the surface water harvesting and channelizing the surface runoff for groundwater recharge.

The impact of each of these three structures types is presented for eight locations for check dams, seven locations for percolation tanks, and seven locations for the recharge shafts in the subsequent section.

Check Dams:

Eight check dams are proposed at the potential locations. The details of all these check dams are given in Table 15.

Table 15. Locations of check dams proposed in the Sot catchment.

Sl. No.	Name	Northing	Easting
1	Check Dam-1	236470	3227170
2	Check Dam-2	236429	3225660
3	Check Dam-3	239498	3209340
4	Check Dam-4	261509	3178440
5	Check Dam-5	264578	3173620
6	Check Dam-6	267524	3167560
7	Check Dam-7	323495	3112410
8	Check Dam-8	331964	3097350

Ponding of water of one meter is assigned to the model considering that the check dam holds water for first six months and for next month does not hold any water. This is considered for a scenario of three years. Recharge from these check dams takes place as per the calibrated model properties. To monitor the groundwater level around each of these check dams, eight observations wells, i.e. OWCD-1 to OWCD-8 (one observation well near each check dam) are placed. The change in the groundwater level around these check dams is presented in Figure 71(a) and 71(b) for a period of three years after the validation period, i.e. after 1615th day with and without check dams. It is seen that the groundwater levels show rise in water table profiles after implementation of recharge interventions. The water table profiles show rise during the period of recharge and declines during the period of no recharge. It is also observed that in general the water table profiles show rising trend after the recharge interventions.

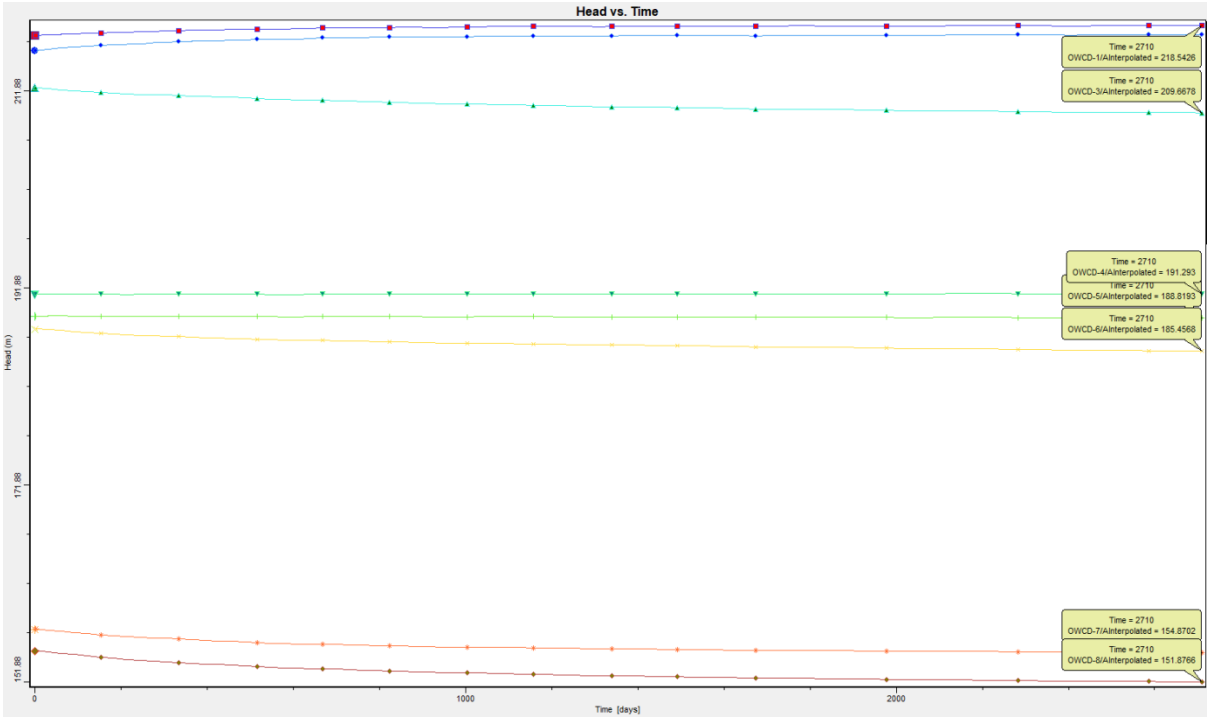

Figure 71(a). Groundwater levels prior to implementation of check dams.

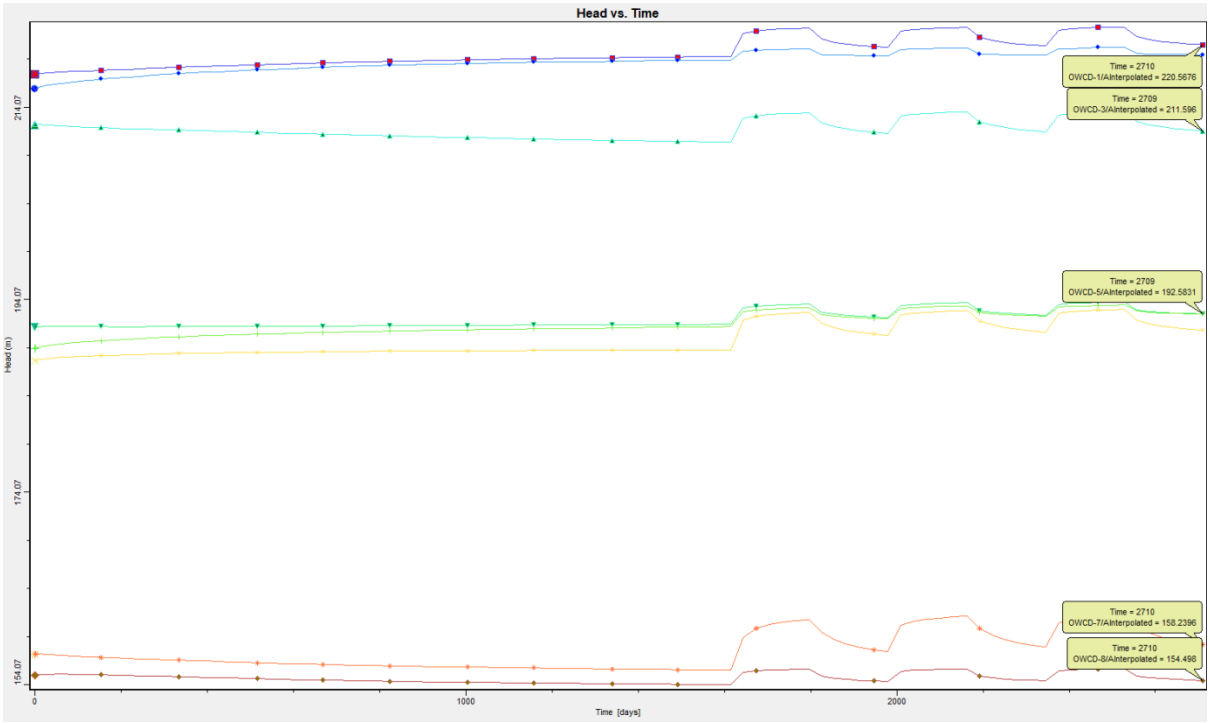

Figure 71(b). Variation of the groundwater levels after implementation of check dams.

Percolation Tanks:

Seven percolation tanks are proposed at the potential locations. The details of all these percolation tanks are given in Table 16.

Table 16. Locations of percolation tanks proposed in the Sot catchment.

Sl. No.	Name	Northing	Easting
1	Percolation Tanks-1	270597	3149510
2	Percolation Tanks-2	287685	3139430
3	Percolation Tanks-3	301852	3121180
4	Percolation Tanks-4	310762	3108180
5	Percolation Tanks-5	326828	3076340
6	Percolation Tanks-6	333838	3098100
7	Percolation Tanks-7	337636	3092260

Ponding of water of one meter on an average is assigned to the model considering that the percolation tank holds water throughout the year. This is considered for a scenario of three years. Recharge from these percolation tanks takes place as per the calibrated model properties. To monitor the groundwater level around each of these percolation tanks, seven observations wells, i.e. OWPT-1 to OWPT-7 (one observation well near each percolation tank) are placed. The change in the groundwater level around these percolation tanks is presented in Figure 72(a) and 72(b) for a period of three years after the validation period, i.e. after 1615^{th} day with and without percolation tanks. It is seen that the groundwater levels show rising trend after implementation of recharge interventions. The magnitude of rise in groundwater level is, however, small which will increase as recharge continues for more years with more no. of structures when net recharge (recharge – discharge) becomes positive.

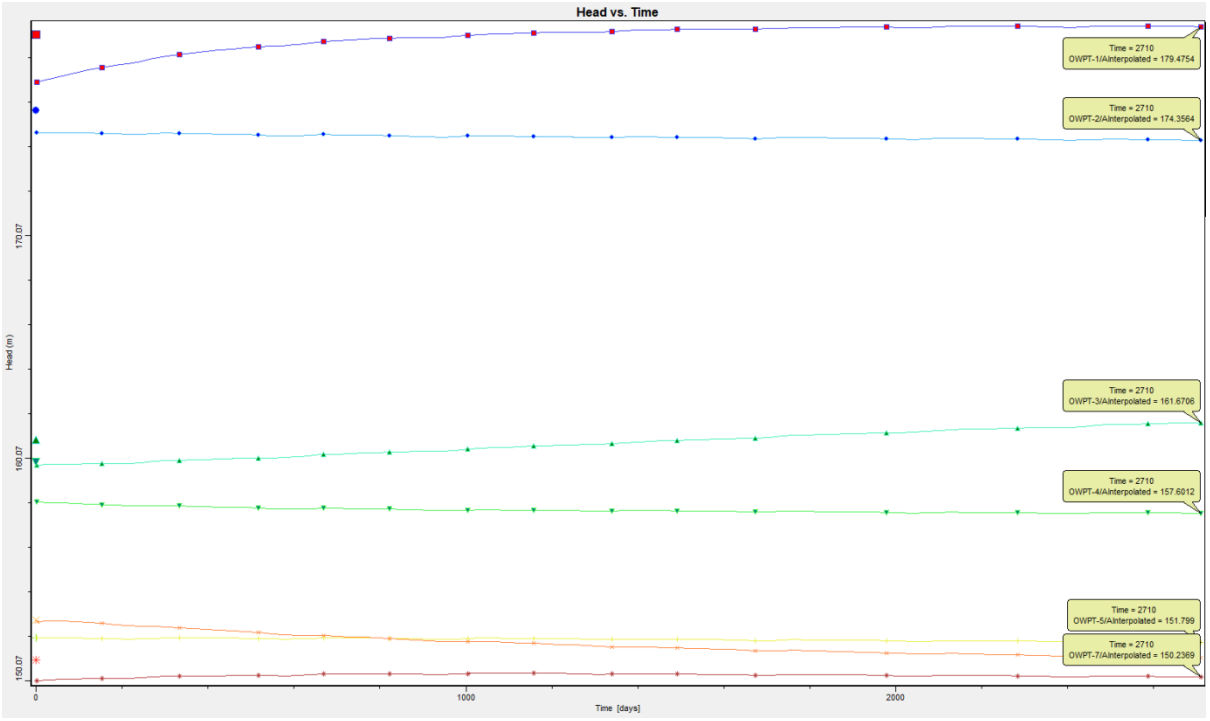

Figure 72(a). Groundwater levels prior to construction of percolation tanks.

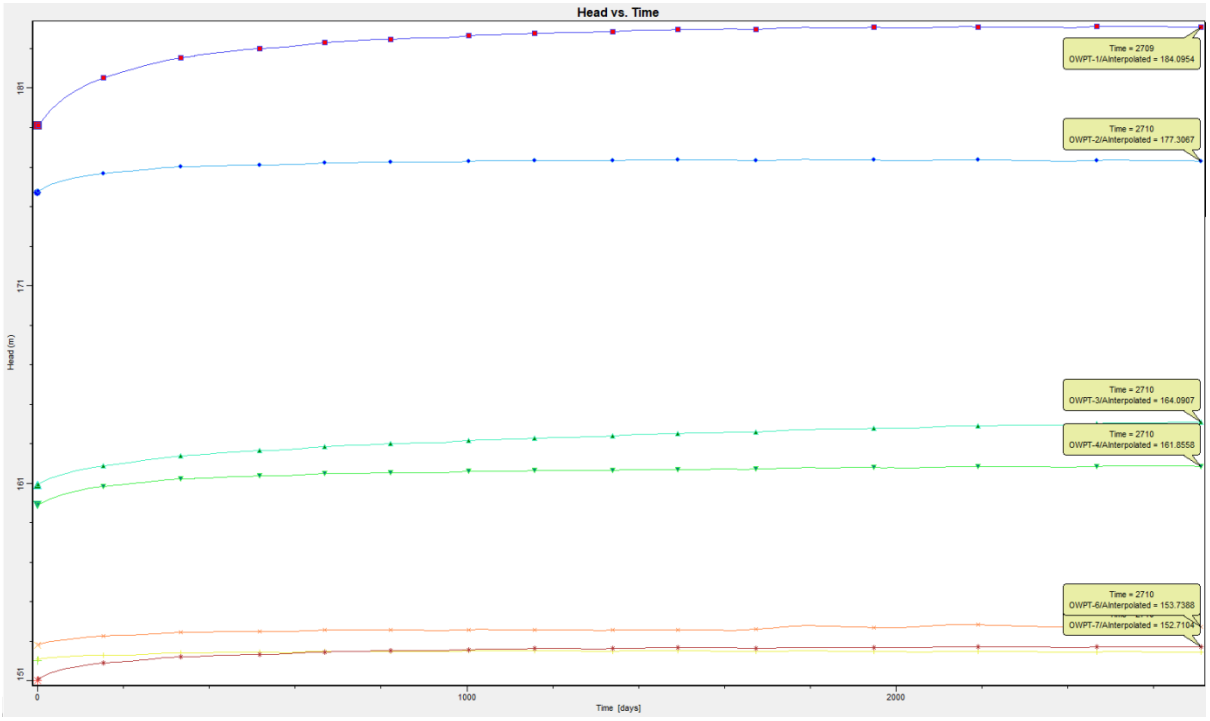

Figure 72(b). Variation of the groundwater levels after construction of percolation tanks.

Recharge Shafts

Seven recharge shafts are proposed at the potential locations. The details of all these recharge shafts is given in Table 17.

Table 17. Locations of recharge shafts proposed in the Sot catchment.

Sl. No.	Name	Northing	Easting
1	Recharge Shafts-1	267125.9	3156875
2	Recharge Shafts-2	271634.5	3148528
3	Recharge Shafts-3	284318.2	3137596
4	Recharge Shafts-4	296669.7	3132644
5	Recharge Shafts-5	305608.7	3118450
6	Recharge Shafts-6	319439.9	3085744
7	Recharge Shafts-7	345471.7	3069648

Injection of water at a rate of 100 m^3/day through the recharge shaft is assigned to the model considering that the recharge through the shaft takes place during the first six months and does not recharge any water during for next six months. This is considered for a scenario of three years. Recharge from these recharge shafts takes place as per the calibrated model properties. To monitor the groundwater level around each of these recharge shafts, seven observations wells, i.e. OWRS-1 to OWRS-7 (one observation well near each recharge shaft) are placed. The change in the groundwater level around these recharge shafts is presented in Figure 73(a) and 73(b) for a period of three years after the validation period, i.e. after 1615^{th} day with and without recharge shafts. It is seen that the groundwater level shows a rising trend after implementation of recharge interventions. The magnitude of rise in groundwater level is varying depending on the existing groundwater withdrawal practices (recharge – discharge).

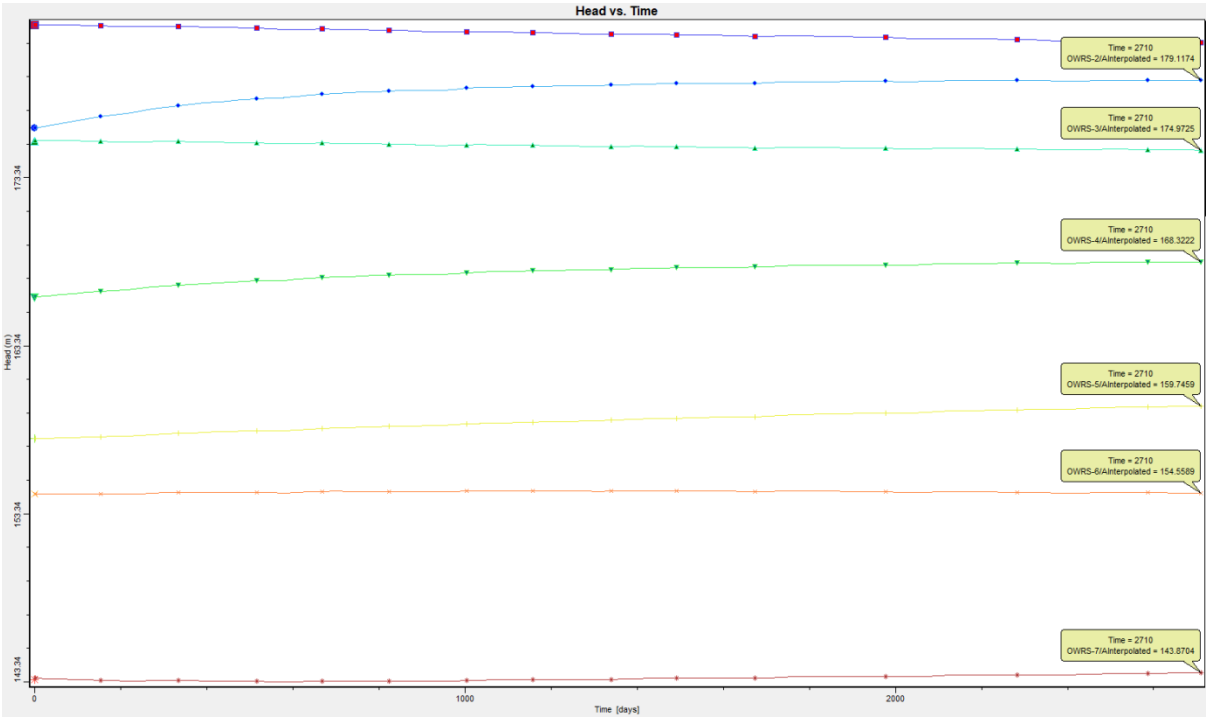

Figure 73(a). Groundwater levels prior to implementation of recharge shafts.

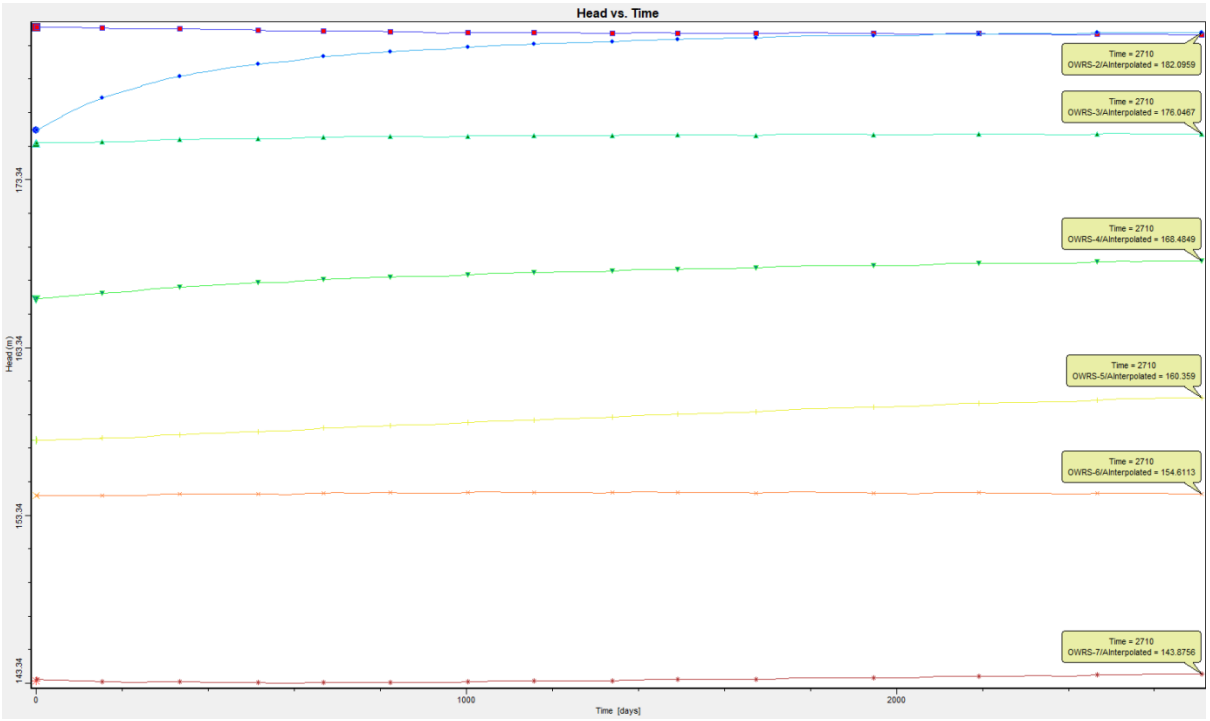

Figure 73(b). Variation of the groundwater levels after implementation of recharge shafts.

6.10 Demand-Side Management of Water Resources

The study focused mainly on the supply-side management as the demand-side management was not the objective of the study. However, the concerned raised by the reviewer is genuine and the study should also focus on the demand-side management of water resource in the catchment. If we look the demand-side management, then the following strategic planning is required for reducing the water demands in the catchment:

(i) Use of drip and sprinkler irrigation systems in the agriculture sector

(ii) Reduce water losses in the water distribution network for both drinking water as well as irrigation water supplies

(iii) Use of low water intensive and high yielding crops

(iv) Recycle and reuse of water across all water related sectors

As per the National Water Policy 2012, future demand can be managed by bringing the maximum possible efficiency in use of water and avoiding wastages.

Demand Management under the Climate Change:

As per the National Water Policy 2012, the adaptation strategies should include adoption of compatible agricultural strategies, cropping patterns and improved water application methods, such as land levelling and/or drip and sprinkler irrigation systems as they enhance the water use efficiency for dealing with increased variability because of climate change. Similarly, industrial processes should be made more water efficient.

6.11 Measures for Revival for Sot River

The condition of the Sot river is already very much deteriorated in past few decades. Lot of sediment and mud is deposited in the river course. Because of this, capacity of river is reduced a lot. Also due to deposition of mud on the river bed, water exchange capacity between river and groundwater is reduced considerably. Developmental activities and land use changes have also impacted the runoff and groundwater recharge conditions in the river catchment. Considering all these aspects, the following measures are suggested:

1. Implementation of groundwater recharge structures in the catchment at the feasible locations.
2. Dredging of river bed material by 1.5 to 2 meters in a planned manner. The dredged material may be used for constructions of roads.

3. Implementation of soil and water conservation practices in general wherever possible.
4. Protection of groundwater pumping within 300 meters of buffer zone of the river.
5. Construction of check dams along river at the feasible locations.
6. Implementation of conjunctive use management practice will be vital for the catchment in maintaining a balance of surface and ground water resource.
7. Development of some kind of surface water irrigation scheme in the middle part of the catchment will benefit in reducing the groundwater pumping.
8. Precise monitoring of river flows is very much needed for better management of surface water resources in the catchment.
9. Revival of old village ponds and tanks is very necessary to conserve and recharge water.
10. Plantations should be done along the banks of river to protect river banks and flourishing of fauna and flora along the river.
11. Removal of weeds like hyacinth, etc. from the river bed wherever present.
12. Restriction of diversion of municipal and industrial wastewater into the river to protect the river water quality and river ecosystem services.
13. Awareness raising among local habitants, farmers and village Panchayat Institutions and their active participation in river health protection and revival would be very much useful.

7 CONCLUSIONS AND SCOPE OF FUTURE WORK

Conclusions

- The annual rainfall varies from 450.5 to 1366.3 mm in the Sot catchment with an average annual rainfall of 881.69 mm. 90% rainfall occurs during June to October. Upper part of catchment receives more rainfall which reduces on moving towards downstream areas. Significant decreasing trend is observed both in monsoon and annual rainfall series in the lower part of the catchment.
- The monthly minimum temperature in the catchment varies from 14°C to 27°C. The monthly maximum temperature ranges from 27°C to 41°C. Temperature increases on moving from u/s to d/s of the catchment. July and August months show rise in the maximum temperature.
- Based on the analysis of 113 years' data (1901-2013), frequent droughts of frequency once in every five years are found. The persistent drought events of 2-, 3- and 4- consecutive years are identified. 3-Month Scale SPI and EDI are also estimated. SPI indicates occurrence of severe and moderate droughts in the catchment.
- Land use changes in the catchment are investigated for the period from 1998 to 2018. An increase of 4.6% has been observed in the settlement while barren land found decreased by 4.86% over this period.
- Cropping pattern indicates increase in area under sugarcane and wheat and reduction in pulses and oilseeds.
- Both minimum and maximum river flows show decreasing trend. The declining trends in minimum flows are very intense. Surface water availability at 80% exceedance probability is found 61.3 cumecs.
- Surface soils are loamy with varying proportions of sand, silt and clay. Infiltration and hydraulic conductivity tests were conducted at 48 locations at uniform grids of size 0.15^{o} x 0.15^{o}. Hydraulic conductivity was found to vary between 0.05 to 2.3 m/d. Infiltration rates were obtained between 0.3 to 51.5 cm/hr.
- Average groundwater levels in the catchment vary from 0.90 to 26.2 mbgl during pre-monsoon and 0.3 to 25.9 mbgl during the post-monsoon. Groundwater levels are shallow in the lower catchment and deeper in the middle part of catchment. Groundwater fluctuation up to 14.85 m is found which is more in the lower part of catchment. Groundwater levels are

found declining during the period of investigation from 2009 to 2018. Average groundwater availability in the catchment is estimated as 10,585.72 Ha-m.

- For river flow modeling and prediction, a total of four ANN models were calibrated and validated by utilizing the different input parameters. It was observed from the results of the study that model 4 (M4) with maximum R values (0.94 and 0.97), MNSE values (0.77 and 0.78), MIA values (0.88 and 0.89), and minimum RMSE values (0.39 and 0.45) during the calibration and validation period can be considered the best suited for predicting river flow of the Sot river catchment.
- Physically distributed ArcSWAT model was applied to the Sot catchment to model the river flow data, and SWATCUP was used to calibrate and validate the daily river flow data using the SUFI-2 algorithms. The results of this study showed that SWAT model performed relatively well in capturing the amount and variability of daily river flow hydrograph both during calibration and validation periods.
- Catchment water balance indicates rainfall 867.10 mm; ET 426.40 mm, surface runoff 145.88 mm, lateral discharge 0.54 mm, percolation 294.04 mm, and groundwater discharge from shallow aquifers as 279.99 mm.
- Litho logs of 49 locations were analyzed and processed for the delineation of aquifer layers. The results show top soil (0-27.4 m), aquifer-1 (0.91-56.4 m), aquifer-2 (16.78-92.9 m), aquifer- 3 (28.9-106.0 m), aquifer-4 (61.9-143.7 m), and aquifer-5 (89.0-150.9 m).
- Groundwater model was developed to model the groundwater system and assess impacts of groundwater recharge interventions in the Sot river catchment. The model was calibrated for the period 2009 to 2014 and validated for the period 2014 to 2018. The calibrated and validated model was used for assessing the impact of groundwater recharge structures in the catchment.
- To implement the groundwater recharge structures in the Sot catchment, potential zones for groundwater recharge were identified considering eleven thematic layers using the Prajal tool. The groundwater potential zones were categorized into six classes viz. unsuitable, very low suitable, low suitable, moderately suitable, suitable and very suitable. The maximum area was found under the moderately suitable condition followed by suitable and very suitable condition. These zones were used to implement the groundwater recharge structures in the catchment.

- Scenarios analysis on impact of groundwater recharge structures was also done for augmentation of groundwater so as to contribute base flow to river. Three types of recharge structures are suggested depending on the local conditions. Eight check dams are suggested mainly in the upper part of the catchment. Seven percolation tanks are distributed in the catchment wherever thickness of surface soil is less. Seven recharge shafts are suggested where upper unconfined aquifer is deeper and separated by thick aquitard layer. The impact of these structures is presented with and without these recharge interventions in the form of groundwater level profiles. It is seen that the groundwater levels show rise in water table profiles after implementation of the recharge interventions. The water table profiles show rise during the period of recharge and decline during the period of no recharge. It is also observed that in general the water table profiles show rising trend after the recharge interventions. Similar structures can be implemented at other feasible locations (falling under the suitable and moderate suitable zones).
- The condition of the Sot river has already very much deteriorated in past few decades and lot of sediment and mud is deposited in the river course. Because of this, capacity of river is reduced a lot. Also due to deposition of mud on the river bed, water exchange capacity between river and groundwater is reduced considerably. Considering these aspects, various measures are suggested for the rejuvenation of the Sot river.

Scope of Future Work

(i) In small tributaries, there is strong need to monitor the river flow precisely through advanced instrumentation.

(ii) River protection measures are needed to protect banks of small rivers from encroachment.

(iii) Efficacy of artificial recharge structures and measures should be tested on existing recharge structures on pilot scale coupled with groundwater modelling.

(iv) River-aquifer interaction study on a polluted river is also a matter of future research.

(v) Demand-side management of water resource in the catchment.

REFERENCES

Annear, T.C.; Hubert, W.; Simpkins, D. and Hebdon, L. 2002. Behavioural and physiological response of trout to winter habitat in tail waters in Wyoming, USA. Hydrological Processes 16: 915- 925.

Bates, B., Kundzewicz, Z., and Wu, S. (2008). *Climate change and water*. Intergovernmental Panel on Climate Change Secretariat.

Bernhardt, E. S., Palmer, M. A., Allan, J. D., Alexander, G., Barnas, K., Brooks, S., ... and Galat, D. (2005). Synthesizing US river restoration efforts.

Butts M B; Payne J T; Kristensen M; Madsen H. 2004. An evaluation of the impact of model structure on hydrological modelling uncertainty for stream flow simulation. Journal of Hydrology, 298(1-4), 242-266.

Central Ground Water Board (CGWB). (2013). District Ground Water Brochure.

Cheng, X., Chen, L., Sun, R., and Kong, P. (2018). Land use changes and socio-economic development strongly deteriorate river ecosystem health in one of the largest basins in China. *Science of the Total Environment*, *616*, 376-385.

Chessman, B. C., Fryirs, K. A., and Brierley, G. J. (2006). Linking geomorphic character, behaviour and condition to fluvial biodiversity: implications for river management. *Aquatic Conservation: Marine and Freshwater Ecosystems*, *16*(3), 267-288.

Fryirs, K., Chessman, B., and Rutherfurd, I. (2013). Progress, problems and prospects in Australian river repair. *Marine and Freshwater Research*, *64*(7), 642-654.

Galay, V. J. (1983). Causes of river bed degradation. *Water resources research*, *19*(5), 1057-1090.

Gore, J. A. (1985). Restoration of rivers and streams.

Gregory, K. J. (2006). The human role in changing river channels. *Geomorphology*, *79*(3-4), 172-191.

Gupta, A. D. (2008). Implication of environmental flows in river basin management. Physics and Chemistry of the Earth, Parts A/B/C, 33(5), 298-303.

Harbaugh, A. W., and McDonald, M. G., (1996). User's documentation for MODFLOW-96, an update to the U.S. Geological Survey modular finite-difference ground-water flow model. Open-File Report 96-485. U.S. Geological Survey.

Harbaugh, Arlen W., (2005). MODFLOW-2005, the U.S. Geological Survey Modular Ground-Water Model—the Ground-Water Flow Process. Techniques and Methods 6–A16. U.S. Geological Survey.

Hermoso, V., Pantus, F., Olley, J. O. N., Linke, S., Mugodo, J., and Lea, P. (2012). Systematic planning for river rehabilitation: integrating multiple ecological and economic objectives in complex decisions. *Freshwater Biology*, *57*(1), 1-9.

Hill, M. T., Platts, W. S., and Beschta, R. L. (1991). Ecological and geomorphological concepts for instream and out-of-channel flow requirements. Rivers, 2(3), 198-210.

ICFR. (2014) India Charter for Rivers adopted by delegates at India Rivers Week, 24-27 November 2014, New Delhi.

IWMI. (2005) Water Policy Briefing, Environmental flows. Planning for environmental water allocation, Report, International Water Management Institute, Sri Lanka, p. 8; http://www. iwmi.cgiar.org/Publications/Water_Policy_Briefs/PDF/wpb15.pdf

Jowett, I.G. 1997. Instream flow methods: a comparison of approaches. Regulated Rivers Research and Management 13: 115-127.

Langhans, S. D., Lienert, J., Schuwirth, N., and Reichert, P. (2013). How to make river assessments comparable: A demonstration for hydromorphology. *Ecological indicators*, *32*, 264-275.

Legates, D.R., McCabe Jr., G.J., 1999. Evaluating the use of "goodness-of-fit" measures in hydrologic and hydroclimatic model validation. Water Resources Research, 35, 233–241.

Linnansaari, T.; Monk, W.A.; Baird, D.J. and Curry, R.A 2012. Review of Approaches and Methods to Assess Environmental Flows across Canada and internationally. Dept Fisheries and Oceans, Can. Sci. Advis. Sec. Res. Doc. 2012/039.

Meier, C. I. (1998). The ecological basis of river restoration: 2. Defining restoration from an ecological perspective. In *Engineering Approaches to Ecosystem Restoration* (pp. 392-397).

Meng, W., Zhang, N., Zhang, Y., and Zheng, B. (2009). Integrated assessment of river health based on water quality, aquatic life and physical habitat. *Journal of Environmental Sciences*, *21*(8), 1017-1027.

Norris, R. H., and Thomas, M. C. (1999). What is river health?. Freshwater biology, 41(2), 197-209.

Pan, B., Yuan, J., Zhang, X., Wang, Z., Chen, J., Lu, J., ... and Xu, M. (2016). A review of ecological restoration techniques in fluvial rivers. *International Journal of Sediment Research*, *31*(2), 110-119.

Paillex, A., Schuwirth, N., Lorenz, A. W., Januschke, K., Peter, A., and Reichert, P. (2017). Integrating and extending ecological river assessment: Concept and test with two restoration projects. *Ecological indicators*, *72*, 131-141.

Piégay, H., Naylor, L. A., Haidvogl, G., Kail, J., Schmitt, L., and Bourdin, L. (2008). Integrative river science and rehabilitation: European experiences. *River Futures: An integrative scientific approach to river repair*, 201-219.

Poff NL, Allan JD, Bain MB, Karr JR, Prestegaard KL, Richter BD, Sparks RE, Stromberg JE (1997). The natural flow regime: a paradigm for river conservation and restoration. Bio Science, 47:769-784

Raju, K.C.B., Rao, G.V.K. and Kumar, B.J., (1989). Analytical aspects of remote sensing techniques for groundwater prospecting in hard rocks, In: Proc. of the 6th Asian Conference on Remote Sensing, 127–132.

Roni, P., Hanson, K., and Beechie, T. (2008). Global review of the physical and biological effectiveness of stream habitat rehabilitation techniques. *North American Journal of Fisheries Management*, *28*(3), 856-890.

Shekhar, S. (2016). Environmental flows and river rejuvenation. *Journal of the Geological Society of India*, *88*(6), 813-814.

Sinha, R., Jain, V., and Tandon, S. K. (2013). River Systems and River Science in India: major drivers and challenges. In *Earth System Processes and Disaster Management* (pp. 67-90). Springer, Berlin, Heidelberg.

Sivakumar, B., Berndtsson, R., and Persson, M. (2001). Monthly runoff prediction using phase space reconstruction. Hydrological sciences journal, 46(3), 377-387.

Stalnaker, C.B. and Arnette, J.L. (Editors). 1976. Methodologies for the Determination of Stream Resource Flow Requirements: An Assessment. U.S. Fish and Wildlife Service, Office of Biological Services. 199 pages.

Vörösmarty, Charles J., Peter B. McIntyre, Mark O. Gessner, David Dudgeon, Alexander Prusevich, Pamela Green, Stanley Glidden et al. "Global threats to human water security and river biodiversity." *Nature* 467, no. 7315 (2010): 555.

Wang and Lu, (2009). "Quantitative Estimation Models and their Application of Ecological Water Use at a Basin Scale." Procedia Environmental Science, 13,1559-1568.

Dunbar, M.J.; Gustard, A.; Acreman, M.C. and Elliot, C.R.N. 1998. Review of Overseas Approaches to Setting River Flow Objectives, Environment Agency R and D Technical Report W6B 96 (4). Institute of Hydrology, Wallingford, U.K. 61 pages.

Wang W C; Chau K W; Cheng C T; Qiu L. 2009. A comparison of performance of several artificial intelligence methods for forecasting monthly discharge time series. Journal of Hydrology, 374(3-4), 294-306.

Willmott, C.J., Ackleson, S.G., Davis, R.E., Feddema, J.J., Klink, K.M., Legates, D.R., O'Donnell, J., Rowe, C.M., 1985. Statistics for the evaluation and comparison of models. Journal of Geophysical Research: Oceans, 90, 8995–9005.

Wohl, E., Palmer, M., Kondolf, G. M., Brierley, G. J., and Fryirs, K. A. (2012). River management in the United States. *River futures: an integrative scientific approach to river repair. Island Press, Washington, DC*, 174-200.

Xu, K., Yang, D., Yang, H., Li, Z., Qin, Y., and Shen, Y. (2015). Spatio-temporal variation of drought in China during 1961–2012: a climatic perspective. Journal of Hydrology, 526, 253-264.